

BROADLY REACTIVE INFLUENZA
NEURAMINIDASE-SPECIFIC ANTIBODY MEDIATED
PROTECTION IN THE MOUSE AND FERRET ANIMAL MODELS

by

AMANDA LEE SKARLUPKA

(Under the Direction of Ted M. Ross)

ABSTRACT

The influenza virus is a human respiratory virus that continues to ravage the world even in the presence of a vaccine. Multiple viral protein targets have been identified to prevent and mitigate disease. However, the most commonly used vaccines - split inactivated virus vaccines - only have standardized concentrations of the hemagglutinin (HA) surface protein and elicit HA-specific antibodies. These responses are strain-specific with limited ability to cross-react with antigenically drifted viruses. Therefore, these current vaccines do not provide protection toward potentially pandemic influenza viruses from the avian, swine, or other animal host reservoirs. The neuraminidase (NA) surface protein is not quantified or standardized even though antibodies that target the NA protein are meaningful correlates of protection in humans and mitigate disease in animal models. New NA vaccine immunogens are being investigated to increase the vaccine's protective breadth and longevity. An N₁ NA subtype vaccine immunogen was designed with the computationally optimized broadly reactive antigen (COBRA) methodology using wild-type NA sequences originating from swine, avian, and human isolated HXN₁ viruses: N₁-I COBRA NA. In the mouse model, the wild-type N₁ antigens elicited antigenically distinct patterns based upon the genetic lineage (human, avian, or swine). The human and avian lineage did not cross-react between each other. However, the N₁-I COBRA NA elicited functional antibodies to all N₁ lineages. Further, this functional antibody profile corresponded with the protection from viral challenge in the ferret model. The N₁-I COBRA NA protected as well as the homologous control proteins an H₁N₁ and an H₅N₁ challenge (two avian lineage viruses), whereas the human lineage N₁ immunogen offered significantly less protection. Lastly, in a contact transmission model, modeling a family unit, vaccination with any immunogen did not inhibit the ability of the vaccinated ferret from transmitting to a naïve ferret, or from a naïve ferret from transmitting to a vaccinated ferret. Overall, this dissertation provides an in-depth analysis of the antigenic and protective profiles of wild-type and the N₁-I COBRA NA immunogen. The inclusion of the N₁-I COBRA NA or, at a minimum, wild-type NA protein into current vaccine compositions will provide increased benefit.

INDEX WORDS: Influenza; Vaccine; Neuramindase; Animal Model; Broadly Protective

BROADLY REACTIVE INFLUENZA NEURAMINIDASE-SPECIFIC ANTIBODY MEDIATED
PROTECTION IN THE MOUSE AND FERRET ANIMAL MODELS

by

AMANDA LEE SKARLUPKA

B.S., University of Wisconsin - Madison, 2014

A Dissertation Submitted to the Graduate Faculty of the
University of Georgia in Partial Fulfillment of the Requirements for the Degree

DOCTOR OF PHILOSOPHY

ATHENS, GEORGIA

2022

©2022

Amanda Lee Skarlupka
All Rights Reserved

BROADLY REACTIVE INFLUENZA NEURAMINIDASE-SPECIFIC ANTIBODY MEDIATED
PROTECTION IN THE MOUSE AND FERRET ANIMAL MODELS

by

AMANDA LEE SKARLUPKA

Major Professor: Ted M. Ross

Committee: Vincent Starai
Melinda Brindley
Donald Harn
Wendy Watford

Electronic Version Approved:

Ron Walcott
Vice Provost for Graduate Education and Dean of the Graduate School
The University of Georgia
May 2022

DEDICATION

This dissertation is dedicated to the rabble-rousers and instigators.

A C K N O W L E D G M E N T S

I want to acknowledge my family, friends, and colleagues who have assisted me in where I am today, including but not limited to: Kara, Joey, Megan, Frank, Grandma and Grandpa, Aunt Fay, Randall, Lane, Dr. Jaehyuk Yu, Dr. Kathy Glass, Abigail, Emily, Stacy, Israel, Valarie, Hamidou, Bodo, Kalyan, Harry, Beau, Laura, Dawn, Maggie, Ying, Rodrigo, Giuseppe, Anne, Lui, Ross, Spencer, James, Dian, Steven, Jason, Lauren, Derek, Hannah and the UGA powerlifting, climbing, salsa, and tango clubs. Without their combined support this process would have been much less enjoyable. Thank you.

CONTENTS

Acknowledgments	v
List of Figures	ix
List of Tables	xii
1 Introduction	I
1.1 Research Aims	2
1.2 Significance	3
1.3 Innovation	5
2 Literature Review	6
2.1 Abstract	7
2.2 Influenza History in the Human Population	8
2.3 Consequences of Influenza Pre-Immunity	9
2.4 Influenza Virion Structure and Morphology	II
2.5 Influenza Virus Genome and Antigenic Shift and Drift	12
2.6 Neuraminidase Structure and Function	14
2.7 Neuraminidase Genetic Diversity	16
2.8 Influenza Entry and Replication Cycle	18
2.9 Neuraminidase-specific Immunobiology	20
2.10 At-risk Populations	22
2.11 Influenza Vaccine History	22
2.12 Influenza Vaccine Platforms	23
2.13 Adjuvants	24
2.14 Neuraminidase as a Vaccine Antigen	25
2.15 COBRA Methodology	26
2.16 Influenza Animal Models	27
2.17 Pre-immunity on the Ferret Immune Response	29
2.18 Conclusion	31

3 Universal Influenza Virus Neuraminidase Vaccine Elicits Protective Immune Responses Against Human Seasonal and Pre-pandemic Strains	32
3.1 Abstract	33
3.2 Introduction	34
3.3 Materials and Methods	36
3.4 Results	44
3.5 Discussion	57
3.6 Acknowledgements	60
3.7 Competing Interests	60
3.8 Funding Information	61
4 Multi-influenza HA Subtype Protection of Ferrets Vaccinated with an Ni COBRA-based Neuraminidase	62
4.1 Abstract	63
4.2 Introduction	65
4.3 Materials and Methods	67
4.4 Results	73
4.5 Discussion	93
4.6 Acknowledgments	96
4.7 Competing Interests	96
4.8 Funding Information	96
5 Discussion	97
5.1 Ni-I COBRA NA as a Vaccine Immunogen	97
5.2 COBRA as Vaccine Antigen Development Tool	100
5.3 Antigenic Cross Reactivity of Wild-type NAs	101
6 Conclusion	104
Bibliography	106
Appendices	147
A Design Considerations for Pre-immune Influenza Ferret Studies	147
A.1 Vaccination as a Surrogate for Viral Infection Pre-Immunity	147
A.2 Low Vaccine Seroconversion Proportions in Naïve Ferrets	148
A.3 Historic Pre-Immune Ferret Models	149
A.4 Current Pre-Immune Ferret Models in Practice	150
A.5 Immune system cool-down	158
A.6 Age/Sex/Vendor specific responses	158
A.7 Validation and Further Work of the Pre-Immune Model	159

A.8	Conclusions	160
B	Inherent Serum Inhibition of Influenza Virus Neuraminidase	162
B.1	Abstract	163
B.2	Introduction	164
B.3	Materials and Methods	166
B.4	Results	170
B.5	Discussion	171
B.6	Acknowledgements	174
B.7	Competing Interests	175
B.8	Funding Information	175
C	COBRA Vaccine Based Upon Swine H1N1 Influenza HA Sequences Protects against both Swine and Human Isolated Viruses	178
C.1	Abstract	178
C.2	Introduction	179
C.3	Materials and Methods	182
C.4	Results	195
C.5	Discussion	205
C.6	Acknowledgements	214
C.7	Competing Interests	214
C.8	Funding Information	214
D	An Influenza Virus Hemagglutinin Computationally Optimized Broadly Reactive Antigen Elicits Antibodies Endowed with Group 1 Heterosubtypic Breadth against Swine Influenza Viruses	215
D.1	Background	216
D.2	Results and Discussion	216
D.3	Acknowledgements	217
D.4	Competing Interests	219
E	Influenza hemagglutinin antigenic distance measures capture trends in HAI differences and infection outcomes, but are not suitable predictive tools	220
E.1	Abstract	221
E.2	Introduction	222
E.3	Materials and Methods	224
E.4	Results	229
E.5	Discussion	239
E.6	Acknowledgments	241
E.7	Competing Interests	241

F Design of N₂ COBRA NA Influenza Antigens	242
F.I Wild-type N ₂ lineages	242

LIST OF FIGURES

2.1	Genetic lineage cladogram of the N1 NA influenza subtype	17
3.1	Neuraminidase activity comparison of influenza A viruses compared to their respective soluble protein	39
3.2	Mouse experimental groups and design used for influenza challenge	45
3.3	Total IgG antibody binding of vaccinated mouse sera to tetrameric NA expressed on the surface of a virus-like particle	47
3.4	NA enzymatic inhibition of N1 influenza viruses with sera from NA vaccinated mice .	48
3.5	Reciprocal NA inhibition (NAI) titers across a panel of N1 influenza viruses with sera from NA vaccinated mice	49
3.6	A/California/07/2009 (H1N1)pdm09 challenge results after vaccination with NA antigens in mice	51
3.7	Vaccine-specific inhibition of influenza inflammatory lung infiltration	52
3.8	A/Brisbane/59/2007 (H1N1)×PR8 challenge results after vaccination with NA antigens in mice	53
3.9	A/Viet Nam/1203/2004 (H5N1)×PR8 challenge results after vaccination with NA antigens in mice	55
3.10	A/Swine/North Carolina/154074/2015 (H1N1) challenge results after vaccination with NA antigens in mice	56
4.1	Naïve, pre-immune, and contact transmission ferret model design	74
4.2	N1-I COBRA NA vaccines performed similarly to CA/o9 HA and NA vaccines in the naïve ferret model intranasally challenged with CA/o9 H1N1	75
4.3	N1-I COBRA NA vaccine induced similar inflammation in the upper and lower respiratory tract as the CA/o9 HA and CA/o9 NA vaccines in naïve ferret model after intranasal challenge with CA/o9 H1N1	78
4.4	H&E staining of CA/o9 challenged ferret lungs	79
4.5	H&E staining of CA/o9 challenged ferret nasal cavity	80
4.6	H&E staining and CD3+ immunohistochemistry of CA/o9 challenged ferret submandibular lymphnode	81

4.7	NA vaccinated ferrets pre-immunized with Sing/86 H ₁ N ₁ exhibited minimal clinical signs after intranasal challenge with CA/09 H ₁ N ₁	83
4.8	N ₁ -I COBRA NA vaccine performed similarly to the Viet/04 NA vaccine in the naïve ferret model intranasally challenged with Viet/04 H ₅ N ₁	84
4.9	N ₁ -I COBRA NA vaccine elicited NA-inhibiting antibodies to a panel of genetically diverse HXN ₁ viruses	86
4.10	NA enzymatic inhibition curves of four N ₁ influenza viruses from sera taken from NA vaccinated ferrets	87
4.11	HAI results of CA/09 HA vaccinated and Sing/86 pre-immunized ferrets	88
4.12	Vaccination of contact transmitting ferrets did not limit the transmission to other ferrets or affect the receiving ferret's clinical or viral outcomes	89
4.13	Vaccination of contact receiving ferrets did not limit transmission	90
4.14	Magnitude of weight loss and viral loads did not change based upon intranasal or contact transmission inoculation method	92
5.1	Antigenic Cartography of the N ₁ NA influenza subtype	99
5.2	Antigenic Cartography of the Dengue Virus Serotypes and COBRA	103
B.1	NA inhibition of influenza virus with addition of raw animal sera.	172
C.1	Designs of Swine COBRA HA sequences	183
C.2	The unrooted human and swine H ₁ HA phylogenetic tree was inferred from database HA amino acid sequences with the inclusion of COBRA HA sequences	186
C.3	Subtle differences in the Sa and Sb regions lead to structural differences among the CO-BRA and wild-type predicted structures surrounding the receptor-binding site.	198
C.4	Differential putative glycosylation sites between the human seasonal-like sequences and the classical swine sequences	199
C.5	A/California/07/2009 H ₁ N ₁ viral challenge of vaccinated BALB/c mice	201
C.6	A/Swine/North Carolina/152702/2015 H ₁ N ₂ viral challenge of COBRA vaccinated BALB/c mice	203
C.7	HAI titers of COBRA VLP vaccinated mice sera against swine H ₁ VLPs	204
C.8	HAI titers of swine and human wild-type HA VLP vaccinated mice sera against swine H ₁ VLPs	206
C.9	HAI titers of swine wild-type HA VLP vaccinated mice sera against human H ₁ N ₁ viruses	207
C.10	ELISA of elicited antibodies against either SW/NC/15 or CA/09 recombinant HA protein	208
C.11	Comparison of antigenic site residues of CA/09 and SW/NC/152702/15	211
D.1	HAI and neutralizing activity breadth of P ₁ - (A), seasonal-, and pandemic-specific (B) MAbs against influenza A H ₁ N ₁ , H ₁ N ₂ , and H ₂ N ₃ swine viruses.	217
D.2	Antigenic cartography map of P ₁ -, seasonal-, and pandemic-specific MAbs.	218

E.1	Amino acid sequence based antigenic distances modeled against the change in HAI titer of H ₁ influenza in the mouse model.	230
E.2	Amino acid sequence based antigenic distances modeled against the change in HAI titer of H ₁ influenza in the mouse model including points below the limit of detection.	231
E.3	The p_{epitope} antigenic distance better describes computationally designed interactions, than wild-type HAI antigen interactions.	233
E.4	The p_{epitope} antigenic distance better describes computationally designed interactions, than wild-type HAI antigen interactions including points below the limit of detection.	234
E.5	The interactions of swine origin HA antigens with HAI antigens are not a function of the p_{epitope} antigenic distance.	235
E.6	The interactions of swine origin HA antigens with HAI antigens are not a function of the p_{epitope} antigenic distance even with inclusion of points below the limit of detection.	236
E.7	Amino acid sequence based antigenic distances modeled against the change in HAI titer for human H ₁ N ₁ subtype HAI data in the ferret model.	237
E.8	Amino acid sequence based antigenic distances modeled against the change in HAI titer for human H ₁ N ₁ subtype HAI data in the ferret model including points below the limit of detection.	237
E.9	The use of in vivo challenge data from the mouse model for linear regression with different antigenic distances.	238
F.1	Genetic lineage cladogram of the N ₂ NA influenza subtype	244

LIST OF TABLES

B.1	Linear regression fit of the NA activity of the viruses tested in the panel.	169
B.2	Non-linear regression fits of raw serum inhibition of Type A influenza viruses.	176
B.3	NA inhibition of raw sera stratified by host origin.	177
C.1	Accession numbers or amino acid sequences of the HA of H1 strains.	185
C.2	Computationally optimized broadly reactive antigens used in the study.	189
C.3	Amino acid residues used to calculate the ADM of vaccine and challenge virus combinations.	189
C.4	Resultant p-values from ordinary one-way ANOVA followed by Tukey's multiple comparisons test.	194
C.5	The dominant p_{epitope} based predictions for vaccine effectiveness against the challenge strains.	196
E.1	HAs used as HAI antigens, vaccine components, and viral challenge strains.	224
E.2	Amino acid residues used to calculate the ADM of vaccine and challenge virus combinations.	228
E.3	Summary of resultant equations from best-fit analysis.	232
E.4	Summary of resultant equations from best-fit analysis including points below the limit of detection.	232
E.5	Summary of resultant equations from best-fit analysis of sub-setted data with and without points below the limit of detection (LOD).	235
F.1	Summary of N2-A and N2-B COBRA NA antigen design. The motivation, wild-type sequences, time frames and methods used to create the N2 COBRA NA antigens. . . .	243

CHAPTER I

INTRODUCTION

Influenza viruses are common human respiratory pathogens transmitted through air-borne droplets and contact with contaminated surfaces. Annually, millions of people are infected with a resulting estimated 0.5 million deaths globally. Commercial vaccines direct the immune response to hemagglutinin (HA) - a significant viral surface protein - and elicit high anti-HA antibody titers. Unfortunately, when there is an antigenic mismatch between the vaccine HA and the circulating influenza strain, there is a decrease in the vaccine effectiveness in vaccinated persons. Therefore, current vaccines are inadequate for long-term protection (>1 year) due to the high epitope variability of the HA protein providing effectiveness between 10-60% depending upon the season (Centers for Disease & Prevention, 2021a). Often these vaccines elicit little or no antibodies against the virus' second-most abundant surface glycoprotein – the neuraminidase (NA) – even though anti-NA antibodies contribute to protection. Furthermore, not only is NA more antigenically stable than HA, vaccinating with only two antigenic subtypes of NA (N₁ and N₂) can widen the elicited antibodies' protective breadth to cover human seasonal epidemics strains (H₁N₁; H₃N₂) in addition to potentially pandemic strains (H₅N₁; H₂N₂, H₅N₂, H₇N₂, H₉N₂). This broad reactivity is a crucial feature for future influenza vaccines. Vaccine researchers and companies have historically overlooked the NA as a universal influenza vaccine antigen in favor of the HA protein. Previously, researchers used the Computationally Optimized Broadly Reactive Antigen (COBRA) methodology to develop HA antigens that elicit a polyclonal antibody response that binds to and inhibits a broader range of HA pro-

teins than wild-type HA antigens. Hence, ***I hypothesize that an N₁ NA antigen designed using the COBRA methodology elicits antibodies with broadly inhibitory and protective activity towards multiple influenza viruses that spans across N₁ genetic lineages and HA subtypes in both mice and ferrets.***

1.1 Research Aims

Specific Aim 1: Design broadly reactive COBRA-based N₁ NA vaccine candidates and define their immunological and protective characteristics to seasonal and pre-pandemic influenza viruses in mice.

Hypothesis: N₁ COBRA NA antigens elicit protective antibodies against a broader panel of N₁ influenza viruses than antibodies produced by wild-type influenza viruses of different subtypes.

Broadly reactive NA proteins designed by COBRA methodology used wild-type NA sequences as the original input. Unique sequences of wild-type N₁ proteins were aligned and clustered for each NA subtype using a multi-layered consensus approach to generate COBRA NA vaccine sequences unique from wild-type sequences. Soluble tetrameric COBRA or wild-type NA protein vaccines were administered to BALB/c mice with adjuvant three times. Mice were bled pre- and post-vaccination, and the collected anti-sera were tested for the ability to bind to the NA (anti-NA ELISA) and to inhibit NA enzymatic activity (NA-inhibition assay) against a panel of wild-type influenza viruses across multiple HA subtypes. Vaccinated mice were challenged with varying challenge viruses (pandemic H₁N₁, seasonal H₁N₁, swine H₁N₁, H₅N₁). Challenged animals were monitored for signs of morbidity for up to 14 days. Lung pathology and viral lung titers were recorded at day three post-infection.

Specific Aim 2: Assess the elicitation of protective immune responses by COBRA NA antigens in the naïve and pre-immune ferret model.

Hypothesis: The COBRA NA vaccines elicit protective immune responses in ferrets against influenza viruses from multiple subtypes and reduce disease pathology in challenged ferrets.

Naïve and pre-immune ferrets will be vaccinated with adjuvanted COBRA and wild-type NA vaccines. The N₁ COBRA antigen will be tested for efficacy in ferrets exposed to a prior sublethal seasonal

H₁N₁ influenza infection to establish pre-existing seasonal influenza immunity. After a period of rest, these pre-immune ferrets will be vaccinated with N₁ COBRA antigens and tested for protection against H₁N₁ or H₅N₁ viral challenges. Elicited serum responses were characterized similarly to mice. After the challenge, ferrets will be assessed for weight loss and viral titers in nasal washes and pathology in tissues of the respiratory tract. Results will be compared to non-pre-immune ferrets vaccinated with the same N₁ COBRA vaccine antigens.

Specific Aim 3: Determine the effect of NA COBRA vaccination on influenza transmission in the ferret model.

Hypothesis: COBRA NA vaccine elicits immune responses in ferrets, and those responses can reduce or block transmission of influenza viruses from host to host.

Ferrets vaccinated with N₁ COBRA vaccines will be challenged with an H₁N₁ virus and subsequently co-housed with an unvaccinated ferret for 14 days to determine if ferrets transmit the virus (both contact and aerosol) to the unvaccinated animal. In a reciprocal experiment, unvaccinated ferrets will be challenged and then housed with vaccinated ferrets to determine if the vaccination protects against influenza virus infection via aerosol or contact transmission. Ferret challenge outcomes will be assessed as described above.

I.2 Significance

With four historical pandemics since 1918, the influenza virus remains at the forefront of communicable diseases. The virus maintains global seasonal epidemics and retains its pandemic potential through animal reservoirs. The infectious virion is a negative-sense single-stranded RNA virus with an eight-segmented genome. The surface of the virion is composed of the hemagglutinin (HA) and neuraminidase (NA) glycoproteins involved in receptor binding and release, respectively. Neutralizing antibodies target these proteins, and current antivirals (zanamivir and oseltamivir) target the NA. The HA and NA are independently subtyped based upon serological cross-reactivity, which are used to classify viral isolates (e.g., H₁N₁, H₅N₁, H₃N₂). Currently, only N₁ or N₂ containing viruses have maintained substantial transmission in humans. The N₆, N₇, N₈ and N₉ have been isolated from human infection but at much lower rates. The

NA has sialidase enzymatic activity contributing to cleavage of mucins, motility, the release of progeny virions, and prevention of self-aggregation (Wohlbold & Krammer, 2014).

Vaccination remains the primary influenza prevention method and elicits protective antibodies against the surface glycoproteins. One of the most commonly used seasonal flu vaccines is a split-inactivated influenza vaccine that does not remove any of the virion components. Although all of the components are present, the structural integrity of the proteins can be destabilized from the split-inactivation process and the final NA protein concentration is not standardized unlike the HA protein (Solano et al., 2017). Vaccination increases antibody titers against the HA protein but not against the NA. The lack of anti-NA titers may be due to this decreased structural integrity from vaccine preparation and to the contribution from the HA being more immunodominant than the NA (Wohlbold & Krammer, 2014).

Antibodies targeting the NA are protective to the host and viral neutralizing. The NA protein is under different selective pressure than the HA, and at times has slower mutation rates compared to the HA protein. Therefore, inclusion of the NA immunogen may elicit an antibody pool that complements the HA elicited pool and may increase the protective lifespan of the vaccine due to the separation of the HA and NA mutation rates.

The goal for influenza vaccine research is the development of a broadly protective vaccine. The Computationally Optimized Broadly Reactive Antigen (COBRA) methodology combines diverse wild-type protein sequences into a layered-consensus sequence. To develop a COBRA antigen, the wild-type protein of interest must be variable in sequence. The antigenic drift of the NA, the high mutation rate of influenza polymerase, and the broad host range introduce and maintain this necessary sequence variability. Therefore, I propose that application of the COBRA methodology to the Ni NA protein may produce an computationally-derived NA antigen that is more broadly protective across viral strains than wild-type Ni NA proteins.

I.3 Innovation

Current approaches for developing a universal or broadly reactive influenza vaccine have focused on eliciting antibodies targeting the HA surface protein with very little interest expressed in NA. However, one broadly protective N₁ COBRA NA vaccine can protect from human seasonal and pandemic H₁ epidemics and decrease the potential for avian H₅N₁ and swine H₁N₁ zoonotic pandemics. The N₁ NA immunogen protects against more HA subtypes and species-of-origin than the use of an HA immunogen. Utilizing the antibody response to the NA protein, in addition to, the HA protein will lead to an increase in the longevity and neutralizing capacity of the influenza vaccine.

Current research has indicated that NA protein as a promising vaccine target. Previously, much of the research focused on the NA protein primarily as a drug target. The NA protein has been directly targeted as a site to prevent infection. Therefore, more preventative responses (such as antibodies induced through vaccination) instead of therapeutic responses (antivirals taken after infection) to the NA protein should be prioritized to decrease the prevalence of influenza. In addition, understanding more about the NA protein as a vaccine antigen, as proposed here, will contribute towards understanding influenza replication and protection from infection.

CHAPTER 2

LITERATURE REVIEW¹

¹Skarupka, A. L., & Ross, T. M. (2020). Immune Imprinting in the Influenza Ferret Model. *Vaccines (Basel)*, 8(2). doi:10.3390/vaccines8020173. Reprinted here with permission of the publisher.

2.1 Abstract

Influenza virus' have been prevalent and important throughout human history. With the initial exposure to influenza virus occurring during childhood, this imprinting has long-lasting effects on the immune responses to subsequent infections and vaccinations. Different vaccine candidates and regimens have been proposed and used to combat the influenza disease symptoms. Thus animal models are used to investigate influenza pathogenesis and vaccination. Therefore, this review covers in depth the influenza virus-life cycle, vaccine candidates, and animals models, all of which are necessary in the development of a broadly-protective influenza vaccine.

2.2 Influenza History in the Human Population

Influenza virus induces a respiratory disease with a broad host range that causes significant morbidity and mortality in humans. The characteristic symptoms of the disease (fever, cough, chills, fatigue) allowed for the classification of influenza outbreaks before the virus' first isolation in 1933 (Potter, 2001; Wozniak-Kosek et al., 2014). Influenza pandemics were recorded throughout human history as early as 1175 AD (Creighton, 1819; Hirsch, 1883), and the 1918 pandemic of H1N1 influenza placed an especially extensive toll on global health. The 1918 pandemic had a conservative estimate of global mortality of 50 million individuals. When accounting for factors such as missing records, misdiagnosis, and location, the count may be as high as 100 million (Johnson & Mueller, 2002). After the pandemic, the H1N1 influenza virus remained prevalent in the population until 1957. In that year, an avian-origin H2N2 pandemic influenza virus replaced the seasonally circulating H1N1 influenza virus, leading to an estimated 1.1 million excess global deaths (Potter, 2001; Reneer & Ross, 2019; Viboud et al., 2016). Nine years later, another avian-origin H3N2 influenza virus led to the subsequent pandemic in 1968, which accumulated between 1 to 4 million global deaths as well, and some postulate the severity of this pandemic was mitigated due to the population having pre-existing antibodies to the neuraminidase component. (Honigsbaum, 2020; Kilbourne, 2006). The last recorded influenza pandemic was in 2009. The pandemic virus arose from a reassortment event between swine and avian influenza viruses, replicated and transmitted efficiently in human hosts (Garten et al., 2009; G. J. Smith et al., 2009).

The pandemics are associated with zoonotic transmission of influenza viruses from animal reservoirs, such as avian or swine, to the human population. This species transmission is possible due to the similarity of the influenza virus receptors for infection. Human- or swine- isolated influenza viruses bind to N-acetylneurameric acids attached to galactose by an α -2,6 linkage (SA α -2,6Gal). In contrast, avian-isolated influenza viruses bind at a higher strength and rate to the α -2,3 linkage (SA α -2,3Gal). In avian species, the influenza virus infections are localized within the SA α -2,3Gal lined gastrointestinal tract. In mammalian hosts, influenza viruses are respiratory pathogens. The human upper respiratory tract contains a higher

prevalence of SA α -2,6Gal expressing cells, and the lower respiratory tract SA α -2,3Gal. However, this species specificity between the receptors is not absolute since the host epithelium cells express both linkages. Furthermore, the receptor-binding site on the HA that recognizes and binds to the sialic acid can have one or two amino acid mutations that allow for recognition of the other moiety. Thus, leading to the zoonotic transmission observed with the avian-origin 1918, 1957, and 1968 pandemics, and swine origin 2009 pandemic. Therefore, zoonotic transmission of influenza from animal reservoirs remains a consistent possibility.

During periods devoid of pandemics, the influenza virus remains endemic throughout the global population. Two types of influenza viruses (Type A and Type B) circulate in a seasonal pattern (Moriyama et al., 2020). Initial exposure to influenza occurs during childhood; at six to nine years old, 80% of children were seropositive to H₃N₂ (F. Liu et al., 2017). Both types of influenza cause morbidity and mortality annually. Currently, public health agencies attribute influenza virus infection to nearly 500,000 annual global deaths (Paget et al., 2019).

2.3 Consequences of Influenza Pre-Immunity

The first influenza strain that infects a human or animal is the imprinting virus for that individual (Francis, McNeil, et al., 2019; Gostic et al., 2016). This initial strain biases the immune memory response to subsequent infections in a phenomenon described as “original antigenic sin” or “immune imprinting” (Arevalo et al., 2020; Gostic et al., 2016; Henry et al., 2018; Vatti et al., 2017). The premise is that when mounting a secondary response to a closely related antigen, instead of creating a wholly new and distinct response, the body recalls memory B-cells that have antibodies that recognize the first antigen (Vatti et al., 2017). This quick recall allows for more robust and faster antibody response, but it may not be as effective as creating a custom response for the second infecting virus. The imprinting strain is associated with the first influenza virus infection. Correlations between the imprinting strain and age of birth result in natural serological groups. In human cohorts, these correlations are due to differences in the circulating influenza

viral subtypes and strains at the time of infection and the individual's age of first exposure (Gostic et al., 2016).

The immune responses of differentially imprinted age groups can be compared to uncover the long-term biases due to differences in pre-immunity. Children from 1957 to 1968 were imprinted with circulating H₂N₂ viruses, whereas children born between 1968 and 1977 were likely imprinted with H₃N₂ subtypes. Furthermore, even within the earlier group of children from 1957 and 1968, the children exposed to pandemic H₂N₂ strains had differential neutralization responses to H₂N₂ viruses compared to children exposed to the late seasonal H₂N₂ strains (Matsuzawa et al., 2019). Hence, antigenic drift contributes to imprinting biases. On a broader scale, the imprinting HA-phylogenetic group (group 1 vs. group 2) is associated with susceptibility to future pandemics (Centers for Disease & Prevention, 2009; Gostic et al., 2016; Novel Swine-Origin Influenza et al., 2009; Simonsen et al., 2004; Skountzou et al., 2010). Immunological imprinting has also been observed with the NA. Individual that were potentially imprinting with H₂N₂ or H₃N₂ due to their year of birth had lower N₁-specific antibodies than individuals born after 1977 (Y. A. Desheva et al., 2015).

Although imprinting was initially characterized by serological results, the basis of this phenomenon is cellular, with the initial infection driving the production of long-lasting virus-specific B- and T-memory cells that bias the immune response to subsequent viruses (Francis, King, et al., 2019). After this initial infection, pre-existing immunity is the culmination of the first and all following exposures and can also be referred to as an individual's entire influenza history (Francis, McNeil, et al., 2019). A pre-immune individual is one with any immune memory to influenza. Using pre-immune models to determine the dangers of zoonotic transmission, especially from swine-origin, is particularly beneficial (Houser et al., 2013; F. Liu et al., 2017). During the H1N1 2009 influenza virus pandemic, the different priming patterns in the population contributed to an unprecedented age-biased distribution in human morbidity (F. Liu et al., 2018). Altogether, these factors highlight the necessity for unraveling the impact of imprinting and pre-immunity on subsequent infection and vaccination.

2.4 Influenza Virion Structure and Morphology

The *Orthomyxoviridae* family of viruses is characterized by its negative-sense, single-stranded segmented RNA genomes, and it consists of the following genera: *Thogotovirus*, *Isavirus*, *Alphainfluenzavirus*, *Betainfluenzavirus*, *Deltainfluenzavirus*, and *Gammainfluenzavirus*. The last four genera correspond to the four types of isolated and identified influenza viruses, Type A influenza, Type B influenza, Type D influenza, and Type C influenza, respectively. Of the four, Types A, B, and C have been documented to infect humans, with Type A previously causing pandemics, Type B remaining endemic in the population, and Type C rarely being isolated from a human host (Kumar, 2017). The influenza virus strains are uniquely named based upon host origin, location, and year of isolation. Type A influenza is further classified into subtypes based upon the surface proteins of the virion. Together those surface protein, HA and NA, subtypes denote an overall viral subtype (e.g., H₁N₁ influenza; H₃N₂ influenza) (Tong et al., 2012).

The envelope of Type A influenza viruses is a lipid membrane derived from the host cell. Influenza viruses are pleomorphic, with the morphology of the virion ranging from spherical with a diameter of 100 nm to filamentous particles as long as 300nm depending on the growth conditions of the virus (Dadonaite et al., 2016; Harris et al., 2006; Hutchinson et al., 2014). The HA, NA, and M₂ ion channel proteins protrude from the surface of the virion. The HA and NA are the majority of the surface proteins in a ratio of 4 HA:1 NA protein (R. Du et al., 2019). The NA proteins form clusters on the surface of the envelope around the HA proteins, leading to some areas of the viral envelope devoid of NA (Harris et al., 2006). The M₁ integral membrane protein is located just beneath the envelope providing structure to the virion, inhibiting the viral polymerase, and assisting genome segment packaging within the virion during budding (M. Itoh & Hotta, 1997). The viral components inside the envelope are encapsulated with the viral ribonucleoprotein complex (vRNP), which contains the RNA genome segments, the polymerase basic 1 (PB₁), and polymerase basic 2 (PB₂) polymerase proteins, the polymerase acid (PA), and the nucle-

oprotein (NP). The nuclear export protein and nonstructural protein (NEP/NS₂) are present within the virion, but the function has yet to be elucidated.

2.5 Influenza Virus Genome and Antigenic Shift and Drift

Type A influenza viruses contain eight RNA segments that encode up to eleven different proteins. The RNA segments are numbered based upon the length. In the order from longest to shortest, the RNA segments are 1. PB₂, 2. PB₁, PB₁-F₂, PB₁-N₄₀, and PB₁-F₂, 3. PA, PA-X, PA-N₁₅₅, and PA-N₁₈₂, 4. HA, 5. NP, 6. NA, 7. M₁, M₂, and M₄₂, and 8. NS₁, NEP/NS₂, and NS₃ (Hao et al., 2020; Jagger et al., 2012; Muramoto et al., 2013; Selman et al., 2012; Wise et al., 2009; Wise et al., 2012). The influenza viruses utilize frameshifted start sites or spliced mRNA to encode different proteins, such as with the M₂ gene within the M₁ RNA segment and the NEP/NS₂ proteins within the NS₁ RNA segment (Garaigorta & Ortín, 2007; Valcarcel et al., 1991). The PB₁-F₂ protein originated from an alternate open reading frame in the PB₁ RNA segment. The PB₁-F₂ and the other nonstructural proteins are accessory proteins associated with virulence and are not essential for some influenza A virus replication (Alymova et al., 2018).

For Type A influenza, the HA and NA molecules are subdivided into different serotypes depending on their ability to react with polyclonal antisera raised against a specific HA type or NA type (R. Yoshida et al., 2009). Currently, there are eleven distinct NA subtypes, with two previously implicated in causing pandemics and seasonal circulation in humans (N₁, N₂). Other NA subtypes (N₃, N₆, N₇, N₈, and N₉) have been isolated from human infections from zoonotic influenza viruses that were short-lived in the population (European Food Safety et al., 2021; Wohlbold & Krammer, 2014). Type B influenza also has different HA subtypes, but they are divided into two lineages: Yamagata-like and Victoria-like. Real-time reverse-transcription polymerase chain reaction (PCR) methods quickly distinguish between Type A and Type B influenza and, with optimization, can distinguish between H₃N₂ and H₁N₁ influenza (Kaul et al., 2010; Wozniak-Kosek et al., 2014).

The influenza genetic segments undergo independent evolution with the RNA-dependent RNA polymerase, which does not have proofreading capabilities (Boivin et al., 2010). The mutation rate is

estimated to be 1.8×10^{-6} substitutions per nucleotide per strand copied (s/n/r) for H₁N₁ and 2.5×10^{-4} s/n/r for H₃N₂ (Pauly et al., 2017). These mutation rates indicate an average of 2-3 mutations for every replicated genome. Although the mutation rate of the influenza polymerase does not change across genome segments, the evolutionary dynamics of the segments differ (Joseph et al., 2015). The proteins have different amino acid mutation rates over time (J. M. Chen et al., 2009; Joseph et al., 2015; Raghwan et al., 2017; Worobey et al., 2014b; Zhuang et al., 2019). The divergence between protein sequences are commonly quantified by estimating the time to the most recent common ancestor (TMRCA) (Zhou & Teo, 2016). Specifically, for the H₃N₂ viruses, the HA gene has the quickest turnover rate (1.90 years TMRCA), followed by the NA gene segment (2.4 years) and then the internal genes, with the M₁ gene having a TMRCA of around seven years (Raghwan et al., 2017). These differences in TMRCA indicate that the phylogeny of the HA, followed by the NA, has more branching and divergence, indicating strong selective pressure.

Combining the high mutation rate of the influenza virus polymerase and the strong selective pressures of the host's immune system, non-silent mutations on the surface glycoproteins become fixed over time. These mutations occur in antigenic sites on both the HA and NA, which are recognized by neutralizing antibodies and allows the virus to not be detected by antibodies in a previously immune host (Air et al., 1985; Caton et al., 1982b; Colman et al., 1983; D. C. Jackson & Webster, 1982; Wiley et al., 1981). This mutational change over time leads to *antigenic drift* of the virus. Antigenically drifted viruses evade the immune system, replicate, and cause disease in what were previously immunologically immune individuals.

In addition to antigenic drift, reassortment of the segments are possible during replication. Reassortment between different types of influenza (Type A, B, C, or D) has not been reported, which further supports the evolutionary distinction between the genera. During co-infection of two or more strains of influenza, the progeny virion may contain a mixture of the two parental virus segments. When the HA and/or NA gene segments are reassorted, this leads to *antigenic shifts*. Within subtypes, there can be distinct shifts in antigenicity, such as with the seasonal H₁N₁, which circulated in humans until the emergence of the swine-origin 2009 pandemic H₁N₁. The internal genes can also undergo reassortment

and may contribute to increased fitness or transmissibility between hosts. These shifts are unprecedented, originate from reassortment with avian, human, or swine-origin viruses, and are often met with no neutralizing antibodies in the host population. Antigenic shifts can also occur from direct zoonotic transmission from an animal host into the human population (Grebe et al., 2008). The lack of immunological memory of these antigens increases the virus' pandemic potential.

2.6 Neuraminidase Structure and Function

The NA is a type II membrane-anchored homo-tetramer glycoprotein. The overall structure has a globular head (residues: 76-470) distal from the membrane attached to a thin stalk portion (residues: 36-75). Near the surface of the virion, the stalk meets with the apical transport and lipid raft association region (residues: 11-33) and transmembrane domain (residues: 7-27), and lastly, the intra-virion region (residues: 1-6) (Laver & Valentine, 1969; UniProt, 2021). (Amino acid residue locations are in reference to A/Puerto Rico/8/1934 H1N1 neuraminidase. UniProtKB accession number: P03468). The protein is about 470 or 450 amino acids in length, depending upon the subtype and host-lineage (Air, 2012). NA proteins isolated for avian hosts may have a deletion of between 20 to 30 amino acids in the stalk region of the protein as a compensatory deletion for poultry adaptation from aquatic avian hosts (Blumenkrantz et al., 2013). The length of the stalk has been associated with infectivity and transmission of the virus and immunogenicity of the protein (Bi et al., 2016; Blumenkrantz et al., 2013; S. Chen et al., 2020; Munier et al., 2010; S. Park et al., 2017; Stech et al., 2015).

Of the protein, the head portion is highly immunogenic and contains the enzymatic cleavage site for sialic acids. X-ray crystallography revealed the three-dimensional structure of the NA head protomer as a six-bladed propeller structure; the other regions (stem, transmembrane domain, and cytoplasmic tail) have not yet been successfully crystallized (Bossart-Whitaker et al., 1993). At least eight disulfide bonds hold together the homo-tetramer conformation in addition to internal protein interactions (Selimova et al., 1982; Shtyrya et al., 2009; Ward et al., 1983). Calcium ions are also necessary for enzymatic activity and maintaining thermostability with a minimum of four Ca^{2+} binding sites for some NA subtypes

(Baker & Gandhi, 1976; Brett & Johansson, 2006; Giurgea et al., 2021; B. E. Johansson & Brett, 2003; H. Wang et al., 2019). The enzymatic cleavage site is highly conserved and is the target of antiviral drugs and monoclonal antibody development. There are four cleavage sites per NA tetramer. The SA α -2,3Gal are cleaved more efficiently than SA α -2,6Gal for all NA subtypes; however, human isolated NAs can cleave SA α -2,6Gal more efficiently than SA α -2,3Gal (W. Du et al., 2018). The enzymatic activity needs a slightly acidic environment to function (5.5-6 pH), with some NAs able to function in pHs as low as 4-5 pH (Takahashi & Suzuki, 2015).

Conversely the head of some NA subtypes also contains a SA α -2,3Gal-preferential sialic acid-binding site (reviewed in W. Du, de Vries, et al., 2020) (W. Du et al., 2019; Varghese et al., 1997). This binding site is not the same as the HA binding site (X. Sun et al., 2014). This binding site is thought to help shuttle sialic acids into the cleavage active site, especially since it may be overlapping or near the cleavage site (Dai et al., 2017). Although the exact mechanism behind the need to the sialic acid binding site is not known, but mutations in the binding site led to compensatory mutations in the HA protein. Avian isolated NAs have highly conserved binding sites but the human isolated sites are less active indicating a potential adaptation from avian influenza to human influenza (W. Du, Wolfert, et al., 2020).

The surface of the NA may be highly glycosylated depending on the specific amino acid sequence, the host, and the evolutionary lineage of the virus. For the N1 and N2 proteins, there are three and four conserved N-linked glycosylation sites, respectively. Glycosylation, protein folding, and translocation are mediated by host enzymes and cell mechanisms when the protein enters the lumen of the endoplasmic reticulum (ER) (N. Wang et al., 2008). After which, the glycans assist with the incorporation of the NA into new virions and viral production (Ostbye et al., 2020). In terms of evading the host immune response, the addition of a glycosylation site increases the ability of the virus to avoid the immune system sterically hindering antibodies from recognizing immunogenic antigenic epitopes and also making the protein inaccessible to antiviral drugs, in a mechanism termed antigenic camouflage or glycan shielding (Kendal, 1987; Seitz et al., 2020). Another mechanism includes allowing the immune system to recognize the glycans as “self,” leading to no elicitation of an immune response (Kendal, 1987). The addition of

N-glycans decreases the overall stability of the protein for the N₁ but has not been found to affect the N₂ stability (Ostbye et al., 2020). For sites not protected by glycans, antigenic drift in the NA contributes to evasion from the host immune system. Therefore, the potential for a vaccine that elicits cross-reactive antibodies to neuraminidase is of great interest.

2.7 Neuraminidase Genetic Diversity

The NA diversity rivals that of the HA. The NAs are characterized into two nucleic acid-based phylogenetic groups. Group 1: N₁, N₄, N₅, and N₈; Group 2: N₂, N₃, N₆, N₇; Bat NA-like Group: N₁₀ and N₁₁; and Type B influenza NA (Air, 2012; Krammer et al., 2018; Q. Li et al., 2012). The subtypes are identified through amino acid sequence and antibody reactivity with the NA-inhibition (NAI or NI) assay. Recent computational advances utilize the DNA sequences and physical and structural properties of the NA protein to determine subtypes (Humayun et al., 2021). Further, the subtypes can be subdivided into genetically distinct lineages (S. Liu et al., 2009; J. Xu et al., 2012; Zhuang et al., 2019).

The N₁ subtype can be subdivided into three main lineages (N_{1.1}, N_{1.2}, and N_{1.3}), which can be subdivided even further if necessary (Fig. 2.1) (Zhuang et al., 2019). The N_{1.1} avian lineage is comprised of the avian-isolated HXN₁ viral subtypes, the highly-pathogenic avian H₅N₁ influenza viruses, the Eurasian swine-isolated HXN₁ viruses, and human-isolated H₁N₁pdm09 viruses. The other two lineages are more restricted in host isolation. The N_{1.2} human lineage is comprised of human-isolated seasonal H₁N₁ prior to the 2009 pandemic. Whereas, the N_{1.3} classical swine lineage is comprised of mostly North American swine-isolated H₁N₁ influenza viruses. All three of the main lineages contain sub-lineages specific to geography and host with a high estimate of 64 sub-lineages (when using nucleotide sequences) for the N₁ subtype (Shi et al., 2010). The genetic diversity has also translated to antigenically distinct groups between divergent N₁ NAs (Gao et al., 2019).

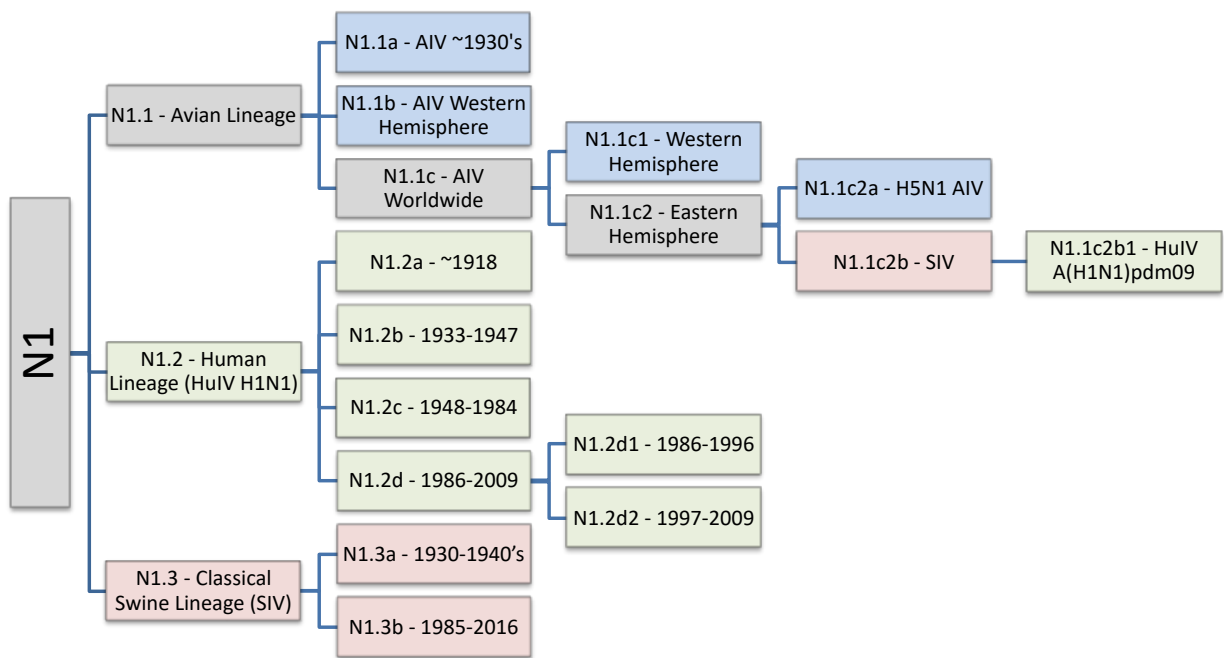


Figure 2.1: The clades of the N1 NA genetic lineages were determined through previous phylogenetic analysis (J. M. Chen et al., 2007; Fanning et al., 2000; S. Liu et al., 2009; Schon et al., 2021; Zhuang et al., 2019). Clades are color coded based upon host viruses are isolated from: grey: multiple host species; blue: avian host species; red: swine host species; green: human host species. AIV: Avian influenza virus; SIV: Swine influenza virus; HuIV: Human influenza virus

2.8 Influenza Entry and Replication Cycle

Before, during and after host cell infection, the neuraminidase contributes to motility, viral attachment, and release of the virions (reviewed in Dou et al., 2018). Upon entering the host's respiratory system, the virion encounters mucins lining upper respiratory tract. The NA cleaves the mucin sialic acids facilitating the movement of the virion until it comes in contact with epithelial cells surfaces that are expressing the appropriate receptors for entry (Cohen et al., 2013; Vahey & Fletcher, 2019; Yang et al., 2014). The NA activity, although dependent on environmental pH, is still functional at neutral pHs. Currently, it is unclear if the microenvironment of the lung is acidic enough for maximum NA cleavage or if the reduced efficiency at neutral pH is permissive for replication. During virus entry, the HA binds cell surface borne sialic acids; if that SA is bound to an entry receptor, entry will be initiated. If the SA is not bound to a receptor or is a decoy SA, the NA will cleave the sialic acid and releasing the HA to bind to other SAs. This mechanism allows the virion to "walk" to a neighboring receptor (reviewed in de Vries et al., 2020) (Hamming et al., 2020). Therefore, the SA that the HA binds to needs to also be recognized by the NA in order to maintain SA-binding-cleaving balance (de Vries et al., 2020; R. Du et al., 2019; W. Du, Wolfert, et al., 2020).

After the HA has bound to an entry receptor, the host cell internalizes the virion primarily through clathrin-coated pits, followed by less common clathrin- and caveolin-independent mechanisms, such as macropinocytosis (de Vries et al., 2011; Rust et al., 2004). Upon entry the low pH in the endosomal compartment triggers a structural change in the HA protein revealing the fusion peptide. The peptide is inserted into the endosomal membrane initiating the fusion with the virion envelope. The M₂ protein pumps hydrogen ions from the endosome into the virion which disrupts and dissociates the vRNP from the M₁ protein. The vRNP travels into the host cell through the pore and is actively shuttled to the nucleus.

The influenza virus replicates using host 5' capped primers and the RNA polymerases in the vRNP. Initially, mRNA is produced to create the proteins needed for the next generation of virions. After

enough viral protein has been created, the production is switched to viral RNA segments for packaging. Preferential temporal gene transcription of the different segments has not been observed for influenza (Kawakami et al., 2011; Vester et al., 2010); usually viruses do not produce the surface proteins until later in the cycle to limit pre-mature budding. However post-transcriptional modulation may contribute to HA and NA production. Dependent on the NS₁ protein levels, the NS₁ may associate with the 5' untranslated region of the HA and NA transcripts. The mRNA is then associated with either the ER-trafficking machinery or ER ribosomes since the surface proteins' transmembrane domains act as an ER targeting sequence (Nordholm et al., 2017), but the mechanism has not been fully elucidated (Dou et al., 2018).

Once the NA protein is associated with the Sec61 protein-conducting channel the transmembrane domain becomes associated with the ER membrane, and the NA inverts during translocation with the C-terminus inside the ER lumen (Bos et al., 1984; Hessa et al., 2007; Mandon et al., 2013). Inside the lumen the NA protein becomes glycosylated with N-linked glycans which are associated with proper folding by recruiting calnexin and calreticulin chaperones and an oxidoreductase which assists with the disulfide bond formation (Daniels et al., 2003; N. Wang et al., 2008). For the N₁ monomers each contain eight disulfide bonds, and the N₂ subtype contains nine bonds. The NA dimers are co-translationally formed first, and then the dimers are oligomerized to form the tetramer. The formation of the tetramer requires at least two more additional disulfide bonds. It is currently not clear if the NA protein actively cleaves SA inside of the Golgi during processing.

Starting from the beginning of protein synthesis the NA protein is present on the cell surface as soon as 30 minutes and reaches a peak content at 1 hour (Hogue & Nayak, 1992). The budding virion is initiated at lipid rafts in the plasma membrane. The NA localizes to the lipid raft locations due to the C-terminus of the transmembrane domain (Barman et al., 2004). The vRNPs are transported to the apical membrane containing the lipid raft. The mechanism of budding is not fully understood, but budding has been observed with expression of only the NA protein (B. J. Chen et al., 2007; J. C. Lai et al., 2010). Once budding is complete the NA cleaves the SA attaching the nascent virion's HA to the parent cell, releasing it to infect a new susceptible cell.

Successful replication can only occur with the cleavage of HAo into the functional disulfide-linked HA₁-HA₂ polymer. In human influenza viruses the single-basic cleavage site is recognized by human type II transmembrane serine proteases such as TMPRSS2 and human airway trypsin-like protease (Beaulieu et al., 2013; Bottcher-Friebertshauser et al., 2011). The serine proteases are present throughout infection and cleavage may occur in the extracellular space, within the host after viral uptake, during protein processing in the Golgi, and during budding of the new virion (Beaulieu et al., 2013). This need for specific proteases restricts the pathogenesis range to only hosts and tissues expressing these specific proteases. Highly-pathogenic avian influenza H₅ and H₇ HAs contain a multibasic cleavage site allowing it to be cleaved by intracellular ubiquitous subtilisin-type proteases which may lead to increased viral tissue tropism and pathogenicity (Sugitan et al., 2012).

The cleavage of the HAo may also be influenced by the NA. NA-dependent cleavage has been observed in an A/WSN/33 H1N1 strain derived from repeated passages of A/WS/33 in mice (closely related to 1918 H1N1 pandemic strain), an H₇N6 avian influenza virus, and an H₃N1 avian influenza virus (Chaipan et al., 2009; Kwon et al., 2019; Schon et al., 2021; Zambon, 2001). With the absence of a glycosylation at position 146 (N1 numbering) the NA binds to plasminogen leading to plasmin and the cleavage of the HAo (Goto & Kawaoka, 1998). This viral replication mechanism is not well studied but has emphasizes the importance of NA glycosylation and role during infection.

2.9 Neuraminidase-specific Immunobiology

During influenza infection both the innate and adaptive immune system are indispensable for controlling and clearing the viral infection (reviewed in X. Chen et al., 2018). The initial infection triggers the innate immune system with the release of cytokines and interferons and the recruitment of monocytes, neutrophils, blood borne dendritic cells, and natural killer cells. After dendritic cells present the viral antigens to naïve and memory T-cells; both CD4+ and CD8+ T-cells are activated and important for influenza virus clearance (D. M. Brown et al., 2012; Ho et al., 2011).

As early as 1972, the connection between NA-specific antibodies and decreased risk of infection was observed (Murphy et al., 1972). Inhibiting antibodies to the protein are created and reach peak NAI titer by day seven post onset of disease (Changsom et al., 2017). The NA specific antibody response is influenced by the age of the individual as well as the NA subtype that is eliciting the response (S. S. Wong et al., 2020). In the human challenge model, pre-existing NA inhibiting antibody titers correlated stronger with the decrease in viral shedding and symptom severity, compared to both the HA inhibiting antibody titer and the HA-stem binding antibody titer (Maier et al., 2020; Memoli et al., 2016; J. K. Park et al., 2018; Weiss et al., 2020). In addition to the direct action of the antibodies, the presence of these pre-existing antibodies may lead to differential gene expression in the peripheral blood leukocytes during infection (Walters et al., 2019).

The NA inhibition titers do not always correlate with HAI titers or microneutralization (MN) titers within the same individual (Y. Desheva et al., 2020; Y. A. Desheva et al., 2015). Polyclonal sera isolated from humans indicate that the NAI antibodies were broader inhibiting than the HAI and MN titer were (Changsom et al., 2017). Further, it was determined that only the serum NAI titers significantly predicted influenza immunity to natural infection when comparing the HAI and NAI titers of both the serum and nasal secretions (Couch et al., 2013).

The main mechanism of action for antibodies targeting the NA is not fully understood (Krammer et al., 2018). The most well studied mechanism is by stopping the virion from egress (Gilchuk et al., 2019). Many of the antibodies target the conserved active site of the protein, or sterically hinder accessibility to the sialic acid for cleavage (Stadlbauer et al., 2019). Further, the antibodies may be used for antibody-dependent cell-mediated cytotoxicity (ADCC) and complement-dependent cytotoxicity (Krammer & Palese, 2015). However, during infection with either H₁N₁ or H₃N₂ individual's antibody-dependent cellular cytotoxicity (ADCC) antibodies were boosted to the both N₁ and N₂ proteins for each infection. Whereas for the H₁N₁ infection, ADCC responses were boosted to also H₁, H₃ and H₇ proteins, for the H₃N₂ infection, boosting was only observed to the NAs (Valkenburg et al., 2019).

2.IO At-risk Populations

Influenza is able to infect the majority of the population, but the disease severity of the virus is not uniformly distributed across populations (Centers for Disease & Prevention, 2021b). Individuals who are five years or younger or are sixty-five years and greater are at increased risk of additional complications from influenza infection (Czaja et al., 2019; Sekiya et al., 2021). Sex has not been identified as a determining factor, but pregnant and postpartum women are at increased risk. Non-Hispanic Black, Hispanic/Latino, and American Indian/Alaska Native racial and ethnic groups have been identified to have increased risk of hospitalization from influenza but have been found to also have lower rates of vaccination (Quinn et al., 2011). Therefore, it cannot be concluded that race or ethnicity is causing the increased risk compared to vaccination rates or socio-economic class (Hadler et al., 2016). In addition, previous medical conditions contribute to the risk associated with influenza infection (Collins et al., 2020). Medical conditions such as asthma, chronic lung disease, blood disorders, obesity ($BMI > 40$), diabetes, heart disease, weakened immune systems, and metabolic disorders, all increase the risk of complications from influenza infection.

2.II Influenza Vaccine History

The current preventative method used to combat influenza is vaccination. The annual vaccine is recommended for all individuals greater than six months of age, especially if the person is within an at-risk population (Uyeki, 2020). The most common vaccine is an intramuscular split-inactivated egg-based influenza vaccine composed of four viral strains, an H₃N₂, an H₁N₁, and two type Bs, one each from the Yamagata and Victoria lineages. For the seasons between 2014 and 2019, the adjusted overall vaccine effectiveness (VE) in the United States ranged between 19% and 48% (Flannery et al., 2019; Flannery et al., 2020; M. L. Jackson et al., 2017; Rolfes et al., 2019; Zimmerman et al., 2016). The VE varies between subtypes and year to year due to numerous viral (antigenic drift/shift), vaccine (egg-adaptive changes, immunogenicity), and host (age, immune-status, pre-immunity) factors. To address the viral contributions, the World Health Organization (WHO) reviews data from its global influenza surveillance network to

identify circulating strains, heavily weighting ferret serological cross-reactivity data to determine antigenic drifts. Vaccine manufacturers are then provided a list of recommended vaccine strains for that particular season for either the Northern or Southern hemisphere. A vaccine is considered to be an effective candidate and protective if the elicited serum titer of antibodies that inhibit the hemagglutination activity of the HA protein is greater than 1:40.

Methods to increase the host response to vaccination and VE include different vaccine compositions, especially in adults older than 65 years of age due to their decreased immune response to vaccination (Wilkinson et al., 2017). The inclusion of adjuvants, varying the amount of antigen, using live-attenuated viral vaccines, and varying the route of administration are all methods used to increase VE.

2.12 Influenza Vaccine Platforms

Inactivated influenza vaccines are intramuscular shots and are the most common influenza vaccine available and readily elicit HA-inhibiting serum antibodies. The vaccines are produced by numerous companies and can be either egg- or mammalian cell-grown. The egg-grown vaccines are the most common, with one FDA licensed vaccine being produced in mammalian cell lines due in part to egg allergens. Flucelvax® Quadrivalent manufactured by Seqirus contains no egg allergens and may also lead to greater protection than egg-based vaccines due to the vaccine strain being grown in the same conditions as the circulating strain and not undergoing egg-adapted changes (Boikos et al., 2020; Rajaram et al., 2020; Raymond et al., 2016). The egg-based intramuscularly delivered vaccines are manufactured by Seqirus (Alfuria®), GSK (Fluarix™), ID Biomedical Corporation of Quebec (FluLaval™), Sanofi-Pasteur (Fluzone®; Fluzone® High-Dose). Standard-dose vaccines are composed of four inactivated influenza viruses, two Type A strains (H1N1 and H3N2 subtypes), and two Type B strains (B-Yamagata and B-Victoria lineages). The HA content of the inactivated viruses is measured, and then the inactivated viruses are combined to contain 15 ug HA of each virus within a 500 ul volume. For elderly individuals (65 years and older), the high-dose trivalent vaccine was initially formulated to contain 60 ug of each HA component (H1, H3, and

one Type B HA). In the 2020-2021 and following seasons, the high-dose trivalent vaccine was replaced with a quadrivalent vaccine that included the other Type B lineages.

Adjuvanted inactivated influenza vaccines, Fluard® and Fluard® Quadrivalent by Seqirus, are also available for elderly individuals in either trivalent or quadrivalent formulations, respectively. The vaccines are egg-based split inactivated vaccines with 15 µg of standardized HA content, but they are formulated with an MF59® (Novartis) adjuvant to stimulate a senescent immune system. The addition of the MF59® adjuvant has not been found to have adverse effects within the elderly population (Yoo et al., 2018).

Live attenuated influenza vaccines (LAIV) contain quadrivalent formulations that are administered as a nasal spray. They are approved for non-pregnant individuals between the ages of two and forty-nine years. The manufacturer, MedImmune, has acknowledged that the mechanism of action for FluMist® is not fully understood. Unlike split inactivated vaccines, live-attenuated vaccines do not elicit high HA-inhibiting serum antibodies. Instead, the localized mucosal responses in the respiratory pathway (nasal cavity) are activated along with cell-mediated immunity. The live-attenuated vaccines rely on the weakened virus actively infecting host cells which then elicit a directed immune response to the virus. This immune response more closely mimics a wild-type infection, which may lead to a more protective adaptive response later.

2.13 Adjuvants

Adjuvants are compounds that stimulate and enhance the immune response to an antigen (Di Pasquale et al., 2015). Vaccines that activate the innate immune system well enough on their own do not need the addition of an adjuvant, such as live attenuated influenza vaccines. One seasonal split inactivated influenza vaccine has been supplemented with an MF59® adjuvant (Fluard® vaccines). Other adjuvants have been approved for inclusion in influenza pandemic vaccine formulations, including AS03, thermo-reversible oil-in-water, and MF59®. The adjuvant is able to increase vaccine efficacy in children and is safe to use in seasonal human vaccines. The mechanism of action for MF59® includes increased recruitment and activation of antigen-presenting cells (APCs) and antigen uptake. The adjuvant elicits a strong T and B

cell response which leads to an increase in antibody breadth. The B cell repertoire with the adjuvant is spread across to include the NA protein instead of focusing the immune response on only the HA protein (O'Hagan et al., 2011).

AddavaxTM (InvivoGen) is approved for preclinical grade adjuvant for research use only. Influenza vaccine studies have used AddavaxTM in place of MF59® for animal studies, including mice and ferrets (Reneer et al., 2020; J. Wang et al., 2018). The adjuvant formulation, a squalene-based oil-in-water nanoemulsion, is similar to MF59®. Which in turn, leads to similar immune activation eliciting a balanced Th1 and Th2 immune response (Calabro et al., 2013).

2.14 Neuraminidase as a Vaccine Antigen

The NA has been associated as a potential vaccine candidate as early as 1972, and then in 1974 when it was tested in an inactivated whole virus vaccine with a mismatched HA protein (Couch et al., 1974; Murphy et al., 1972). Since then, the NA has been included in vaccines as an afterthought. Split-inactivated whole virus vaccines do not provide the NA antigen in an accessible format for a cellular adaptive immune response. This in turn can lead to low or non-responders of NAI activity (Ito et al., 2020). There are different factors that contribute to this, such as the age of the recipient, the structural integrity of the NA protein during the formulation process, the immunodominance of the other proteins, and the lack of quantification, standardization, and regulation of the NA quantity in the vaccine preparations (Shultz et al., 2020; Sultana et al., 2014). When NAI antibodies are measured the kinetics are similar to the HAI antibodies in their longevity after vaccination in healthy adults (Petrie et al., 2015). Further, when supplemented into split-inactivated vaccines, the immune response was broadened to encompass more strains potentially due to the decrease in the immunodominance of the HA (B. Johansson, 1998).

The other vaccine formats provide more antibody response to the NA. The inclusion of adjuvants for the elderly population has been shown to increase the breadth of the antibody response to include B cell responses to the NA protein in addition to the HA protein. Adjuvanted vaccines are only used for elderly individuals or in pandemic vaccine formulations for emergency use. The LAIVs do not have the issue

of protein degradation and stability like the split-inactivated vaccines. Individuals that were immunized with LAIV vaccines had an increase in inhibitory NA antibodies (Y. Desheva et al., 2020).

Inclusion of the NA into the development of influenza vaccines will do more than add another strain-specific antigen for antibodies to target. Broadly binding anti-NA monoclonal antibodies have been isolated from human subjects and were shown to be protective in mice (Stadlbauer et al., 2019). The polyclonal sera for the N1 subtype have been found to be cross-reactive, with antibodies inhibiting both the H1N1 2009 pandemic and the H5N1 highly pathogenic NAs (Y. Desheva et al., 2020; Y. A. Desheva et al., 2015; Krammer et al., 2018; Pei et al., 2015; Wan et al., 2013). In addition, it has been found that across a range of different concentrations NA concentrations used for vaccination, the NA vaccines did not inhibit infection, however there was a limit on the viral load in the lung tissue of mice (B. E. Johansson et al., 1989). This permissive infection vaccine allows the body to mitigate the symptoms and still mount an immune response which can contribute to boosting the response during reinfection.

The lack of reagents for working with the NA protein is a major hurdle that is beginning to be overcome. The amount of NA in each vaccine dose varies widely based upon the vaccine platform, the manufacturer, and the lot (Gerentes et al., 1999). In 2019, an experimental high-throughput technique for quantifying the NA content in a variety of vaccine platforms was developed (Byrne-Nash et al., 2019). Ideally, with the increase in tools, and more calls for its inclusion the NA, especially the N1 which was shown to be cross-reactive, will be more thoughtfully designed into vaccine production (Eichelberger & Monto, 2019; Eichelberger et al., 2018; Eichelberger & Wan, 2015; Giurgea et al., 2020; Krammer et al., 2018).

2.15 COBRA Methodology

Of the candidates proposed in the race to design broadly-neutralizing influenza vaccines that remain effective longer against circulating viruses longer than the current standard-of-care vaccines, the computationally optimized broadly reactive antigen (COBRA) methodology was conceptualized in 2011 (Giles & Ross, 2011a). This approach can be utilized for protein antigens that showcase a large variability in

their antigenic sites and amino acid sequences. For influenza, the wild-type protein sequences for either HA or the NA protein are retrieved from the surveillance databases (NCBI Influenza Virus Resource or GISAID) (Bao et al., 2008; Elbe & Buckland-Merrett, 2017). After cleaning the sequences to trim the ends and remove sequences with ambiguities, only the unique sequences are moved forward to reduce the bias of over sampling (Machalaba et al., 2015). The unique sequences are then combined in multiple rounds of consensus layering to obtain a final HA or NA protein sequence that captures the genetic variability of the original wild-type input sequences.

The COBRA methodology has been shown to be effective in animal models with different subtypes of influenza. Specifically, antigens for the H₁, H₂, H₃, H₅ and H₇ HA proteins, and for the dengue virus envelope glycoprotein have been shown to be more broadly reactive than wild-type proteins (Allen et al., 2019; Allen, Ray, et al., 2018a; Carter et al., 2017; Carter et al., 2016a; Crevar et al., 2015; Fadlallah et al., 2020; Giles & Ross, 2011a; Reneer et al., 2020; Ross et al., 2019; Skarlupka et al., 2019; Skarlupka, Reneer, et al., 2020; Uno & Ross, 2020; T. M. Wong et al., 2017). Further these antigens elicited antibody responses in variety of animal models including: mice, ferrets, chickens, swine, and non-human primates. The mechanism of action of how COBRA antigens induce antibody breadth is not fully understood, but is thought to be a combination of structural stability, antigenic regions exhibiting epitopes that are partial matches for distinct viruses, and glycosylation (Y. Huang et al., 2020). Although, the COBRA methodology has only been used for the HA protein, the NA protein is also an ideal candidate for a COBRA construct and described further in this dissertation fruitful (Skarlupka et al., 2021).

2.16 Influenza Animal Models

Animal models are used to study influenza vaccination and infection. Mice, hamsters, guinea pigs, cotton rats, rats, ferrets, and non-human primates are used for human influenza research. Swine, chickens, guinea fowl, and horses have also been used to study non-human species-specific influenza. The mouse model is commonly used due to the plethora of genetic tools and the availability of reagents. In addition, pre-immunity can be established in the mouse model (Dong et al., 2018; Kreijtz et al., 2009; Kreijtz et al.,

2007; Min et al., 2010; Nachbagauer et al., 2017; Novel Swine-Origin Influenza et al., 2009; Schulman & Kilbourne, 1965; Yetter, Lehrer, et al., 1980). Within mice, pre-infection compared to vaccination elicited similar innate immunity and antibody responses. Sterilizing immunity was achieved in pre-immune animals that had reduced viral receptors and increased T-cell responses in the lungs (Dutta et al., 2016). Although less utilized than mice or ferrets, guinea pigs produce similar results (Nachbagauer et al., 2017; Steel et al., 2010). However, mice are not naturally susceptible to influenza infection, and the virus may need to be mouse-adapted before challenge (Matsuoka et al., 2009b). Ideally, work done in the mouse model, will be confirmed in other animal models that more closely match the human system, such as the ferret model.

2.16.1 Influenza Ferret Model

The gold standard for influenza vaccine research is the ferret animal model (Belser et al., 2011). Ferrets capture the physiological and immunological aspects of influenza vaccination infection. These include similar lung architecture, natural susceptibility to human influenza viruses, and similar antibody responses (Matsuoka et al., 2009a). Currently, there are models developed that capture infants (S. S. Huang et al., 2012), aged (Paquette et al., 2014), naïve, and pre-immune scenarios (Allen et al., 2019). During vaccine selection, experts consider only data generated from the naïve ferret model for the determination of recommended strains for currently administered human vaccines. However, the immune response in a naïve host, compared to a pre-immune individual, differs during subsequent vaccination and/or infection (Ellebedy et al., 2011; McLaren & Potter, 1974). Therefore, the use of naïve ferret sera for vaccine strain selection is potentially misrepresentative of the pre-immune human population that receives each season's influenza virus vaccines, contributing to the observed VE.

This initial infection primes the immune system and biases future immune responses to subsequent infections and vaccinations (Gostic et al., 2016; Hancock et al., 2009; Lessler et al., 2012; Miller et al., 2013; Monsalvo et al., 2011; Tesini et al., 2019; Worobey et al., 2014a). Due to the cost and resources of human clinical trials, there are numerous animal models designed to study this viral pathogen (Bouvier

& Lowen, 2010). The ferret model remains indispensable due to similarities in lung physiology (Enkirch & von Messling, 2015; Maher & DeStefano, 2004), anatomical distribution of sialylated glycan receptors (Jayaraman et al., 2012), and glycomic profile of ferret respiratory tissues (Jia et al., 2014; P. S. Ng et al., 2014). These animal models are commonly used to study viral characteristics, host immune responses, and vaccine/antiviral therapies. Therefore, animal models that mimic pre-existing human immunity to influenza viruses may better represent the human immune responses to infection and vaccination.

2.17 Pre-immunity on the Ferret Immune Response

The effects of imprinting and pre-immunity on subsequent humoral and cellular responses are still under investigation. During initial pre-immune ferret infection, there are increased nasal protein secretions compared to naïve ferrets during a heterologous challenge (McLaren & Potter, 1974). Characterization of the influenza virus infection during different stages of the infectious process, with and without prior specific immunity to influenza, has recently been reported (Leon et al., 2013). The differences in protection of a pre-immune animal compared to a naïve animal may be due to the recall of antibodies specific to shared epitopes that do not necessarily need to be neutralizing (Belongia et al., 2017). Infection induces T-cell responses to T-cell epitopes within the HA and other proteins, and even neuraminidase inhibiting antibodies that are not elicited by split-inactivated vaccines (Y. Q. Chen et al., 2018; Dutta et al., 2016). These responses may be either synergistic or antagonistic when paired with vaccination. For instance, vaccination may boost the non-neutralizing antibodies leading to decreased vaccine efficacy compared to a naïve animal.

This back-boosting, also described as an anamnestic response, has been observed in the human population (Carlock et al., 2019; deBruijn et al., 1997; McElhaney et al., 1993; Nunez et al., 2017) and has been recapitulated within the ferret model. This similarity makes it a useful tool for determining vaccine performance in a setting where back-boosting is present (Allen et al., 2019). Specifically, back-boosting was observed when imprinted with H1N1/Singapore/6/1986 followed by H1N1/California/07/2009 VLP vaccination. The breadth of HAI-specific antibody response was wider than just H1N1/Singapore/6/1986

alone and covered more viruses. The breadth increased to include viruses before and after the 1986 seasonal virus (Carter et al., 2017). The back-boosting observed after a VLP-vaccination was dependent on the recognition of memory B-cell and T-helper cell epitopes specific to the HA of the virus. This increase in the breadth was also observed after sequential infections with ELISA titers to total antibody binding (Nachbagauer et al., 2017). This back-boosting is what contributed to the difference in the naïve vs. pre-immune antigenic maps of different H₃N₂ viruses (Kosikova et al., 2018). The exact mechanism of back-boosting is not completely elucidated (Carlock et al., 2019).

Heterosubtypic protection between the Type A influenza strains suggest that cross-reactive cellular immune responses may be contributing to virus control (Hatta et al., 2018). Protective T-cell responses are elicited through recognition of cross-reactive epitopes (Gooch et al., 2019; Pulit-Penaloza et al., 2018). Cross-reactive memory B-cells can also be elicited post-imprinting (Webster, 1966). Characterization of the cellular and humoral responses, similar to the human-based study conducted by Ryan et al. (Ryan et al., 2018), with imprinted and sequentially infected ferrets is a priority to determine if cellular immune responses differ with H₁N₁ and H₃N₂ subtype infections (Ryan et al., 2018) or during H₃N₂ and H₅N₁ influenza virus co-infection (Cameron et al., 2008), or with seasonal vs. pandemic H₁N₁ influenza virus infections (S. S. Huang et al., 2011; Rowe et al., 2010).

As the reagents for the ferret animal model continue to expand, the opportunities to investigate different correlates of infection and/or protection magnify. Before this reagent development, research was limited to characterizing serum and nasal washes for neutralizing antibodies and measuring clinical signs after infection. Therefore, future studies can capture the cellular immune reactions of T-cell responses with IFN- γ ELISAs (Ochi et al., 2008), peripheral blood leukocyte tracking (Music et al., 2014), and ELISpots (DiPiazza et al., 2016; Gooch et al., 2019), as well as the humoral immunity (Cheng et al., 2009; Francis, McNeil, et al., 2019; Kirchenbaum et al., 2017; Upadhyay et al., 2018).

2.18 Conclusion

With the possibility of future pandemics due to zoonotic transmission and antigenic shifts the design of a longer-lasting broadly-reactive influenza vaccine is necessary. The NA surface protein of the virion is a great vaccine candidate given its important roles in viral replication, host and tissue tropism, and pathogenicity. NA inhibiting antibodies are protective in animal models and correlate with decreased influenza-like symptoms in humans. With innovation in vaccine development, such as the COBRA methodology, NA COBRA antigens can be designed to be tested in the mouse and ferret animal models, before being tested in human clinical trials. Therefore, N1 subtype which includes both endemic human H1N1 influenza virus and highly pathogenic H5N1 influenza virus is the highest priority antigen for COBRA design to protect the human population for both these and other influenza viruses.

CHAPTER 3

UNIVERSAL INFLUENZA VIRUS NEURAMINIDASE VACCINE ELICITS PROTECTIVE IMMUNE RESPONSES AGAINST HUMAN SEASONAL AND PRE-PANDEMIC STRAINS¹

¹Skarupka, A. L., Bebin-Blackwell, A. G., Sumner, S. F., & Ross, T. M. (2021). Universal influenza virus neuraminidase vaccine elicits protective immune responses against human seasonal and pre-pandemic strains. *J. Virol.* 2021 Aug 10;95(17):e0075921. doi: 10.1128/JVI.00759-21. Epub 2021 Aug 10. PMID: 34160258; PMCID: PMC8354223. Reprinted here with permission of the publisher.

3.1 Abstract

The hemagglutinin (HA) surface protein is the primary immune target for most influenza vaccines. The neuraminidase (NA) surface protein is often a secondary target for vaccine designs. In this study, computationally optimized broadly reactive antigen methodology was used to generate the Ni-I NA vaccine antigen that was designed to cross-react with avian, swine, and human influenza viruses of Ni NA subtype. The elicited antibodies bound to NA proteins derived from A/California/07/2009 (H1N1)pdm09, A/Brisbane/59/2007 (H1N1), A/Swine/North Carolina/154074/2015 (H1N1) and A/Viet Nam/1203/2004 (H5N1) influenza viruses, with NA-neutralizing activity against a broad panel of HXN1 influenza strains. Mice vaccinated with the Ni-I COBRA NA vaccine were protected from mortality and viral lung titers were lower when challenged with four different viral challenges: A/California/07/2009, A/Brisbane- /59/2007, A/Swine/North Carolina/154074/2015 and A/Viet Nam/1203/2004. Vaccinated mice had little to no weight loss against both homologous, but also cross-NA genetic clade challenges. Lung viral titers were lower compared to the mock vaccinated mice, and at times, equivalent to the homologous control. Thus, the Ni-I COBRA NA antigen has the potential to be a complimentary component in a multi-antigen universal influenza virus vaccine formulation that also contains HA antigens.

Importance The development and distribution of a universal influenza vaccines would alleviate global economic and public health stress from annual influenza virus outbreaks. The influenza virus NA vaccine antigen allows for protection from multiple HA subtypes and virus host origins, but it has not been the focus of vaccine development. The Ni-I NA antigen described here protected mice from direct challenge of four distinct influenza viruses and inhibited the enzymatic activity of a Ni influenza virus panel. The use of the NA antigen in combination with the HA widens the breadth of protection against various virus strains. Therefore, this research opens the door to the development of a longer lasting vaccine with increased protective breadth.

3.2 Introduction

Influenza remains in the forefront of communicable diseases due to reoccurring global seasonal epidemics with pandemic potential. This negative-sense, single-stranded RNA virus contains an eight-segmented genome with the virion surface studded with viral hemagglutinin (HA) and neuraminidase (NA) glycoproteins. The sialic acid binding activity of the HA controls receptor binding specificity and thus host-cell fusion. Comparatively, the sialidase enzymatic activity of the NA contributes to cleavage of mucins, motility, release of progeny virions and prevention of self-aggregation [1]. During infection, viruses can be neutralized by antibodies targeting one of these two proteins (Eichelberger et al., 2018; Zhu et al., 2019). Viral isolates are classified by the HA and NA subtypes that are independently characterized based upon serological cross-reactivity (e.g. H₁N₁, H₅N₁, H₃N₂).

The N₁ NA subtype can be matched with different HA subtypes and three distinct genetic NA clades are defined by phylogenetic analysis based on the NA nucleic acid sequences: N_{1.1}, N_{1.2}, and N_{1.3} genetic clade which correspond to avian-like, classical swine-like, and human-like respectively (J. M. Chen et al., 2007; Fanning et al., 2000). The N_{1.1} clade is the most diverse, and the N_{1.2} and N_{1.3} clades follow more closely a temporal evolution pattern. Prior to the pandemic in 2009, the N₁ that dominated the human infections belonged to the human-like N_{1.2} clade. Further, the Eurasian swine viruses commonly contain the avian-like N_{1.1} clade NA protein. Thus, the 2009 pandemic NA which originated from the Eurasian swine lineage with protein sequences more similar to the NA protein from highly pathogenic avian H₅N₁ viruses (N_{1.1}) than either the seasonal human (N_{1.2}) or classical swine NA (N_{1.3}). The classical swine NA proteins continue to circulate throughout the North American swine populations. Furthermore, through reassortment, some isolated swine-origin influenza viruses contain human-seasonal NA, which were introduced to the swine population through human interactions. Each of the three clades: N_{1.1} (highly pathogenic avian H₅N₁ influenza, 2009 pandemic H₁N₁ influenza), N_{1.2} (seasonal H₁N₁ influenza; e.g. A/Brisbane/59/2007), and N_{1.3} (H₁N₁ variant influenza) has been isolated from virus-infected humans.

NA from the three clades have been isolated from humans, indicating a potential for human adaptability and designating NA as a promising vaccine target (Gaydos et al., 2006; S. Lai et al., 2016).

Indeed, vaccination remains the main method for prevention of influenza virus induced disease. One of the most commonly used seasonal influenza virus vaccines for humans is a split-inactivated virus vaccine without removal of components of the virion. Although all of the components are present, the immunological response to the NA protein is limited. The structural integrity of the protein, the relative ratio of HA to NA, and immunodominance between antigens contribute to a minimal NA-specific immune response after vaccination (Eichelberger & Wan, 2015; Sultana et al., 2014), even though influenza virus infection elicits NA antibodies (Y. Q. Chen et al., 2018). Split-virion vaccination increases antibody titers against the HA protein, but not against the NA protein (Ito et al., 2020). This differential antigenicity may be due to the vaccine preparation, but is difficult to determine due to the lack of methods for quantifying and standardizing NA protein content in vaccine doses. Despite the NA not being a standardized vaccine antigen, the clinical use of NA inhibiting antivirals have led the reduction of influenza disease severity, duration, mortality, and hospitalization (Bassetti et al., 2019; Ison, 2013; S. Ng et al., 2010; Treanor et al., 2000), and the anti-NA antibody titers are virus neutralizing (Couch et al., 2013; Kilbourne et al., 1968; Murphy et al., 1972) and meaningful serological correlates of protection in humans (Clements et al., 1986; Gilchuk et al., 2019; Monto et al., 2015).

Approaches towards the development of a universal or broadly-reactive influenza virus vaccine have focused on eliciting antibodies targeting the HA surface protein with less interest focused on the NA (Berlanda Scorza et al., 2016). However, with a broadly-protective NI-based vaccine, both human seasonal and pandemic HI epidemics can be managed along with decreasing the potential for zoonotic pandemics from avian H5NI and another swine-origin H1NI pandemic. The use of the NA as an immunogen crosses more HA subtypes and species-of-origin than the use of one HA subtype immunogen. Specific monoclonal antibodies (mAbs) bind conserved epitopes on human seasonal HI NI, human 2009 pandemic HI NI and pandemic H5NI NA proteins (Wan et al., 2013). Within the human host the HA has higher nucleic acid substitution rates than NA (J. Jang & Bae, 2018), therefore, HA-specific protective antibodies

are not as effective over many seasons compared to antibodies against NA. The use of an NA-based vaccine may potentially provide a longer lasting vaccine antigen than current vaccination methods that rely primarily on immune responses against HA. The standardization of NA antigen in the influenza virus vaccine may contribute to increased vaccine efficacy. Clinical symptoms, peak viral titers and viral shedding are inversely correlated with NA-inhibiting antibody titers (Clements et al., 1986).

In this report, the development and characterization of a computationally optimized broadly (COBRA) reactive N₁ NA antigen is described. Previously, the COBRA methodology was used to design broadly-reactive HA-based vaccine candidates for H₁, H₂, H₃, and H₅ influenza A virus subtypes. These COBRA HA candidates are effective in mice, ferrets, chickens and non-human primates (Carter et al., 2017; Giles, Crevar, et al., 2012; Giles & Ross, 2011a; Reneer et al., 2020; Ross et al., 2019; T. M. Wong et al., 2017). The design of a COBRA antigen requires variability in the target antigen amino acid sequence to produce a unique immunogen protein sequence after consecutive consensus layering. The diverse genetic clades of NA, antigenic drift, and influenza virus antigen sequencing surveillance contributes to the variability of the available wild-type NA sequences. N₁ COBRA NA protein immunogens were designed using wild-type NA sequences from human, avian and swine influenza isolates. N₂ COBRA NA antigens were also produced and covered in more detail in Appendix F. The N₁ COBRA and wild-type NA proteins are immunogenic as tetrameric soluble protein vaccines. They elicit broadly-reactive antibodies across a panel of N₁ viruses.

3.3 Materials and Methods

3.3.1 COBRA NA antigen construction and synthesis

Full length N₁ NA amino acid sequences for avian (2000-2015; 4891 sequences), swine (1990-2015; 3515 sequences), and human (2001-2014; 9976 sequences) influenza A viruses were downloaded from the GISAID database (www.gisaid.org) (Elbe & Buckland-Merrett, 2017). Full length sequences were aligned using Geneious alignment (global alignment with free end gaps; Blosum62 cost matrix: open gap penalty

12, gap extension penalty 3; 2 refinement iterations) (Geneious VII.1.5). After alignment the most common amino acid at each position was determined, and resulted in primary consensus sequences. The resulting primary sequences from each clade were then realigned to generate a secondary consensus. This process was continued until a single final consensus was obtained. Finally, the ultimate amino acid sequence was reverse translated and optimized for expression in mammalian cells, including codon usage and RNA optimization (Genewiz, Washington, DC, USA). The resulting sequences were termed computationally optimized broadly reactive antigens (COBRA). The Ni-I NA COBRA gene was synthesized and inserted into the pcDNA3.3 vector for soluble tetrameric recombinant NA protein production which contained the tetramerization domain in replace of the stem region (replaced amino acid residues 1-74).

3.3.2 Viruses and Wild-type NA antigens

Ni viruses were obtained through the Influenza Reagents Resource (IRR), BEI Resources, the Centers for Disease Control (CDC), or a generous gift from Dr. Mark Tompkins laboratory at the University of Georgia. Viruses were passaged once in the same growth conditions as they were received or as per the instructions provided by the WHO, in either embryonated chicken eggs or Madin-Darby canine kidney (MDCK) cell culture (Organization & Network, 2011). Virus lots were aliquoted for single-use applications and stored at -80°C. Hemagglutination titer of the frozen aliquots was determined with turkey RBCs. Viruses with NA protein GenBank accession numbers and NA genetic clade distinctions were as follows: A/California/07/2009 (H1Ni)pdm09 (ACQ63272.1; CA/09; Ni.Ic2b1), recombinant virus containing HA and NA from A/Brisbane/59/2007 (H1Ni) and all internal genes from A/Puerto Rico/8/1934 (H1Ni) (PR8) virus (AHG96686.1; Bris/07; Ni.2d), A/Swine/North Carolina/154074/2015 (H1Ni) (Amino acid sequence available upon request; Sw/NC/15; Ni.3b), and BSL-2 recombinant virus containing HA and NA from A/Viet Nam/1203/2004 (H5Ni) and all internal genes from A/Puerto Rico/8/1934 (H1Ni) virus (AAW80723.1; Viet/04; Ni.Ic2a). Viruses included in the enzyme-linked lectin assay panel included: A/Texas/36/1991 (H1Ni) (TX/91; Ni.2d), A/Brisbane/02/2018 (H1Ni)pdm09 (Bris/18; Ni.Ic2b1), A/Hubei/1/2010 (H5Ni) (Hub/10; Ni.Ic2a), A/Swine/Iowa/1931-

(H₁N₁) (Sw/IA/1931; N₁.3a), and A/Swine/Nebraska/Ao144614/2013 (H₁N₁) (Sw/NE/13; N₁.3b). The NA genetic clade distinctions were classified with widely utilized designations used previously through rigorous phylogenetic analysis (J. M. Chen et al., 2007; Fanning et al., 2000; S. Liu et al., 2009; Schon et al., 2021; Zhuang et al., 2019). Viruses were chosen to from each genetic clades to account for the breadth of the N₁ protein diversity and to provide a range of antigenic diversity.

3.3.3 Phylogenetic comparison of avian, swine, human, and COBRA NA sequences

NA amino acid sequences were visualized on a phylogenetic tree (Fig. 3.2A). Briefly, the truncated NA sequences were aligned, and the Geneious Tree Builder, which observed the same alignment characteristics as Geneious alignment, was used to obtain a neighbor-joining Jukes-Cantor phylogenetic tree with no indicated outgroup. The scale bar represents 0.02 amino acid substitutions per site of the region between the amino acid residues 74 through 470 (Kearse et al., 2012).

3.3.4 Soluble tetrameric recombinant NA (tetNA)

The full NA codon optimized sequences were originally commercially sourced in the pTR600 vector for virus-like particle (VLP) production (Genewiz, Washington, DC, USA). The wild-type NA amino acid sequences were aligned to CA/09 NA and truncated between residues 74 and 75. Truncated NA coding regions were subcloned into pcDNA3.3 vector containing a soluble tetramerization sequence for tetNA production. Starting from the N-terminal of the protein, the tetramerization region is composed of a CD₅ signal sequence (for efficient secretion of protein), a hexahistidine affinity tag (used for protein purification), a thrombin cleavage domain (maybe used to remove hexahistidine tag), the tetrabrachion domain from *Staphylothermus marinus* (forms and stabilizes the tetramer), and followed by the NA coding sequence (Fig. 3.2B). The NA sequences of the H₁N₁ influenza viruses included the amino acid residues 74 to 470 and NA sequences from H₅N₁ influenza viruses included the residues 55 to 449. All sequences ended with a dual stop codon (nucleic acid sequence: TGATGA, TAATGA or TGATAG).

N-terminal truncation of the original NA sequence was necessary to replace the transmembrane and stem domain with the soluble tetramerization region. After successful cloning, plasmids were sequence verified.

Soluble tetrameric NA proteins were expressed through individual transient plasmid DNA transfections of EXPI293F cells (ThermoFisher Scientific) following the ExpiFectamine 293 transfection kit protocol. Cell supernatant from transiently transfected cells were collected, centrifuged to remove cellular debris, and filtered through a 0.22 µm pore membrane. Proteins were purified through a HisTrapExcel column and washed and eluted using the AKTA Pure System following manufacturer's protocol (GE Healthcare Bio-Sciences AB, Uppsala, Sweden). Eluted protein fractions were concentrated in phosphate buffered saline + 0.1% w/v sodium azide (PBSA) using Amicon Ultra-15 centrifugal filter unit (Millipore-Sigma, Burlington, MA, USA). Total protein content was determined with the Micro BCA Protein Assay Reagent kit (Pierce Biotechnology, Rockford, IL, USA). Single use aliquots were stored at -80°C until use. The NA proteins were confirmed to have NA sialidase activity, and thus be a tetramer, with the ELLA assay 3.i.²

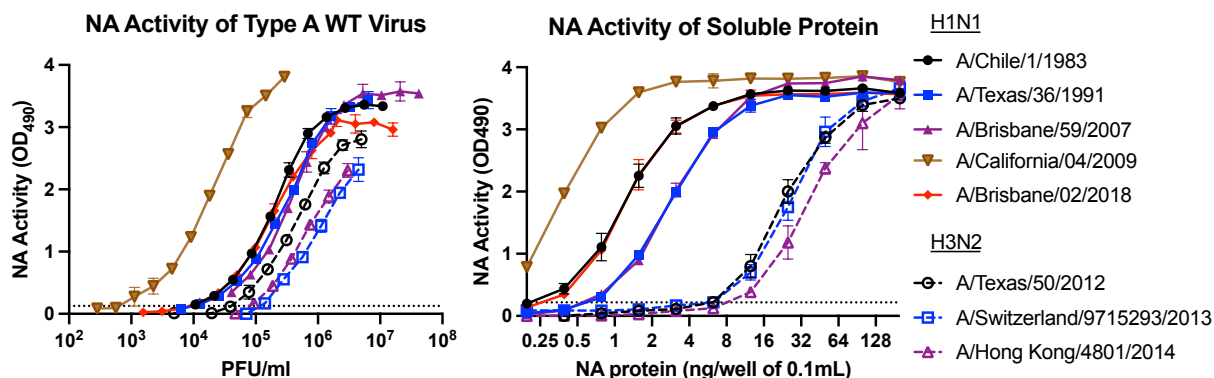


Figure 3.i: Neuraminidase activity of: wild-type influenza A virus (A); and the corresponding recombinantly expressed and purified NA proteins from stably-transfected cell lines (B). Recombinant NA proteins from H1N1 strains and H3N2 strains were evaluated for neuraminidase activity measured as the ability to cleave sialic acid displayed on the fetuin glycoprotein. LOD represents the limit of detection.

²Figure from: Ecker JW, Kirchenbaum GA, Pierce SR, **Skarlupka AL**, Abreu RB, Cooper RE, Taylor-Mulneix D, Ross TM, Sautto GA. High-Yield Expression and Purification of Recombinant Influenza Virus Proteins from Stably-Transfected Mammalian Cell Lines. *Vaccines (Basel)*. 2020 Aug 21;8(3):462. doi: 10.3390/vaccines8030462. PMID: 32825605; PMCID: PMC7565037. Reprinted here with permission from the publisher.

3.3.5 Mouse vaccination and challenge studies

BALB/c mice (*Mus musculus*, females, 6 to 8 weeks old) were purchased from Jackson Laboratory (Bar Harbor, ME, USA) and housed in microisolator units and allowed free access to food and water. Mice (10 mice per group) were vaccinated with a 1:1 mixture of soluble tetNA in PBS (1.0 µg tetNA/mouse) and AddaVax squalene-based oil-in-water adjuvant (InvivoGen, San Diego, CA, USA) in a total volume of 100 µl. Mice were vaccinated via intramuscular injection at week 0 and boosted with the same vaccine formulation at the same dose at weeks 4 and 8. PBS mixed 1:1 by volume with adjuvant served as a mock vaccination. Blood samples were collected from mice via cheek bleeds twenty-eight days after final vaccination in 1.5 ml microcentrifuge tubes. The samples were incubated at RT for 30 min and then centrifuged at 10,000 rpm for 10 min. Serum samples were removed and stored at -20°C.

Four weeks after final vaccination, mice were challenged intranasally with one of four challenge viruses. Mice were challenged with 5×10^4 plaque forming units (PFU) of CA/09; 1×10^7 PFU of Sw/NC/15; 4.375×10^5 PFU of Bris/07; or 1×10^6 PFU of Viet/04. Infectious doses were determined to be ten times the 50% lethal dose, except for Bris/07 which was a non-lethal dose. The viral inoculum were delivered in a volume of 50 µl. Mice were monitored, at minimum, daily for weight loss, disease signs, and death for 14 days post-infection. Individual body weights were recorded daily post-infection for each group during weight loss until stable recovery. Any animal exceeding 25% weight loss or a humane-endpoint score greater than two was humanely euthanized. Surviving mice were confirmed for successful infection indicated by HA titer seroconversion to the challenge virus.

Lung samples were harvested three days post-infection. Mice (n=3) were anesthetized using tribromoethanol (Avertin; Sigma Aldrich, Darmstadt, Germany). The right lung was clamped and excised, and the tissue was snap frozen on dry ice in a 2.0 mL cryogenic vial for storage at -80°C. After right lung excision, the trachea was intubated and the remaining lung lobes were perfused with 10% buffered formalin. After the perfusion, the lung was excised and placed in a 15 mL conical tube with minimum 10 mL of 10% buffered formalin. The fixed lung tissues were embedded in paraffin wax, sectioned, and stained with hematoxylin and eosin (H&E). All procedures were performed in accordance with the Guide for the Care

and Use of Laboratory Animals, Animal Welfare Act, and Biosafety in Microbiological and Biomedical Laboratories (AUP: A2018 06-018-Y3-A13).

3.3.6 ELISA for elicited antibody quantification

A high-affinity, 96-well flat-bottom enzyme-linked immunosorbent assay (ELISA; Immulon 4HBX) plate was coated with 50 µl of 10 mg/ml of virus-like particles with NA expressed on the surface in ELISA carbonate buffer (50mM carbonate buffer (pH 9.5) with 5 µg/ml bovine serum albumin (BSA)), and the plate was incubated overnight at 4°C. The next morning, nonspecific epitopes were blocked with 1% BSA in PBS with 0.05% Tween 20 (PBST+BSA) solution for 1 h at RT or overnight at 4°C. Buffer was removed and three-fold serial dilutions of raw sera were added to the plate with an initial dilution of 1:100. Plates were incubated at 37°C for 90 min. The plates were washed in PBS, and goat anti-mouse IgG-HRP was added 1:4000 in PBST+BSA (cat. no. 1030-05, Southern Biotech, Birmingham, AL, USA). Plates were incubated at 37°C for 1 hr. After washing, 2,2'-azino-bis(3-ethylbenzothiazoline-6-sulphonic acid) (ABTS) substrate in McIlvain's Buffer (pH 5) was added to each well, and incubated at 37°C for 15 min. The colorimetric reaction was stopped with the addition of 1% SDS in dH₂O, and the absorbance was measured at 414 nm using a spectrophotometer (PowerWave XS; BioTek, Winooski, VT, USA). Endpoint titers were determined as the last dilution above five standard deviations of the negative control wells after subtracting the background absorbance.

3.3.7 ELLA for NA inhibition

High affinity Immunoblot 4HBX 96-well flat-bottom plates (ThermoFisher Scientific, Waltham, MA, USA) were coated overnight with 100µl of 25µg/ml fetuin (Sigma-Aldrich, St. Louis, MO) in commercial KPL coating buffer (Seracare Life Sciences Inc, Milford, MA, USA) and stored at 4°C until use. Influenza virus was diluted in sample diluent (Dulbecco's phosphate-buffered saline containing 0.133 g/L CaCl₂ and 0.1 g/L MgCl₂ (DPBS), 1% BSA, 0.5% Tween-20) to an initial dilution of 1:10. Before virus addition, fetuin plates were washed three times in PBS-T (PBS + 0.05% Tween-20). After which, 50µl of two-fold serial

dilutions of virus were added to the fetuin-coated plate containing 50 μ l of sample diluent in duplicate. A negative control column was included containing 100 μ l of only sample diluent. Plates were sealed and incubated for 18 h at 37°C and 5% CO₂. After incubation, plates were washed six times in PBS-T, and 100 μ l of peanut agglutinin-HRPO (Sigma-Aldrich, St. Louis, MO) diluted 1000-fold in conjugate diluent (DPBS, 1% BSA) was added. Plates were incubated at RT for 2 h. Plates were washed three times in PBS-T, and 100 μ l (500 μ g/ml) of o-phenylenediamine dihydrochloride (OPD; Sigma-Aldrich, St. Louis, MO) in 0.05 M phosphate-citrate buffer with 0.03% sodium perborate pH 5.0 (Sigma-Aldrich, St. Louis, MO) was added to the plates. Plates were immediately incubated in the dark for 10 mins at RT. The reaction was stopped with 100 μ l of 1 N sulfuric acid. The absorbance was read at 490nm using a spectrophotometer (PowerWave XS; BioTek, Winooski, VT, USA). NA activity was determined after subtracting the mean background absorbance of the negative control wells. Linear regression analysis was used to determine the dilution of the influenza viruses used in the assay necessary to achieve 90-95% NA activity and was used for subsequent NA inhibition enzyme-linked lectin assays (ELLAs).

Mouse sera was treated with 3 parts receptor destroying enzyme (RDE, Seneka, Japan), incubated at 37°C for 16-18 h and heat inactivated at 55 °C for 6 h to completely inactivate the NA activity from the *Vibrio cholera* NA; this inactivation procedure has previously been shown to be efficient (Westgeest et al., 2015). From an initial dilution of 1:100, NI ELLA titers were determined by two-fold serially diluting treated sera in sample diluent. Duplicate dilutions were added to fetuin plates in 50 μ l. The virus diluted to 90-95% NA activity in sample diluent was added to the plate in 50 μ l. Controls were each a minimum of 8 wells, and included a positive NA antigen control (50 μ l virus + 50 μ l sample diluent) and a negative control (100 μ l of sample diluent) on each plate. Plates were incubated for 16-18 h at 37°C and 5% CO₂ after which they were processed as described above. NA percent activity was determined by subtracting the mean background absorbance of the negative control wells, and then dividing the serum absorbance by the mean virus positive control wells multiplied by 100. Nonlinear regression lines were fit using Prism, and the log 50% NI titer was estimated.

3.3.8 Determination of viral lung titers

Frozen right lung samples were thawed on ice, weighed and per 0.1 g tissue a volume of 1 ml of Dulbecco modified Eagle medium (DMEM) supplemented with penicillin-streptomycin (P/S) was added. The tissue was macerated through a 0.70 µm nylon filter (Corning Cell Strainer, Sigma Aldrich, St. Louis, MO, USA) until thoroughly homogenized. Ten-fold serial dilutions of lung homogenate were overlaid onto MDCK cells seeded at 1×10^6 cells per well of a six-well plate for enumeration of viral lung titers. Samples were incubated for 1 h at RT with intermittent shaking every 15 min. Medium was removed, and the cells were washed twice with DMEM + P/S. Wash medium was replaced with 4 ml of L15 medium TPCK-trypsin plus 1.2% avicel (Cambrex, East Rutherford, NJ, USA) and incubated at 37°C with 5% CO₂ for 48-72 h. After incubation, avicel was removed and discarded. MDCK cells were washed with PBS and then fixed with 10% buffered formalin for 15 min and stained with 1% crystal violet for 15 min. The human viruses were incubated with 1 µg/ml of TPCK trypsin, and the Viet/o₄ and Sw/NC/15 were incubated with 2 µg/ml. The plates were thoroughly washed in distilled water to remove excess crystal violet, and the plaques were counted and recorded to determine the PFU per ml lung homogenate.

3.3.9 Statistical analysis

Statistical significance was defined as a p-value less than 0.05. The means of the viral lung titers and day 6 weights were analyzed by an ordinary one-way ANOVA followed by Tukey's multiple comparisons test, with a single pooled variance. The viral lung titers were transformed by \log_{10} and the mean calculated. The lowest limit of detection for viral lung titers was 1.0 \log_{10} (PFU/ml lung homogenate), and this value was used for the statistical analysis of samples below that. Comparisons of peak weight loss were determined by dividing the measured weight on the peak of weight loss by the pre-challenge weight on day 0, multiplied by 100. The standard deviations for weight curves, viral lung titers and peak weight loss were determined. If an animal was sacrificed before the peak due to a greater than 25% drop in original weight or a humane-endpoint score of greater than or equal to three, a percent weight of 75 was used as the limit of detection

for the statistical analysis. The mean \log_{10} (NA 50% inhibitory (NAI) titers) were presented with the 95% confidence interval. Analyses were done using GraphPad Prism software.

3.3.10 COBRA sequences

The amino acid sequence for the COBRA NA has been reported in U.S. patent filings PCT/US21/12695.

3.4 Results

3.4.1 Design of Ni COBRA NA sequences

The computationally optimized broadly reactive NA antigen was designed from sequences obtained from the GISAID database(Elbe & Buckland-Merrett, 2017). The Ni-I COBRA NA antigen was designed using human, avian and swine origin influenza virus NA sequences from 1990-2015 depending on host origin. The Ni-I COBRA NA was phylogenetically located close to the branch point of the human-like NA clade Ni.2 (Fig. 3.2A). When aligned to representative wild-type sequences, the Ni-I COBRA NA had between 31 to 44 amino acids differences. The Sw/IA/1931 NA protein was the most similar to Ni-I COBRA NA and the Bris/18 and Sw/NE/13 NA proteins were the least similar with 44 amino acids different compared to the Ni-I COBRA NA.

3.4.2 Soluble recombinant tetrameric NA protein vaccines are immunogenic

Sera was collected at week 12 (Fig. 3.2C) from mice (BALB/c) vaccinated at week 0, 4, and 8 with one of five tetNA (Fig. 3.2D). The adjuvanted tetNA soluble protein vaccines elicited an NA-specific antibody response and were confirmed to be immunogenic (Fig. 3.3). All NA vaccinations elicited IgG antibodies that bound to all four wild-type NA antigens which were presented in a tetramer formation on the surface of a virus-like particle. The Ni-I COBRA NA group had endpoint titers of 1:1000 or greater to each of the challenge virus NA proteins (Fig. 3.3A). The greatest titers were to CA/09 and Viet/04 NA antigens, and

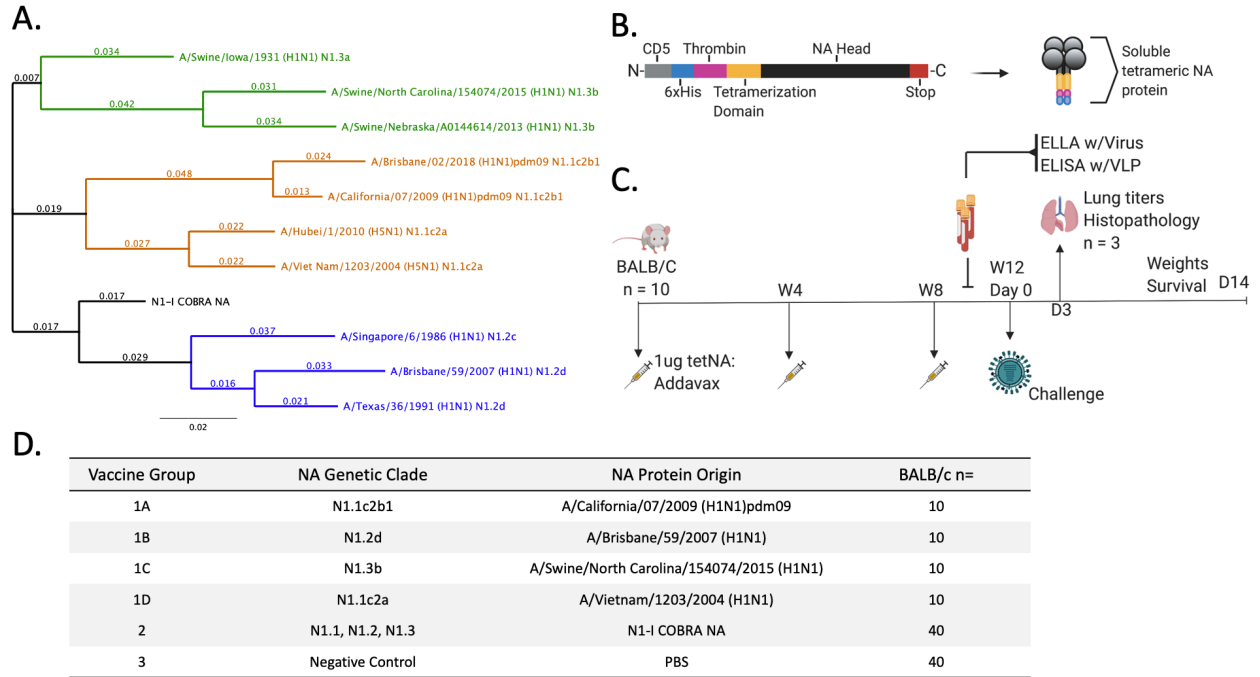


Figure 3.2: Experimental groups and design used for influenza challenge. (A) Phylogenetic tree of truncated NA amino acid sequences (74 to 470). The N1-I COBRA NA (black) branched closer to the root of the tree than all other wild-type NA proteins. Representative viruses for each N1 clade (N1.1, orange; N1.2, blue; N1.3, green) were included. Scale bar = substitutions per site; total sites = 396 amino acids. (B) Cartoon schematic of soluble tetrameric NA protein used for vaccinations. From the N-terminal to C-terminal ends of the protein sequence, the domains were CD5 signal sequence (CD5; cleaved during protein processing), hexahistidine domain (6×His), thrombin cleavage domain (Thrombin), *Staphylothermus marinus tetrabrachion* domain (Tetramerization Domain), the NA head region of the select antigen (NA Head), and a double stop codon (Stop). (C) Vaccination and challenge regimen followed for each challenge. Female BALB/c mice ($n = 10$) were vaccinated with tetrameric soluble NA (tetNA) in a prime-boost-boost at 4-week intervals. Sera were collected after vaccinations and prior to challenge for serological assays (enzyme-linked lectin assay [ELLA]; enzyme-linked immunosorbent assay [ELISA] with virus-like particles [VLP]). Each of the four vaccine groups were challenged with one of the four challenge viruses. Over the course of infection, weights were monitored for up to 14 days, and lungs ($n = 3$) were harvested on day 3. (D) The vaccine groups for each challenge varied and was the homologous control for the matched virus.

the lowest endpoint titer was to the Sw/NC/15 antigen. But the binding to Sw/NC/15 was comparable to the what the wild-type Sw/NC/15 NA vaccination elicited endpoint titers of 1:890 and 1:5620 respectively (Fig. 3.3E). Mice vaccinated with the Viet/o4 NA had the highest anti-NA IgG titers when binding to the homologous protein of 1:316,000 (Fig. 3.3D). CA/o9 and Viet/o4 NA antigens, elicited the highest binding towards the Ni.1 clade proteins (Fig. 3.3B and D). Whereas, Bris/o7 had higher titers to itself and Viet/o4 (Fig. 3.3C). Sw/NC/15 NA antigen elicited antibodies bound at similar titers to Bris/o7, Viet/o4 and Sw/NC/15 NA protein. All vaccine antigens elicited antibodies that were able to bind to the Viet/o4 NA protein. The mock vaccinated group did not elicit detectable antibodies to the tested proteins (data not shown).

3.4.3 Soluble recombinant tetrameric NA protein vaccines elicit NA inhibiting antibodies

Collected antisera was examined for the ability to inhibit the NA enzymatic activity through an enzyme-linked lectin assay (ELLA) (Fig. 3.4; Fig. 3.5). The ELLA measures the ability of NA to cleave sialic acids from the terminal ends of fetuin. Mice vaccinated with the COBRA Ni-I NA vaccine had antibodies that inhibited all tested HXN1 viruses in the Ni.1, Ni.2 and Ni.3 genetic clades (Fig. 3.5A). Mice vaccinated with CA/o9 NA protein had broad NA inhibition with cross reactivity in the Ni.1 and swine-like Ni.3 clades (Fig. 3.5B). Conversely, sera collected from mice vaccinated with the Bris/o7 NA had the narrowest response, only inhibiting the human-like clade Ni.2 H1N1 viruses (TX/91 and Bris/o7) and no viruses from either clade Ni.1 or Ni.3 (Fig. 3.5C). Mice vaccinated Viet/o4 NA proteins had a NA inhibition activity pattern similar to CA/o9 vaccinated mice (3D). However, the CA/o9 NA vaccinated sera were able to inhibit Bris/18, and the Viet/o4 sera had higher NA inhibition titers to Viet/o4, Hubei/10, and Sw/NE/13 viruses. The Sw/NC/15 NA elicited sera had a narrow breadth and inhibited the swine origin viruses and Hubei/10 (Fig. 3.5E). In conclusion the COBRA Ni-I NA protein elicited a broad inhibitory response mediated by antibody binding.

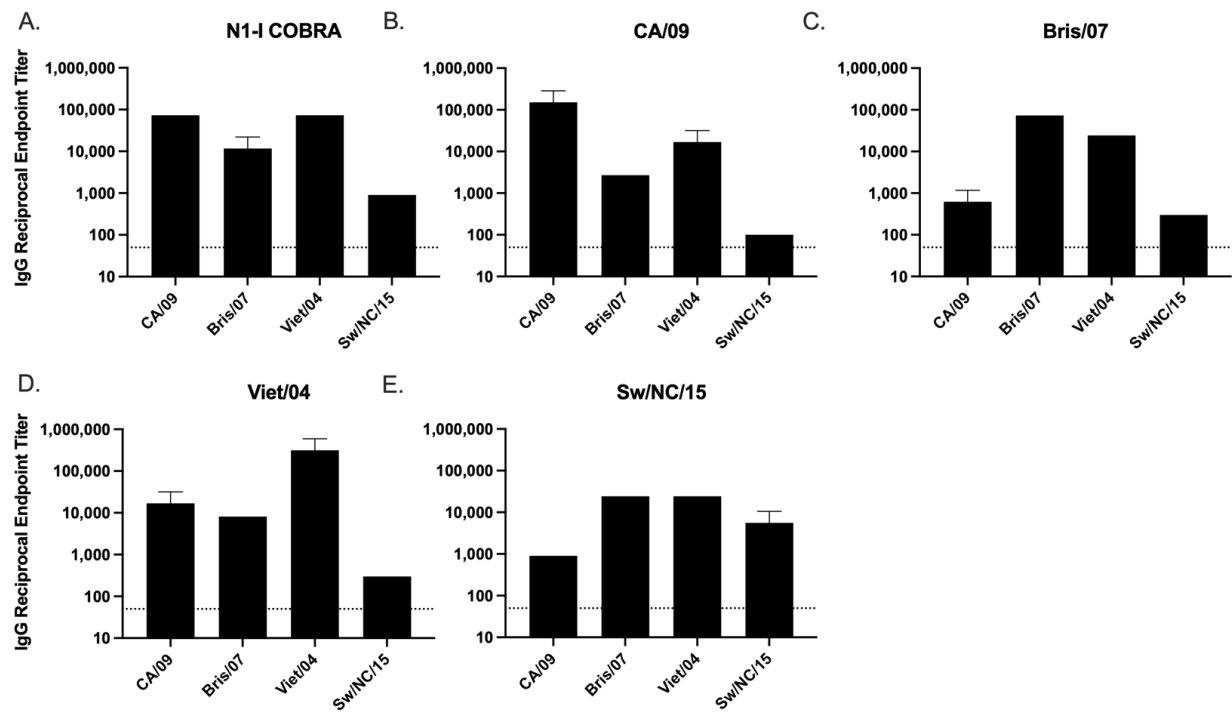


Figure 3.3: Total IgG antibody binding of vaccinated mouse sera to tetrameric NA expressed on the surface of a virus-like particle. The homologous sera had the highest reciprocal endpoint titer for each challenge virus. The N1-I COBRA NA elicited binding to all four challenge NAs, and the mock vaccinations produced no measurable binding (not shown). Reciprocal serum endpoint titers were determined with raw serum starting from an initial dilution of 1:100 after a prime-boost-boost vaccination regimen with soluble tetNA. The endpoint titer was the last serum titer that produced an absorbance greater than 5 standard deviations above the background absorbance. Serum that did not produce an absorbance greater than the cutoff was defined as below the limit of detection (LOD), depicted as 50 reciprocal endpoint titer. The serum was analyzed in triplicate and the geometric mean reciprocal endpoint titer was calculated. Error bars represent the geometric standard deviation.

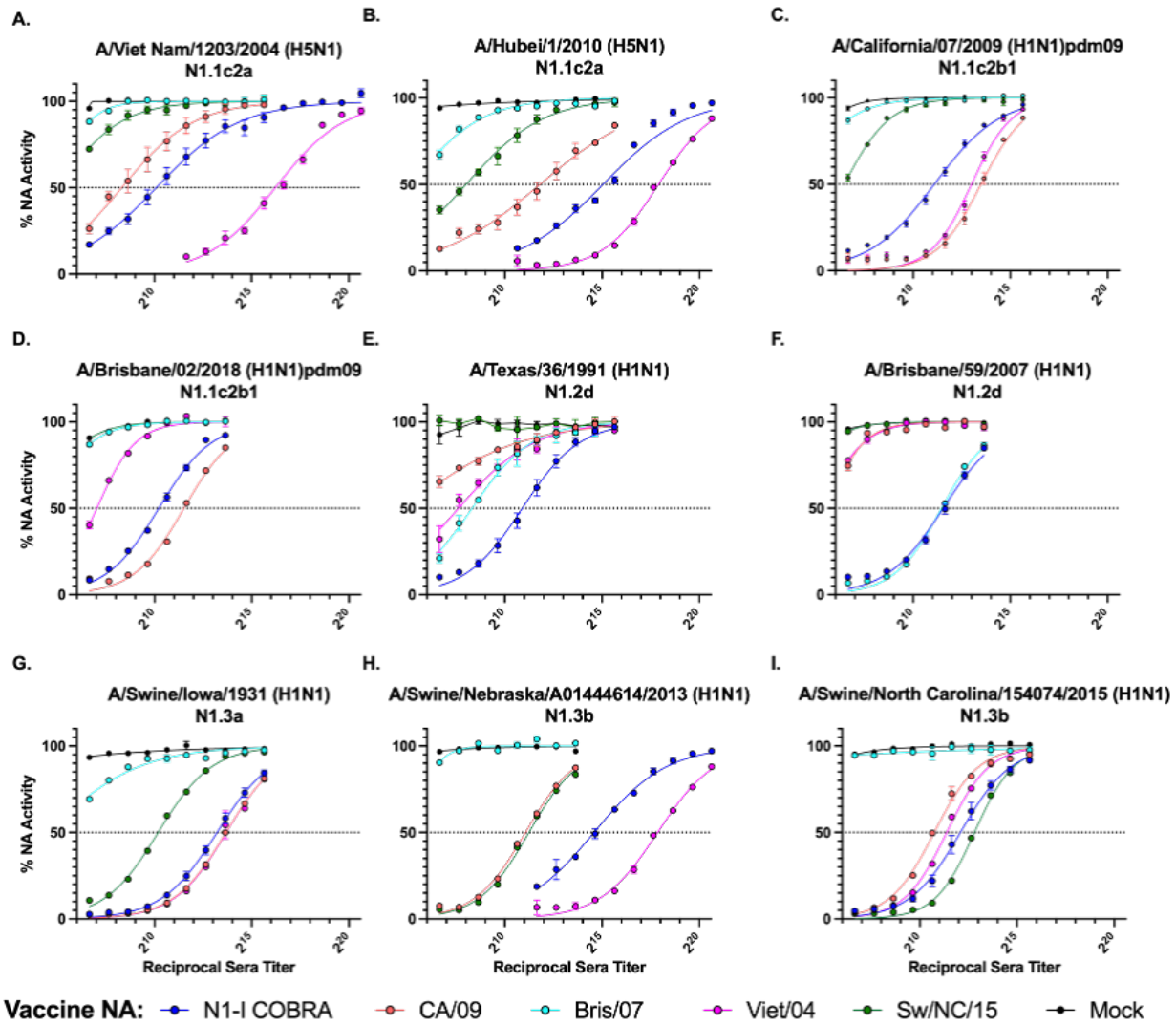


Figure 3.4: NA enzymatic inhibition of N1 influenza viruses with sera from NA vaccinated mice. The sera were two-fold serially diluted from the starting dilution of 1:100 to a dilution necessary to quantify the NAI titer. Non-linear regression (resulting fit: solid line) was conducted from these results to obtain the \log_{10} (NAI reciprocal titer) that inhibited 50% of the NA activity (dotted horizontal line). Before conducting non-linear regression, the NA activity was normalized with 100% NA activity being defined with a ‘virus only with no sera’ control that included at least 8 wells. Error bars represent the standard error of the mean.

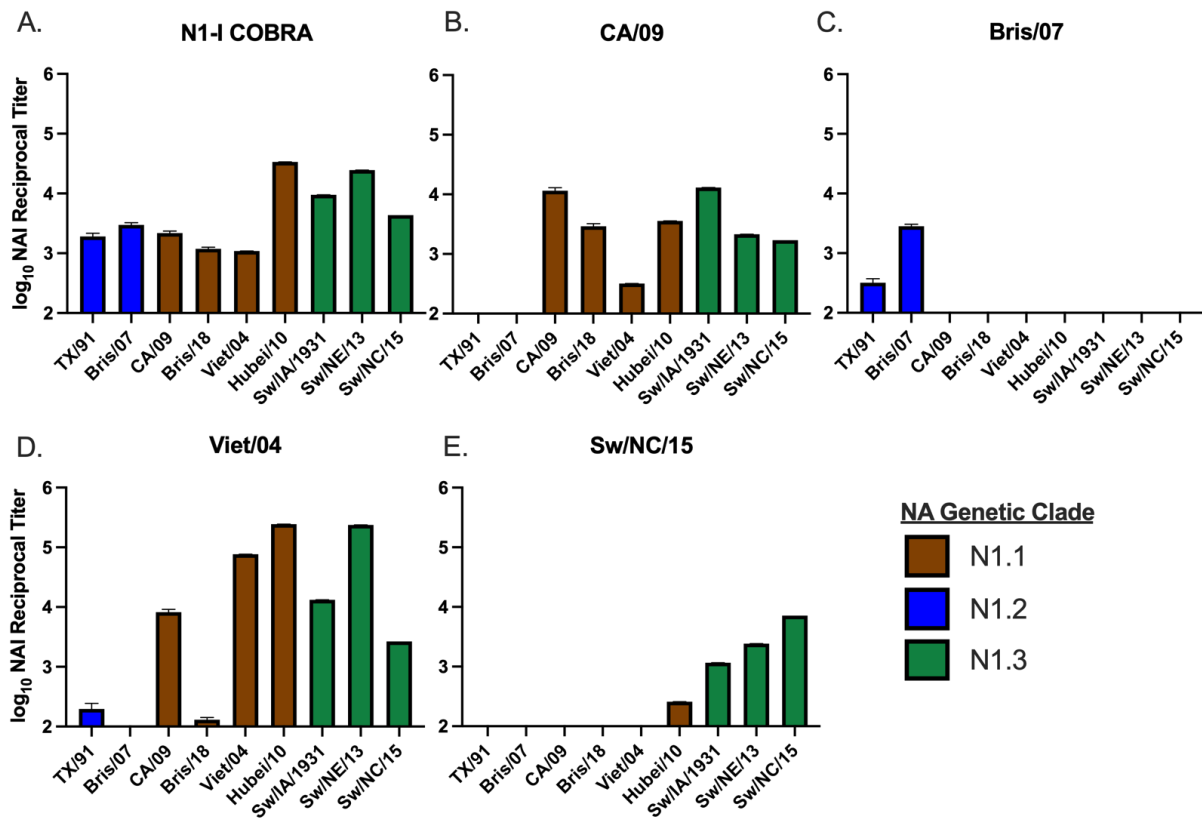


Figure 3.5: Reciprocal NA inhibition (NAI) titers across a panel of N1 influenza viruses. The N1-I COBRA vaccinated sera (A) inhibited all representative viruses in the panel (B). The wild-type sera (B to E) elicited various levels of inhibition breadth from very broad (D) to narrow (C and E), but was not as broad as the N1-I COBRA. The enzyme-linked lectin assays (ELLAs) were performed with RDE-treated and heat-inactivated sera initially diluted to 1:100 followed by 2-fold dilutions. The limit of detection was defined as $2.0 \log_{10}(\text{NAI reciprocal titer})$. The mean $\log_{10}(\text{NAI reciprocal titer})$ that inhibited 50% of the NA activity with 95% confidence intervals was estimated with nonlinear regression of the ELLA dilution curves in 3.4.

3.4.4 Vaccinated mice challenged with human pandemic H1N1 influenza virus.

To determine if the antibody binding to an NA molecule correlates with inhibition of NA enzymatic activity and protection against infection, mice were challenged intranasally with CA/09 virus (Fig. 3.6). During the course of infection, all of the mock vaccinated mice reached humane endpoints and were sacrificed by days 5-6 post-infection (Fig. 3.6A). The COBRA Ni-I NA and CA/09 NA vaccinated mice survived challenge, but lost 14-17% weight between days 3-5 post-vaccination, but recovered almost all body weight by day 12 (Fig. 3.6B). At day 6, the average weight of the CA/09 vaccinated mice was not significantly different from the COBRA Ni-I NA vaccinated mice (Fig. 3.6C). The CA/09 NA vaccinated mice had the lowest mean viral titer of $2.24 \log_{10}(\text{PFU/ml})$ on day 3 (Fig. 3.6D). The titer was significantly lower than the mean viral titer of $4.72 \log_{10}(\text{PFU/ml})$ from mice vaccinated with COBRA Ni-I NA. Although greater than the CA/09 homologous control, the Ni-I COBRA NA also had a significantly lower titer than the mock negative control with mean viral titer of $6.41 \log_{10}(\text{PFU/ml})$ (Fig. 3.6D). Formalin-fixed lung tissue stained with hemolysin and eosin (H&E) showed more inflammatory infiltration for the mock vaccinated group in the CA/09 challenge than either the CA/09 (homologous) or the Ni-I COBRA vaccinated groups (Fig. 3.7A-C). Visually the CA/09 and Ni-I COBRA NA were similar in the amount inflammatory reaction.

3.4.5 Vaccinated mice challenged with human seasonal H1N1 influenza virus.

In addition to enzymatic inhibition of the human pandemic virus CA/09 NA, the COBRA Ni-I NA also inhibited the human seasonal virus Bris/07 NA enzymatic activity. All Bris/07 challenged mouse groups did not reach humane endpoints, and all the mice survived challenge (Fig. 3.8A), with a peak weight loss at day 3 post-infection with quick recovery (Fig. 3.8B and C). However, there were significant differences in the lung viral titers on day 3 between the vaccinated groups (Fig. 3.8D). Mice vaccinated with the Ni-I COBRA NA had a mean viral lung titer of $1.97 \log_{10}(\text{PFU/ml})$ that was not significantly different from the Bris/07 NA vaccinated control group of $1.00 \log_{10}(\text{PFU/ml})$ (Fig. 3.8D). Furthermore, the Ni-I

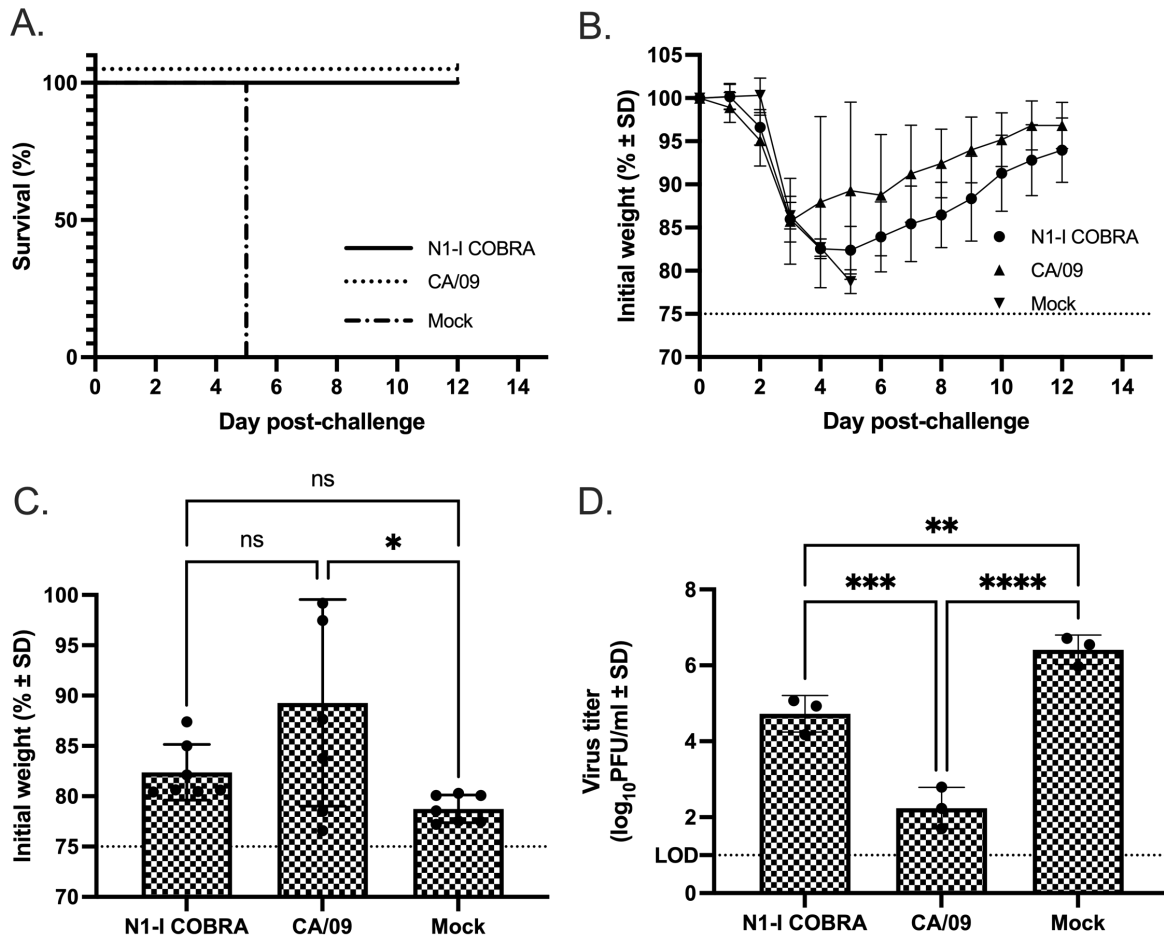


Figure 3.6: A/California/07/2009 (H1N1)pdm09 challenge results after vaccination with NA antigens. (A and B) Survival (A) and weight loss (B) curves of mice postinfection are shown. (C) The day 5 peak weight loss of the CA/09-vaccinated mice was significantly different than the mock vaccinated. The variation of the CA/09 NA-vaccinated group was greater than the N1-I-vaccinated group. (D) The viral lung titers determined through plaque assay from lung tissue on day 3 postinfection. All error bars depict standard deviations, and the statistical analysis was conducted using a one-way ANOVA with Tukey's multiple comparison. Not significant (ns); P value < 0.05 (*); P value < 0.01 (**); P value < 0.001 (***); P value < 0.0001 (****).

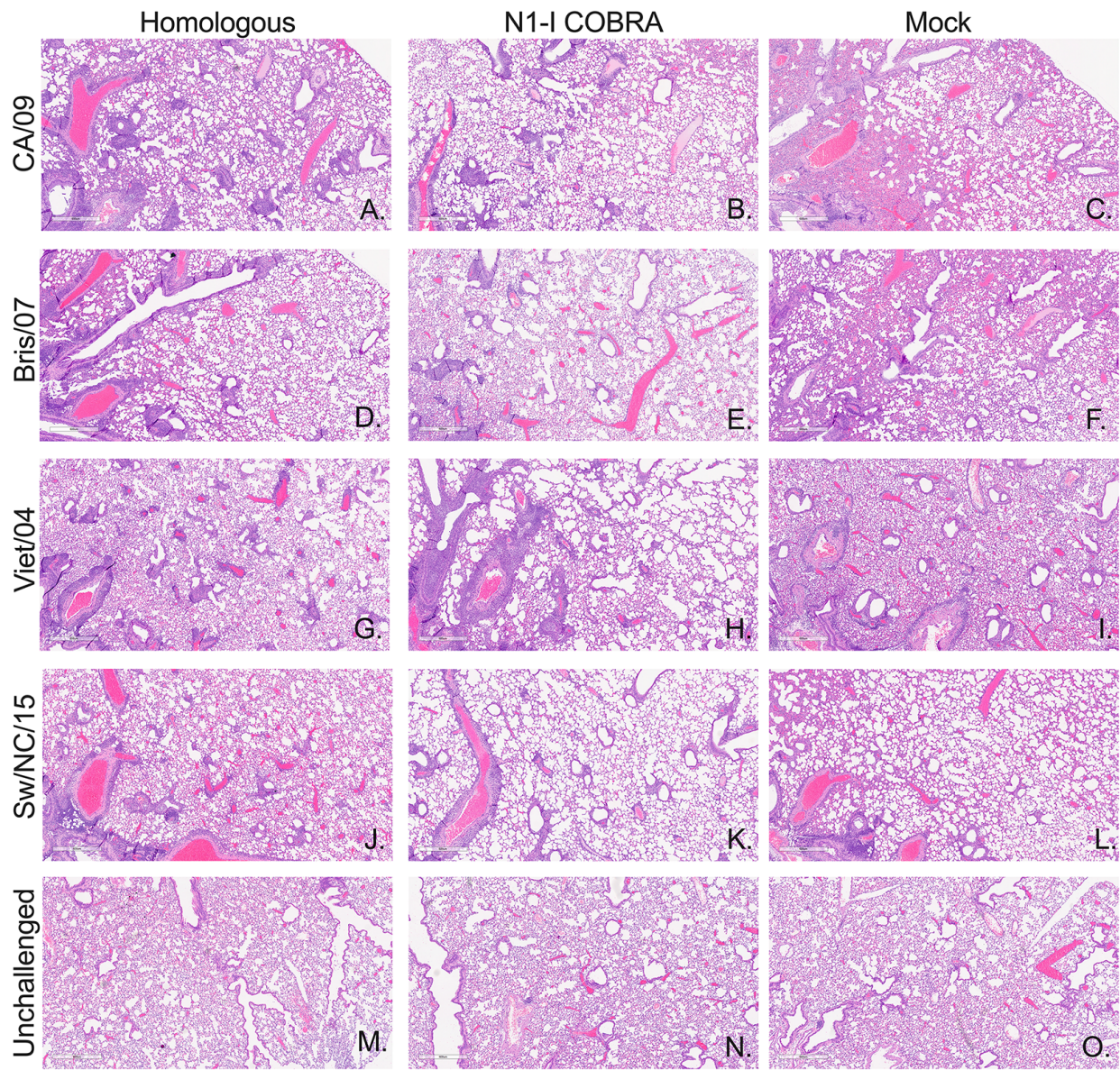


Figure 3.7: Vaccine-specific inhibition of influenza inflammatory lung infiltration. Day 3 postinfection lungs were perfused and fixed with 10% buffered formalin. Representative images from hematoxylin and eosin (H&E)-stained sections are depicted. The vaccine groups along the horizontal axis include the homologous control vaccine groups in the first column with the appropriate vaccine per challenge virus listed in the vertical axis: CA/09 challenge (A to C), Bris/07 challenge (D to F), Viet/04 challenge (G to I), and Sw/NC/15 challenge (J to L). The unchallenged controls were age-matched unvaccinated, unchallenged mouse lungs (M to O). Each image represents separate individual mice. The magnification for all images was 4 \times , and the scale bar represents 0.6 mm.

COBRA NA vaccinated mice had significantly lower mean viral lung titers than the mock vaccinated mice with a mean titer of $4.39 \log_{10}(\text{PFU/ml})$. In addition to the difference in viral lung titer, the mock vaccinated lung H&E resulted in greater inflammatory infiltration compared to the Bris/07 and Ni-I COBRA NA vaccinated mice (Fig. 3.7D-F). The Bris/07 and Ni-I COBRA NA lung stains were similar to each other and to the unchallenged mouse lung (Fig. 3.7M-O).

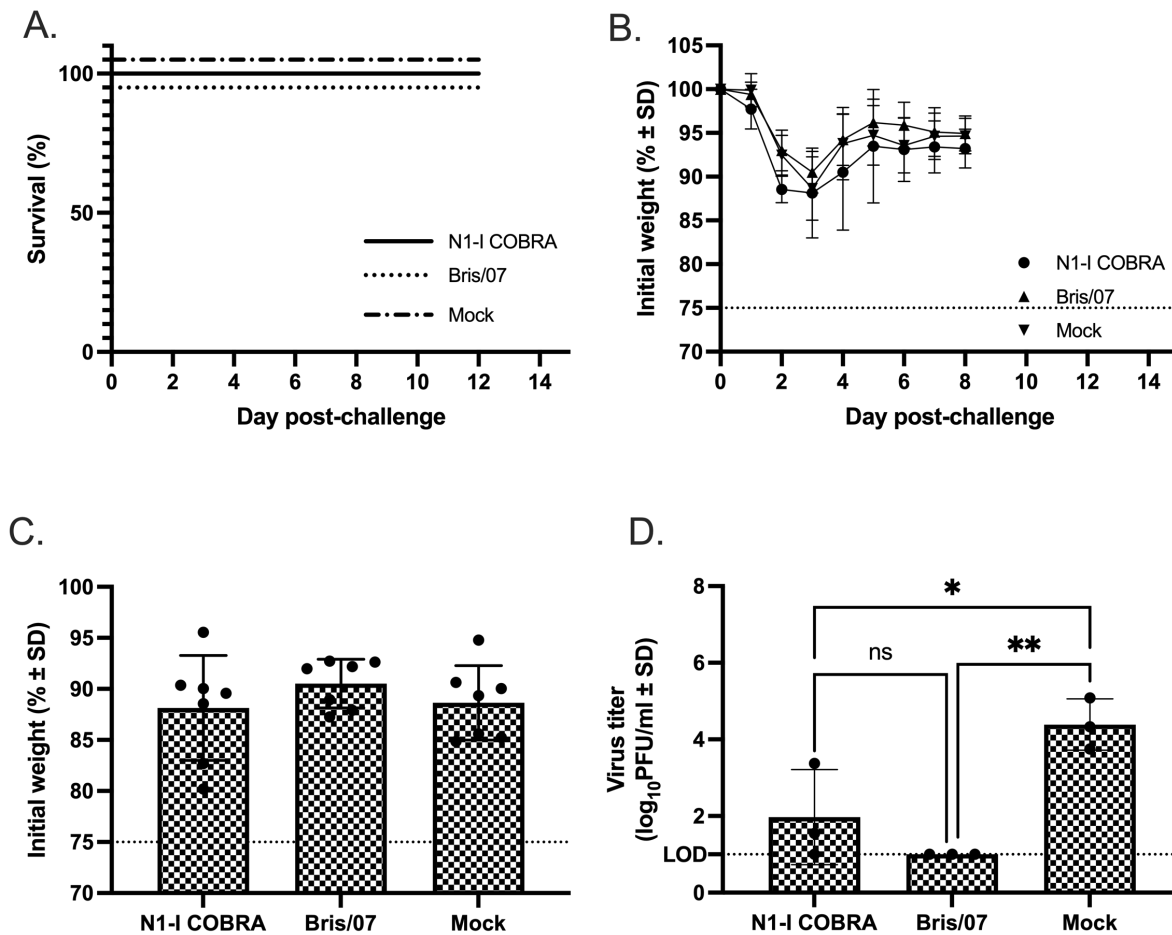


Figure 3.8: A/Br/59/2007 (H1N1) x PR8 challenge results after vaccination with NA antigens. (A and B) Survival (A) and weight loss (B) curves of mice postinfection. (C) The day 3 peak weight loss was not significantly different between any of the groups. (D) The viral lung titers were determined through plaque assay from lung tissue on day 3 postinfection. All error bars depict standard deviations, and the statistical analysis was conducted using a one-way ANOVA with Tukey's multiple comparison. Not significant (ns); P value < 0.05 (*); P value < 0.01 (**).

3.4.6 Vaccinated mice challenged with avian H₅N₁ reassortant influenza virus.

The reassortant H₅N₁ avian virus, Viet/o₄ challenge virus contains the HA and NA gene segments originating from the highly pathogenic Viet/o₄ wild-type virus, but the multi-basic cleavage site of the HA is mutated to infer a low pathogenic phenotype. Mice vaccinated with Viet/o₄ NA and challenged with the Viet/o₄ virus containing the homologous NA protein all survived viral challenge (Fig. 3.9A) with little weight loss (Fig. 3.9B). In contrast, mock vaccinated mice all reached humane endpoint by day 4 (Fig. 3.9A). Ninety percent of mice vaccinated with Ni-I COBRA NA survived challenge (Fig. 3.9A), but these mice did lose between 10-15% of their body weight between days 4-6 post-challenge and then returned to full body weight by day 14 (Fig. 3.9B). At the peak of weight loss on day 5 post-infection, mice vaccinated with the Ni-I COBRA NA had significantly more weight loss than mice vaccinated with the homologous Viet/o₄ NA, but had statistically less weight loss than mock vaccinated (Fig. 3.9C). At day 3, mice vaccinated with Ni-I COBRA NA vaccine had $3.67 \log_{10}(\text{PFU/ml})$ mean lung viral titers that were significantly lower than viral titers in mock vaccinated mice (Fig. 3.9D). The mock vaccinated mean lung titer was $4.77 \log_{10}(\text{PFU/ml})$. The mock vaccinated group challenged with Viet/o₄ had the greatest amount of infiltration of all groups of mice across all challenge viruses (Fig. 3.7). As such, the Viet/o₄ and Ni-I COBRA NA vaccinated groups had comparatively less infiltration (Fig. 3.7G-I).

3.4.7 Vaccinated mice challenged with swine-isolate H₁N₁ influenza virus.

While all mice in the Ni-I COBRA NA, Sw/NC/15 NA, and mock vaccinated groups had significant weight loss following infection with Sw/NC/15 (Fig. 3.10B), few mice reached humane endpoint and were sacrificed (Fig. 3.10A). At day 6, the weight of the Ni-I COBRA NA vaccinated mice was not significantly different from the Sw/NC/15 NA vaccinated mice, but was significantly higher than the mock vaccinated mice (Fig. 3.10C). The Sw/NC/15 NA vaccinated mice was not statistically greater than the mock vaccinated animals. Furthermore, mice vaccinated with the Ni-I COBRA NA had lower lung titers on day 3 post-infection (mean viral titer of $3.25 \log_{10}(\text{PFU/ml})$) compared to the mock vaccinated mice

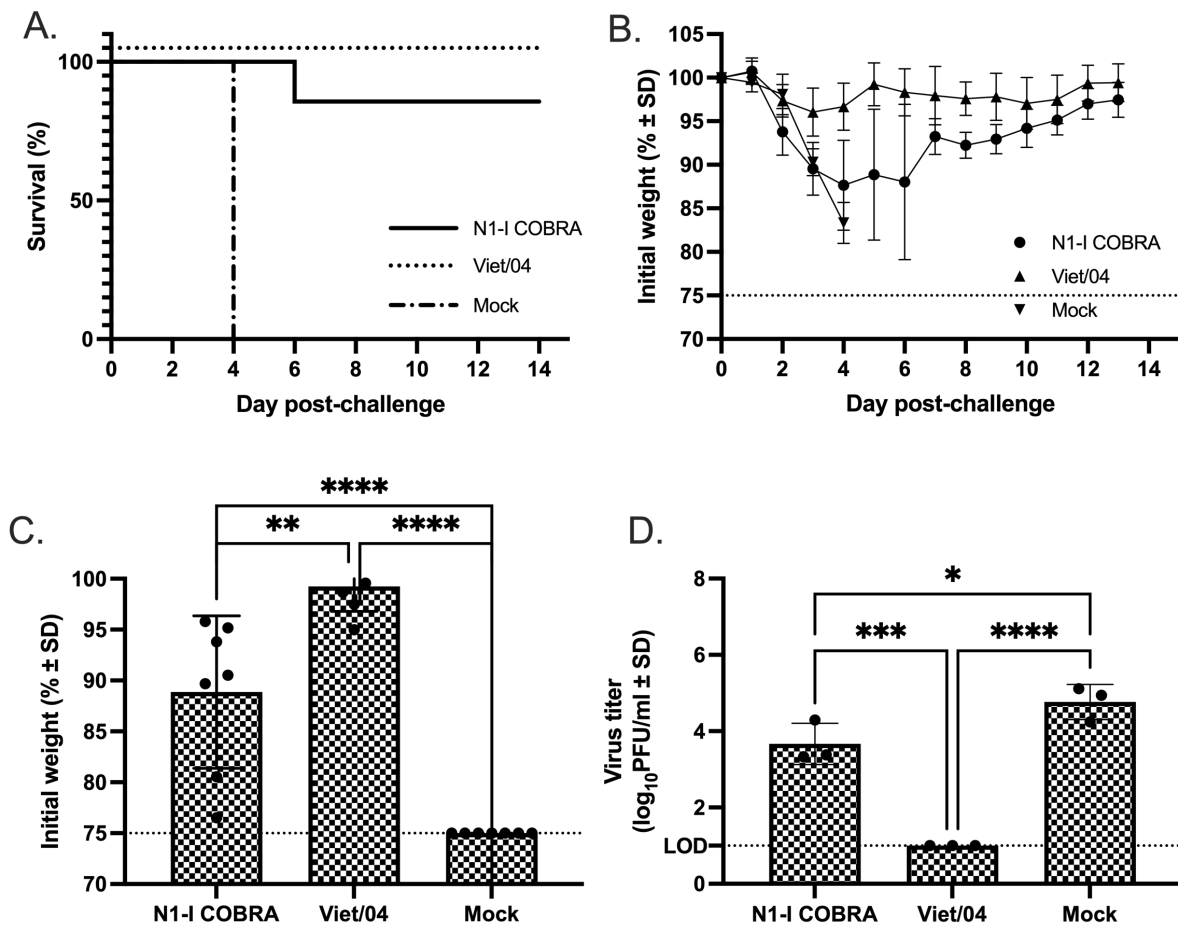


Figure 3.9: A/Viet Nam/1203/2004 (H5N1)×PR8 challenge results after vaccination with NA antigens. (A and B) Survival (A) and weight loss (B) curves of mice postinfection. (C) The day 5 peak weight loss was significantly different between all vaccination groups. The weights that reached humane endpoint before day 5 were analyzed at the limit of detection (75% body weight). (D) The viral lung titers determined through plaque assay from lung tissue on day 3 postinfection. All error bars depict standard deviations, and the statistical analysis was conducted using a one-way ANOVA with Tukey's multiple comparison. P value < 0.05 (*); P value < 0.01 (**); P value < 0.001 (***); P value < 0.0001 (****).

($5.88 \log_{10}(\text{PFU/ml})$) (Fig. 3.10D). There was no significant difference between the mean viral lung titer in Ni-I COBRA NA vaccinated mice and mice vaccinated with the Sw/NC/15 NA ($4.64 \log_{10}(\text{PFU/ml})$). The mice vaccinated with Ni-I COBRA NA had less inflammatory infiltration than either the Sw/NC/15 and mock vaccinated groups (Fig. 3.7J-L), and was more similar to the unchallenged controls (Fig. 3.7M-O).

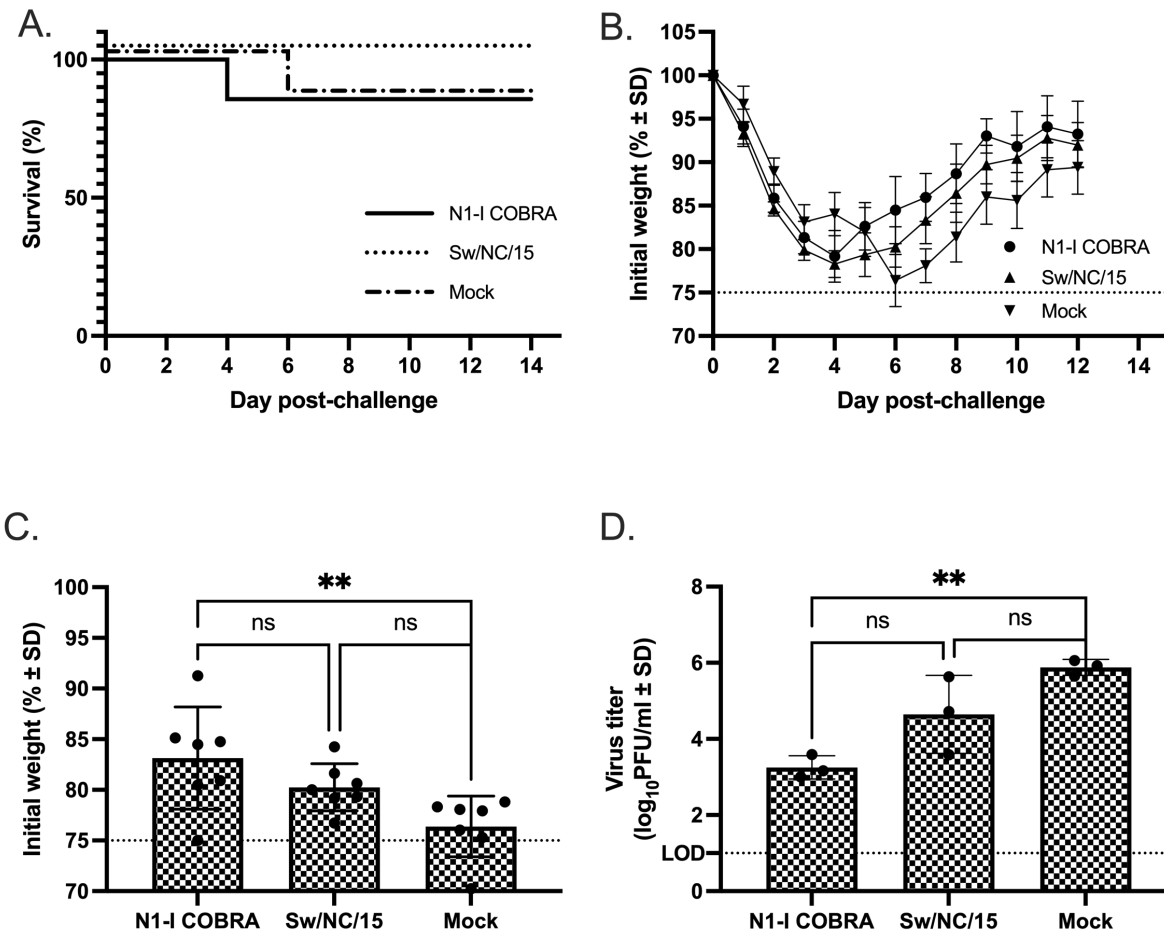


Figure 3.10: A/Swine/North Carolina/154074/2015 (H1N1) challenge results after vaccination with NA antigens. (A and B) Survival (A) and weight loss (B) curves of mice postinfection. (C) The day 6 peak weight loss was significantly different between the Ni-I COBRA and mock groups. The weights that reached humane endpoint before day 6 were analyzed at the limit of detection (75% body weight). (D) Viral lung titers were determined through plaque assay from lung tissue on day 3 postinfection. All error bars depict standard deviations, and the statistical analysis was conducted using a one-way ANOVA with Tukey's multiple comparison. Not significant (ns); P value < 0.01 (**).

3.5 Discussion

Following influenza virus infection, the HA surface glycoprotein binds to sialic acids on the surface of ciliated epithelial cells lining the respiratory tract (Gottschalk & Lind, 1949; Suzuki et al., 2000). Following entry, genome replication, and viral protein production, nascent virions assemble and bud from the infected cell surfaces (Pohl et al., 2016). The influenza virus NA is expressed on the surface of viral particles and infected cells and the protein assists in the budding and release of nascent virions from the cell surface (B. J. Chen et al., 2007; J. C. Lai et al., 2010; Rossman & Lamb, 2011). The NA sialidase enzymatic activity cleaves the host sialic acid receptors allowing newly formed virions to efficiently bud from the cells surface, and also increases viral penetration through mucus (Cohen et al., 2013; Wagner et al., 2002).

Both influenza virus HA and NA proteins are targets for the immune system to protect the host against infection and disease. Antibodies directed against HA bind to the protein and block receptor binding, viral fusion with and release from host cells, and NA activity (Y. Q. Chen et al., 2019; Kosik et al., 2019; Kosik & Yewdell, 2017; Whittle et al., 2011; Williams et al., 2018; Yamayoshi et al., 2017). Several mechanism(s) may inhibit NA responses following antibody binding. In addition to steric hinderance from the anti-HA antibodies, anti-NA antibodies can bind multiple epitopes on the NA protein on the cell surface during budding and sterically hinder NA activity (Y. Q. Chen et al., 2019; Gilchuk et al., 2019). For Bris/07 NA-specific elicited antibodies bound to the NA protein of Viet/04 (Fig. 3.3C), but they did not inhibit the NA enzymatic activity of the Viet/04 (H₅N₁) virus (Fig. 3.5C). Antibody binding to NA can inhibit the enzymatic activity of molecule to cleave sialic acid residues thereby reducing virus release from infected cells. In this study, NA protein vaccinations were immunogenic and antigenic. The elicited anti-NA antibodies successfully bound NA proteins as observed through ELISA (Fig. 3.3) and blocked the NA activity of several N₁ viral NA genetic clades as observed through the ELLA assay (Fig. 3.5). NA antibodies can also target infected cells for destruction via the bound antibody Fc receptor to attract macrophages and other cells for antibody-dependent cellular cytotoxicity (ADCC) but those functions were not measured here (Broecker et al., 2019; Wohlbold et al., 2017).

Overall, influenza NA proteins are attractive targets in the development of a universal influenza virus vaccines (Eichelberger & Wan, 2015; W. Sun et al., 2020; Sylte & Suarez, 2009). As outlined by the U.S. National Institutes of Allergy and Infectious Diseases, a next generation influenza virus vaccine should be 75% effective against symptomatic influenza and virus induced disease and elicit protective immunity that lasts for a minimum of one year (Erbelding et al., 2018). A broadly-reactive NA antigen was generated from N1 NA amino acid sequences using COBRA algorithms (Giles & Ross, 2011a) and termed N1-I. The N1-I COBRA NA elicited protective antibodies against four different HXN1 influenza viruses. These elicited antibodies inhibited sialidase enzymatic activity and inhibited virus replication of N1.1, N1.2, and N1.3 HXN1 influenza viruses (Fig. 3.5). In addition, these vaccines mitigated clinical signs of disease in vaccinated mice following challenge with four diverse influenza virus strains (Fig. 3.6, 3.7, 3.8, 3.9, 3.10). The ELLA assay quantifies the serological titers necessary to inhibit the influenza virus NA from cleaving 2,3- or 2,6- α sialic acids presented on fetuin, the host receptors utilized during infection (Baenziger & Fiete, 1979). In humans and animal models, polyclonal NA inhibition titers have been correlated positively with increased influenza virus protection, similar to hemagglutination inhibition titers (Monto et al., 2015; Walz et al., 2018; Weiss et al., 2020). Anti-NA antibodies are not able to inhibit the initial entry of the virus into the host cells, but they limit the viral spread during infection and contribute to immunity (Clements M-L. & Murphy, 1986; Kilbourne et al., 1968; Murphy et al., 1972; Rockman et al., 2013).

Conserved epitopes on NA proteins that are responsible for eliciting broadly reactive antibodies have been identified using monoclonal antibodies (mAbs) (Jiang et al., 2020; Shoji et al., 2011; Wan et al., 2013). For example, there was a single conserved epitope on the H1N1 and H5N1 NA proteins that elicited cross-reactive antibodies against both H1N1 seasonal, H1N1pdm, and H5N1 NA proteins (Wan et al., 2013). Prophylactic treatment of mice with mAbs that bound these conserved epitopes resulted in less weight loss and mortality in virally challenged mice compared to non-treated mice. The N1-I COBRA NA immunogen retains this conserved epitope (amino acid residues 273, 338, 339) and mice vaccinated with N1-I COBRA NA elicited antibodies that reduced the overall viral titer (Fig. 3.8D), as a result of potentially eliciting antibodies specific to this conserved NA epitope. However, this does not rule out

that neutralization and protection against viral challenge are a result of binding to multiple NA epitopes on each NA protein. Total antibody binding may not always be associated with sialidase activity, since Viet/o₄ NA and Sw/NC/1₅ NA elicited sera bound to Bris/o₇, but did not inhibit Bris/o₇ NA enzymatic activity (Fig. 3.5E, F). The similar antibody binding and NA inhibition profiles of CA/o₉ and Viet/o₄ are a combined contribution of conserved epitopes regions and originating from the same N1.1c2 clade (Job et al., 2018).

There may be a direct correlation between antibody binding to severity of disease. Mice vaccinated with the Viet/o₄ NA and then challenged with the Viet/o₄ virus had little weight loss and undetectable lung virus titers (Fig. 3.9B-D). These mice had high anti-NA antibody titers (Fig. 3.3D). Mice vaccinated with NA derived from CA/o₉ or Sw/NC/1₅ had more weight loss and higher viral titers when challenged with their respective homologous viruses (Fig. 3.6 and 3.8), but had lower titer antibodies that bound to each NA protein. Soluble tetramerized NA proteins were used to provide appropriate NA protein conformation to elicit protective antibodies, as previously described (McMahon et al., 2020). However, differences in protein integrity and chemistry could have played a role in the variation in the magnitude of antibodies elicited (Fox et al., 2013; Scheiblhofer et al., 2017). It is unlikely that glycans shielded differential epitopes between NA proteins since all NA proteins were predicted to express the same N-linked glycans (NetNGlyc 1.0) (R. Gupta et al., 2004). Other factors, such as protein stability, folding, or hydrophobicity, may have contributed to the protein's ability to elicit the immune responses. To further elucidate whether the lack of protection was due to protein integrity, different vaccine platforms can be used to deliver the NA antigen. Attenuated live reassortant viruses or virus-like particles that express NA antigens may be used in future studies to determine the contribution of the soluble protein format to these titer differences.

The addition of a standardized NA antigen component to a multi-antigen influenza vaccine provides advantages and disadvantages. The inclusion of the NA protein may slow the overall antigenic drift of the vaccine since the HA and NA antigens evolve independent of each other (Kilbourne et al., 1990), and the NA protection is not dependent on the HA subtype of the infecting virus. However, with the addition, immunodominance between proteins may occur, and studies to determine the optimal ratio

of protein will be necessary to overcome this similar to previous vaccine optimization (Y. H. Jang et al., 2014). Lastly, in a live-attenuated virus vaccine platform, the computationally derived NA protein will need maintain stability and functionality to allow viral infection to be immunogenic. Before inclusion into a multi-valent vaccine platform, the NA antigen should be confirmed to elicit NA inhibition titers and mitigate clinical signs independently of the other antigens.

The COBRA methodology was previously used to design broadly-protective influenza HA antigens (Allen, Ray, et al., 2018a; Fadlallah et al., 2020; Reneer et al., 2020; Ross et al., 2019), as well as other viral antigens, such as the E protein of dengue viruses (Uno & Ross, 2020). In this study, the COBRA methodology was applied to NA to design an antigen that elicited broadly-reactive antibodies against NI proteins from different subtypes. The COBRA NI-I antigen has the possibility of eliciting protective immune responses against both current human influenza viruses, but also zoonotic and pre-pandemic viruses from multiple subtypes, which moves a step closer to a universal vaccine antigen.

3.6 Acknowledgements

The authors would like to thank Ying Huang for technical assistance, Z. Beau Reneer for insightful discussions, Dr. Mark Tompkins' laboratory for graciously providing the A/Swine/North Carolina/154074/2015 virus, and Dr. Ralph Tripp's laboratory for graciously providing A/Swine/Nebraska/Ao1444614/2013 virus. Certain HXNI influenza A viruses were obtained through the Prevention and Control of Influenza, Centers for Disease Control and Prevention, Atlanta, GA, USA. The authors would like to thank the University of Georgia Animal Resource staff, technicians, and veterinarians for animal care, the University of Georgia Pathology and Histopathology staff for preparation of histopathology slides, and the Center for Vaccines and Immunology Protein Expression and Purification Core for providing purified protein.

3.7 Competing Interests

No competing interests.

3.8 Funding Information

This work has been funded by the National Institute of Allergy and Infectious Diseases, a component of the NIH, Department of Health and Human Services, under the Collaborative Influenza Vaccine Innovation Centers (CIVICs) contract 75N93019C00052 and in part, by the University of Georgia (UGA) (MRA-001). In addition, TMR is supported by the Georgia Research Alliance as an Eminent Scholar.

CHAPTER 4

MULTI-INFLUENZA HA SUBTYPE PROTECTION OF FERRETS VACCINATED WITH AN NI COBRA-BASED NEURAMINIDASE^I

^ISkarlupka, A. L., Blas-Machado, U., Sumner, S. F., & Ross, T. M. Submitted to PLOS Pathogens, November 2021

4.I Abstract

The neuraminidase (NA) of the influenza virus presents a promising target for next-generation influenza vaccines. Even with current vaccines, influenza continues to negatively impact the global economy, with the US facing a total estimated burden of \$11.2 billion in 2018. The Ni-I computationally optimized broadly reactive NA antigen (Ni-I COBRA NA) resulted from the combination of avian, human, and swine isolated Ni virus NA protein sequences and elicits NA inhibition titers across a panel of Ni viruses. The protection induced by vaccination with the Ni-I COBRA NA was characterized in the both the naïve and pre-immune ferret animal models with A/California/07/2009 (H1N1; CA/09) and A/Vietnam/1203/2004 (H5N1; Viet/04) influenza challenges, as well as in the CA/09 contact transmission model. Ferrets were naïve or pre-immunized with A/Singapore/6/1986 (H1N1; Sing/86) to mimic individuals imprinted and after 1986. The ferrets were prime-boost vaccinated with Addavax adjuvanted NA or HA protein (15 µg) vaccines including: mock, Ni-I COBRA NA, Viet/04 NA, CA/09 NA, A/Brisbane/59/2007 (Bris/07) NA and CA/09 HA. In both the naïve and pre-immune CA/09 challenge model, the Ni-I COBRA NA vaccinated animals maintained similar weight as the CA/09 HA control and significantly reduced viral titers compared the mock control. In the naïve Viet/04 challenge model, the Ni-I COBRA NA and Viet/04 NA vaccinated ferrets were well protected with minimal clinical symptoms and negligible weight loss. Whereas, the CA/09 NA group lost weight with 25% mortality. Vaccination with either HA or NA vaccines did not inhibit contact transmission of CA/09 to a naïve cage mate. When the receiving ferrets were vaccinated, the Ni-I COBRA NA and positive controls still mitigated disease compared to the mock group. The route of infection, intranasal or contact, adjusted the viral kinetics but did not significantly change the magnitude of the viral titer observed over the course of infection. Overall, the Ni-I COBRA elicited protection in the naïve and pre-immune ferret model with H1N1 and H5N1 infections, and mitigated disease in a contact transmission model for the vaccinated receivers. The current results indicate that the Ni-I COBRA NA performed similarly to the CA/09 HA and NA positive controls. Therefore, the Ni-I COBRA NA alone induces protection from both highly pathogenic H5N1

and human 2009 pandemic H1N1, indicating its value as a vaccine component to increase the breadth of protection induced by vaccination.

4.2 Introduction

Influenza viruses, type A and B, circulate pervasively in the global human population and upon infection, induces a contagious upper respiratory illness. Influenza virus infection often results in fatigue, fever, sneezing, body aches, nausea, and in severe cases, pneumonia and death. Type A influenza virus has a broad host species range, whereas Type B influenza viruses are mainly human isolated. Avian, swine and other host species act as reservoirs for zoonotic transmission, and lead to constant reintroduction of influenza viruses with pandemic potential due to individuals lacking pre-existing immunity to novel strains. The two major surface proteins, hemagglutinin (HA) and neuraminidase (NA), classify the influenza A viruses into subtypes. The sequentially numbered protein subtypes denote antigenically distinct groups. In humans, the H₁N₁ and H₃N₂ viral subtypes co-circulate seasonally with occasional zoonotic spillover infections, most commonly with avian-origin H₅N₁ and H₇N₉ viruses (Philippon et al., 2020). Broadly protective influenza virus vaccines are currently unavailable for seasonal human influenza or zoonotic pandemic viral variants (Levine et al., 2019). Governmental agencies prioritized the funding of the development of such a vaccine in 2019 (Y. H. Jang & Seong, 2019; Krammer et al., 2020). Influenza viruses transmit primarily through airborne transmission or direct contact with infectious individuals and surfaces. Ideally, an effective influenza virus vaccine will prevent infection and prevent transmission to another person. Vaccination can also lower viral shedding from virally exposed vaccinated individuals by either reducing the peak viral load or decreasing the shedding timeframe (Music et al., 2019). Currently, split-inactivated vaccines are non-sterilizing and infection-permissive, but vaccination reduces disease signs and adverse outcomes following infection (A. Choi et al., 2020; Ferdinands et al., 2021).

Influenza virus vaccine development has often overlooked the influenza virus neuraminidase as a potential vaccine candidate antigen. Split-inactivated vaccines are standardized based upon HA content and not quantified or standardized for NA content. The immunodominance of the HA further dampens the immune response to NA (B. E. Johansson et al., 1987; Zheng et al., 2020). The NA surface protein cleaves sialic acid receptors on the surface of cells, which the HA protein of the virus then uses as a

receptor to mediate entry into cells. In addition, NA improves viral motility, allowing the release of nascent virions from host cells and preventing self-aggregation (Krammer et al., 2018). Anti-NA polyclonal and monoclonal antibodies protect mice and ferrets from influenza virus infection (Y. Q. Chen et al., 2018; G. E. Smith et al., 2017; Wohlbold et al., 2015). The NA inhibiting antibodies decrease influenza virus disease severity; the vaccine effectiveness can be enhanced through the synergy of NA and HA inhibiting antibodies (Couch et al., 2013; Krammer et al., 2020; Monto et al., 2015).

The goal of the current study was to evaluate a next-generation neuraminidase vaccine based upon computationally optimized broadly reactive antigen (COBRA) methodology in ferrets (Giles & Ross, 2011a; Skarlupka et al., 2021). The NA antigen was designed for the N₁ influenza subtype, designated N₁-I (Giles & Ross, 2011a; Skarlupka et al., 2021). This COBRA NA antigen elicited inhibitory antibody responses to a panel of HXN₁ viruses encompassing all three genetic lineages of N₁: N_{1.1} (avian; human pandemic), N_{1.2} (human seasonal), and N_{1.3} (classical swine). In contrast, wild-type N_{1.1} and N_{1.3} antigens elicited cross-reactive NAI antibodies among the lineages, but could not inhibit the NA of H₁N₁ N_{1.2} viruses. Likewise, the antisera to the N_{1.2} NA did not inhibit the N_{1.1} or N_{1.3} clade viruses. Previously, our group demonstrated that mice vaccinated with a recombinant N₁-I COBRA NA protein were protected against viral influenza challenge. The challenge results of the N₁-I COBRA NA vaccinated groups and homologous vaccine groups were similar. Further, the N₁-I COBRA NA groups maintained lower viral titers than the mock vaccinated animals. Consequently, the protective efficacy of the NA COBRA vaccine was quantified in the ferret model.

The ferret model is the gold standard for vaccine efficacy testing due to its natural susceptibility to human influenza, the ferret's sizeable respiratory system, and similar immunological and physiological responses to vaccination and infection (Roubidoux & Schultz-Cherry, 2021). The ferret is an excellent model for pre-immunity studies that more closely model human infection due to humans experiencing immune imprinting from previous viral infections (Skarlupka & Ross, 2020). In this study, we tested the ability of the N₁-I COBRA NA to elicit protective immune responses in a naïve and H₁N₁ pre-immune ferret model. The N₁-I COBRA NA results were compared to ferrets vaccinated with homologous and

heterologous wild-type NA and HA antigens following challenges with either A/California/07/2009 (H₁N₁) or A/Vietnam/1203/2004 (H₅N₁). Vaccines were evaluated for the ability to elicit broadly reactive antibodies, protection against both morbidity and mortality, as well as the inhibition of viral transmission between ferrets.

4.3 Materials and Methods

4.3.1 Viruses

The historical H₁N₁ A/Singapore/06/1986 (Sing/86; H₁N₁; BSL-2) virus was used for establishing pre-immunity, while A/California/07/2009 (CA/09; H₁N₁; BSL-2) and A/Vietnam/1203/2004 (Viet/04; H₅N₁; BSL-3 select agent) were used for challenge infections. In addition to Sing/86 and CA/09, the following viruses were used in the hemagglutination inhibition assay (HAI) and enzyme-linked lectin assay (ELLA): A/Vietnam/1203/2004 PR8 reassortant (Viet/04xPR8; H₅N₁; BSL-2; 6:2 reassortant virus with A/Puerto Rico/8/1934 internal genes and Viet/04 HA and NA gene segments), A/Brisbane/59/2007 (Bris/07; H₁N₁; BSL-2), and A/swine/North Carolina/154704/2015 (Sw/NC/15; H₁N₁; BSL-2). Sw/NC/15 was cultured in Madin-Darby canine kidney (MDCK) cells; all other viruses were grown in egg-culture. MDCK cells were maintained with Dulbecco's modified Eagle's medium (DMEM) with 10% heat-inactivated fetal bovine serum (FBS) with 1% penicillin-streptomycin (P/S) at 37°C with 5% CO₂.

4.3.2 Vaccines

Recombinant soluble proteins were used for vaccination included: CA/09 NA, Viet/04 NA, Bris/07 NA, Ni-I COBRA NA, and CA/09 HA. The optimized coding sequence for wild-type and COBRA proteins in a pcDNA3.3 vector was expressed into soluble protein using a HEK-293T cell expression line as described previously (Ecker et al., 2020; Skarlupka et al., 2021). Protein was extracted using HisTrapExcel columns with the AKTA Pure System (GE Healthcare Bio-Sciences AB, Uppsala, Sweden). Purified proteins were concentrated with phosphate-buffered saline + 0.1% w/v sodium azide (PBSA). Protein concentration

was determined using Micro BCA Protein Assay Reagent kits (Pierce Biotechnology, Rockford, IL, USA) and stored at -80°C until used for vaccination.

4.3.3 Animals

Female Fitch ferrets (*Mustela putorius furo*) between six to fifteen months of age were sourced from Triple F Farms after descending and spaying (Gillett, PA, USA). Each animal was confirmed to be serologically naive to the A/California/07/2009 H1N1 influenza virus with sera collected prior to vaccination or pre-immunization. When not infected, ferrets were pair housed with free access to food, water, and enrichment. Ferrets were anesthetized with vaporized isoflurane before bleeds, vaccination, infection, nasal washes, and euthanasia. All animal procedures were performed following the Guide for the Care and Use of Laboratory Animals, Animal Welfare Act, and Biosafety in Microbiological and Biomedical Laboratories (AUP: A2020 II-016-YI-A6).

Ferrets were vaccinated intramuscularly in the thigh muscle with 15 µg of protein in a total volume of 500 µL. Addavax adjuvant (InvivoGen, San Diego, CA, USA), was mixed in a 1:1 ratio (250 µL sterile PBS with protein: 250 µL Addavax). Mock vaccinated groups received 250 µL of sterile PBS with 250 µL of Addavax. Four weeks following the prime vaccination, the animals received a booster vaccine of the same mixture. At least two weeks after the boost, blood was collected in BD Vacutainer SST tubes. After 30 min at room temperature (RT), serum was separated by processing the tubes at 2500 rpm for 10 min. Purified serum was stored at -20°C until analysis.

4.3.4 Direct and contact transmission ferret infections

Ferrets were directly infected either to establish pre-immunity before vaccination (Sing/86) or to challenge the vaccine groups for protection characteristics (CA/o9; Viet/o4). Direct infection was performed intranasally with 1 mL total volume with 500 µL administered to each naris. The infection dose used for Sing/86 and CA/o9 was 1×10^6 plaque-forming units (PFU)/mL. Whereas the infection dose used for Viet/o4 was 1×10^5 PFU/mL. After infection, animals were observed twice daily for clinical signs and

weighed once daily until two consecutive days without signs. On days 1, 3, 5, and 7 post-infection (p.i.) nasal washes were performed with 3 mL of sterile PBS. The receiving ferret was placed with the directly infected ferret on day 1 p.i. after nasal wash to evaluate contact transmission. The receiving ferret remained pair housed with the transmitting ferret until the end of the observation period. The receiving ferret was nasal washed on days 3, 5, 7, and 9 p.i. of the transmitting ferret, i.e., days 2, 4, 6, 8 post-contact. All nasal wash samples were stored at -80°C until viral titration.

When a cumulative clinical score of three was reached, the animal was humanely euthanized. Clinical signs with their scores were as follows: nasal discharge/sneezing/diarrhea (0.5; not used for humane endpoint calculation but used for graphical representation), lethargy (1), dyspnea (2), cyanosis (2), neurological signs (3), moribund (3), laterally recumbent (3), failure to respond to stimuli (3), weight loss of 20-25% (2), and weight loss of greater than 25% (3). The maximum of the two clinical scores recorded for each day was used for analysis.

4.3.5 Histopathological analysis

Histopathological samples were collected from designated animals prior to challenge and were euthanized with B-euthanasia on day 5 p.i. The left cranial and caudal lobes were sectioned into quarters, placed on dry ice, and stored at -80°C until viral titration. The right cranial, middle, caudal lobe, and accessory lobe were infused intratracheally with neutral-buffered, 10% formalin fixative solution (BF). The trachea and right lung were extracted and placed in BF. The submandibular lymph node was extracted and set in BF. The head was removed at the junction of the cricoid cartilage and tracheal rings. The nasal cavity was fixed with BF administration through the pharyngeal isthmus until BF drained from both nares. All samples were stored in BF for one week, after which 70% ethanol solution replaced the BF. The skull was decalcified in Kristensen's solution for two weeks. All tissues were embedded in paraffin, and sectioned as follows: coronal sections through the nasal cavity, transverse sections through the middle and inner ear, and cross sections through the submandibular lymph node, trachea, and right lung lobes. The 5 µm thick sections were stained with hematoxylin and eosin (H&E). To assess proliferation of T-cells in

the submandibular lymph nodes, CD3+ immunohistochemistry for T-cells (polyclonal rabbit anti-CD3 antibody (Dako Ao452) was performed.

Microscopic exam consisted of evaluation of the nasal cavity (at 9 levels), ear (middle and inner), trachea, and the right lung lobes (cranial, middle, and caudal) for the presence or absence of inflammation. Microscopically, lesion (tissue change or alteration) incidence, severity, and distribution were recorded. If absent (i.e., histologically normal), a score of 0 was assigned. If present, the severity of the lesions was recorded as minimal, mild, moderate, or severe, with severity scores of 1 through 4, respectively, based on an increasing extent and/or complexity of change, unless otherwise specified. Lesion distribution was recorded as focal, multifocal, or diffuse, with distribution scores of 1, 2, or 3, respectively.

All histopathological work was conducted following the US FDA Good Laboratory Practice regulations (21 CFR Part 58 and subsequent amendments) and all microscopic evaluations of the H&E stained sections was performed by a board-certified pathologist (UBM).

4.3.6 Influenza virus plaque assay

The nasal wash and lung samples were processed for viral titration. The nasal wash samples were diluted in 10-fold serial dilutions in DMEM+P/S before addition to the cells. The lung samples were weighed and then homogenized in a corresponding quantity of DMEM+P/S such that 0.1 g was resuspended in 1 mL DMEM+P/S. The homogenized lung was passed through a 0.70 µm nylon filter (Corning Cell Strainer, Sigma Aldrich, St. Louis, MO, USA). The filtrate was then diluted in 10-fold serial dilutions in DMEM+P/S before addition to the cells. The upper right quadrant of the left cranial lobe and the lower left quadrant of the left caudal lobe were processed for viral lung titers.

MDCK cells were seeded at 2.5×10^5 cells per well of a 12-well tissue-culture treated plate. The next day the confluent cells were washed with DMEM+P/S and overlaid with 100 µL of the viral sample. Plates were incubated at RT with shaking every 15 min. The cells were then washed with DMEM+P/S and overlaid with 1 mL of plaque medium (minimum essential media with P/S, 2 mM L-glutamine, 1.5 mg/mL NaHCO₃, 10 mM HEPES, 5 µg/mL Gentamycin, and 1.2% Avicel RC-591 NF (MFC corporation, PA,

USA). For Viet/o₄ virus, trypsin was not added, but for CA/o₉ virus, 1.5 µg/mL TPCK-treated trypsin was added (Sigma-Aldrich). Plates were incubated at 37°C with 5% CO₂. After 48 hours (Viet/o₄) or 72 hours (CA/o₉), plates were removed, washed with PBS, and fixed with BF for 15 min. After, the plaques were visualized by staining with 1% crystal-violet for 10 min. The plaques were counted and back-calculated to determine the PFU/mL for nasal wash viral titers and the PFU/g for lung tissue viral titers. All plaques were conducted in duplicate for each sample, and the average value was taken for analysis. The limit of detection of nasal wash and viral lung titers were 1.0 \log_{10} (PFU/mL) and 2.0 \log_{10} (PFU/g). The limit of quantification was defined as greater than or equal to 10 countable plaques, which led to reliable lower limits of 2.0 \log_{10} (PFU/mL) and 3.0 \log_{10} (PFU/g) for nasal wash and viral lung titer values respectively.

4.3.7 Hemagglutination inhibition (HAI) assay

Ferret sera were treated with three parts receptor destroying enzyme (RDE, Seneka, Japan). Sera and RDE were incubated at 37°C for 18-20 hours and then heat-inactivated at 56°C for 1 hour. After reaching RT, six parts PBS was added to the samples. The HAI assay was performed as previously described. The H₁N₁ viruses and Viet/o₄xPR8 virus were titered to 1:8 HA units/50 µL with 0.8% turkey erythrocytes (Lampire Biologicals, Pipersville, PA, USA) and 1% horse erythrocytes (Lampire Biologicals, Pipersville, PA, USA), respectively. The serum was diluted two-fold in V-bottom 96 well plates and incubated in equal volume with the virus for 20 min at RT. After which, an equal volume of the respective erythrocytes was added. After 30 min for H₁N₁ viruses and 60 min for Viet/o₄xPR8 H₅N₁ virus, the plates were tilted, and the reciprocal dilution of the last well to not be agglutinated was recorded as the HAI titer. The last column of the plate contained no sera – only PBS, virus, and erythrocytes – and served as the negative control.

4.3.8 Neuraminidase inhibition assay (NAI); Enzyme-linked lectin assay (ELLA)

Sera treatment for the ELLA assay was similar to the treatment for the HAI assay, except heat inactivation was for 8 hours to completely deactivate the NA activity of the *Vibrio cholerae* neuraminidase. The NA activity of the virus was determined as previously described and diluted to a concentration providing

90-95% NA activity (Skarlupka & Ross, 2021). From an initial dilution of 1:100, sera was diluted two-fold in Dulbecco's phosphate-buffered saline containing 0.133 g/L CaCl₂ and 0.1 g/L MgCl₂ (DPBS), 1% BSA, 0.5% Tween-20 (DPBS-BT). The sera were added to a PBS+Tween-20 (PBS-T) washed fetuin plated coated previously overnight with 100 µL of 25 µg/mL fetuin. The serial dilutions were added in 25 µL in duplicate per ferret sample. In the control wells, 50 µL of DPBS-BT was added in substitution of sera. The control wells included at least six wells with no sera and no virus for the subtraction of the background absorbance and another minimum of six wells with no sera and only virus to serve as the 100% NA activity threshold. The diluted virus was added in 50 µL, and the plate was rocked to mix. Plates were incubated at 37°C with 5% CO₂ for 16-18 hours. After which, they were washed 6X with PBS-T, and 100 µL of peanut agglutinin-HRPO (Sigma-Aldrich, St. Louis, MO) was added at a dilution of 1:1000 in DPBS-T. Plates were incubated in the dark for 2 hours at RT. After washing 3X in PBS-T, 100 µL of o-phenylenediamine dihydrochloride (OPD; Sigma-Aldrich, St. Louis, MO) in 0.05 M phosphate-citrate buffer with 0.03% sodium perborate pH 5.0 (Sigma-Aldrich, St. Louis, MO) was added to the plates. They were incubated in the dark at RT for 10 min and stopped with 100 µL of 1 N sulfuric acid. The absorbance was read at 490 nm using a spectrophotometer (PowerWave XS; BioTek, Winooski, VT, USA). The background absorbance was subtracted, and the serum-containing wells were normalized with the average of the virus-only wells defining 100% NA activity. Nonlinear regression was conducted in Prism 9.1 using the duplicates to provide the average estimated $\log_{10}(50\% \text{ NAI titer})$ for individual ferrets.

4.3.9 Statistical analysis

The data were analyzed by either a two-way ANOVA or a REML mixed effects model if data were missing. Repeated measures were used to account for the ferret variation. Initially, the interactions were fit between the two main effects (usually vaccine group and day p.i.). If the interaction was not significant with an F-test, the analysis was then conducted with only the main effects. Tukey's multiple comparison test was conducted first. If there was no significant difference between the vaccinated groups to each other, a Dunnett's multiple comparison test was conducted using the mock vaccinated as the control group.

Survival curves were analyzed using the log-rank Mantel-Cox test with asymmetrical 95% confidence intervals. The mean value with standard deviation error bars were depicted on all figures except for clinical scores. Clinical score figures depicted the standard error of the mean, with the individual values shown in the background. The offsetting values of the weight loss and viral nasal wash titers were determined by adjusting the days in increments of one, until the mock vaccinated groups were visually aligned with each other.

4.4 Results

4.4.1 Ni-I COBRA NA mitigated clinical signs and viral titers in naïve ferrets directly challenged with CA/o9 H1N1

Ferrets were vaccinated with the Ni-I COBRA NA or one of the wild-type NA or HA vaccines. Following vaccination, immunologically naïve ferrets were infected with the CA/o9 virus (Fig. 4.1A). Mock vaccinated ferrets infected with CA/o9 lost 15-20% of their body weight by day 7 p.i. (Fig. 4.2A). In contrast, ferrets vaccinated with Ni-I COBRA NA lost significantly less weight (5-7% of their original body weight) by day 3 p.i. (adj. p-value < 0.05) and then maintained that weight for the remainder of the study (Fig. 4.2A). This weight loss was similar to ferrets vaccinated with CA/o9 HA, and less than those ferrets vaccinated with wild-type NA vaccines (Fig. 4.2A). Higher clinical scores and morbidity were observed for ferrets with greater weight loss (Fig. 4.2B-C). As an example, by day 2 p.i., ferrets vaccinated with Ni-I COBRA NA or CA/o9 NA vaccines had lower scores than ferrets vaccinated with the Viet/o4 NA group. At day 4 p.i., mock vaccinated ferrets had greater clinical scores than the Ni-I COBRA NA, Viet/o4 NA, and CA/o9 NA vaccinated ferrets (Fig. 4.2B). Four of the eight mock vaccinated ferrets had high clinical scores, reached the clinical endpoint, and were sacrificed by day 5 p.i. (Fig. 4.2C). The Bris/o7 NA and mock vaccinated groups exhibited 50% and 60% survival by the end of the observation period, respectively. All other vaccinated ferrets maintained 100% survival.

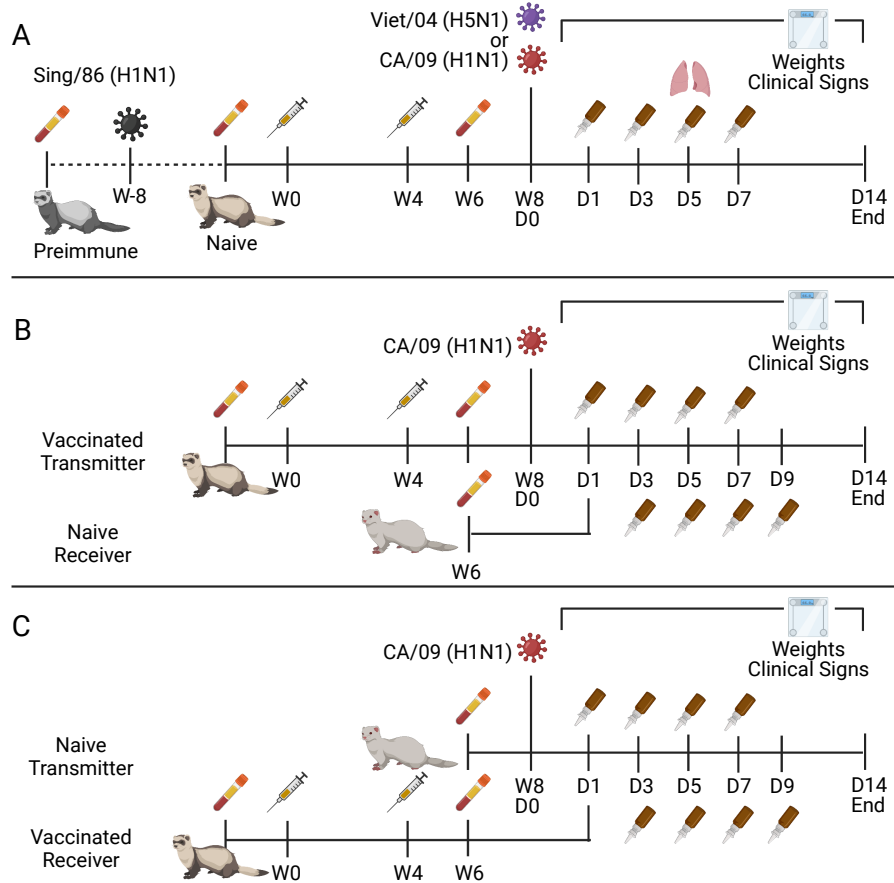


Figure 4.1: Naïve, pre-immune, and contact transmission ferret model design. Naïve or pre-immune ferrets were vaccinated with 15 µg of adjuvanted recombinant protein in a prime-boost schema after prebleeding and pre-immunization if necessary (A). Animals were challenged with either Viet/04 or CA/09. Day 5 p.i. four animals were harvested for lung viral titers and histopathology for CA/09 challenge. Contact transmission between vaccinated transmitters and influenza naïve receivers was studied by vaccinating the transmitter with 15 µg recombinant protein with adjuvant in a prime-boost, infecting with CA/09, and on day 1 p.i. co-housing the intranasally infected ferret with the naïve receiver after nasal wash (B). Contact transmission between influenza naïve infected transmitters and vaccinated receivers was similar, except the naïve ferret was infected and then the vaccinated ferret was co-housed on day 1 p.i. (C). Weights and clinical signs were recorded for all ferrets for a maximum of 14 days post-influenza exposure. Nasal washes were harvested on days 1, 3, 5, and 7 p.i. for intranasally infected animals and on days 3, 5, 7, and 9 p.i. relative to the day of infection for the transmitting ferret for the contact transmission animals.

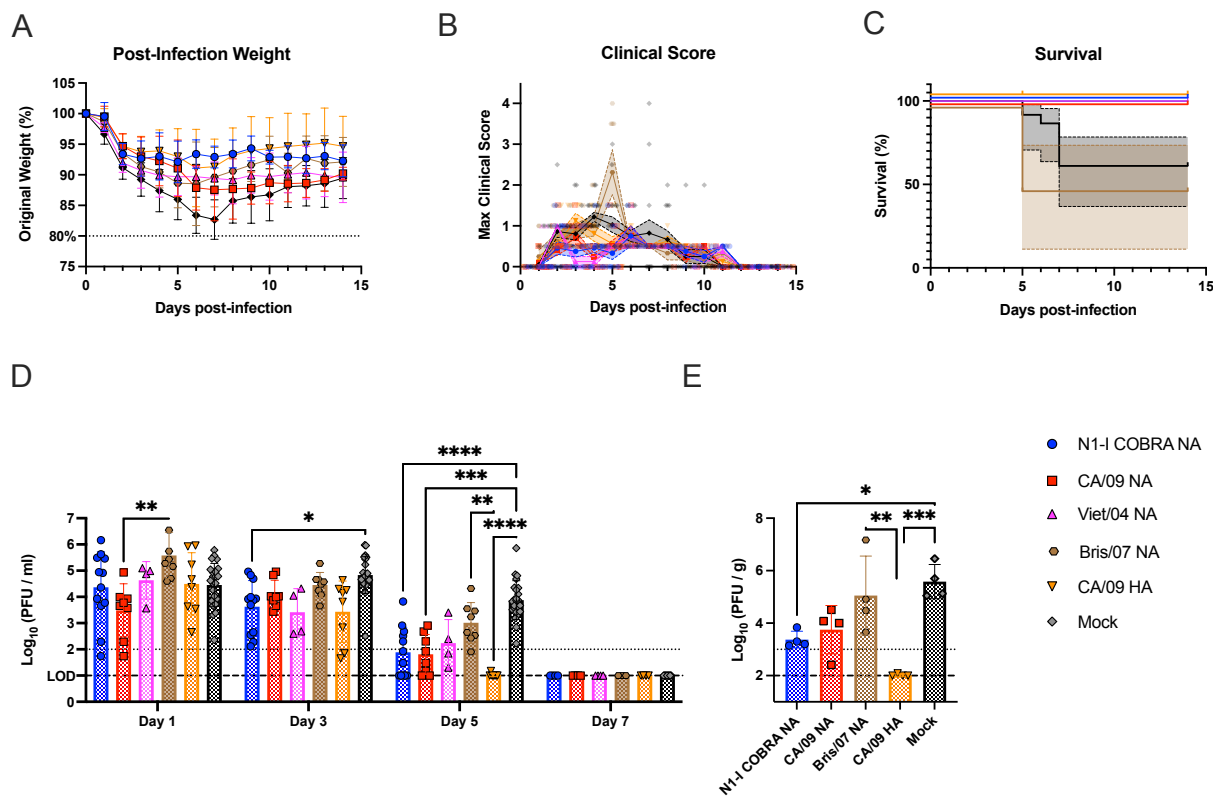


Figure 4.2: N1-I COBRA NA vaccines performed similarly to CA/o9 HA and NA vaccines in the naive ferret model intranasally challenged with CA/o9 H1Ni. (A) After challenge with CA/o9, the weight during challenge was normalized to the percentage of the original starting weight before infection. (B) The maximum clinical scores from the morning and evening checks were displayed with a score of three or greater indicating clinical endpoint. Individual ferret clinical scores are shown with the line connecting the mean score and the range of the standard error of the mean shaded. (C) The survival was determined while accounting for the censored ferrets on day 5 p.i. that were purposefully removed from the study for sample collection. The 95% asymmetrical confidence intervals are shown for the groups that did not have 100% survival. (D) The viral nasal wash titers for all vaccinated groups were determined through plaque assay and analyzed with a mixed effects model. (E) The viral lung titers were quantified by plaquing homogenized tissue each the upper and lower left lung lobes. The lobe location was not a significant factor, and thus the titers were analyzed with a one-way ANOVA. Viral lung titers were not harvested for the Viet/o4 NA group. The limit of detection (LOD; dashed line) was 1.0 \log_{10} (PFU/ml) and 2.0 \log_{10} (PFU/g) for the nasal wash titers and lung titers, respectively. The limit of quantification (dotted line) was 2.0 \log_{10} (PFU/ml) and 3.0 \log_{10} (PFU/g) for the nasal wash titers and lung titers, respectively. Tukey's test for multiple comparisons was used for viral titer comparisons. All error bars represent standard deviation. The minimum weight before clinical endpoint was 75% with 80% denoting an increase in clinical scoring. Adjusted p-value: * = < 0.05, ** = < 0.01, *** = < 0.001, **** = < 0.0001.

Over the course of infection, nasal wash samples were taken every other day to quantify viral titer in the upper respiratory tract (Fig. 4.2D). Virus was recovered from all vaccinated ferrets at day 1 p.i. and not detectable by day 7 p.i. On day 3 p.i., Ni-I COBRA NA vaccinated ferrets had significantly lower viral titers than the mock group. By day 5 p.i., the CA/o9 HA, Ni-I COBRA NA, and CA/o9 NA ferrets had viral titers significantly lower than the mock, and at or near the limit of detection ($1.0 \log_{10}(\text{PFU/mL})$). The Bris/o7 NA and Viet/o4 NA groups were not significantly different from mock, with the Bris/o7 NA having a higher mean titer on day 5 p.i. than Viet/o4 NA. These results were corroborated by the viral lung titers of the left lung lobes collected on day 5 p.i. (Fig. 4.2E). The CA/o9 HA group was below the limit of detection ($2.0 \log_{10}(\text{PFU/g lung tissue})$). The Ni-I COBRA NA group had significantly lower viral loads compared to the mock group (adj. p-value = 0.0167). The antigenically distinct Bris/o7 NA group was not significantly different from mock, and had a greater mean titer than the CA/o9 HA group. Again, the Ni-I COBRA NA performed similarly to the CA/o9 positive controls.

In addition to lung viral titers, histopathological samples were analyzed at day 5 p.i. (Fig. 4.3, 4.4, 4.5 and 4.6). Of all tissues examined, significant tissue alterations consisted of tissue inflammation, which was most consistently observed in the lungs, followed by the nose. The severity and distribution of the inflammation in the right lung was significantly greater in all vaccine groups compared to the unchallenged unvaccinated control group (Fig. 4.3A and Fig. 4.4). The inflamed lung tissue was hyperemic and hypercellular about the airways (bronchi and bronchioles), respiratory (or terminal) bronchioles, and blood vessels. In the most severe cases, the terminal bronchioles had necrosis and sloughing of the mucosa, with hypertrophy and hyperplasia of the adjacent mucosal epithelia. The sloughed, necrotic epithelia extended into the adjacent alveoli, which contained foamy macrophages. In the adjacent blood vessels, mild to moderate collections of lymphocytes obscured and expanded the perivascular tissues and extended into the adjacent alveolar and terminal bronchiolar interstitial tissue. In the larger bronchioles, the mucosa was thickened and hypercellular, with loss of cilia. Within a loose fibrocollagen tissue stroma, lymphocytic, plasmacytic and neutrophilic infiltrates obscured and expanded the peribronchiolar and peribronchial tissues; infiltrates often extended into the lumens through the mucosal walls and periph-

erally into and between the bronchiolar smooth muscles, peribronchiolar and bronchial blood vessels, and spaced bronchiolar glands. The lumens of the larger bronchioles and bronchi contained sloughed necrotic cells, neutrophils, necrotic debris, and proteinaceous material mixed with mucus.

Of the vaccine groups, the CA/o9 HA had significantly less inflammation compared to all NA vaccine groups. Comparing the degree of inflammation of the Ni-I COBRA and CA/o9 NA groups, they had the same mean severity score, which was lower than that of the mock vaccinated although insignificantly. Inflammation was observed in the lung of all challenged animals. Inflammation in the trachea was more variable (Fig. 4.3B). The CA/o9 NA group had a greater inflammation score than the unchallenged animals, and 100% of the animals having signs of inflammation. The mock challenged animals had similar inflammation levels with 75% of the animals having inflammation in the trachea. Comparatively, Ni-I COBRA NA and CA/o9 HA vaccine groups had an inflammation incidence of 50% and 25% respectively. The middle/inner ear was similar to the trachea, with the prevalence of inflammation varying between groups (Fig. 4.3C). Ni-I COBRA NA, CA/o9 NA and unchallenged animals had the similar profile of 25% prevalence with one animal exhibiting a score of two. The CA/o9 HA vaccinated group had 50% prevalence with two severity scores of three and four. The mock vaccinated animals had 100% prevalence of inflammation with a mean of 2.5 severity score. There were no statistically significant comparisons between the middle/inner ear samples.

Of the nasal cavity sections, the unchallenged animals had a low level of inflammation further in the nasal cavity between sections three to eight (Fig. 4.3D and Fig. 4.5). The inflamed nose tissue was diffusely hyperemic and hypercellular. Large number of neutrophils and macrophages, mixed with debris and embedded in basophilic mucinous material filled the nasal meatus and covered the mucosa. In some areas, there was loss of ciliated epithelia and replacement with low cuboidal to squamous epithelia. Neutrophils expanded the loose tissues of the underlying lamina propria and often extended into the overlying mucosa (leukocytic exocytosis). Neutrophil, macrophage, and lymphocytic infiltrates extended along the loosely arranged lamina propria/submucosa between the spaced nasal glands and dilated lymphatics and blood-engorged vessels. For all challenged animals regardless of vaccine group, the inflammation was greater than

the unchallenged, but no different when compared to each other. The submandibular lymph node had no inflammation, lymphocyte necrosis, or lymphoid depletion across all groups. The T-cell populations were investigated through immunohistochemistry. The lymphoid hyperplasia of the CD₃+ cells were elevated in all challenged groups when compared to the unchallenged, but not different among each other (Fig. 4.6).

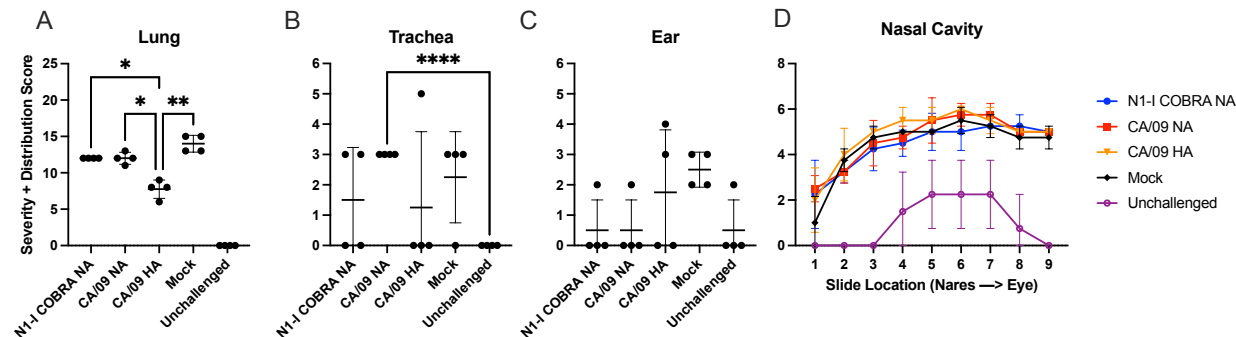


Figure 4.3: Ni-I COBRA NA vaccine induced similar inflammation in the upper and lower respiratory tract as the CA/09 HA and CA/09 NA vaccines in naïve ferret model after intranasal challenge with CA/09 H₁N₁. H&E-stained formalin-fixed and embedded tissues were scored for the severity and distribution of inflammation. (A) The NA-based vaccines had the same mean severity score and were significantly greater than the CA/09 HA vaccine group. All groups were significantly different ($p < 0.01$) compared to the unchallenged group (not shown). (B) The trachea was examined for inflammation and the CA/09 NA vaccinated group had higher incidence and mean severity scores compared to all other groups. (C) The inflammation in the middle and inner ear were mild. The mock group had 100% incidence. (D) Sections of the nasal cavity from the nares to the eye were examined for inflammation. All challenged animals were similar in inflammation compared to the unchallenged group. A two-way repeated measures ANOVA with Tukey's test for multiple comparisons was used for statistical analysis of the lung, trachea, and ear sections, and the same analysis conducted separately for the nasal cavity sections.

4.4.2 Ni-I COBRA NA mitigated clinical signs and viral nasal wash titers in H₁N₁ pre-immune ferrets directly challenged with CA/09 H₁N₁

pre-immunity to a historical H₁N₁ influenza virus was established in ferrets by intranasal inoculation of Sing/86 H₁N₁ influenza virus, (Fig. 4.1A) and they were vaccinated after with NA protein vaccines. After challenge with CA/09, pre-immune ferrets that were mock vaccinated lost 10% of their original

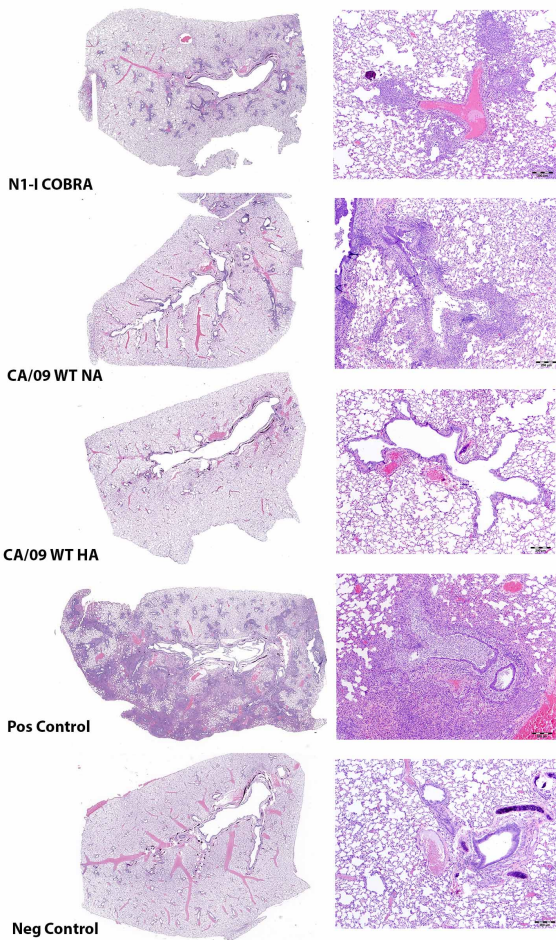


Figure 4.4: H&E staining of CA/09 challenged ferret lungs. Ferrets were vaccinated with Ni-I COBRA NA, CA/09 NA, and CA/09 HA proteins in a prime-boost regimen. Vaccinated and unvaccinated (Pos Control) were challenged with CA/09 virus intranasally, and lungs harvested on day 5 p.i. Tissues from unvaccinated unchallenged ferrets were also harvested (Neg Control). Formalin-fixed paraffin embedded tissue was stained with H&E for visualizing inflammation. (Left) Lower magnification of lung sections. (Right) Closer examination of the bronchioles of the lung with a scale bar of 200 μm .

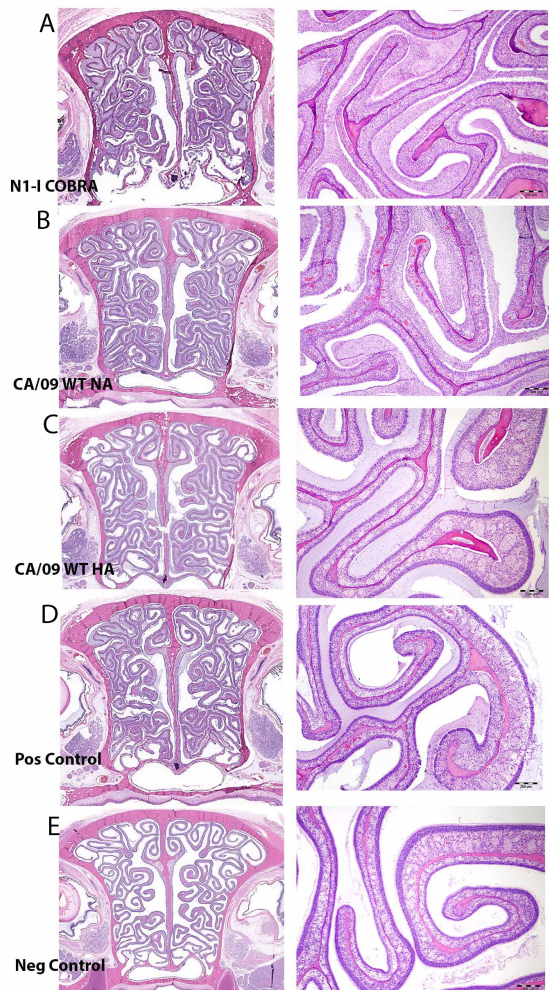


Figure 4.5: H&E staining of CA/09 challenged ferret nasal cavity. Ferrets were vaccinated with N1-I COBRA NA, CA/09 NA, and CA/09 HA proteins in a prime-boost regimen. Vaccinated and unvaccinated (Pos Control) were challenged with CA/09 virus intranasally, and nasal cavities harvested on day 5 p.i.. Tissues from unvaccinated unchallenged ferrets were also harvested (Neg Control). Formalin-fixed paraffin embedded tissue was stained with H&E for visualizing inflammation. (Left) Entire nasal cavity section. (Right) Closer examination of the nasal cavity turbinates with a scale bar of 200 μm .

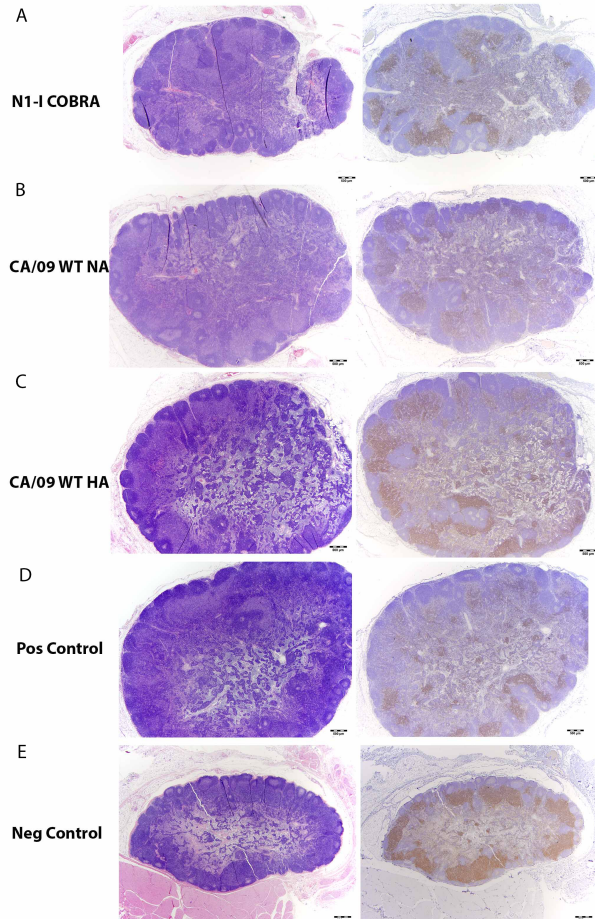


Figure 4.6: H&E staining and CD3+ immunohistochemistry of CA/09 challenged ferret submandibular lymphnode. Ferrets were vaccinated with N1-I COBRA NA, CA/09 NA, and CA/09 HA proteins in a prime-boost regimen. Vaccinated and unvaccinated (Pos Control) were challenged with CA/09 virus intranasally, and the submandibular lymphnode was harvested on day 5 p.i.. Tissues from unvaccinated unchallenged ferrets were also harvested (Neg Control). (Left) Formalin-fixed paraffin embedded tissue was stained with H&E for visualizing inflammation, lymphocyte necrosis, and lymphoid depletion or atrophy with a scale bar of 500 μ m. (Right) Lymphode section stained for CD3+ for visualizing CD3+ lymphoid hyperplasia with a scale bar of 500 μ m.

body weight by day 5 p.i (Fig. 4.7A). There was little or no weight loss for pre-immune ferrets that were vaccinated with the Ni-I COBRA NA, Viet/o₄ NA, and CA/o₉ NA vaccines. pre-immune vaccinated ferrets had an average clinical sign score of 0.5 (Fig. 4.7B) with the mock vaccinated ferrets maintaining an average score of 1 for days 2 to 4 p.i.. During infection, three mock ferrets recovered, and one reached the clinical endpoint (Fig. 4.7C). pre-immune, mock vaccinated ferrets had significantly higher viral nasal wash titers (1.0-2.0 \log_{10} (PFU/mL) compared to pre-immune NA vaccinated ferrets, regardless of the NA vaccine (Fig. 4.7D). There was no statistical difference in the nasal wash titers between any of the pre-immune, NA vaccinated ferret groups. Viral nasal wash titers were undetectable by day 5 p.i.

4.4.3 Ni-I COBRA NA mitigated clinical signs in naïve ferrets directly challenged with Viet/o₄ H₅N₁ virus

The efficacies of the vaccines were tested in the highly pathogenic Viet/o₄ virus challenge model with naïve vaccinated ferrets. Mock vaccinated naïve ferrets had a continuous weight loss after infection, and all of the ferrets reached clinical endpoint by day 6 p.i. (Fig. 4.8A-C). Naïve ferrets vaccinated with CA/o₉ NA vaccines lost 5% of their original weight by day 4 p.i. with slow decline to 10% of their body weight by day 9 p.i. (Fig. 4.8A). Ferrets vaccinated with the Ni-I COBRA NA or the Viet/o₄ NA all survived challenge with little to no weight loss or clinical signs over the 14 days of observation (Fig. 4.8A-C). There were no viral nasal wash titers detected at any time point post-infection.

4.4.4 pre-immunity to historical H₁N₁ influenza viruses mitigated clinical signs and mortality when directly challenged with Viet/o₄ H₅N₁ influenza virus compared to naïve animals

Ferrets that were initially pre-immunized with the Sing/86 H₁N₁ influenza virus, then vaccinated, and then challenged with Viet/o₄ virus had no weight loss, had minimal clinical signs, and no mortality over the course of the infection (Fig. 4.8D-E). No viral nasal wash titers were detected over the course of

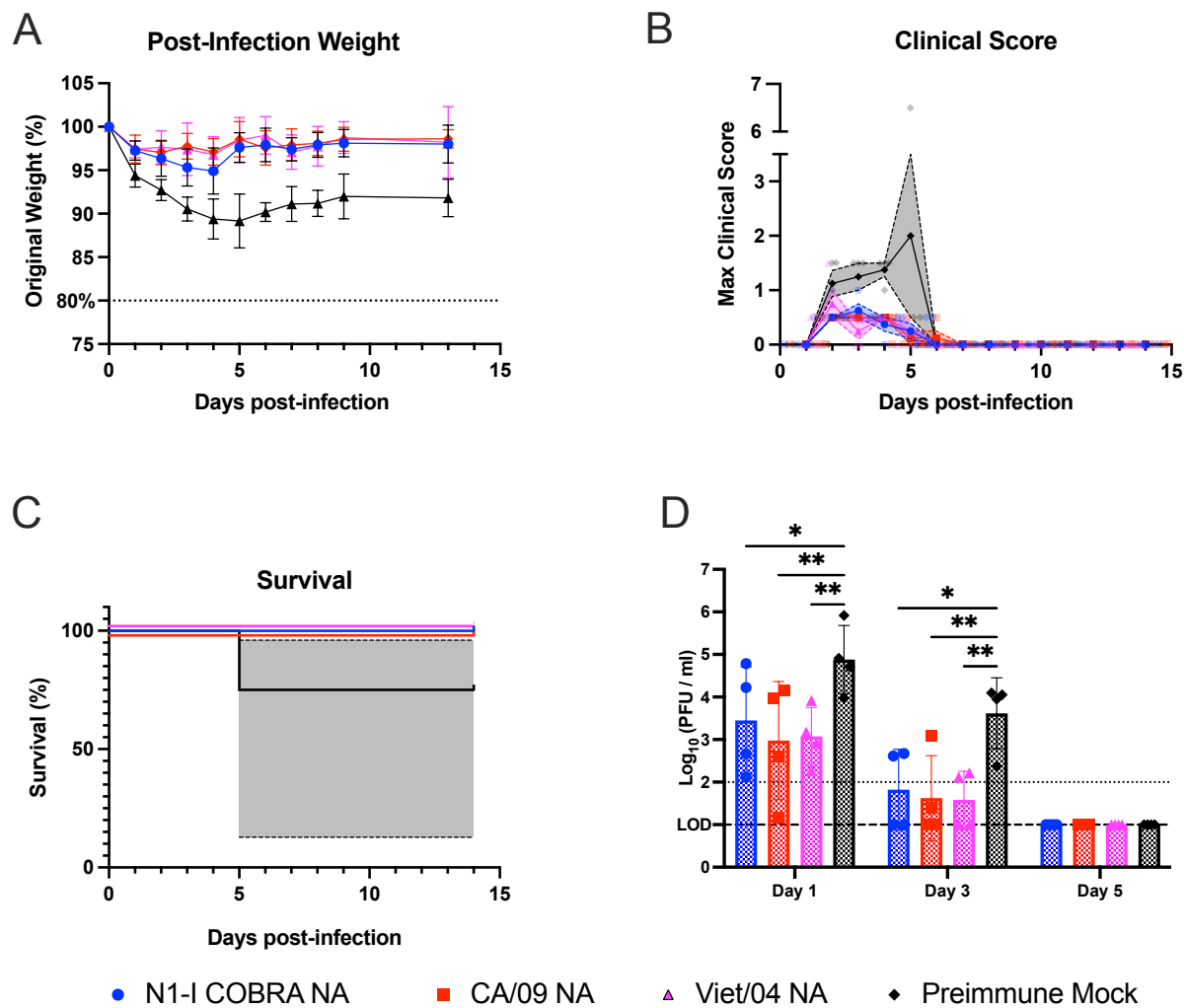


Figure 4.7: NA vaccinated ferrets pre-immunized with Sing/86 H1N1 exhibited minimal clinical signs after intranasal challenge with CA/09 H1N1. (A) After challenge with CA/09, the weight during challenge was normalized to the percentage of the original starting weight before infection. (B) The maximum clinical scores from the morning and evening checks were displayed with a score of three or greater indicating clinical endpoint. Individual ferret clinical scores are shown with the line connecting the mean score and the range of the standard error of the mean shaded. (C) The survival percentage for each group was determined. (D) The nasal wash titers for all vaccinated groups were determined through plaque assay. The limit of detection (LOD; dashed line) was $1.0 \log_{10}(\text{PFU}/\text{ml})$, and the limit of quantification (dotted line) was $2.0 \log_{10}(\text{PFU}/\text{ml})$. A two-way repeated measures ANOVA and Dunnett's test for multiple comparisons was used for statistical analysis with the mock vaccinated as the control group. All error bars represent standard deviation. The minimum weight before clinical endpoint was 75% with 80% denoting an increase in clinical scoring. Adjusted p-value: * = < 0.05, ** = < 0.01, *** = < 0.001, **** = < 0.0001.

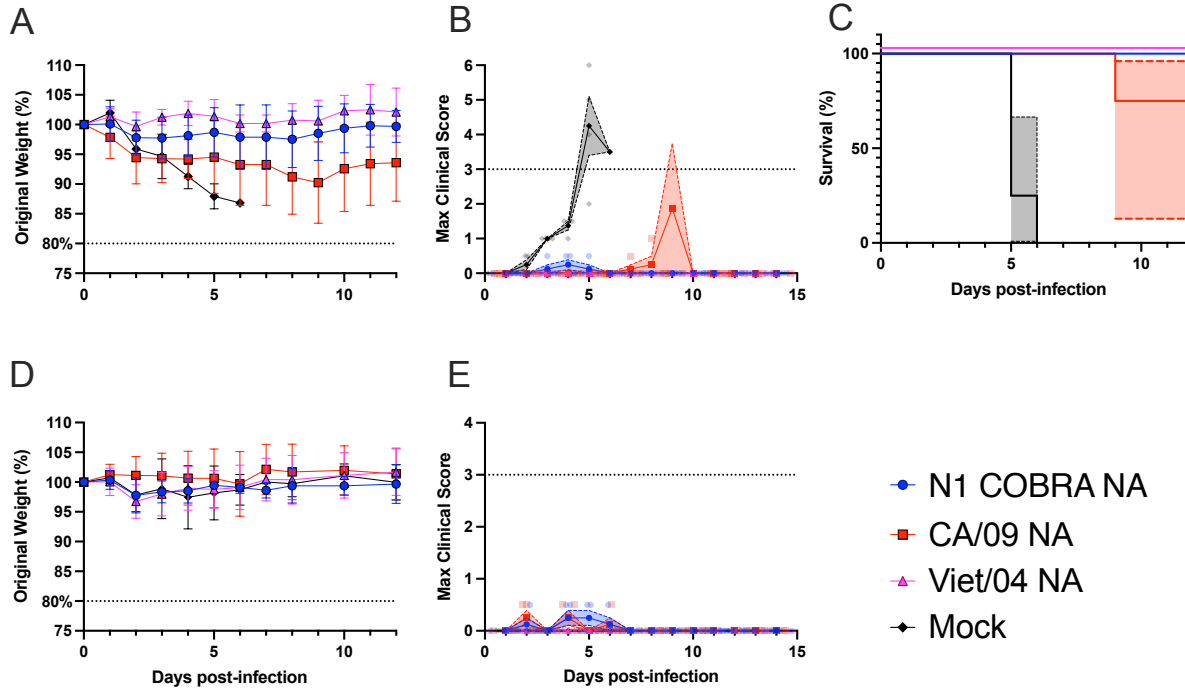


Figure 4.8: Ni-I COBRA NA vaccine performed similarly to the Viet/o₄ NA vaccine in the naïve ferret model intranasally challenged with Viet/o₄ H₅N₁. (A) After challenge with Viet/o₄, the weight during challenge was normalized to the percentage of the original starting weight before infection. (B) The maximum clinical scores from the morning and evening checks were displayed with a score of three or greater indicating clinical endpoint. Individual ferret clinical scores are shown with the line connecting the mean score and the range of the standard error of the mean shaded. (C) The survival percentage for naïve ferret model were determined for each vaccine group. (D) Weights were also monitored for the Sing/86 H₁N₁ pre-immune group, in addition to the clinical signs (E). Survival was 100% for all groups in the pre-immune vaccinated Viet/o₄ challenge model. All error bars represent standard deviation. The minimum weight before clinical endpoint was 75% with 80% denoting an increase in clinical scoring.

infection. There was no distinguishable difference between pre-immune ferrets vaccinated with the Ni-COBRA NA, CA/o9 NA, or Viet/o4 NA vaccines and pre-immune mock vaccinated ferrets. When compared to the mock vaccinated naïve ferret group in Fig. 4.8A-C, the mock vaccinated pre-immune ferrets had less clinical manifestations due to Sing/86 pre-immunity.

4.4.5 Serological responses following vaccination

Serum samples were collected from each ferret (4.1) and assayed for the elicitation of anti-NA antibodies with the ability to inhibit NA enzymatic activity against a panel of HxN1 viruses (Fig. 4.9 and Fig. 4.10). The Ni-I COBRA NA elicited antibodies with ELLA activity to all four viruses in the panel. Not all of the Ni-I COBRA NA vaccinated animals seroconverted to Bris/o7 (Clade: Ni.2). The CA/o9 NA and Viet/o4 NA vaccinated animals only had ELLA titers to the CA/o9 (Clade: Ni.1), Viet/o4 (Clade: Ni.1) and Sw/NC/15 (Clade: Ni.3) viruses. The Bris/o7 NA antibodies was even more restricted in breadth, with ELLA titers to only Bris/o7 and Sw/NC/15 viruses.

Sera with HAI activity against CA/o9 was detected in naïve ferret vaccinated with CA/o9 HA (Fig. 4.11A). The CA/o9 HA vaccine-elicited titers ranged between $4.32\text{-}9.32 \log_2(\text{HAI titer})$, with a mean of $7.031 \log_2(\text{HAI titer})$. All ferrets pre-immunized with Sing/86 H1N1 seroconverted with an average \log_2 titer of 7.978 ± 0.5453 standard deviation (Fig. 4.11B). pre-immunity elicited no cross-reactive HA antibodies that inhibited either the CA/o9 H1N1 or Viet/o4xPR8 H5N1 influenza virus HA activity.

4.4.6 Contact transmission from vaccinated ferrets to naïve ferrets

To determine if NA vaccination reduces the ability of infected ferrets to transmit virus to another co-housed ferret, naïve receiver ferrets were co-housed with CA/o9 influenza virus infected, HA- or NA-vaccinated transmitter ferrets 1 day p.i. (4.1). Contact transmission occurred between all vaccinated transmitter and influenza-naïve receiver pairs. All naïve receiving ferrets lost body weight that was not statistically different compared to mock-vaccinated animals, regardless of the transmitting ferret's vaccination (F-statistic: 0.1029; DF: 4, 15; p-value: 0.9797) (Fig. 4.12A). Further, the transmitting ferret's vaccine

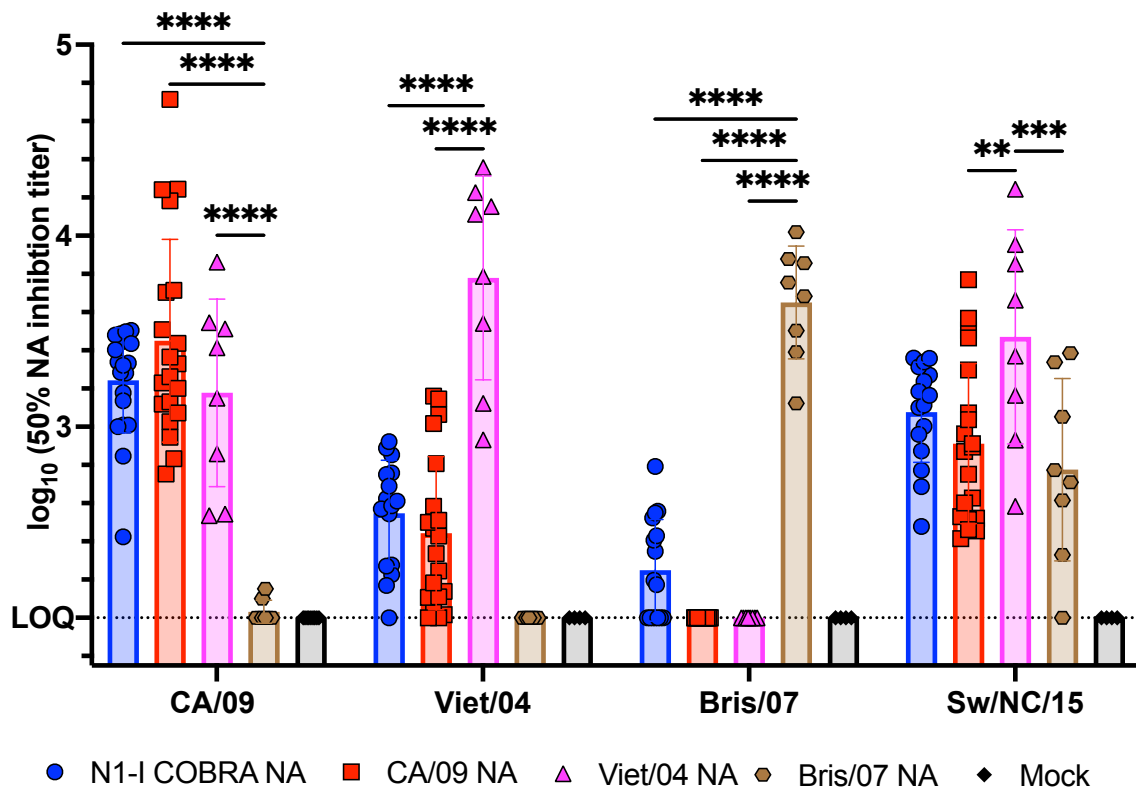


Figure 4.9: N1-I COBRA NA vaccine elicited NA-inhibiting antibodies to a panel of genetically diverse HXN1 viruses. The 50% NA inhibition (NAI) titers elicited by the NA-based vaccines were measured for a panel of N1 influenza viruses that belong to different N1 genetic clades. Nonlinear regression of the ELLA results using RDE treated ferret sera was used to determine the 50% NAI titers (Fig. 4.10). The N1-I COBRA NA vaccination elicited inhibitory antibodies to viruses in the panel. The CA/09 NA and Viet/04 NA elicited cross-reactive NAI antibodies to each other. The Bris/07 NA vaccine elicited NAI antibodies to itself. All NA vaccines elicited antibodies that inhibited the Sw/NC/15 virus. The initial serum dilution used for the ELLA assay (1:100) was defined as the limit of quantification at $2.0 \log_{10}(50\% \text{NAI titer})$.

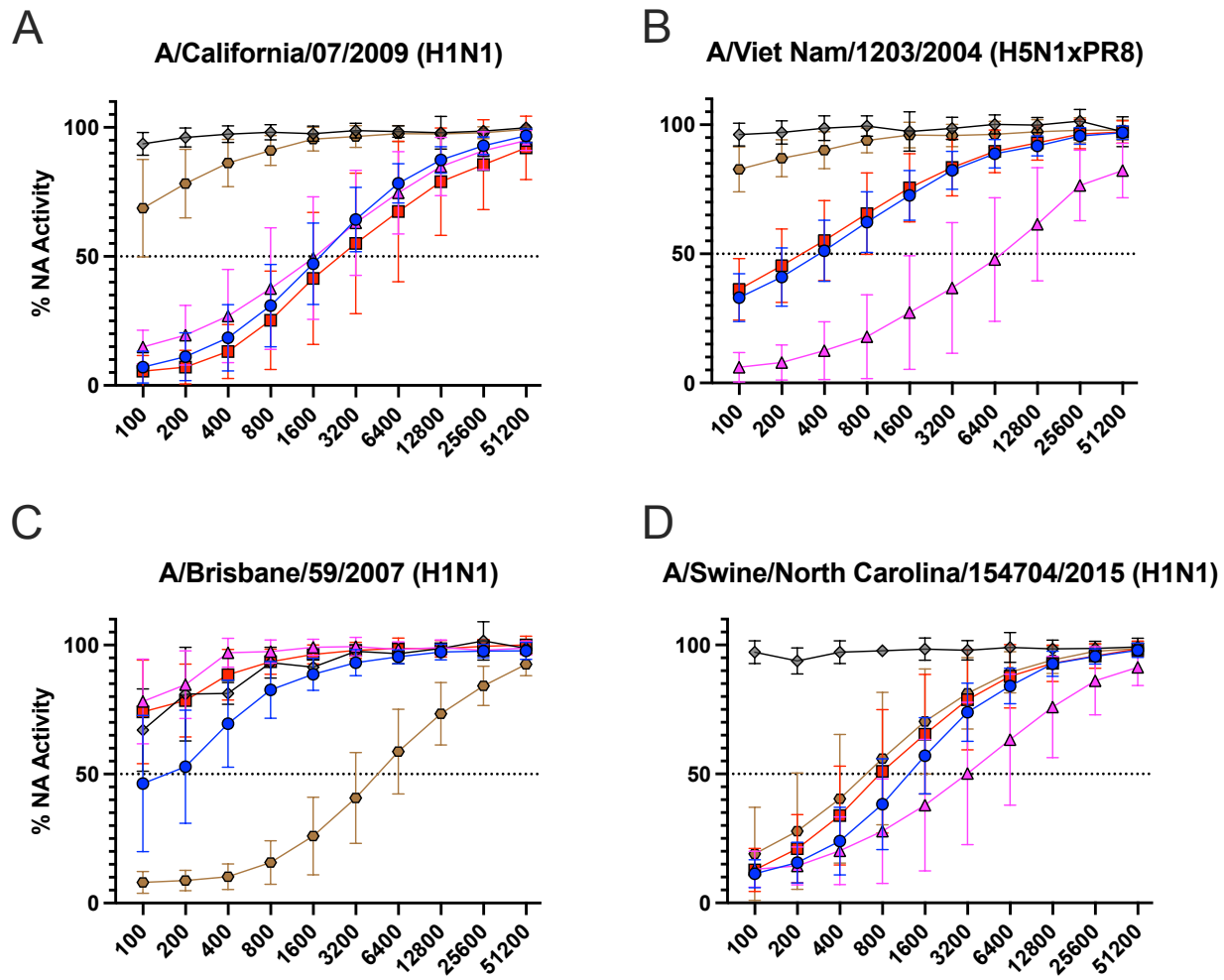


Figure 4.10: NA enzymatic inhibition curves of four N1 influenza viruses from sera taken from NA vaccinated ferrets. On average the Ni-I COBRA NA antigen inhibited all four strains, reducing NA activity by at least 50%. The RDE treated sera were two-fold diluted from a starting dilution of 1:100 to a dilution necessary to quantify the NAI titer. The mean of ferret curves in duplicate is shown as the solid line with standard deviation error bars. NA activity was normalized with 100% NA activity being defined with a ‘virus only with no sera’ control that included at least 8 wells. The dotted line indicates 50% NA activity.

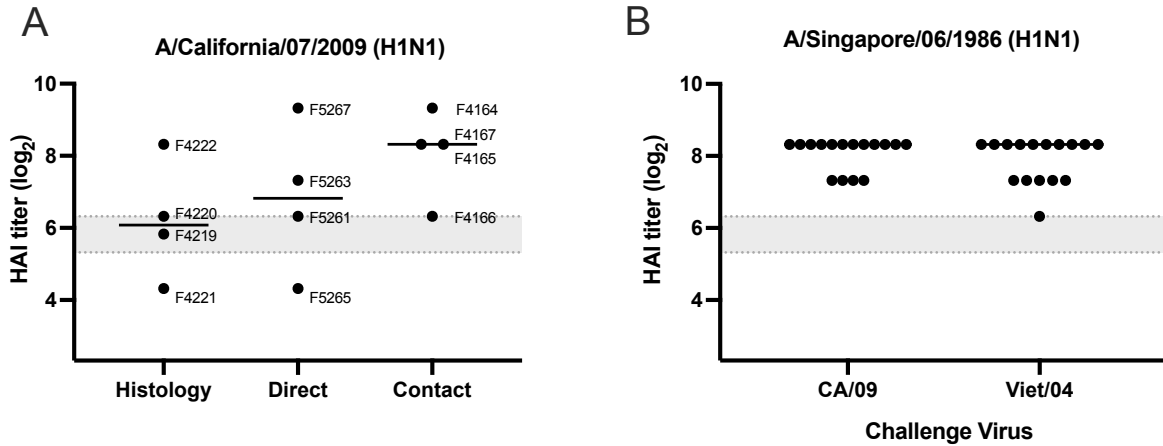


Figure 4.II: HAI results of CA/09 HA vaccinated and Sing/86 pre-immunized ferrets. (A) HAI titers for ferrets vaccinated with CA/09 HA, split up by study group, with the mean of all ferrets in that group shown as a solid line. Ferret identification numbers are also given to identify each data point. (B) HAI titers to Sing/86 were measured after Sing/86 pre-immunization and before vaccination. The x-axis indicates the challenge virus group of either CA/09 and Viet/04. Dotted lines indicate 1:40 and 1:80 HAI titers.

group did not significantly contribute to the naïve receiving ferrets' clinical scores (F-statistic: 1.916; DF: 3, 12; p-value: 0.1809), or nasal wash titer (F-statistic: 2.549; DF: 4, 15; p-value: 0.0825) (Fig. 4.12B and D).

4.4.7 Contact transmission from naïve ferrets to vaccinated ferrets

A second set of vaccinated ferrets were designated as the receiver ferrets and co-housed with naïve ferrets that were intranasally infected with CA/09 virus (Fig. 4.13). All the naïve transmitting ferrets exhibited similar weight loss, clinical scores, and nasal wash titers amongst each other (Fig. 4.2A-D). The mock receiver ferrets lost 15-20% of their body weight, whereas CA/09 HA vaccinated receiver ferrets only lost marginal weight over the 14 days of co-housing (Fig. 4.13A). In contrast, ferrets vaccinated with the Ni-I COBRA NA lost 10% of their original body weight by day 7 p.i., which was not statistically different to ferrets vaccinated with CA/09 NA vaccine (Fig. 4.13A). The Ni-I COBRA NA was statistically different to CA/09 HA on days 4, 9, and 12 p.i. The CA/09 NA group initially maintained weight, but steadily lost

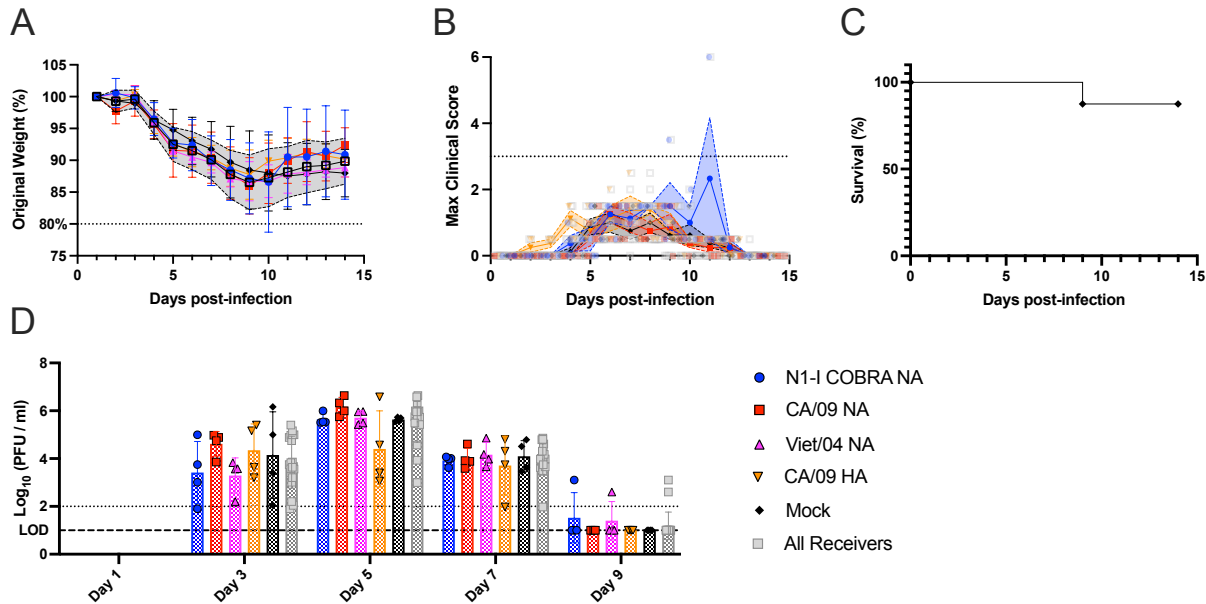


Figure 4.12: Vaccination of contact transmitting ferrets did not limit the transmission to other ferrets or affect the receiving ferret's clinical or viral outcomes. Naïve ferrets were co-housed one day after the CA/09 intranasal infection of ferrets vaccinated with different influenza protein antigens (see legend; Fig. 4.1B). The normalized weights, regardless of the transmitting ferret's vaccination status, were not significantly different, and the combination of all the naïve receivers is shown in grey with the 'All Receivers' group (A). The clinical scores (B), and survival (C) were recorded over the course of the study and shown as All Receivers. (D) The viral lung titers determined through plaque assay were also unsignificant. The maximum clinical scores from the morning and evening checks were displayed with a score of three or greater indicating clinical endpoint. Individual ferret clinical scores are shown with the line connecting the mean score and the range of the standard error of the mean shaded. Mixed effects analysis or two-way ANOVA with repeated measures were used for statistical analysis. All error bars represent standard deviation. The minimum weight before clinical endpoint was 75% with 80% denoting an increase in clinical scoring.

weight over time, never dropping below an average of 5% of their original body weight. This decrease in the group's average weight and large standard deviation bars was due to two of the four ferrets experiencing considerable weight loss and the others maintaining their original weight during infection (Fig. 4.14B). Overall, the HA vaccine provided complete mitigation of weight loss, and the NA vaccines, including the N1-I COBRA NA, provided partial mitigation of weight loss with few clinical signs observed (Fig. 4.13A-B). All vaccinated ferrets survived the challenge (Fig. 4.13C).

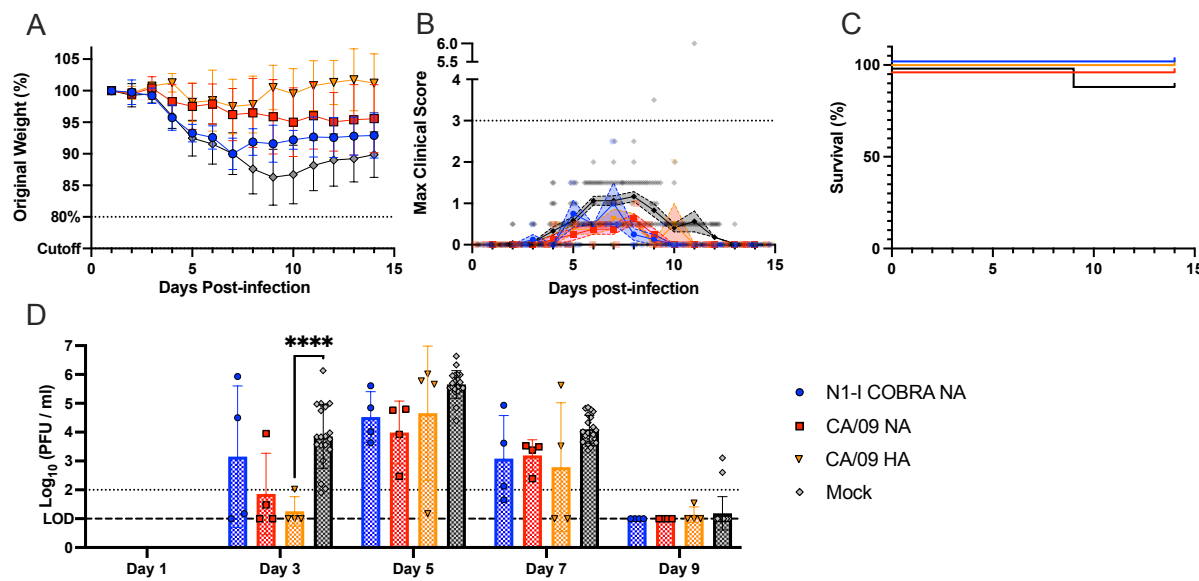


Figure 4.13: Vaccination of contact receiving ferrets did not limit transmission. Vaccinated ferrets were co-housed one day after the CA/o9 intranasal infection of naive ferrets (Fig. 4.1C). (A) The weight during challenge were normalized to the percentage of the original starting weight before co-housing on day 1 p.i. (B) The maximum clinical scores from the morning and evening checks were displayed with a score of three or greater indicating clinical endpoint. Individual ferret clinical scores are shown with the line connecting the mean score and the range of the standard error of the mean shaded. (C) The survival percentage for each group was determined. (D) The nasal wash titers for all vaccinated groups were determined through plaque assay. The limit of detection (LOD; dashed line) was $1.0 \log_{10}(\text{PFU}/\text{ml})$, and the limit of quantification (dotted line) was $2.0 \log_{10}(\text{PFU}/\text{ml})$. Mixed effects analysis with repeated measures was used for statistical analysis. Tukey's test for multiple comparisons was used for the weight analysis, and Dunnett's test was used for nasal wash titers with the mock receivers as the control group. All error bars represent standard deviation. The minimum weight before clinical endpoint was 75% with 80% denoting an increase in clinical scoring. Adjusted p-value: * = < 0.05, ** = < 0.01, *** = < 0.001, **** = < 0.0001.

The viral nasal wash titers did not differ significantly between the HA and NA vaccinated receivers (Fig. 4.13D). In comparison to the mock vaccinated receiver ferrets, only the CA/09 HA vaccinated receivers had significantly lower viral nasal wash titers on day 3 p.i. Contact transmission provided increased variability in the nasal wash titers on day 3 p.i. The standard deviation of the mock receivers was ranged from 0.478 to $1.104 \log_{10}(\text{PFU/mL})$ between days 3-9 p.i. The Ni-I COBRA NA vaccinated receiver ferrets had a wide standard deviation of $2.453 \log_{10}(\text{PFU/mL})$ on day 3, followed by more narrow intervals up to day 9 p.i. Viral titers peaked for all groups of ferrets at day 5 p.i. and then declined to undetectable levels on day 9 p.i. (Fig. 4.13D).

4.4.8 Comparison of the inoculation methods

The results from the two ferret transmission studies were compared to determine differences in vaccine effectiveness between the two routes of virus administration: intranasal and contact. The contact transmission weights were normalized by three days to match the intranasal inoculated ferret study (Fig. 4.14A-D). The Ni-I COBRA NA vaccinated ferrets had similar weight loss profiles regardless of the inoculation method. Ferrets maintained between 90-97% of their original body weight (Fig. 4.14A). CA/09 NA vaccinated receiver ferrets lost less body weight than the intranasally inoculated transmission ferrets, however these animals also had the largest variability (Fig. 4.14B). The receiver ferrets that lost weight when using the direct contact method had weight loss curves that were similar to the weights of transmission ferret directly receiving virus via the intranasal method. Similar results were observed for CA/09 HA vaccinated ferrets (Fig. 4.14C). The mock ferrets had similar responses to both inoculation methods, but had greater variability with a range of peak weight loss (80-95%) (some animals reached clinical endpoint at bodyweight 80% from the resulting increase in clinical score) (Fig. 4.14D).

The nasal wash titers from intranasal and contact transmission were also compared by offsetting the contact groups by two days (Fig. 4.14E-H). The mean peak viral titer did not differ between the intranasal and contact methods in any of the vaccine groups. The mock vaccinated contact group had a significantly higher peak titer compared to the intranasal inoculated ferrets (adj. p-value: 0.0001). All groups reached

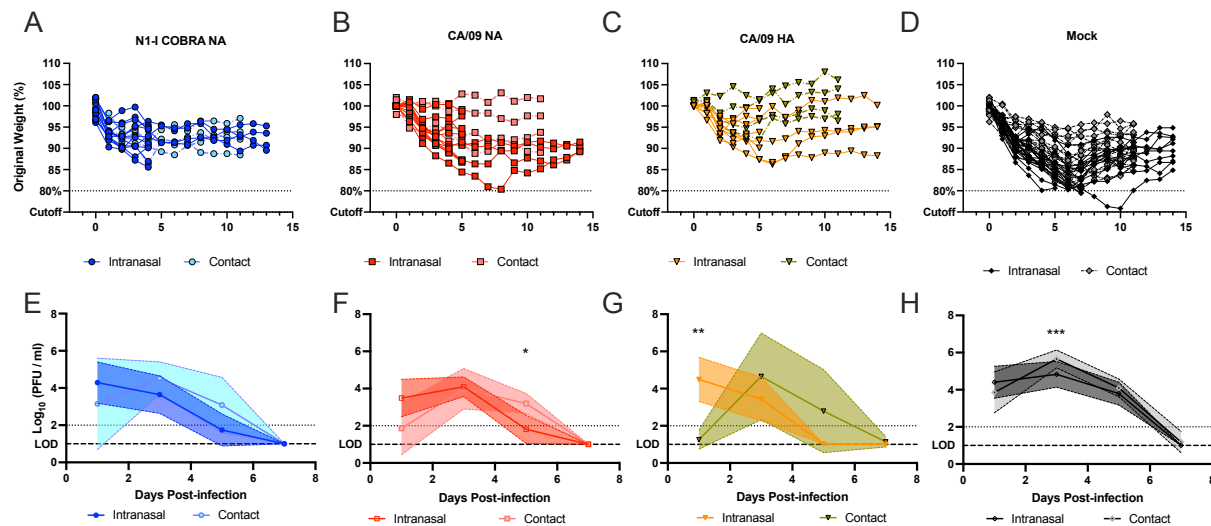


Figure 4.14: Magnitude of weight loss and viral loads did not change based upon intranasal or contact transmission inoculation method. Vaccinated animals that were challenged by either direct intranasal inoculation (intranasal) or through contact transmission from an intranasally inoculated cage mate (contact) were compared by offsetting the contact weights by three days and the nasal wash titers by two days. The offset days were chosen by to maximize the alignment of the mock vaccinated animals (D and H). Each individual ferret's weight loss over time was depicted for each vaccine group (A-D). The average nasal wash titer with standard deviations were depicted for each vaccine group as well (E-H). Comparisons were conducted within vaccine groups with a two-way repeated measured ANOVA and Sidak's multiple comparison test. The minimum weight before clinical endpoint was 75% with 80% denoting an increase in clinical scoring. The limit of detection (LOD; dashed line) was 1.0 \log_{10} (PFU/ml), and the limit of quantification (dotted line) was 2.0 $\log_{10}(\text{PFU}/\text{ml})$. Adjusted p-value: * = < 0.05, ** = < 0.01, *** = < 0.001, **** = < 0.0001.

a peak titer between 4 to 6 \log_{10} (PFU/mL). The viral dynamics differed between the vaccinated groups. For instance, the intranasal CA/o9 NA group had significantly lower titers on the third day compared to the contact CA/o9 NA group (Fig. 4.14F). The contact CA/o9 HA vaccinated ferrets had a delay in the increase in viral titers (Fig. 4.14G), but still reached the same viral peak titer observed on day 1 p.i. for the intranasal group.

4.5 Discussion

Antibodies elicited to the influenza NA protein have been associated with decreased influenza H₁N₁ shedding and illness in humans (Maier et al., 2020). Therefore, the Ni-I COBRA NA was investigated for its potential as an influenza vaccine antigen. The naïve CA/o9 ferret model was used to thoroughly characterize the protective responses elicited by the Ni-I COBRA NA after infection. The Ni-I COBRA NA induced similar ferret responses and viral titers compared to the CA/o9 HA and NA positive controls. The Bris/o7 NA vaccine was included as a heterologous NA and does not elicit NAI antibodies to either the H₁N₁ or H₅N₁ challenge viruses. The Ni-I COBRA NA and positive controls consistently had lower mean viral titers in nasal washes and lung tissue compared both the Bris/o7 NA and mock vaccine groups. Although differences in the mean weight loss compared to other vaccines were similar, the survival of the Bris/o7 NA group was only 50%. The severity and distribution of inflammation in the vaccinated animals were similar in the ear and nasal cavity. Even in the CA/o9 HA vaccinated group, which had below detectable viral titers in both the nasal wash and lung tissue, the inflammation levels were similar to all other challenged groups. The Ni-I COBRA NA reduced inflammation similarly to the CA/o9 NA control, but less than the CA/o9 HA. These results correlate with the presence of virus still in the lungs in the NA vaccinated animals on day 5 p.i. compared to the CA/o9 HA group, which was below the limit of detection.

The Ni-I COBRA NA provides protection against seasonal and pandemic Ni viruses. In concordance with the naïve CA/o9 ferret model, the Ni-I COBRA NA performed identically to the Viet/o4 NA positive control in the naïve Viet/o4 ferret model. The Ni-I COBRA NA vaccine elicited lower NAI

titors than the Viet/o₄ NA vaccinated animals, but both were equally protected. This implies that the NAI titers and magnitude of protection for the H₅N₁ virus may not be a linear relationship, and there potentially is a minimum NAI titer threshold for protection. Further, the Ni-I COBRA NA avoided the weight loss and mortality observed in the CA/o₉ NA vaccine group over the course of infection.

The protective responses in ferrets corresponded with the elicited serological responses. The Ni-I COBRA NA elicited strong responses to both CA/o₉ and Viet/o₄ viruses for 100% of the ferrets. The inhibition was lower for Bris/o₇, but was similar for the Sw/NC/o₅. The wild-type NA's showed antigenic profiles based upon their lineages similar to what has previously been observed (Skarlupka et al., 2021). One contrasting observation was that the Bris/o₇ NA elicited antibodies that inhibited the NA of Sw/NC/o₅. Previously in the mouse model, there was no cross-reaction between clades (Ni.2 and Ni.3) (Skarlupka et al., 2021). This difference in specificity may be due to the change in animal models, from mice to ferrets.

The majority of the human population has pre-existing immunity to influenza through both vaccination and infection. This pre-existing immunity biases the immune recall response is termed immune imprinting. The Ni-I COBRA NA was tested in a pre-immune ferret model to mimic individuals exposed to H_iN₁ influenza viruses. The Ni-I COBRA NA vaccine performed equally well as the CA/o₉ controls in the naïve and pre-immune ferret models. Therefore, even with the pre-existing anti-Sing/86 Ni antibodies, a protective response was elicited when vaccinated with the Ni-I COBRA NA. This effect was prominent in the CA/o₉ challenge. In the Viet/o₄ pre-immune challenge, there was no weight loss for any group. Contrary to expectations, the pre-immunity to Sing/86 H_iN₁ was more protective in the Viet/o₄ H₅N₁ challenge than in the CA/o₉ H_iN₁ challenge. It was expected that due to the shared H_i subtype that the Sing/86 pre-immunity would be more protective in the CA/o₉ challenge than in the Viet/o₄ challenge. Since, the serum from Sing/86 pre-immunized ferrets did not have HAI activity to either of the challenge viruses (all HAI titers were less than 1:10), the differences in protection may be from stem binding antibodies or T-cell responses induced from pre-immunization with a live virus infection.

Vaccination with either NA- or HA-based vaccines did not inhibit the contact transmission of the CA/o₉ virus. This was previously observed in the pig model as well (Everett et al., 2021). These vaccina-

tions thus should protect just the individuals who are vaccinated. In the contact transmission model, the ferrets were co-housed for the entirety of the observation period. This transmission model mimicked family transmission between individuals who are frequently in contact. One of the limitations of this model is that it does not capture shorter exposure periods. Since the viral dynamics differed in the vaccinated groups, it may suggest varying windows for transmission post-infection.

There were a few limitations of this study. Previously mentioned was the limitation of only observing direct contact transmission with a long period of exposure, similar to a family structure or co-housing instance. The viral dynamics after aerosol transmission in vaccinated ferrets may also differ due the differences in inoculum particulate size. In addition to this, inflammatory responses were only measured on day 5 p.i. This day, although informative for the lung tissue, may have been past the day necessary for nasal cavity inflammation quantification. Earlier time points of the upper respiratory tract may have provided differential results when comparing vaccine groups. Lastly, within the pre-immune ferret model, the pre-existing antibodies to the HA protein of Sing/86 interfere with the measurement of the functional NA-specific antibodies and prohibit comparison between the elicited NA antibodies in a naïve and pre-immune models.

Ni-I COBRA NA is a promising candidate for a broadly protective influenza vaccine. Inclusion of the Ni-I COBRA NA can enhance current split-inactivated vaccines or be included in new influenza vaccine formulations. Split-inactivated vaccines elicit mostly an HA-specific antibody response with minimal NA response. Inclusion of the broadly-protective NA antigens, such as the Ni-I COBRA NA, opens the door to eliciting a more balanced response after vaccination. New influenza vaccine candidates, whether subunit or microparticles, can also be designed to include the Ni-I COBRA NA. The Ni-I COBRA NA can help us achieve the future of the influenza vaccines eliciting a broadly-protective response to multiple antigens and increasing the potential protection that individuals receive.

4.6 Acknowledgments

We would like to thank Ying Huang for her insightful discussions. We also thank Mark Tompkins' laboratory for graciously providing the A/Swine/North Carolina/154074/2015 virus. Certain HXN1 influenza A viruses were obtained through the Prevention and Control of Influenza, Centers for Disease Control and Prevention, Atlanta, GA, USA and the International Reagent Resource. We thank the University of Georgia animal resources and veterinary staff, especially Vanessa Thornton, Trey Wills, and Dr. Steve Harvey. All animal studies were conducted in accordance with UGA's IACUC guidelines. We thank the Athens Veterinary Diagnostic Laboratory of the University of Georgia for processing the histopathological samples.

4.7 Competing Interests

No competing interests.

4.8 Funding Information

This study was supported by the Collaborative Influenza Vaccine Innovation Centers (CIVIC) contract by the National Institute of Allergy and Infectious Diseases, a component of the NIH, Department of Health and Human Services, under contract 75N93019C00052. In addition, TMR was supported by the Georgia Research Alliance as an Eminent Scholar.

CHAPTER 5

DISCUSSION

5.1 NI-I COBRA NA as a Vaccine Immunogen

The high incidence of influenza virus infection with the availability of a vaccine has spurred the research and development of vaccines with a wider protective range that is resistant to the antigenic drift observed currently in the human population, as well as the different subtypes that may contribute to a viral pandemic from zoonotic reservoirs. The computationally optimized broadly reactive antigen (COBRA) methodology was developed to overcome the antigenic variability that pathogens use to circumvent the immune system response.

The influenza viruses of the H₃N₂ and H₁N₁ subtype circulate globally among the human population. Since 1918, the H₁N₁ viruses that have seasonally infected humans are from two of the three N₁ genetic lineages. From 1918 to 1958, and 1977 to 2009, the human-lineage (N_{1.2}) NAs were dominated. After 2009, the H₁N₁ swine influenza arose from a reassortment with a Eurasian swine virus contained the N₁ protein from the avian-lineage (N_{1.1c2b}). In addition to these lineages, constant reassortment between swine and human influenza viruses indicates that viruses with a swine-lineage NAs (N_{1.3}) may also induce a productive infection in humans. Further, swine are seen as a 'mixing vessel' that catalyzes the reassortment of avian and mammalian viruses since swine are susceptible to both. Since arising in a mammalian host,

these reassortments may have more efficient transmission in humans, than viruses directly crossing the species barrier from avian to human.

Therefore, a vaccine that induces protection to influenza viruses that contains any of the three N_I genetic lineages greatly increases the value of the vaccine. Similar to HA, the N_I genetic lineages are antigenically distinct. Antigenic maps created with the serological NAI titers in mice (Chapter 3) show the clustering of the lineages (Fig. 5.1). The human pandemic CA/09 and Bris/18 antisera and CA/09 virus have antigenically drifted from the original avian lineage N_Is (Viet/04 virus; Viet/04 and Hubei/10 antisera). The human lineage clusters well amongst themselves and are the furthest from the avian and swine lineages. The presence of antigenic diversity in the N_I subtype indicates that vaccination with one wild-type NA protein will not be sufficient for protection from antigenically distinct NA lineages.

To develop an NA vaccine antigen that does elicit NA inhibiting antibodies to the three different N_I lineages the COBRA methodology was utilized to design the N_I-I COBRA NA. The input sequences for the N_I-I COBRA NA included wild-type NA sequences from isolated viruses from all three lineages. In the mouse model, the N_I-I COBRA NA vaccination elicited protection to all three of the different lineages compared to mock vaccinated animals and depending upon the measurement of protection equivalent to homologous NA vaccinated animals (Chapter 3). However, the mouse model has some limitations; mice are not naturally susceptible to human influenza infection, their inbred nature does not represent the heterogeneity of the human population, and their respiratory system does not accurately model that of humans.

To alleviate these limitations, the N_I-I COBRA NA was introduced in to the naive ferret model - the gold standard of influenza animal models. These cross protective characteristics of the N_I-I COBRA NA were still observed (Chapter 4). The N_I-I COBRA NA in some measures (body weight loss, clinical signs, survival, and nasal wash titers) performed equivalent to the CA/09 HA protein. Protection induced by vaccination with the HA protein is the current standard-of-care, since all the current vaccines are designed around the HA-inhibiting antibody elicitation. The remaining measures (lung viral titer and lung inflammation) were equivalent to the CA/09 NA homologous control. In the highly pathogenic

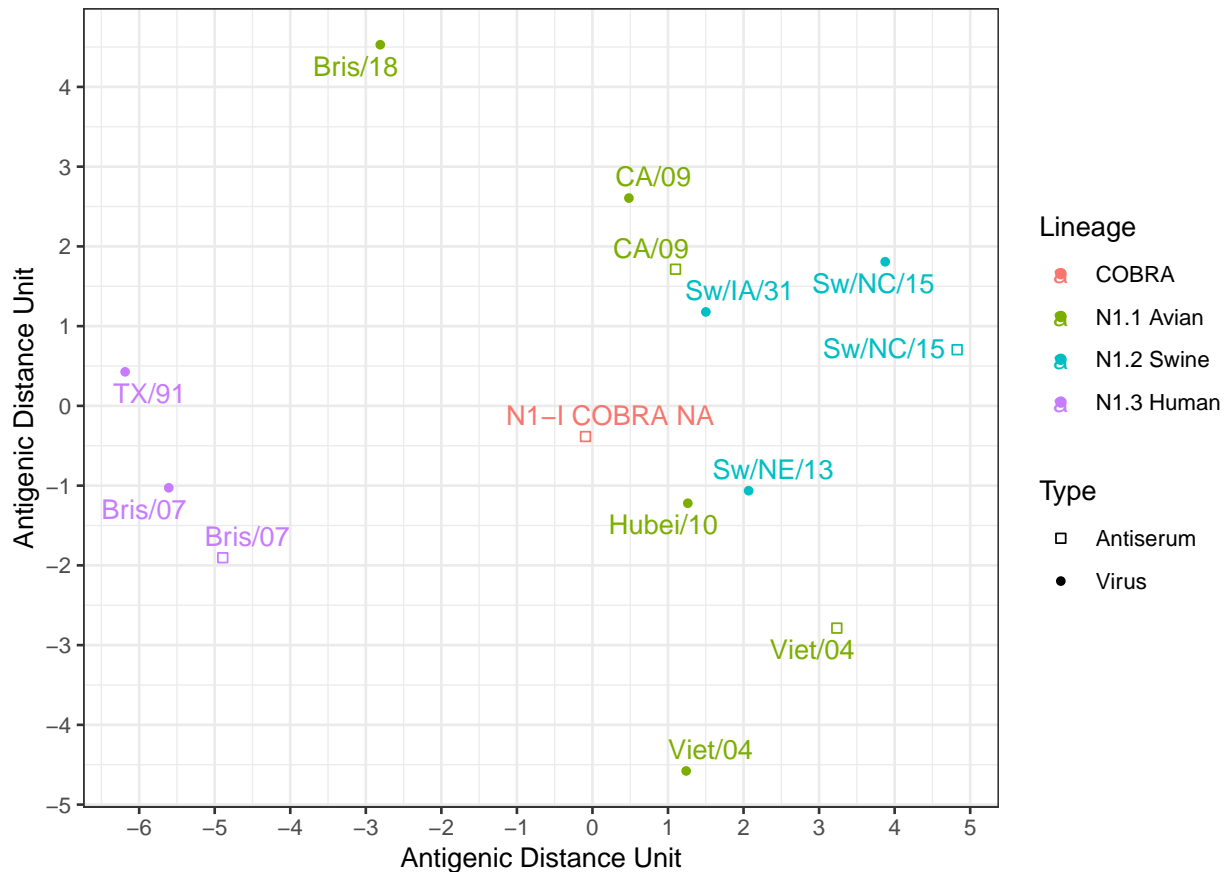


Figure 5.1: The resulting 50% NAI titers of antisera from mice thrice vaccinated with N1 antigens to N1 influenza viruses were visualized through antigenic cartography. Cartography analysis was completed using AcmaCS Web Cherry application (<https://acmacs-web.antigenic-cartography.org/>). The multidimensional scaling was conducted with no minimum column basis, 100 optimizations, and dodgy titer set to false. The final stress was 82.3393. 1 Antigenic distance unit = 1.0 \log_2 change in the 50% NAI titer.

H₅N₁ avian influenza challenge, the Ni-I COBRA NA again performed as well as the homologous control NA (weight loss, survival and clinical scores). Therefore, ferret animal model the Ni-I COBRA NA performed as well as can be expected in both an H₁N₁ and H₅N₁ challenge.

All together, the Ni-I COBRA NA is a good candidate component for future influenza vaccines.

5.2 COBRA as Vaccine Antigen Development Tool

The COBRA method for vaccine antigen development has been utilized for at least three different proteins for two different virus families. The HA and NA surface glycoproteins of the influenza A virus, and the envelope glycoprotein (E) of Dengue virus (DNV) have been tested in numerous animal models including mice, ferrets, and non-human primates (Uno & Ross, 2020). The production of a broadly-reactive antigen from the COBRA method remains consistent even across different research groups (Carter et al., 2016b; Fadlallah et al., 2020). In addition to the Ni-I COBRA NA, there has been only one other COBRA antigen that attempted to increase the breadth between species isolates. The P-I COBRA HA was developed with input wild-type sequences of both swine- and human-isolated H₁ influenza viruses and elicited protection two both groups (See Appendix C; Skarupka et al., 2019).

The main response to a COBRA designed protein is suspected to be a B-cell response (Sautto, Kirchenbaum, Ecker, et al., 2018). To more thoroughly investigate the profile of antibodies produced, the monoclonal antibodies elicited to the P-I COBRA HA was conducted. The mainly IgG antibodies recognized both either conformational or linear epitopes with the proportions not being greatly biased either way (Sautto et al., 2020). Overall, the monoclonal antibody profile indicated that COBRA antigen vaccination elicited broadly-reactive monoclonal antibodies with diverse functions that bind to conserved epitopes. Elicited antibody functionality profiles and epitope identification for the Ni-I COBRA NA provide a future set of experiments that will assist with uncovering the mechanism behind the broadly-reactive response. Effector functional characterization of the antibodies includes antibody-dependent cellular-mediated cytotoxicity (ADCC), antibody-dependent cellular phagocytosis (ADCP) and complement-

dependent cytotoxicity. Lastly, the T-cell mediated responses induced from a COBRA vaccination are currently being investigated.

The COBRA methodology has produced protective vaccine antigens from a myriad of scenarios. The N₁-I COBRA NA and the P-I COBRA HA are examples of the cross-isolated species COBRAs, whereas the DNV COBRA E, influenza COBRA H₁, and influenza COBRA N₁ antigens are constructed from different glycoproteins. Promising future applications of the COBRA methodology include other surface glycoproteins that are the target of antibody responses that also exhibit epitope variability, such as norovirus (Parra et al., 2012; Tan & Jiang, 2014).

5.3 Antigenic Cross Reactivity of Wild-type NAs

The antigenic diversity of the influenza NA subtypes has not been thoroughly characterized. Seminal research analyzed the cross-reactome of antibody binding (Nachbagauer et al., 2017). However, in the panel of representative N₁ viruses there was only one human-lineage N₁ virus (A/Texas/1991) and two avian-lineage N₁ viruses (A/California/2009; A/Viet nam/1203/2004). A broader N₁ panel including the diversity of the lineages has not been conducted. Further, this research focused only on antibody binding, and not a functional response such as inhibition of NA enzymatic activity. Antigenic diversity of the HA is classified by the hemagglutination inhibition functional assay results and not by total antibody binding. Therefore, the NA proteins should be similarly classified into antigenic groups based upon functional assays correlated to protection, such as enzyme-linked lectin assay (ELLA) titers.

Research into antigenic clustering and drift of the NA has been conducted. Human-lineage N₁ viruses and human H₃N₂ N₂ viruses were analyzed with using the NI assay (the precursor assay to the ELLA, which measures small molecule cleavage) (Sandbulte et al., 2011). They found that the NA protein undergoes antigenic drift that does not coincide with the HA antigenic drift, and that one amino acid mutation provided a major shift in antibody recognition from the A/Solomon Islands/2006 H₁N₁ virus to the A/Brisbane/59/2007 H₁N₁ virus. Another group has characterized the antigenic drift of the human H₁N₁ viruses from 2009 onward. Antigenic drift of the N₁ protein from the original A/California/07/2009

virus through time to H₁N₁ viruses isolated in 2016 (Gao et al., 2019). The most recent isolates had been drifting away from the original pandemic strain. This drift was also observed in these studies specifically comparing the distance between the CA/09 and Bris/18 antisera and CA/09 virus (Fig. 5.1). Thus, the antigenic clustering research of the N₁ subtype has mainly focused on the human-isolated viruses. Due to this, the N₁ swine genetic lineage and the avian-isolated N₁ virus strains have not been thoroughly investigated. Recent work that has focused on zoonotic viruses was specifically for the N₂ swine-isolated viruses, but did not characterize N₁ swine-isolated viruses (Kaplan et al., 2021).

Characterization of the antigenic clustering informs on the inhibition range of the antibodies elicited by an antigen. Therefore, if two N₁ antigens are close together (TX/91; Bris/07 of Fig. 5.1), they have similar inhibition profiles against a panel of diverse sera. As they become more distant, they do not react similarly to the same sera (Bris/07 and CA/09). If one wild-type protein was able to elicit inhibitory antibodies to all other N₁ proteins, there would be no need for COBRA vaccine antigen. However, as observed in the animal models, the N₁ are antigenically distinct. Ideally, a vaccine antigen should be in the middle of all target viruses since it should inhibit a wide panel of N₁ viruses and not a single cluster. As such, the N₁-I COBRA NA was placed between the three different genetic lineages assisting with the visualization of the cross-reactive nature of the antigen (Fig. 5.1). This centering of a COBRA antigen between different antigenic clusters has been previously observed with the P-I COBRA HA (See Appendix D; Skarupka, Reneer, et al., 2020). The P-I COBRA HA was situated between both the swine-isolated H₁N_X viruses and the human-isolated H₁N₁ viruses. The most promising DNV COBRA (COBRA I) was also positioned between the four different serotypes of DNV (Fig. 5.2). Hence visualization of the multidimensional data generated during vaccine animal trials may assist with vaccine selection for future studies.

Advances in computational biology have been used to predict antigenic relatedness from the amino acid sequence of the protein. A computational method instead of the experimental techniques used currently would be a great benefit. Computational approaches use less time, money, and do not need access to the virus, unlike the HAI or ELLA assays traditionally used. Methods have included analyzing tree

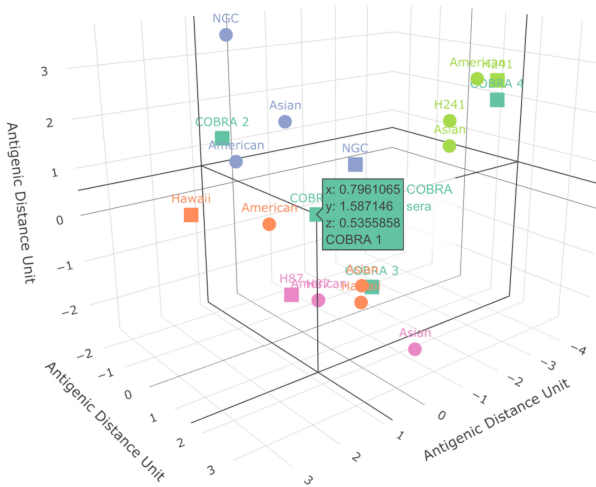


Figure 5.2: The resulting 50% focus reduction neutralization results (FRNT) from mice twice vaccinated with DNV E subviral particles were visualized through antigenic cartography. Colors indicate different DNV serotypes, and shapes indicate sera (square) and viruses (circle). Cartography analysis was completed using the Racmacs package in R statistical software (R-Project, 2017). The multidimensional scaling was conducted with no minimum column basis and 100 optimizations. The final stress was 74.77. 1 Antigenic distance unit = 1.0 \log_2 change in the 50% FRNT titer. Original data from Fig. 3 of Uno and Ross, 2020 was extracted using the WebPlotDigitizer application (<https://apps.automeris.io/wpd/>; Rohatgi, 2020).

distances and biased percentages of the number of amino acid differences in specifically the epitope regions (C. S. Anderson et al., 2018; Neher et al., 2016; Pan et al., 2011). Currently the HA computational antigenic distances have been studied and have been found to correlate with vaccine effectiveness in humans and animal studies (See Appendix E; Pan et al., 2011). However, if used to predict the efficacy of a vaccine antigen in animal models the computational antigenic distance measures' prediction confidence intervals were too wide to be conclusive. Therefore, more refinement may be necessary before computational methods can be used as a vaccine selection tool.

To be prepared for future zoonotic pandemics, future experiments should include further characterization of the antigenic clustering of the wild-type NAs from different genetic clades and host isolates. Only after characterization of the breadth of inhibition will we be more informed how much protection can be expected to other circulating viruses after vaccination.

CHAPTER 6

CONCLUSION

Humans have been developing vaccines to protect against influenza viruses since the 1930s. Initially starting from monovalent split-inactivated virus vaccines available to a select portion of the population to a quadrivalent formulation using egg-manufacturing that cost fractions of an American dollar per dose to produce. Vaccine manufacturing has expanded to include egg-based, cell-based, and recombinant protein based designs. As the influenza virus vaccine platforms continue to evolve, so must the antigens used for vaccination.

Historically and currently, the influenza hemagglutinin (HA) protein is the target protein for determining vaccine responses. Functional antibodies to the HA protein can be measured quickly with a technically easy assay (hemagglutination inhibition assay) which was identified in the 1930s at the beginning of influenza research. However, recent advances into characterizing the immune response after influenza virus infection have revealed that in addition to HA-specific antibodies, neuraminidase (NA) specific antibodies are also elicited. These antibodies are protective against clinical signs and are correlates of protection and are inversely related to all negative disease signs of influenza. The NA surface protein was initially investigated in the 1970s, but fell out of favor for the HA as the main target for antibody elicitation.

In addition to evolving the composition of the antigens used for vaccination, humans have been working on changing the antigens themselves. The wild-type proteins have been modified to increase the

breadth and/or the magnitude of the immune response. Researchers are modifying wild-type proteins, for instance by removing portions of the wildtype protein sequence to direct a response to a specific region (remove head region from virus A) or by combining two strains together (head region from virus A attached to stem region of virus B). Others have created completely new proteins by either a mosaic approach (replacing immunodominant sites with unrelated epitopes to redirect the immune response) and by a consensus layering technique to create a computationally optimized broadly reactive antigen (COBRA). All of these techniques and more have been developed and are being refined for use as an addition to the influenza vaccine.

Therefore, the future of the influenza vaccines will entail a formulation that elicits protection against a broader range of viruses than what is observed with the current strain-specific split-inactivated virus vaccines. The Ni-I COBRA NA vaccine antigen and the COBRA methodology described in this dissertation provides a promising addition to the future influenza vaccines. The wider protective breadth compared to the wildtype NA proteins increases the potential of the antigen as it provided protection not only against seasonal H₁N₁ influenza but also towards the highly-pathogenic avian H₅N₁ influenza. Regardless of which platform is used to deliver the future generations of vaccines this COBRA NA antigen can be included as it is stable membrane bound as well as in a soluble recombinant format. Future influenza vaccines will be a combination of different antigens, manufacturing, delivery platforms, and adjuvants, all of which the Ni-I COBRA NA can be incorporated into to assist with increasing the breadth and protection of the influenza virus vaccine.

BIBLIOGRAPHY

- Air, G. M. (2012). Influenza neuraminidase. *Influenza Other Respir Viruses*, 6(4), 245–56. <https://doi.org/10.1111/j.1750-2659.2011.00304.x>
- Air, G. M., Els, M. C., Brown, L. E., Laver, W. G., & Webster, R. G. (1985). Location of antigenic sites on the three-dimensional structure of the influenza n2 virus neuraminidase. *Virology*, 145(2), 237–248. [https://doi.org/10.1016/0042-6822\(85\)90157-6](https://doi.org/10.1016/0042-6822(85)90157-6)
- Allen, J. D., Jang, H., DiNapoli, J., Kleanthous, H., & Ross, T. M. (2018). Elicitation of protective antibodies against 20 years of future h3n2 co-circulating influenza virus variants in ferrets preimmune to historical h3n2 influenza viruses. *J Virol*. <https://doi.org/10.1128/JVI.00946-18>
- Allen, J. D., Jang, H., DiNapoli, J., Kleanthous, H., & Ross, T. M. (2019). Elicitation of protective antibodies against 20 years of future h3n2 cocirculating influenza virus variants in ferrets preimmune to historical h3n2 influenza viruses. *J Virol*, 93(3). <https://doi.org/10.1128/JVI.00946-18>
- Allen, J. D., Ray, S., & Ross, T. M. (2018a). Split inactivated cobra vaccine elicits protective antibodies against h1n1 and h3n2 influenza viruses. *PLoS One*, 13(9), e0204284. <https://doi.org/10.1371/journal.pone.0204284>
- Allen, J. D., Ray, S., & Ross, T. M. (2018b). Split inactivated cobra vaccine elicits protective antibodies against h1n1 and h3n2 influenza viruses. *PLoS One*, 13(9), e0204284. <https://doi.org/10.1371/journal.pone.0204284>
- Allkofer, A., Garvey, M., Ryan, E., Lyons, R., Ryan, M., Lukaseviciute, G., Walsh, C., Venner, M., & Cullinane, A. (2021). Primary vaccination in foals: A comparison of the serological response to equine influenza and equine herpesvirus vaccines administered concurrently or 2 weeks apart. *Arch Virol*, 166(2), 571–579. <https://doi.org/10.1007/s00705-020-04846-6>
- Altman, M. O., Angel, M., Kosik, I., Trovao, N. S., Zost, S. J., Gibbs, J. S., Casalino, L., Amaro, R. E., Hensley, S. E., Nelson, M. I., & Yewdell, J. W. (2019). Human influenza a virus hemagglutinin glycan evolution follows a temporal pattern to a glycan limit. *MBio*, 10(2). <https://doi.org/10.1128/mBio.oo204-19>
- Altschul, S. F., Madden, T. L., Schaffer, A. A., Zhang, J., Zhang, Z., Miller, W., & Lipman, D. J. (1997). Gapped blast and psi-blast: A new generation of protein database search programs. *Nucleic Acids Res*, 25(17), 3389–402. <https://www.ncbi.nlm.nih.gov/pubmed/9254694>
- Alymova, I. V., McCullers, J. A., Kamal, R. P., Vogel, P., Green, A. M., Gansebom, S., & York, I. A. (2018). Virulent pbi-f2 residues: Effects on fitness of h1n1 influenza a virus in mice and changes during evolution of human influenza a viruses. *Sci Rep*, 8(1), 7474. <https://doi.org/10.1038/s41598-018-25707-y>

- Anders, E. M., Hartley, C. A., & Jackson, D. C. (1990). Bovine and mouse serum beta inhibitors of influenza a viruses are mannose-binding lectins. *Proc Natl Acad Sci USA*, *87*(12), 4485–9. <https://doi.org/10.1073/pnas.87.12.4485>
- Anderson, C. S., McCall, P. R., Stern, H. A., Yang, H. M., & Topham, D. J. (2018). Antigenic cartography of h1n1 influenza viruses using sequence-based antigenic distance calculation. *Bmc Bioinformatics*, *19*. <https://doi.org/ARTN5110.1186/s12859-018-2042-4>
- Anderson, T. K., Campbell, B. A., Nelson, M. I., Lewis, N. S., Janas-Martindale, A., Killian, M. L., & Vincent, A. L. (2015). Characterization of co-circulating swine influenza a viruses in north america and the identification of a novel h1 genetic clade with antigenic significance. *Virus Res*, *201*, 24–31. <https://doi.org/10.1016/j.virusres.2015.02.009>
- Anderson, T. K., Macken, C. A., Lewis, N. S., Scheuermann, R. H., Van Reeth, K., Brown, I. H., Swenson, S. L., Simon, G., Saito, T., Berhane, Y., Ciacci-Zanella, J., Pereda, A., Davis, C. T., Donis, R. O., Webby, R. J., & Vincent, A. L. (2016). A phylogeny-based global nomenclature system and automated annotation tool for h1 hemagglutinin genes from swine influenza a viruses. *mSphere*, *1*(6). <https://doi.org/10.1128/mSphere.00275-16>
- Anderson, T. K., Nelson, M. I., Kitikoon, P., Swenson, S. L., Korslund, J. A., & Vincent, A. L. (2013). Population dynamics of co-circulating swine influenza a viruses in the united states from 2009 to 2012. *Influenza and Other Respiratory Viruses*, *7*(S4), 42–51.
- Angeletti, D., Gibbs, J. S., Angel, M., Kosik, I., Hickman, H. D., Frank, G. M., Das, S. R., Wheatley, A. K., Prabhakaran, M., Leggat, D. J., McDermott, A. B., & Yewdell, J. W. (2017). Defining b cell immunodominance to viruses. *Nat Immunol*, *18*(4), 456–463. <https://doi.org/10.1038/ni.3680>
- Archetti, I., & Horsfall, J., F. L. (1950). Persistent antigenic variation of influenza a viruses after incomplete neutralization in ovo with heterologous immune serum. *J Exp Med*, *92*(5), 441–62. <https://doi.org/10.1084/jem.92.5.441>
- Arevalo, P., McLean, H. Q., Belongia, E. A., & Cobey, S. (2020). Earliest infections predict the age distribution of seasonal influenza a cases. *eLife*, *9*. <https://doi.org/10.7554/eLife.50060>
- Baenziger, J. U., & Fiete, D. (1979). Structure of the complex oligosaccharides of fetuin. *Journal of Biological Chemistry*, *254*(3), 789–795. [https://doi.org/10.1016/S0021-9258\(17\)37874-2](https://doi.org/10.1016/S0021-9258(17)37874-2)
- Baker, N. J., & Gandhi, S. S. (1976). Effect of ca++ on the stability of influenza virus neuraminidase. *Arch Virol*, *52*(1-2), 7–18. <https://doi.org/10.1007/BF01317860>
- Bao, Y. M., Bolotov, P., Dernovoy, D., Kiryutin, B., Zaslavsky, L., Tatusova, T., Ostell, J., & Lipman, D. (2008). The influenza virus resource at the national center for biotechnology information. *Journal of Virology*, *82*(2), 596–601. <https://doi.org/10.1128/JVI.02005-07>
- Barman, S., Adhikary, L., Chakrabarti, A. K., Bernas, C., Kawaoka, Y., & Nayak, D. P. (2004). Role of transmembrane domain and cytoplasmic tail amino acid sequences of influenza a virus neuraminidase in raft association and virus budding. *J Virol*, *78*(10), 5258–69. <https://doi.org/10.1128/jvi.78.10.5258-5269.2004>
- Bart, S. A., Hohenboken, M., Della Cioppa, G., Narasimhan, V., Dormitzer, P. R., & Kanesa-Thasan, N. (2014). A cell culture-derived mf59-adjuvanted pandemic a/h7n9 vaccine is immunogenic in adults. *Sci Transl Med*, *6*(234), 234ra55. <https://doi.org/10.1126/scitranslmed.3008761>
- Bassetti, M., Castaldo, N., & Cornelutti, A. (2019). Neuraminidase inhibitors as a strategy for influenza treatment: Pros, cons and future perspectives. *Expert Opin Pharmacother*, *20*(14), 1711–1718. <https://doi.org/10.1080/14656566.2019.1626824>

- Beaulieu, A., Gravel, E., Cloutier, A., Marois, I., Colombo, E., Desilets, A., Verreault, C., Leduc, R., Marsault, E., & Richter, M. V. (2013). Matriptase proteolytically activates influenza virus and promotes multicycle replication in the human airway epithelium. *J Virol*, *87*(8), 4237–51. <https://doi.org/10.1128/JVI.03005-12>
- Bedford, T., Suchard, M. A., Lemey, P., Dudas, G., Gregory, V., Hay, A. J., McCauley, J. W., Russell, C. A., Smith, D. J., & Rambaut, A. (2014). Integrating influenza antigenic dynamics with molecular evolution. *eLife*, *3*, e01914. <https://doi.org/10.7554/eLife.01914>
- Belongia, E. A., Skowronski, D. M., McLean, H. Q., Chambers, C., Sundaram, M. E., & De Serres, G. (2017). Repeated annual influenza vaccination and vaccine effectiveness: Review of evidence. *Expert Rev Vaccines*, *16*(7), 1–14. <https://doi.org/10.1080/14760584.2017.1334554>
- Belser, J. A., Katz, J. M., & Tumpey, T. M. (2011). The ferret as a model organism to study influenza a virus infection. *Disease Models & Mechanisms*, *4*(5), 575–579. <https://doi.org/10.1242/dmm.007823>
- Belshe, R. B., Frey, S. E., Graham, I., Mulligan, M. J., Edupuganti, S., Jackson, L. A., Wald, A., Poland, G., Jacobson, R., Keyserling, H. L., Spearman, P., Hill, H., Wolff, M., National Institute of, A., Infectious Diseases-Funded, V., & Treatment Evaluation, U. (2011). Safety and immunogenicity of influenza a h5 subunit vaccines: Effect of vaccine schedule and antigenic variant. *J Infect Dis*, *203*(5), 666–73. <https://doi.org/10.1093/infdis/jiq093>
- Belshe, R. B., Gruber, W. C., Mendelman, P. M., Mehta, H. B., Mahmood, K., Reisinger, K., Treanor, J., Zangwill, K., Hayden, F. G., Bernstein, D. I., Kotloff, K., King, J., Piedra, P. A., Block, S. L., Yan, L., & Wolff, M. (2000). Correlates of immune protection induced by live, attenuated, cold-adapted, trivalent, intranasal influenza virus vaccine. *J Infect Dis*, *181*(3), 1133–7. <https://doi.org/10.1086/315323>
- Benkert, P., Biasini, M., & Schwede, T. (2011). Toward the estimation of the absolute quality of individual protein structure models. *Bioinformatics*, *27*(3), 343–50. <https://doi.org/10.1093/bioinformatics/btq662>
- Berlanda Scorza, F., Tsvetnitsky, V., & Donnelly, J. J. (2016). Universal influenza vaccines: Shifting to better vaccines. *Vaccine*, *34*(26), 2926–2933. <https://doi.org/10.1016/j.vaccine.2016.03.085>
- Bi, Y., Xiao, H., Chen, Q., Wu, Y., Fu, L., Quan, C., Wong, G., Liu, J., Haywood, J., Liu, Y., Zhou, B., Yan, J., Liu, W., & Gao, G. F. (2016). Changes in the length of the neuraminidase stalk region impact h7n9 virulence in mice. *J Virol*, *90*(4), 2142–9. <https://doi.org/10.1128/JVI.02553-15>
- Bienert, S., Waterhouse, A., de Beer, T. A., Tauriello, G., Studer, G., Bordoli, L., & Schwede, T. (2017). The swiss-model repository-new features and functionality. *Nucleic Acids Res*, *45*(D1), D313–D319. <https://doi.org/10.1093/nar/gkw1132>
- Blackburne, B. P., Hay, A. J., & Goldstein, R. A. (2008). Changing selective pressure during antigenic changes in human influenza h3. *PLoS Pathog*, *4*(5), e1000058. <https://doi.org/10.1371/journal.ppat.1000058>
- Blumenkrantz, D., Roberts, K. L., Shelton, H., Lycett, S., & Barclay, W. S. (2013). The short stalk length of highly pathogenic avian influenza h5n1 virus neuraminidase limits transmission of pandemic h5n1 virus in ferrets. *J Virol*, *87*(19), 10539–51. <https://doi.org/10.1128/JVI.00967-13>
- Bodewes, R., Kreijtz, J. H., Geelhoed-Mieras, M. M., van Amerongen, G., Verburgh, R. J., van Trierum, S. E., Kuiken, T., Fouchier, R. A., Osterhaus, A. D., & Rimmelzwaan, G. F. (2011). Vaccination against seasonal influenza a/h3n2 virus reduces the induction of heterosubtypic immunity against

- influenza a/h5n1 virus infection in ferrets. *J Virol*, 85(6), 2695–702. <https://doi.org/10.1128/JVI.02371-10>
- Boikos, C., Sylvester, G. C., Sampalis, J. S., & Mansi, J. A. (2020). Relative effectiveness of the cell-cultured quadrivalent influenza vaccine compared to standard, egg-derived quadrivalent influenza vaccines in preventing influenza-like illness in 2017-2018. *Clin Infect Dis*, 71(10), e665–e671. <https://doi.org/10.1093/cid/ciaa371>
- Boivin, S., Cusack, S., Ruigrok, R. W., & Hart, D. J. (2010). Influenza a virus polymerase: Structural insights into replication and host adaptation mechanisms. *J Biol Chem*, 285(37), 28411–7. <https://doi.org/10.1074/jbc.R110.117531>
- Bonomo, M. E., & Deem, M. W. (2018). Predicting influenza h3n2 vaccine efficacy from evolution of the dominant epitope. *Clin Infect Dis*. <https://doi.org/10.1093/cid/ciy323>
- Bos, T. J., Davis, A. R., & Nayak, D. P. (1984). N_H2-terminal hydrophobic region of influenza virus neuraminidase provides the signal function in translocation. *Proc Natl Acad Sci U S A*, 81(8), 2327–31. <https://doi.org/10.1073/pnas.81.8.2327>
- Bossart-Whitaker, P., Carson, M., Babu, Y. S., Smith, C. D., Laver, W. G., & Air, G. M. (1993). Three-dimensional structure of influenza a n9 neuraminidase and its complex with the inhibitor 2-deoxy 2,3-dehydro-n-acetyl neuraminic acid. *J Mol Biol*, 232(4), 1069–83. <https://doi.org/10.1006/jmbi.1993.1461>
- Bottcher-Friebertshauser, E., Stein, D. A., Klenk, H. D., & Garten, W. (2011). Inhibition of influenza virus infection in human airway cell cultures by an antisense peptide-conjugated morpholino oligomer targeting the hemagglutinin-activating protease tmprss2. *J Virol*, 85(4), 1554–62. <https://doi.org/10.1128/JVI.01294-10>
- Bouvier, N. M., & Lowen, A. C. (2010). Animal models for influenza virus pathogenesis and transmission. *Viruses*, 2(8), 1530–1563. <https://doi.org/10.3390/v20801530>
- Brett, I. C., & Johansson, B. E. (2006). Variation in the divalent cation requirements of influenza a virus n1 neuraminidases. *J Biochem*, 139(3), 439–47. <https://doi.org/10.1093/jb/mvj051>
- Bright, R. A., Carter, D. M., Daniluk, S., Toapanta, F. R., Ahmad, A., Gavrilov, V., Massare, M., Pushko, P., Mytle, N., Rowe, T., Smith, G., & Ross, T. M. (2007). Influenza virus-like particles elicit broader immune responses than whole virion inactivated influenza virus or recombinant hemagglutinin. *Vaccine*, 25(19), 3871–8. <https://doi.org/10.1016/j.vaccine.2007.01.106>
- Broecker, F., Zheng, A., Suntrronwong, N., Sun, W., Bailey, M. J., Krammer, F., & Palese, P. (2019). Extending the stalk enhances immunogenicity of the influenza virus neuraminidase. *J Virol*, 93(18). <https://doi.org/10.1128/JVI.00840-19>
- Brown, D. M., Lee, S., Garcia-Hernandez Mde, L., & Swain, S. L. (2012). Multifunctional cd4 cells expressing gamma interferon and perforin mediate protection against lethal influenza virus infection. *J Virol*, 86(12), 6792–803. <https://doi.org/10.1128/JVI.07172-11>
- Brown, I. H. (2000). The epidemiology and evolution of influenza viruses in pigs. *Vet Microbiol*, 74(1-2), 29–46. <https://www.ncbi.nlm.nih.gov/pubmed/10799776>
- Burke, D. F., & Smith, D. J. (2014). A recommended numbering scheme for influenza a ha subtypes. *PLoS One*, 9(11), e112302. <https://doi.org/10.1371/journal.pone.0112302>
- Buxton, R. C., Edwards, B., Juo, R. R., Voyta, J. C., Tisdale, M., & Bethell, R. C. (2000). Development of a sensitive chemiluminescent neuraminidase assay for the determination of influenza virus

- susceptibility to zanamivir. *Anal Biochem*, 280(2), 291–300. <https://doi.org/10.1006/abio.2000.4517>
- Byrne-Nash, R. T., Gillis, J. H., Miller, D. F., Bueter, K. M., Kuck, L. R., & Rowlen, K. L. (2019). A neuraminidase potency assay for quantitative assessment of neuraminidase in influenza vaccines. *NPJ Vaccines*, 4, 3. <https://doi.org/10.1038/s41541-019-0099-3>
- Calabro, S., Tritto, E., Pezzotti, A., Taccone, M., Muzzi, A., Bertholet, S., De Gregorio, E., O'Hagan, D. T., Baudner, B., & Seubert, A. (2013). The adjuvant effect of mf59 is due to the oil-in-water emulsion formulation, none of the individual components induce a comparable adjuvant effect. *Vaccine*, 31(33), 3363–9. <https://doi.org/10.1016/j.vaccine.2013.05.007>
- Camacho, C., Coulouris, G., Avagyan, V., Ma, N., Papadopoulos, J., Bealer, K., & Madden, T. L. (2009). Blast+: Architecture and applications. *BMC Bioinformatics*, 10, 421. <https://doi.org/10.1186/1471-2105-10-421>
- Cameron, C. M., Cameron, M. J., Bermejo-Martin, J. F., Ran, L., Xu, L., Turner, P. V., Ran, R., Danesh, A., Fang, Y., Chan, P. K., Mytle, N., Sullivan, T. J., Collins, T. L., Johnson, M. G., Medina, J. C., Rowe, T., & Kelvin, D. J. (2008). Gene expression analysis of host innate immune responses during lethal h5n1 infection in ferrets. *J Virol*, 82(22), 11308–17. <https://doi.org/10.1128/JVI.00691-08>
- Canine influenza. (2021). <https://www.avma.org/resources-tools/animal-health-and-welfare/canine-influenza>
- Carlock, M. A., Ingram, J. G., Clutter, E. F., Cecil, N. C., Ramgopal, M., Zimmerman, R. K., Warren, W., Kleanthous, H., & Ross, T. M. (2019). Impact of age and pre-existing immunity on the induction of human antibody responses against influenza b viruses. *Hum Vaccin Immunother*, 15(9), 2030–2043. <https://doi.org/10.1080/21645515.2019.1642056>
- Carter, D. M., Bloom, C. E., Nascimento, E. J., Marques, E. T., Craig, J. K., Cherry, J. L., Lipman, D. J., & Ross, T. M. (2013). Sequential seasonal h1n1 influenza virus infections protect ferrets against novel 2009 h1n1 influenza virus. *J Virol*, 87(3), 1400–10. <https://doi.org/10.1128/JVI.02257-12>
- Carter, D. M., Darby, C. A., Johnson, S. K., Carlock, M. A., Kirchenbaum, G. A., Allen, J. D., Vogel, T. U., Delagrave, S., DiNapoli, J., Kleanthous, H., & Ross, T. M. (2017). Elicitation of protective antibodies against a broad panel of h1n1 viruses in ferrets preimmune to historical h1n1 influenza viruses. *J Virol*, 91(24). <https://doi.org/10.1128/JVI.01283-17>
- Carter, D. M., Darby, C. A., Lefoley, B. C., Crevar, C. J., Alefantis, T., Oomen, R., Anderson, S. F., Strugnell, T., Cortes-Garcia, G., Vogel, T. U., Parrington, M., Kleanthous, H., & Ross, T. M. (2016a). Design and characterization of a computationally optimized broadly reactive hemagglutinin vaccine for h1n1 influenza viruses. *J Virol*, 90(9), 4720–4734. <https://doi.org/10.1128/JVI.03152-15>
- Carter, D. M., Darby, C. A., Lefoley, B. C., Crevar, C. J., Alefantis, T., Oomen, R., Anderson, S. F., Strugnell, T., Cortes-Garcia, G., Vogel, T. U., Parrington, M., Kleanthous, H., & Ross, T. M. (2016b). Design and characterization of a computationally optimized broadly reactive hemagglutinin vaccine for h1n1 influenza viruses. *J Virol*, 90(9), 4720–4734. <https://doi.org/10.1128/JVI.03152-15>
- Carter, D. M., Darby, C. A., Lefoley, B. C., Crevar, C. J., Alefantis, T., Oomen, R., Anderson, S. F., Strugnell, T., Cortes-Garcia, G., Vogel, T. U., Parrington, M., Kleanthous, H., & Ross, T. M. (2016c). Design and characterization of a computationally optimized broadly reactive hemagglu-

- tinin vaccine for h1n1 influenza viruses. *J Virol*, 90(9), 4720–34. <https://doi.org/10.1128/JVI.03152-15>
- Castrucci, M. R., Donatelli, I., Sidoli, L., Barigazzi, G., Kawaoka, Y., & Webster, R. G. (1993). Genetic reassortment between avian and human influenza a viruses in italian pigs. *Virology*, 193(1), 503–6. <https://doi.org/10.1006/viro.1993.1155>
- Caton, A. J., Brownlee, G. G., Yewdell, J. W., & Gerhard, W. (1982a). The antigenic structure of the influenza virus a/pr/8/34 hemagglutinin (h1 subtype). *Cell*, 31(2 Pt 1), 417–27. <https://www.ncbi.nlm.nih.gov/pubmed/6186384>
- Caton, A. J., Brownlee, G. G., Yewdell, J. W., & Gerhard, W. (1982b). The antigenic structure of the influenza virus a/pr/8/34 hemagglutinin (h1 subtype). *Cell*, 31(2), 417–427. [https://doi.org/10.1016/0092-8674\(82\)90135-0](https://doi.org/10.1016/0092-8674(82)90135-0)
- Cattoli, G., Milani, A., Temperton, N., Zecchin, B., Buratin, A., Molesti, E., Aly, M. M., Arafa, A., & Capua, I. (2011). Antigenic drift in h5n1 avian influenza virus in poultry is driven by mutations in major antigenic sites of the hemagglutinin molecule analogous to those for human influenza virus. *J Virol*, 85(17), 8718–24. <https://doi.org/10.1128/JVI.02403-10>
- Centers for Disease, C., & Prevention. (2009). Serum cross-reactive antibody response to a novel influenza a (h1n1) virus after vaccination with seasonal influenza vaccine. *MMWR Morb Mortal Wkly Rep*, 58(19), 521–4. <https://www.ncbi.nlm.nih.gov/pubmed/19478718>
- Centers for Disease, C., & Prevention. (2021a). <https://www.cdc.gov/flu/vaccines-work/effectiveness-studies.htm>
- Centers for Disease, C., & Prevention. (2021b). <https://www.cdc.gov/flu/highrisk/index.htm>
- Chaipan, C., Kobasa, D., Bertram, S., Glowacka, I., Steffen, I., Tsegaye, T. S., Takeda, M., Bugge, T. H., Kim, S., Park, Y., Marzi, A., & Pohlmann, S. (2009). Proteolytic activation of the 1918 influenza virus hemagglutinin. *J Virol*, 83(7), 3200–11. <https://doi.org/10.1128/JVI.02205-08>
- Changsom, D., Jiang, L., Lerdsamran, H., Iamsirithaworn, S., Kitphati, R., Pooruk, P., Auewarakul, P., & Puthavathana, P. (2017). Kinetics, longevity, and cross-reactivity of antineuraminidase antibody after natural infection with influenza a viruses. *Clin Vaccine Immunol*, 24(12). <https://doi.org/10.1128/CVI.00248-17>
- Chen, B. J., Leser, G. P., Morita, E., & Lamb, R. A. (2007). Influenza virus hemagglutinin and neuraminidase, but not the matrix protein, are required for assembly and budding of plasmid-derived virus-like particles. *J Virol*, 81(13), 7111–23. <https://doi.org/10.1128/JVI.00361-07>
- Chen, C. J., Wu, G. H., Kuo, R. L., & Shih, S. R. (2017). Role of the intestinal microbiota in the immunomodulation of influenza virus infection. *Microbes Infect*, 19(12), 570–579. <https://doi.org/10.1016/j.micinf.2017.09.002>
- Chen, J. M., Ma, H. C., Chen, J. W., Sun, Y. X., Li, J. M., & Wang, Z. L. (2007). A preliminary panorama of the diversity of n1 subtype influenza viruses. *Virus Genes*, 35(1), 33–40. <https://doi.org/10.1007/s11262-006-0025-4>
- Chen, J. M., Sun, Y. X., Chen, J. W., Liu, S., Yu, J. M., Shen, C. J., Sun, X. D., & Peng, D. (2009). Panorama phylogenetic diversity and distribution of type a influenza viruses based on their six internal gene sequences. *Virol J*, 6, 137. <https://doi.org/10.1186/1743-422X-6-137>
- Chen, S., Quan, K., Wang, D., Du, Y., Qin, T., Peng, D., & Liu, X. (2020). Truncation or deglycosylation of the neuraminidase stalk enhances the pathogenicity of the h5n1 subtype avian influenza virus in mallard ducks. *Front Microbiol*, 11, 583588. <https://doi.org/10.3389/fmicb.2020.583588>

- Chen, X., Liu, S., Goraya, M. U., Maarouf, M., Huang, S., & Chen, J. L. (2018). Host immune response to influenza a virus infection. *Front Immunol*, 9, 320. <https://doi.org/10.3389/fimmu.2018.00320>
- Chen, Y. Q., Lan, L. Y., Huang, M., Henry, C., & Wilson, P. C. (2019). Hemagglutinin stalk-reactive antibodies interfere with influenza virus neuraminidase activity by steric hindrance. *J Virol*, 93(4). <https://doi.org/10.1128/JVI.01526-18>
- Chen, Y. Q., Wohlbold, T. J., Zheng, N. Y., Huang, M., Huang, Y., Neu, K. E., Lee, J., Wan, H., Rojas, K. T., Kirkpatrick, E., Henry, C., Palm, A. E., Stamper, C. T., Lan, L. Y., Topham, D. J., Treanor, J., Wrammert, J., Ahmed, R., Eichelberger, M. C., ... Wilson, P. C. (2018). Influenza infection in humans induces broadly cross-reactive and protective neuraminidase-reactive antibodies. *Cell*, 173(2), 417–429 e10. <https://doi.org/10.1016/j.cell.2018.03.030>
- Cheng, X., Eisenbraun, M., Xu, Q., Zhou, H., Kulkarni, D., Subbarao, K., Kemble, G., & Jin, H. (2009). H5ni vaccine-specific b cell responses in ferrets primed with live attenuated seasonal influenza vaccines. *PLoS One*, 4(2), e4436. <https://doi.org/10.1371/journal.pone.0004436>
- Choi, A., Ibanez, L. I., Strohmeier, S., Krammer, F., Garcia-Sastre, A., & Schotsaert, M. (2020). Non-sterilizing, infection-permissive vaccination with inactivated influenza virus vaccine reshapes subsequent virus infection-induced protective heterosubtypic immunity from cellular to humoral cross-reactive immune responses. *Front Immunol*, 11, 1166. <https://doi.org/10.3389/fimmu.2020.01166>
- Choi, Y. K., Goyal, S. M., & Joo, H. S. (2002). Prevalence of swine influenza virus subtypes on swine farms in the united states. *Arch Virol*, 147(6), 1209–20. <https://doi.org/10.1007/s00705-002-0788-4>
- Clark, T. W., Pareek, M., Hoschler, K., Dillon, H., Nicholson, K. G., Groth, N., & Stephenson, I. (2009). Trial of 2009 influenza a (hini) monovalent mf59-adjuvanted vaccine. *N Engl J Med*, 361(25), 2424–35. <https://doi.org/10.1056/NEJMoa0907650>
- Clements, M. L., Betts, R. F., Tierney, E. L., & Murphy, B. R. (1986). Serum and nasal wash antibodies associated with resistance to experimental challenge with influenza a wild-type virus. *J Clin Microbiol*, 24(1), 157–60. <https://doi.org/10.1128/JCM.24.1.157-160.1986>
- Clements M-L., E. T., R. Betts, & Murphy, B. (1986). Serum and nasal wash antibodies associated with resistance to experimental challenge with influenza a wild-type virus. *Journal of Clinical Microbiology*, (July), 157–160.
- Cohen, M., Zhang, X. Q., Senaati, H. P., Chen, H. W., Varki, N. M., Schooley, R. T., & Gagneux, P. (2013). Influenza a penetrates host mucus by cleaving sialic acids with neuraminidase. *Virol J*, 10, 321. <https://doi.org/10.1186/1743-422X-10-321>
- Collins, J. P., Campbell, A. P., Openo, K., Farley, M. M., Cummings, C. N., Hill, M., Schaffner, W., Lindegren, M. L., Thomas, A., Billing, L., Bennett, N., Spina, N., Bargsten, M., Lynfield, R., Eckel, S., Ryan, P., Yousey-Hindes, K., Herlihy, R., Kirley, P. D., ... Anderson, E. J. (2020). Outcomes of immunocompromised adults hospitalized with laboratory-confirmed influenza in the united states, 2011-2015. *Clin Infect Dis*, 70(10), 2121–2130. <https://doi.org/10.1093/cid/ciz638>
- Colman, P. M., Varghese, J. N., & Laver, W. G. (1983). Structure of the catalytic and antigenic sites in influenza virus neuraminidase. *Nature*, 303(5912), 41–4. <https://doi.org/10.1038/303041a0>
- Couch, R. B., Atmar, R. L., Franco, L. M., Quarles, J. M., Wells, J., Arden, N., Nino, D., & Belmont, J. W. (2013). Antibody correlates and predictors of immunity to naturally occurring influenza in humans and the importance of antibody to the neuraminidase. *J Infect Dis*, 207(6), 974–81. <https://doi.org/10.1093/infdis/jis935>

- Couch, R. B., Kasel, J. A., Gerin, J. L., Schulman, J. L., & Kilbourne, E. D. (1974). Induction of partial immunity to influenza by a neuraminidase-specific vaccine. *J Infect Dis*, 129(4), 411–20. <https://doi.org/10.1093/infdis/129.4.411>
- Council, N. R. (2011). *Guide for the care and use of laboratory animals* (8th ed.). The National Academies Press.
- Couzens, L., Gao, J., Westgeest, K., Sandbulte, M., Lugovtsev, V., Fouchier, R., & Eichelberger, M. (2014). An optimized enzyme-linked lectin assay to measure influenza a virus neuraminidase inhibition antibody titers in human sera. *J Virol Methods*, 210, 7–14. <https://doi.org/10.1016/j.jviromet.2014.09.003>
- Cox, N. J., & Subbarao, K. (2000). Global epidemiology of influenza: Past and present. *Annu Rev Med*, 51, 407–21. <https://doi.org/10.1146/annurev.med.51.1.407>
- Creighton, C. (1819). *A history of epidemics in britain* (Vol. 1). Cambridge. <https://www.gutenberg.org/files/42686/42686-h/42686-h.htm>
- Crevar, C. J., Carter, D. M., Lee, K. Y., & Ross, T. M. (2015). Cocktail of h5n1 cobra ha vaccines elicit protective antibodies against h5n1 viruses from multiple clades. *Hum Vaccin Immunother*, 11(3), 572–83. <https://doi.org/10.1080/21645515.2015.1012013>
- Crevar, C. J., & Ross, T. M. (2008). Elicitation of protective immune responses using a bivalent h5n1 vlp vaccine. *Virol J*, 5, 131. <https://doi.org/10.1186/1743-422X-5-131>
- Cwach, K. T., Sandbulte, H. R., Klonoski, J. M., & Huber, V. C. (2012). Contribution of murine innate serum inhibitors toward interference within influenza virus immune assays. *Influenza Other Respir Viruses*, 6(2), 127–35. <https://doi.org/10.1111/j.1750-2659.2011.00283.x>
- Czaja, C. A., Miller, L., Alden, N., Wald, H. L., Cummings, C. N., Rolfes, M. A., Anderson, E. J., Bennett, N. M., Billing, L. M., Chai, S. J., Eckel, S., Mansmann, R., McMahon, M., Monroe, M. L., Muse, A., Risk, I., Schaffner, W., Thomas, A. R., Yousey-Hindes, K., ... Herlihy, R. K. (2019). Age-related differences in hospitalization rates, clinical presentation, and outcomes among older adults hospitalized with influenza-u.s. influenza hospitalization surveillance network (flusurv-net). *Open Forum Infect Dis*, 6(7). <https://doi.org/10.1093/ofid/ofz225>
- Dadonaite, B., Vijayakrishnan, S., Fodor, E., Bhella, D., & Hutchinson, E. C. (2016). Filamentous influenza viruses. *J Gen Virol*, 97(8), 1755–1764. <https://doi.org/10.1099/jgv.0.000535>
- Dai, M., McBride, R., Dortmans, J., Peng, W., Bakkers, M. J. G., de Groot, R. J., van Kuppeveld, F. J. M., Paulson, J. C., de Vries, E., & de Haan, C. A. M. (2017). Mutation of the second sialic acid-binding site, resulting in reduced neuraminidase activity, preceded the emergence of h7n9 influenza a virus. *J Virol*, 91(9). <https://doi.org/10.1128/JVI.00049-17>
- Daniels, R., Kurowski, B., Johnson, A. E., & Hebert, D. N. (2003). N-linked glycans direct the co-translational folding pathway of influenza hemagglutinin. *Molecular Cell*, 11(1), 79–90. [https://doi.org/10.1016/S1097-2765\(02\)00821-3](https://doi.org/10.1016/S1097-2765(02)00821-3)
- deBruijn, I. A., Remarque, E. J., Beyer, W. E. P., leCessie, S., Masurel, N., & Ligthart, G. J. (1997). Annually repeated influenza vaccination improves humoral responses to several influenza virus strains in healthy elderly. *Vaccine*, 15(12-13), 1323–1329. [https://doi.org/10.1016/S0264-410X\(97\)00019-4](https://doi.org/10.1016/S0264-410X(97)00019-4)
- Deem, M. W., & Pan, K. (2009). The epitope regions of hi-subtype influenza a, with application to vaccine efficacy. *Protein Eng Des Sel*, 22(9), 543–6. <https://doi.org/10.1093/protein/gzp027>

- Deem, M. W., & Pan, K. Y. (2009). The epitope regions of h1-subtype influenza a, with application to vaccine efficacy. *Protein Engineering Design & Selection*, 22(9), 543–546. <https://doi.org/10.1093/protein/gzp027>
- Desheva, Y., Smolonogina, T., Donina, S., & Rudenko, L. (2020). Study of neuraminidase-inhibiting antibodies in clinical trials of live influenza vaccines. *Antibodies (Basel)*, 9(2). <https://doi.org/10.3390/antib9020020>
- Desheva, Y. A., Smolonogina, T. A., Donina, S. A., & Rudenko, L. G. (2015). Serum strain-specific or cross-reactive neuraminidase inhibiting antibodies against pandemic capital a, cyrillic/california/07/2009(h1n1) influenza in healthy volunteers. *BMC Res Notes*, 8, 136. <https://doi.org/10.1186/s13104-015-1086-z>
- de Vries, E., Du, W., Guo, H., & de Haan, C. A. M. (2020). Influenza a virus hemagglutinin-neuraminidase-receptor balance: Preserving virus motility. *Trends Microbiol*, 28(1), 57–67. <https://doi.org/10.1016/j.tim.2019.08.010>
- de Vries, E., Tscherne, D. M., Wienholts, M. J., Cobos-Jimenez, V., Scholte, F., Garcia-Sastre, A., Rotter, P. J., & de Haan, C. A. (2011). Dissection of the influenza a virus endocytic routes reveals macropinocytosis as an alternative entry pathway. *PLoS Pathog*, 7(3), e1001329. <https://doi.org/10.1371/journal.ppat.1001329>
- Di Pasquale, A., Preiss, S., Tavares Da Silva, F., & Garcon, N. (2015). Vaccine adjuvants: From 1920 to 2015 and beyond. *Vaccines (Basel)*, 3(2), 320–43. <https://doi.org/10.3390/vaccines3020320>
- Dickson, R. P., Erb-Downward, J. R., Falkowski, N. R., Hunter, E. M., Ashley, S. L., & Huffnagle, G. B. (2018). The lung microbiota of healthy mice are highly variable, cluster by environment, and reflect variation in baseline lung innate immunity. *Am J Respir Crit Care Med*, 198(4), 497–508. <https://doi.org/10.1164/rccm.201711-2180OC>
- DiPiazza, A., Richards, K., Batarse, F., Lockard, L., Zeng, H., Garcia-Sastre, A., Albrecht, R. A., & Sant, A. J. (2016). Flow cytometric and cytokine elispot approaches to characterize the cell-mediated immune response in ferrets following influenza virus infection. *J Virol*, 90(17), 7991–8004. <https://doi.org/10.1128/JVI.01001-16>
- Dong, W., Bhide, Y., Sicca, F., Meijerhof, T., Guilfoyle, K., Engelhardt, O. G., Boon, L., de Haan, C. A. M., Carnell, G., Temperton, N., de Vries-Idema, J., Kelvin, D., & Huckriede, A. (2018). Cross-protective immune responses induced by sequential influenza virus infection and by sequential vaccination with inactivated influenza vaccines. *Front Immunol*, 9, 2312. <https://doi.org/10.3389/fimmu.2018.02312>
- Dou, D., Revol, R., Ostbye, H., Wang, H., & Daniels, R. (2018). Influenza a virus cell entry, replication, virion assembly and movement. *Front Immunol*, 9, 1581. <https://doi.org/10.3389/fimmu.2018.01581>
- Du, R., Cui, Q., & Rong, L. (2019). Competitive cooperation of hemagglutinin and neuraminidase during influenza a virus entry. *Viruses*, 11(5). <https://doi.org/10.3390/vi11050458>
- Du, W., Dai, M., Li, Z., Boons, G. J., Peeters, B., van Kuppeveld, F. J. M., de Vries, E., & de Haan, C. A. M. (2018). Substrate binding by the second sialic acid-binding site of influenza a virus ni neuraminidase contributes to enzymatic activity. *J Virol*, 92(20). <https://doi.org/10.1128/JVI.01243-18>
- Du, W., de Vries, E., van Kuppeveld, F. J. M., Matrosovich, M., & de Haan, C. A. M. (2020). Second sialic acid-binding site of influenza a virus neuraminidase: Binding receptors for efficient release. *FEBSJ*. <https://doi.org/10.1111/febs.15668>

- Du, W., Guo, H., Nijman, V. S., Doedt, J., van der Vries, E., van der Lee, J., Li, Z., Boons, G. J., van Kuppeveld, F. J. M., de Vries, E., Matrosovich, M., & de Haan, C. A. M. (2019). The 2nd sialic acid-binding site of influenza a virus neuraminidase is an important determinant of the hemagglutinin-neuraminidase-receptor balance. *PLoS Pathog*, 15(6), e1007860. <https://doi.org/10.1371/journal.ppat.1007860>
- Du, W., Wolfert, M. A., Peeters, B., van Kuppeveld, F. J. M., Boons, G. J., de Vries, E., & de Haan, C. A. M. (2020). Mutation of the second sialic acid-binding site of influenza a virus neuraminidase drives compensatory mutations in hemagglutinin. *PLoS Pathog*, 16(8), e1008816. <https://doi.org/10.1371/journal.ppat.1008816>
- Dutta, A., Huang, C. T., Lin, C. Y., Chen, T. C., Lin, Y. C., Chang, C. S., & He, Y. C. (2016). Sterilizing immunity to influenza virus infection requires local antigen-specific t cell response in the lungs. *Sci Rep*, 6, 32973. <https://doi.org/10.1038/srep32973>
- Ecker, J. W., Kirchenbaum, G. A., Pierce, S. R., Skarupka, A. L., Abreu, R. B., Cooper, R. E., Taylor-Mulneix, D., Ross, T. M., & Sautto, G. A. (2020). High-yield expression and purification of recombinant influenza virus proteins from stably-transfected mammalian cell lines. *Vaccines (Basel)*, 8(3). <https://doi.org/10.3390/vaccines8030462>
- Eichelberger, M. C., & Monto, A. S. (2019). Neuraminidase, the forgotten surface antigen, emerges as an influenza vaccine target for broadened protection. *J Infect Dis*, 219(Suppl_1), S75–S80. <https://doi.org/10.1093/infdis/jiz017>
- Eichelberger, M. C., Morens, D. M., & Taubenberger, J. K. (2018). Neuraminidase as an influenza vaccine antigen: A low hanging fruit, ready for picking to improve vaccine effectiveness. *Curr Opin Immunol*, 53, 38–44. <https://doi.org/10.1016/j.coi.2018.03.025>
- Eichelberger, M. C., & Wan, H. (2015). Influenza neuraminidase as a vaccine antigen. *Curr Top Microbiol Immunol*, 386, 275–99. https://doi.org/10.1007/82__2014__398
- Elbe, S., & Buckland-Merrett, G. (2017). Data, disease and diplomacy: Gisaid's innovative contribution to global health. *Glob Chall*, 1(1), 33–46. <https://doi.org/10.1002/gch2.1018>
- Ellebedy, A. H., Ducatez, M. F., Duan, S., Stigger-Rosser, E., Rubrum, A. M., Govorkova, E. A., Webster, R. G., & Webby, R. J. (2011). Impact of prior seasonal influenza vaccination and infection on pandemic a (h1n1) influenza virus replication in ferrets. *Vaccine*, 29(17), 3335–9. <https://doi.org/10.1016/j.vaccine.2010.08.067>
- Enkirch, T., & von Messling, V. (2015). Ferret models of viral pathogenesis. *Virology*, 479-480, 259–70. <https://doi.org/10.1016/j.virol.2015.03.017>
- Erbelding, E. J., Post, D. J., Stemmy, E. J., Roberts, P. C., Augustine, A. D., Ferguson, S., Paules, C. I., Graham, B. S., & Fauci, A. S. (2018). A universal influenza vaccine: The strategic plan for the national institute of allergy and infectious diseases. *J Infect Dis*, 218(3), 347–354. <https://doi.org/10.1093/infdis/jiy103>
- European Food Safety, A., European Centre for Disease, P., Control, European Union Reference Laboratory for Avian, I., Adlhoch, C., Fusaro, A., Gonzales, J. L., Kuiken, T., Marangon, S., Niqueux, E., Staubach, C., Terregino, C., Munoz Guajardo, I., Lima, E., & Baldinelli, F. (2021). Avian influenza overview december 2020 - february 2021. *EFSA J*, 19(3), e06497. <https://doi.org/10.2903/j.efsa.2021.6497>
- Everett, H. E., van Diemen, P. M., Aramouni, M., Ramsay, A., Coward, V. J., Pavot, V., Canini, L., Holzer, B., Morgan, S., Dynamics sLoLa, C., Woolhouse, M. E. J., Tchilian, E., Brookes, S. M., Brown,

- I. H., Charleston, B., & Gilbert, S. (2021). Vaccines that reduce viral shedding do not prevent transmission of h1n1 pandemic 2009 swine influenza a virus infection to unvaccinated pigs. *J Virol*, 95(4). <https://doi.org/10.1128/JVI.01787-20>
- Fadlallah, G. M., Ma, F., Zhang, Z., Hao, M., Hu, J., Li, M., Liu, H., Liang, B., Yao, Y., Gong, R., Zhang, B., Liu, D., & Chen, J. (2020). Vaccination with consensus h7 elicits broadly reactive and protective antibodies against eurasian and north american lineage h7 viruses. *Vaccines (Basel)*, 8(1). <https://doi.org/10.3390/vaccines8010143>
- Fanning, T. G., Reid, A. H., & Taubenberger, J. K. (2000). Influenza a virus neuraminidase: Regions of the protein potentially involved in virus-host interactions. *Virology*, 276(2), 417–23. <https://doi.org/10.1006/viro.2000.0578>
- Fedson, D. S. (2018). Influenza, evolution, and the next pandemic. *Evol Med Public Health*, 2018(1), 260–269. <https://doi.org/10.1093/emph/eoy027>
- Ferdinands, J. M., Thompson, M. G., Blanton, L., Spencer, S., Grant, L., & Fry, A. M. (2021). Does influenza vaccination attenuate the severity of breakthrough infections? a narrative review and recommendations for further research. *Vaccine*, 39(28), 3678–3695. <https://doi.org/10.1016/j.vaccine.2021.05.011>
- Fischinger, S., Boudreau, C. M., Butler, A. L., Streeck, H., & Alter, G. (2019). Sex differences in vaccine-induced humoral immunity. *Semin Immunopathol*, 41(2), 239–249. <https://doi.org/10.1007/s00281-018-0726-5>
- Flannery, B., Chung, J. R., Monto, A. S., Martin, E. T., Belongia, E. A., McLean, H. Q., Gaglani, M., Murthy, K., Zimmerman, R. K., Nowalk, M. P., Jackson, M. L., Jackson, L. A., Rolfes, M. A., Spencer, S., Fry, A. M., & Investigators, U. S. F. V. (2019). Influenza vaccine effectiveness in the united states during the 2016-2017 season. *Clin Infect Dis*, 68(11), 1798–1806. <https://doi.org/10.1093/cid/ciy775>
- Flannery, B., Kondor, R. J. G., Chung, J. R., Gaglani, M., Reis, M., Zimmerman, R. K., Nowalk, M. P., Jackson, M. L., Jackson, L. A., Monto, A. S., Martin, E. T., Belongia, E. A., McLean, H. Q., Kim, S. S., Blanton, L., Kniss, K., Budd, A. P., Brammer, L., Stark, T. J., ... Patel, M. (2020). Spread of antigenically drifted influenza a(h3n2) viruses and vaccine effectiveness in the united states during the 2018-2019 season. *J Infect Dis*, 221(1), 8–15. <https://doi.org/10.1093/infdis/jiz543>
- Fonville, J. M., Wilks, S. H., James, S. L., Fox, A., Ventresca, M., Aban, M., Xue, L., Jones, T. C., Le, N. M. H., Pham, Q. T., Tran, N. D., Wong, Y., Mosterin, A., Katzelnick, L. C., Labonte, D., Le, T. T., van der Net, G., Skepner, E., Russell, C. A., ... Smith, D. J. (2014). Antibody landscapes after influenza virus infection or vaccination. *Science*, 346(6212), 996–1000. <https://doi.org/10.1126/science.1256427>
- Fox, C. B., Kramer, R. M., Barnes, V. L., Dowling, Q. M., & Vedvick, T. S. (2013). Working together: Interactions between vaccine antigens and adjuvants. *Ther Adv Vaccines*, 1(1), 7–20. <https://doi.org/10.1177/2051013613480144>
- Francis, M. E., King, M. L., & Kelvin, A. A. (2019). Back to the future for influenza preimmunity-looking back at influenza virus history to infer the outcome of future infections. *Viruses*, 11(2). <https://doi.org/10.3390/v11020122>
- Francis, M. E., McNeil, M., Dawe, N. J., Foley, M. K., King, M. L., Ross, T. M., & Kelvin, A. A. (2019). Historical h1n1 influenza virus imprinting increases vaccine protection by influencing the activity

- and sustained production of antibodies elicited at vaccination in ferrets. *Vaccines (Basel)*, 7(4). <https://doi.org/10.3390/vaccines7040133>
- Fries, L. F., Smith, G. E., & Glenn, G. M. (2013). A recombinant viruslike particle influenza a (h7n9) vaccine. *N Engl J Med*, 369(26), 2564–6. <https://doi.org/10.1056/NEJMci131186>
- Gao, J., Couzens, L., Burke, D. F., Wan, H., Wilson, P., Memoli, M. J., Xu, X., Harvey, R., Wrammert, J., Ahmed, R., Taubenberger, J. K., Smith, D. J., Fouchier, R. A. M., & Eichelberger, M. C. (2019). Antigenic drift of the influenza a(h1n1)pdm09 virus neuraminidase results in reduced effectiveness of a/california/7/2009 (h1n1pdm09)-specific antibodies. *mBio*, 10(2). <https://doi.org/10.1128/mBio.00307-19>
- Garaigorta, U., & Ortín, J. (2007). Mutation analysis of a recombinant ns replicon shows that influenza virus ns1 protein blocks the splicing and nucleo-cytoplasmic transport of its own viral mrna. *Nucleic Acids Res*, 35(14), 4573–82. <https://doi.org/10.1093/nar/gkm230>
- Garten, R. J., Davis, C. T., Russell, C. A., Shu, B., Lindstrom, S., Balish, A., Sessions, W. M., Xu, X., Skepner, E., Deyde, V., Okomo-Adhiambo, M., Gubareva, L., Barnes, J., Smith, C. B., Emery, S. L., Hillman, M. J., Rivailler, P., Smagala, J., de Graaf, M., ... Cox, N. J. (2009). Antigenic and genetic characteristics of swine-origin 2009 a(h1n1) influenza viruses circulating in humans. *Science*, 325(5937), 197–201. <https://doi.org/10.1126/science.1176225>
- Gaush, C. R., & Smith, T. F. (1968). Replication and plaque assay of influenza virus in an established line of canine kidney cells. *Appl Microbiol*, 16(4), 588–94. <https://www.ncbi.nlm.nih.gov/pubmed/5647517>
- Gaydos, J. C., Top, J., F. H., Hodder, R. A., & Russell, P. K. (2006). Swine influenza a outbreak, fort dix, new jersey, 1976. *Emerg Infect Dis*, 12(1), 23–8. <https://doi.org/10.3201/eid1201.050965>
- Gerentes, L., Kessler, N., & Aymard, M. (1999). Difficulties in standardizing the neuraminidase content of influenza vaccines. *Dev Biol Stand*, 98, 189–96, discussion 197. <https://www.ncbi.nlm.nih.gov/pubmed/10494973>
- Ghendon, Y. (1990). The immune response to influenza vaccines. *Acta Virol*, 34(3), 295–304. <https://www.ncbi.nlm.nih.gov/pubmed/1980401>
- Gibbs, A. J., Armstrong, J. S., & Downie, J. C. (2009). From where did the 2009 'swine-origin' influenza a virus (h1n1) emerge? *Virol J*, 6, 207. <https://doi.org/10.1186/1743-422X-6-207>
- Gilbert, P. B., Fong, Y., Juraska, M., Carpp, L. N., Monto, A. S., Martin, E. T., & Petrie, J. G. (2019). HAI and nai titer correlates of inactivated and live attenuated influenza vaccine efficacy. *BMC Infect Dis*, 19(1), 453. <https://doi.org/10.1186/s12879-019-4049-5>
- Gilchuk, I. M., Bangaru, S., Gilchuk, P., Irving, R. P., Kose, N., Bombardi, R. G., Thornburg, N. J., Creech, C. B., Edwards, K. M., Li, S., Turner, H. L., Yu, W., Zhu, X., Wilson, I. A., Ward, A. B., & Crowe, J., J. E. (2019). Influenza h7n9 virus neuraminidase-specific human monoclonal antibodies inhibit viral egress and protect from lethal influenza infection in mice. *Cell Host Microbe*, 26(6), 715–728 e8. <https://doi.org/10.1016/j.chom.2019.10.003>
- Giles, B. M., Bissel, S. J., Dealmeida, D. R., Wiley, C. A., & Ross, T. M. (2012). Antibody breadth and protective efficacy are increased by vaccination with computationally optimized hemagglutinin but not with polyvalent hemagglutinin-based h5n1 virus-like particle vaccines. *Clin Vaccine Immunol*, 19(2), 128–39. <https://doi.org/10.1128/CVI.05533-11>
- Giles, B. M., Crevar, C. J., Carter, D. M., Bissel, S. J., Schultz-Cherry, S., Wiley, C. A., & Ross, T. M. (2012). A computationally optimized hemagglutinin virus-like particle vaccine elicits broadly

- reactive antibodies that protect nonhuman primates from h5n1 infection. *J Infect Dis*, 205(10), 1562–70. <https://doi.org/10.1093/infdis/jis232>
- Giles, B. M., & Ross, T. M. (2011a). A computationally optimized broadly reactive antigen (cobra) based h5n1 vlp vaccine elicits broadly reactive antibodies in mice and ferrets. *Vaccine*, 29(16), 3043–54. <https://doi.org/10.1016/j.vaccine.2011.01.100>
- Giles, B. M., & Ross, T. M. (2011b). A computationally optimized broadly reactive antigen (cobra) based h5n1 vlp vaccine elicits broadly reactive antibodies in mice and ferrets. *Vaccine*, 29(16), 3043–54. <https://doi.org/10.1016/j.vaccine.2011.01.100>
- Giurgea, L. T., Morens, D. M., Taubenberger, J. K., & Memoli, M. J. (2020). Influenza neuraminidase: A neglected protein and its potential for a better influenza vaccine. *Vaccines (Basel)*, 8(3). <https://doi.org/10.3390/vaccines8030409>
- Giurgea, L. T., Park, J. K., Walters, K. A., Scherler, K., Cervantes-Medina, A., Freeman, A., Rosas, L. A., Kash, J. C., Taubenberger, J. K., & Memoli, M. J. (2021). The effect of calcium and magnesium on activity, immunogenicity, and efficacy of a recombinant n1/n2 neuraminidase vaccine. *NPJ Vaccines*, 6(1), 48. <https://doi.org/10.1038/s41541-021-00310-x>
- Gooch, K. E., Marriott, A. C., Ryan, K. A., Yeates, P., Slack, G. S., Brown, P. J., Fothergill, R., Whittaker, C. J., & Carroll, M. W. (2019). Heterosubtypic cross-protection correlates with cross-reactive interferon-gamma-secreting lymphocytes in the ferret model of influenza. *Sci Rep*, 9(1), 2617. <https://doi.org/10.1038/s41598-019-38885-o>
- Gostic, K. M., Ambrose, M., Worobey, M., & Lloyd-Smith, J. O. (2016). Potent protection against h5n1 and h7n9 influenza via childhood hemagglutinin imprinting. *Science*, 354(6313), 722–726. <https://doi.org/10.1126/science.aag1322>
- Goto, H., & Kawaoka, Y. (1998). A novel mechanism for the acquisition of virulence by a human influenza a virus. *Proc Natl Acad Sci U S A*, 95(17), 10224–8. <https://doi.org/10.1073/pnas.95.17.10224>
- Gottschalk, A., & Lind, P. E. (1949). Product of interaction between influenza virus enzyme and ovo-mucin. *Nature*, 164(4162), 232. <https://doi.org/10.1038/164232ao>
- Grebe, K. M., Yewdell, J. W., & Bennink, J. R. (2008). Heterosubtypic immunity to influenza a virus: Where do we stand? *Microbes Infect*, 10(9), 1024–9. <https://doi.org/10.1016/j.micinf.2008.07.002>
- Green, T. D., Montefiori, D. C., & Ross, T. M. (2003). Enhancement of antibodies to the human immunodeficiency virus type 1 envelope by using the molecular adjuvant c3d. *Journal of Virology*, 77(3), 2046–2055. <https://doi.org/10.1128/JVI.77.3.2046-2055.2003>
- Grohskopf, L. A., Alyanak, E., Broder, K. R., Walter, E. B., Fry, A. M., & Jernigan, D. B. (2019). Prevention and control of seasonal influenza with vaccines: Recommendations of the advisory committee on immunization practices - united states, 2019-20 influenza season. *MMWR Recomm Rep*, 68(3), 1–21. <https://doi.org/10.15585/mmwr.rr6803a1>
- Guex, N., & Peitsch, M. C. (1997). Swiss-model and the swiss-pdbviewer: An environment for comparative protein modeling. *Electrophoresis*, 18(15), 2714–23. <https://doi.org/10.1002/elps.1150181505>
- Guex, N., Peitsch, M. C., & Schwede, T. (2009). Automated comparative protein structure modeling with swiss-model and swiss-pdbviewer: A historical perspective. *Electrophoresis*, 30 Suppl 1, S162–73. <https://doi.org/10.1002/elps.200900140>
- Guideline on influenza vaccines. (2014). http://www.ema.europa.eu/docs/en%5C_GB/document%5C_library/Scientific%5C_guideline/2014/07/WC500170300.pdf

- Gupta, R., Jung, E., & Brunak, S. (2004). Prediction of n-glycosylation sites in human proteins. <http://www.cbs.dtu.dk/services/NetNGlyc/>
- Gupta, V., Earl, D. J., & Deem, M. W. (2006). Quantifying influenza vaccine efficacy and antigenic distance. *Vaccine*, 24(18), 3881–8. <https://doi.org/10.1016/j.vaccine.2006.01.010>
- Hadler, J. L., Yousey-Hindes, K., Perez, A., Anderson, E. J., Bargsten, M., Bohm, S. R., Hill, M., Hogan, B., Laidler, M., Lindgren, M. L., Lung, K. L., Mermel, E., Miller, L., Morin, C., Parker, E., Zansky, S. M., & Chaves, S. S. (2016). Influenza-related hospitalizations and poverty levels - united states, 2010-2012. *MMWR Morb Mortal Wkly Rep*, 65(5), 101–5. <https://doi.org/10.15585/mmwr.mm6505a1>
- Hagan, T., Cortese, M., Rouphael, N., Boudreau, C., Linde, C., Maddur, M. S., Das, J., Wang, H., Guthmiller, J., Zheng, N. Y., Huang, M., Upadhyay, A. A., Gardinassi, L., Petitdemange, C., McCullough, M. P., Johnson, S. J., Gill, K., Cervasi, B., Zou, J., ... Pulendran, B. (2019). Antibiotics-driven gut microbiome perturbation alters immunity to vaccines in humans. *Cell*, 178(6), 1313–1328 e13. <https://doi.org/10.1016/j.cell.2019.08.010>
- Hamming, P. H. E., Overeem, N. J., & Huskens, J. (2020). Influenza as a molecular walker. *Chem Sci*, 11(1), 27–36. <https://doi.org/10.1039/c9sc05149j>
- Hancock, K., Veguilla, V., Lu, X., Zhong, W., Butler, E. N., Sun, H., Liu, F., Dong, L., DeVos, J. R., Gargiullo, P. M., Brammer, T. L., Cox, N. J., Tumpey, T. M., & Katz, J. M. (2009). Cross-reactive antibody responses to the 2009 pandemic h1n1 influenza virus. *N Engl J Med*, 361(20), 1945–52. <https://doi.org/10.1056/NEJMoa0906453>
- Hao, W., Wang, L., & Li, S. (2020). Roles of the non-structural proteins of influenza a virus. *Pathogens*, 9(10). <https://doi.org/10.3390/pathogens9100812>
- Harris, A., Cardone, G., Winkler, D. C., Heymann, J. B., Brecher, M., White, J. M., & Steven, A. C. (2006). Influenza virus pleiomorphy characterized by cryoelectron tomography. *Proc Natl Acad Sci U S A*, 103(50), 19123–7. <https://doi.org/10.1073/pnas.0607614103>
- Harvey, W. T., Benton, D. J., Gregory, V., Hall, J. P., Daniels, R. S., Bedford, T., Haydon, D. T., Hay, A. J., McCauley, J. W., & Reeve, R. (2016). Identification of low- and high-impact hemagglutinin amino acid substitutions that drive antigenic drift of influenza a(h1n1) viruses. *PLoS Pathog*, 12(4), e1005526. <https://doi.org/10.1371/journal.ppat.1005526>
- Hatta, Y., Boltz, D., Sarawar, S., Kawaoka, Y., Neumann, G., & Bilsel, P. (2018). Novel influenza vaccine m2sr protects against drifted h1n1 and h3n2 influenza virus challenge in ferrets with pre-existing immunity. *Vaccine*, 36(33), 5097–5103. <https://doi.org/10.1016/j.vaccine.2018.06.053>
- Hay, J. A., Laurie, K., White, M., & Riley, S. (2019). Characterising antibody kinetics from multiple influenza infection and vaccination events in ferrets. *PLoS Comput Biol*, 15(8), e1007294. <https://doi.org/10.1371/journal.pcbi.1007294>
- Hebert, D. N., Zhang, J. X., Chen, W., Foellmer, B., & Helenius, A. (1997). The number and location of glycans on influenza hemagglutinin determine folding and association with calnexin and calreticulin. *J Cell Biol*, 139(3), 613–23. <https://www.ncbi.nlm.nih.gov/pubmed/9348279>
- Henry, C., Palm, A. E., Krammer, F., & Wilson, P. C. (2018). From original antigenic sin to the universal influenza virus vaccine. *Trends Immunol*, 39(1), 70–79. <https://doi.org/10.1016/j.it.2017.08.003>
- Hessa, T., Meindl-Beinker, N. M., Bernsel, A., Kim, H., Sato, Y., Lerch-Bader, M., Nilsson, I., White, S. H., & von Heijne, G. (2007). Molecular code for transmembrane-helix recognition by the sec61 translocon. *Nature*, 450(7172), 1026–30. <https://doi.org/10.1038/nature06387>

- Hilgers, L. A. T., Platenburg, P., Bajramovic, J., Veth, J., Sauerwein, R., Roeffen, W., Pohl, M., van Amerongen, G., Stittelaar, K. J., & van den Bosch, J. F. (2017). Carbohydrate fatty acid monosulphate esters are safe and effective adjuvants for humoral responses. *Vaccine*, 35(24), 3249–3255. <https://doi.org/10.1016/j.vaccine.2017.04.055>
- Hirsch, A. (1883). Handbook of geographical and historical pathology. Volume i. acute infective diseases (pp. 7–54). The New Sydenham Society.
- Ho, A. W., Prabhu, N., Betts, R. J., Ge, M. Q., Dai, X., Hutchinson, P. E., Lew, F. C., Wong, K. L., Hanson, B. J., Macary, P. A., & Kemeny, D. M. (2011). Lung cd103+ dendritic cells efficiently transport influenza virus to the lymph node and load viral antigen onto mhc class i for presentation to cd8 t cells. *J Immunol*, 187(11), 6011–21. <https://doi.org/10.4049/jimmunol.1100987>
- Hogue, B. G., & Nayak, D. P. (1992). Synthesis and processing of the influenza virus neuraminidase, a type ii transmembrane glycoprotein. *Virology*, 188(2), 510–517. [https://doi.org/10.1016/0042-6822\(92\)90505-j](https://doi.org/10.1016/0042-6822(92)90505-j)
- Honigsbaum, M. (2020). Revisiting the 1957 and 1968 influenza pandemics. *The Lancet*, 395(10240), 1824–1826. [https://doi.org/10.1016/S0140-6736\(20\)31201-0](https://doi.org/10.1016/S0140-6736(20)31201-0)
- Houser, K. V., Pearce, M. B., Katz, J. M., & Tumpey, T. M. (2013). Impact of prior seasonal h3n2 influenza vaccination or infection on protection and transmission of emerging variants of influenza a(h3n2)v virus in ferrets. *J Virol*, 87(24), 13480–9. <https://doi.org/10.1128/JVI.02434-13>
- Huang, S. S., Banner, D., Degousee, N., Leon, A. J., Xu, L., Paquette, S. G., Kanagasabai, T., Fang, Y., Rubino, S., Rubin, B., Kelvin, D. J., & Kelvin, A. A. (2012). Differential pathological and immune responses in newly weaned ferrets are associated with a mild clinical outcome of pandemic 2009 h1n1 infection. *J Virol*, 86(24), 13187–201. <https://doi.org/10.1128/JVI.01456-12>
- Huang, S. S., Banner, D., Fang, Y., Ng, D. C., Kanagasabai, T., Kelvin, D. J., & Kelvin, A. A. (2011). Comparative analyses of pandemic h1n1 and seasonal h1n1, h3n2, and influenza b infections depict distinct clinical pictures in ferrets. *PLoS One*, 6(11), e27512. <https://doi.org/10.1371/journal.pone.0027512>
- Huang, Y., Owino, S. O., Crevar, C. J., Carter, D. M., & Ross, T. M. (2020). N-linked glycans and k147 residue on hemagglutinin synergize to elicit broadly reactive h1n1 influenza virus antibodies. *J Virol*, 94(6). <https://doi.org/10.1128/JVI.01432-19>
- Hufeldt, M. R., Nielsen, D. S., Vogensen, F. K., Midtvedt, T., & Hansen, A. K. (2010). Variation in the gut microbiota of laboratory mice is related to both genetic and environmental factors. *Comp Med*, 60(5), 336–47.
- Humayun, F., Khan, F., Fawad, N., Shamas, S., Fazal, S., Khan, A., Ali, A., Farhan, A., & Wei, D. Q. (2021). Computational method for classification of avian influenza a virus using dna sequence information and physicochemical properties. *Front Genet*, 12, 599321. <https://doi.org/10.3389/fgene.2021.599321>
- Hutchinson, E. C., Charles, P. D., Hester, S. S., Thomas, B., Trudgian, D., Martinez-Alonso, M., & Fodor, E. (2014). Conserved and host-specific features of influenza virion architecture. *Nat Commun*, 5, 4816. <https://doi.org/10.1038/ncomms5816>
- Ison, M. G. (2013). Clinical use of approved influenza antivirals: Therapy and prophylaxis. *Influenza Other Respir Viruses*, 7 Suppl 1, 7–13. <https://doi.org/10.1111/irv.12046>
- Ito, H., Nishimura, H., Kisu, T., Hagiwara, H., Watanabe, O., Kadji, F. M. N., Sato, K., Omiya, S., Takashita, E., & Nobusawa, E. (2020). Low response in eliciting neuraminidase inhibition activ-

- ity of sera among recipients of a split, monovalent pandemic influenza vaccine during the 2009 pandemic. *PLoS One*, 15(5), e0233001. <https://doi.org/10.1371/journal.pone.0233001>
- Itoh, M., & Hotta, H. (1997). [structure, function and regulation of expression of influenza virus matrix m₁ protein]. *Nihon Rinsho*, 55(10), 2581–6. <https://www.ncbi.nlm.nih.gov/pubmed/9360375>
- Itoh, Y., Shinya, K., Kiso, M., Watanabe, T., Sakoda, Y., Hatta, M., Muramoto, Y., Tamura, D., Sakai-Tagawa, Y., Noda, T., Sakabe, S., Imai, M., Hatta, Y., Watanabe, S., Li, C., Yamada, S., Fujii, K., Murakami, S., Imai, H., ... Kawaoka, Y. (2009). In vitro and in vivo characterization of new swine-origin h1n1 influenza viruses. *Nature*, 460(7258), 1021–5. <https://doi.org/10.1038/nature08260>
- Jackson, D. C., & Webster, R. G. (1982). A topographic map of the enzyme active center and antigenic sites on the neuraminidase of influenza virus a/tokyo/3/67 (h2n2). *Virology*, 123(1), 69–77. [https://doi.org/10.1016/0042-6822\(82\)90295-1](https://doi.org/10.1016/0042-6822(82)90295-1)
- Jackson, M. L., Chung, J. R., Jackson, L. A., Phillips, C. H., Benoit, J., Monto, A. S., Martin, E. T., Belongia, E. A., McLean, H. Q., Gaglani, M., Murthy, K., Zimmerman, R., Nowalk, M. P., Fry, A. M., & Flannery, B. (2017). Influenza vaccine effectiveness in the united states during the 2015-2016 season. *NEnglJ Med*, 377(6), 534–543. <https://doi.org/10.1056/NEJMoa1700153>
- Jagger, B. W., Wise, H. M., Kash, J. C., Walters, K. A., Wills, N. M., Xiao, Y. L., Dunfee, R. L., Schwartzman, L. M., Ozinsky, A., Bell, G. L., Dalton, R. M., Lo, A., Efstatithiou, S., Atkins, J. F., Firth, A. E., Taubenberger, J. K., & Digard, P. (2012). An overlapping protein-coding region in influenza a virus segment 3 modulates the host response. *Science*, 337(6091), 199–204. <https://doi.org/10.1126/science.1222213>
- Jang, J., & Bae, S. E. (2018). Comparative co-evolution analysis between the ha and na genes of influenza a virus. *Virology (Auckl)*, 9, i178122X18788328. <https://doi.org/10.1177/1178122X18788328>
- Jang, Y. H., Lee, E. Y., Byun, Y. H., Jung, E. J., Lee, Y. J., Lee, Y. H., Lee, K. H., Lee, J., & Seong, B. L. (2014). Protective efficacy in mice of monovalent and trivalent live attenuated influenza vaccines in the background of cold-adapted a/x-31 and b/lee/40 donor strains. *Vaccine*, 32(5), 535–43. <https://doi.org/10.1016/j.vaccine.2013.12.002>
- Jang, Y. H., & Seong, B. L. (2019). The quest for a truly universal influenza vaccine. *Front Cell Infect Microbiol*, 9, 344. <https://doi.org/10.3389/fcimb.2019.00344>
- Jayaraman, A., Chandrasekaran, A., Viswanathan, K., Raman, R., Fox, J. G., & Sasisekharan, R. (2012). Decoding the distribution of glycan receptors for human-adapted influenza a viruses in ferret respiratory tract. *PLoS One*, 7(2), e27517. <https://doi.org/10.1371/journal.pone.0027517>
- Jennings, R., & Potter, C. W. (1973). Enhanced response to influenza a vaccines in hamsters primed by prior heterotype influenza infection. *Arch Gesamte Virusforsch*, 42(2), 197–206. <https://doi.org/10.1007/bf01270840>
- Jeong, J. H., Kim, E. H., Lloren, K. K. S., Kwon, J. J., Kwon, H. I., Ahn, S. J., Kim, Y. I., Choi, W. S., Si, Y. J., Lee, O. J., Han, H. J., Baek, Y. H., Song, M. S., Choi, Y. K., & Kim, C. J. (2019). Preclinical evaluation of the efficacy of an h5n8 vaccine candidate (idcdc-rg43a) in mouse and ferret models for pandemic preparedness. *Vaccine*, 37(3), 484–493. <https://doi.org/10.1016/j.vaccine.2018.11.064>
- Jia, N., Barclay, W. S., Roberts, K., Yen, H. L., Chan, R. W., Lam, A. K., Air, G., Peiris, J. S., Dell, A., Nicholls, J. M., & Haslam, S. M. (2014). Glycomic characterization of respiratory tract tissues of ferrets: Implications for its use in influenza virus infection studies. *J Biol Chem*, 289(41), 28489–504. <https://doi.org/10.1074/jbc.M114.588541>

- Jiang, H., Peng, W., Qi, J., Chai, Y., Song, H., Bi, Y., Rijal, P., Wang, H., Oladejo, B. O., Liu, J., Shi, Y., Gao, G. F., Townsend, A. R., & Wu, Y. (2020). Structure-based modification of an anti-neuraminidase human antibody restores protection efficacy against the drifted influenza virus. *mBio*, *11*(5). <https://doi.org/10.1128/mBio.02315-20>
- Job, E. R., Schotsaert, M., Ibanez, L. I., Smet, A., Ysenbaert, T., Roose, K., Dai, M., de Haan, C. A. M., Kleanthous, H., Vogel, T. U., & Saelens, X. (2018). Antibodies directed toward neuraminidase n1 control disease in a mouse model of influenza. *J Virol*, *92*(4). <https://doi.org/10.1128/JVI.01584-17>
- Johansson, B. (1998). Supplementation of conventional influenza a vaccine with purified viral neuraminidase results in a balanced and broadened immune response. *Vaccine*, *16*(9-10), 1009–1015. [https://doi.org/10.1016/S0264-410X\(97\)00279-X](https://doi.org/10.1016/S0264-410X(97)00279-X)
- Johansson, B. E., & Brett, I. C. (2003). Variation in the divalent cation requirements of influenza a virus n2 neuraminidases. *J Biochem*, *134*(3), 345–52. <https://doi.org/10.1093/jb/mvg151>
- Johansson, B. E., Bucher, D. J., & Kilbourne, E. D. (1989). Purified influenza virus hemagglutinin and neuraminidase are equivalent in stimulation of antibody response but induce contrasting types of immunity to infection. *J Virol*, *63*(3), 1239–46. <https://doi.org/10.1128/JVI.63.3.1239-1246.1989>
- Johansson, B. E., Moran, T. M., & Kilbourne, E. D. (1987). Antigen-presenting b cells and helper t cells cooperatively mediate intravirionic antigenic competition between influenza a virus surface glycoproteins. *Proc Natl Acad Sci USA*, *84*(19), 6869–73. <https://doi.org/10.1073/pnas.84.19.6869>
- Johnson, N. P. A. S., & Mueller, J. (2002). Updating the accounts: Global mortality of the 1918-1920 "spanish" influenza pandemic. *Bulletin of the History of Medicine*, *76*(1), 105–115. <https://doi.org/10.1353/bhm.2002.0022>
- Joseph, U., Linster, M., Suzuki, Y., Krauss, S., Halpin, R. A., Vijaykrishna, D., Fabrizio, T. P., Bestebroer, T. M., Maurer-Stroh, S., Webby, R. J., Wentworth, D. E., Fouchier, R. A., Bahl, J., Smith, G. J., & Group, C. H. N. W. (2015). Adaptation of pandemic h2n2 influenza a viruses in humans. *J Virol*, *89*(4), 2442–7. <https://doi.org/10.1128/JVI.02590-14>
- Jurchott, K., Schulz, A. R., Bozzetti, C., Pohlmann, D., Stervbo, U., Warth, S., Malzer, J. N., Waldner, J., Schweiger, B., Olek, S., Grutzkau, A., Babel, N., Thiel, A., & Neumann, A. U. (2016). Highly predictive model for a protective immune response to the a(h1n1)pdm2009 influenza strain after seasonal vaccination. *PLoS One*, *11*(3), e0150812. <https://doi.org/10.1371/journal.pone.0150812>
- Kaplan, B. S., Anderson, T. K., Chang, J., Santos, J., Perez, D., Lewis, N., & Vincent, A. L. (2021). Evolution and antigenic advancement of n2 neuraminidase of swine influenza a viruses circulating in the united states following two separate introductions from human seasonal viruses. *J Virol*, *95*(20), e0063221. <https://doi.org/10.1128/JVI.00632-21>
- Kaplan, B. S., & Vincent, A. L. (2020). Detection and titration of influenza a virus neuraminidase inhibiting (nai) antibodies using an enzyme-linked lectin assay (ella). *Methods Mol Biol*, *2123*, 335–344. https://doi.org/10.1007/978-1-0716-0346-8__24
- Karasin, A. I., Landgraf, J., Swenson, S., Erickson, G., Goyal, S., Woodruff, M., Scherba, G., Anderson, G., & Olsen, C. W. (2002). Genetic characterization of h1n2 influenza a viruses isolated from pigs throughout the united states. *J Clin Microbiol*, *40*(3), 1073–9. <https://www.ncbi.nlm.nih.gov/pubmed/11880444>

- Kaul, K. L., Mangold, K. A., Du, H., Pesavento, K. M., Nawrocki, J., & Nowak, J. A. (2010). Influenza a subtyping: Seasonal h1n1, h3n2, and the appearance of novel h1n1. *J Mol Diagn*, 12(5), 664–9. <https://doi.org/10.2353/jmoldx.2010.090225>
- Kawakami, E., Watanabe, T., Fujii, K., Goto, H., Watanabe, S., Noda, T., & Kawaoka, Y. (2011). Strand-specific real-time rt-pcr for distinguishing influenza vrna, crna, and mrna. *J Virol Methods*, 173(1), 1–6. <https://doi.org/10.1016/j.jviromet.2010.12.014>
- Kearse, M., Moir, R., Wilson, A., Stones-Havas, S., Cheung, M., Sturrock, S., Buxton, S., Cooper, A., Markowitz, S., Duran, C., Thierer, T., Ashton, B., Meintjes, P., & Drummond, A. (2012). Geneious basic: An integrated and extendable desktop software platform for the organization and analysis of sequence data. *Bioinformatics*, 28(12), 1647–9. <https://doi.org/10.1093/bioinformatics/bts199>
- Kendal, A. P. (1987). Epidemiologic implications of changes in the influenza virus genome. *The American Journal of Medicine*, 82(6), 4–14. [https://doi.org/10.1016/0002-9343\(87\)90554-7](https://doi.org/10.1016/0002-9343(87)90554-7)
- Kilbourne, E. D. (1976). Comparative efficacy of neuraminidase-specific and conventional influenza virus vaccines in induction of antibody to neuraminidase in humans. *J Infect Dis*, 134(4), 384–94. <https://doi.org/10.1093/infdis/134.4.384>
- Kilbourne, E. D. (2006). Influenza pandemics of the 20th century. *Emerg Infect Dis*, 12(1), 9–14. <https://doi.org/10.3201/eid1201.051254>
- Kilbourne, E. D., Johansson, B. E., & Grajower, B. (1990). Independent and disparate evolution in nature of influenza a virus hemagglutinin and neuraminidase glycoproteins. *Proc Natl Acad Sci USA*, 87(2), 786–90. <https://doi.org/10.1073/pnas.87.2.786>
- Kilbourne, E. D., Laver, W. G., Schulman, J. L., & Webster, R. G. (1968). Antiviral activity of antiserum specific for an influenza virus neuraminidase. *J Virol*, 2(4), 281–8. <https://doi.org/10.1128/JVI.2.4.281-288.1968>
- Kim, H. H., Yang, D. K., Seo, B. H., & Cho, I. S. (2018). Serosurvey of rabies virus, canine distemper virus, parvovirus, and influenza virus in military working dogs in korea. *J Vet Med Sci*, 80(9), 1424–1430. <https://doi.org/10.1292/jvms.18-0012>
- Kim, J. I., & Park, M. S. (2012). N-linked glycosylation in the hemagglutinin of influenza a viruses. *Yonsei Med J*, 53(5), 886–93. <https://doi.org/10.3349/ymj.2012.53.5.886>
- Kirchenbaum, G. A., Allen, J. D., Layman, T. S., Sautto, G. A., & Ross, T. M. (2017). Infection of ferrets with influenza virus elicits a light chain-biased antibody response against hemagglutinin. *J Immunol*, 199(11), 3798–3807. <https://doi.org/10.4049/jimmunol.1701174>
- Kirchenbaum, G. A., Carter, D. M., & Ross, T. M. (2016). Sequential infection in ferrets with antigenically distinct seasonal h1n1 influenza viruses boosts hemagglutinin stalk-specific antibodies. *J Virol*, 90(2), 1116–28. <https://doi.org/10.1128/JVI.02372-15>
- Klingen, T. R., Reimering, S., Guzman, C. A., & McHardy, A. C. (2018). In silico vaccine strain prediction for human influenza viruses. *Trends Microbiol*, 26(2), 119–131. <https://doi.org/10.1016/j.tim.2017.09.001>
- Koedijk, D., Pastrana, F. R., Hoekstra, H., Berg, S. V. D., Back, J. W., Kerstholt, C., Prins, R. C., Bakker-Woudenberg, I., van Dijl, J. M., & Buist, G. (2017). Differential epitope recognition in the immunodominant staphylococcal antigen a of staphylococcus aureus by mouse versus human igg antibodies. *Sci Rep*, 7(1), 8141. <https://doi.org/10.1038/s41598-017-08182-9>

- Koel, B. F., Burke, D. F., Bestebroer, T. M., van der Vliet, S., Zondag, G. C., Vervaet, G., Skepner, E., Lewis, N. S., Spronken, M. I., Russell, C. A., Eropkin, M. Y., Hurt, A. C., Barr, I. G., de Jong, J. C., Rimmelzwaan, G. F., Osterhaus, A. D., Fouchier, R. A., & Smith, D. J. (2013). Substitutions near the receptor binding site determine major antigenic change during influenza virus evolution. *Science*, 342(6161), 976–9. <https://doi.org/10.1126/science.1244730>
- Koel, B. F., Mogling, R., Chutinimitkul, S., Fraaij, P. L., Burke, D. F., van der Vliet, S., de Wit, E., Bestebroer, T. M., Rimmelzwaan, G. F., Osterhaus, A. D., Smith, D. J., Fouchier, R. A., & de Graaf, M. (2015). Identification of amino acid substitutions supporting antigenic change of influenza a(h1n1)pdm09 viruses. *J Virol*, 89(7), 3763–75. <https://doi.org/10.1128/JVI.02962-14>
- Koel, B. F., van der Vliet, S., Burke, D. F., Bestebroer, T. M., Bharoto, E. E., Yasa, I. W., Herliana, I., Laksono, B. M., Xu, K., Skepner, E., Russell, C. A., Rimmelzwaan, G. F., Perez, D. R., Osterhaus, A. D., Smith, D. J., Prajitno, T. Y., & Fouchier, R. A. (2014). Antigenic variation of clade 2.1 h5n1 virus is determined by a few amino acid substitutions immediately adjacent to the receptor binding site. *MBio*, 5(3), e01070-14. <https://doi.org/10.1128/mBio.01070-14>
- Kosik, I., Angeletti, D., Gibbs, J. S., Angel, M., Takeda, K., Kosikova, M., Nair, V., Hickman, H. D., Xie, H., Brooke, C. B., & Yewdell, J. W. (2019). Neuraminidase inhibition contributes to influenza a virus neutralization by anti-hemagglutinin stem antibodies. *J Exp Med*, 216(2), 304–316. <https://doi.org/10.1084/jem.20181624>
- Kosik, I., & Yewdell, J. W. (2017). Influenza a virus hemagglutinin specific antibodies interfere with virion neuraminidase activity via two distinct mechanisms. *Virology*, 500, 178–183. <https://doi.org/10.1016/j.virol.2016.10.024>
- Kosikova, M., Li, L., Radvak, P., Ye, Z., Wan, X. F., & Xie, H. (2018). Imprinting of repeated influenza a/h3 exposures on antibody quantity and antibody quality: Implications for seasonal vaccine strain selection and vaccine performance. *Clin Infect Dis*, 67(10), 1523–1532. <https://doi.org/10.1093/cid/ciy327>
- Krammer, F., Fouchier, R. A. M., Eichelberger, M. C., Webby, R. J., Shaw-Saliba, K., Wan, H., Wilson, P. C., Compans, R. W., Skountzou, I., & Monto, A. S. (2018). Naction! how can neuraminidase-based immunity contribute to better influenza virus vaccines? *MBio*, 9(2). <https://doi.org/10.1128/mBio.02332-17>
- Krammer, F., & Palese, P. (2015). Advances in the development of influenza virus vaccines. *Nat Rev Drug Discov*, 14(3), 167–82. <https://doi.org/10.1038/nrd4529>
- Krammer, F., Weir, J. P., Engelhardt, O., Katz, J. M., & Cox, R. J. (2020). Meeting report and review: Immunological assays and correlates of protection for next-generation influenza vaccines. *Influenza Other Respir Viruses*, 14(2), 237–243. <https://doi.org/10.1111/irv.12706>
- Kreijtz, J. H., Bodewes, R., van den Brand, J. M., de Mutsert, G., Baas, C., van Amerongen, G., Fouchier, R. A., Osterhaus, A. D., & Rimmelzwaan, G. F. (2009). Infection of mice with a human influenza a/h3n2 virus induces protective immunity against lethal infection with influenza a/h5n1 virus. *Vaccine*, 27(36), 4983–9. <https://doi.org/10.1016/j.vaccine.2009.05.079>
- Kreijtz, J. H., Bodewes, R., van Amerongen, G., Kuiken, T., Fouchier, R. A., Osterhaus, A. D., & Rimmelzwaan, G. F. (2007). Primary influenza a virus infection induces cross-protective immunity against a lethal infection with a heterosubtypic virus strain in mice. *Vaccine*, 25(4), 612–20. <https://doi.org/10.1016/j.vaccine.2006.08.036>

- Krivanova, O., & Rathova, V. (1969). Serum inhibitors of myxoviruses. *Curr Top Microbiol Immunol*, 47, 125–51. https://doi.org/10.1007/978-3-642-46160-6__6
- Kumar, V. (2017). Influenza in children. *Indian J Pediatr*, 84(2), 139–143. <https://doi.org/10.1007/s12098-016-2232-x>
- Kwon, H. I., Kim, Y. I., Park, S. J., Kim, E. H., Kim, S., Si, Y. J., Song, M. S., Pascua, P. N. Q., Govorkova, E. A., Webster, R. G., Webby, R. J., & Choi, Y. K. (2019). A novel neuraminidase-dependent hemagglutinin cleavage mechanism enables the systemic spread of an h7n6 avian influenza virus. *mBio*, 10(6). <https://doi.org/10.1128/mBio.02369-19>
- Lai, J. C., Chan, W. W., Kien, F., Nicholls, J. M., Peiris, J. S., & Garcia, J. M. (2010). Formation of virus-like particles from human cell lines exclusively expressing influenza neuraminidase. *J Gen Virol*, 91(Pt 9), 2322–30. <https://doi.org/10.1099/vir.0.019935-o>
- Lai, S., Qin, Y., Cowling, B. J., Ren, X., Wardrop, N. A., Gilbert, M., Tsang, T. K., Wu, P., Feng, L., Jiang, H., Peng, Z., Zheng, J., Liao, Q., Li, S., Horby, P. W., Farrar, J. J., Gao, G. F., Tatem, A. J., & Yu, H. (2016). Global epidemiology of avian influenza a h5n1 virus infection in humans, 1997–2015: A systematic review of individual case data. *The Lancet Infectious Diseases*, 16(7), e108–e118. [https://doi.org/10.1016/s1473-3099\(16\)00153-5](https://doi.org/10.1016/s1473-3099(16)00153-5)
- Lantos, P. M., Hoffman, K., Hohle, M., Anderson, B., & Gray, G. C. (2016). Are people living near modern swine production facilities at increased risk of influenza virus infection? *Clin Infect Dis*, 63(12), 1558–1563. <https://doi.org/10.1093/cid/ciw646>
- Laurie, K. L., Carolan, L. A., Middleton, D., Lowther, S., Kelso, A., & Barr, I. G. (2010). Multiple infections with seasonal influenza a virus induce cross-protective immunity against a(h1n1) pandemic influenza virus in a ferret model. *J Infect Dis*, 202(7), 1011–20. <https://doi.org/10.1086/656188>
- Laursen, N. S., & Wilson, I. A. (2013). Broadly neutralizing antibodies against influenza viruses. *Antiviral Res*, 98(3), 476–83. <https://doi.org/10.1016/j.antiviral.2013.03.021>
- Laver, W. G., & Valentine, R. C. (1969). Morphology of the isolated hemagglutinin and neuraminidase subunits of influenza virus. *Virology*, 38(1), 105–119. [https://doi.org/10.1016/0042-6822\(69\)90132-9](https://doi.org/10.1016/0042-6822(69)90132-9)
- Lee, M. S., & Chen, J. S. (2004). Predicting antigenic variants of influenza a/h3n2 viruses. *Emerg Infect Dis*, 10(8), 1385–90. <https://doi.org/10.3201/eid1008.040107>
- Lee, M. S., Mahmood, K., Adhikary, L., August, M. J., Cordova, J., Cho, I., Kemble, G., Reisinger, K., Walker, R. E., & Mendelman, P. M. (2004). Measuring antibody responses to a live attenuated influenza vaccine in children. *Pediatr Infect Dis J*, 23(9), 852–6. <https://doi.org/10.1097/01.inf.0000137566.87691.3b>
- Lees, W. D., Moss, D. S., & Shepherd, A. J. (2010). A computational analysis of the antigenic properties of haemagglutinin in influenza a h3n2. *Bioinformatics*, 26(11), 1403–8. <https://doi.org/10.1093/bioinformatics/btq160>
- Lemey, P., Suchard, M., & Rambaut, A. (2009). Reconstructing the initial global spread of a human influenza pandemic: A bayesian spatial-temporal model for the global spread of h1n1pdm. *PLoS Curr*, 1, RRN1031. <https://doi.org/10.1371/currents.RRN1031>
- Leon, A. J., Banner, D., Xu, L., Ran, L., Peng, Z., Yi, K., Chen, C., Xu, F., Huang, J., Zhao, Z., Lin, Z., Huang, S. H., Fang, Y., Kelvin, A. A., Ross, T. M., Farooqui, A., & Kelvin, D. J. (2013). Sequencing, annotation, and characterization of the influenza ferret infectome. *J Virol*, 87(4), 1957–66. <https://doi.org/10.1128/JVI.02476-12>

- Lessler, J., Riley, S., Read, J. M., Wang, S., Zhu, H., Smith, G. J., Guan, Y., Jiang, C. Q., & Cummings, D. A. (2012). Evidence for antigenic seniority in influenza a (h3n2) antibody responses in southern china. *PLoS Pathog*, 8(7), e1002802. <https://doi.org/10.1371/journal.ppat.1002802>
- Levine, M. Z., Holiday, C., Jefferson, S., Gross, F. L., Liu, F., Li, S., Friel, D., Boutet, P., Innis, B. L., Mallett, C. P., Tumpey, T. M., Stevens, J., & Katz, J. M. (2019). Heterologous prime-boost with a(h5n1) pandemic influenza vaccines induces broader cross-clade antibody responses than homologous prime-boost. *NPJ Vaccines*, 4, 22. <https://doi.org/10.1038/s41541-019-0114-8>
- Lewis, N. S., Russell, C. A., Langat, P., Anderson, T. K., Berger, K., Bielejec, F., Burke, D. F., Dudas, G., Fonville, J. M., Fouchier, R. A., Kellam, P., Koel, B. F., Lemey, P., Nguyen, T., Nuansrichy, B., Peiris, J. M., Saito, T., Simon, G., Skepner, E., ... Vincent, A. L. (2016). The global antigenic diversity of swine influenza a viruses. *eLife*, 5, e12217. <https://doi.org/10.7554/eLife.12217>
- Li, Q., Sun, X., Li, Z., Liu, Y., Vavricka, C. J., Qi, J., & Gao, G. F. (2012). Structural and functional characterization of neuraminidase-like molecule n10 derived from bat influenza a virus. *Proc Natl Acad Sci U S A*, 109(46), 18897–902. <https://doi.org/10.1073/pnas.1211037109>
- Li, X., & Deem, M. W. (2016). Influenza evolution and h3n2 vaccine effectiveness, with application to the 2014/2015 season. *Protein Engineering, Design and Selection*, 29(8), 309–315.
- Li, Y., Myers, J. L., Bostick, D. L., Sullivan, C. B., Madara, J., Linderman, S. L., Liu, Q., Carter, D. M., Wrammert, J., Esposito, S., Principi, N., Plotkin, J. B., Ross, T. M., Ahmed, R., Wilson, P. C., & Hensley, S. E. (2013). Immune history shapes specificity of pandemic h1n1 influenza antibody responses. *J Exp Med*, 210(8), 1493–500. <https://doi.org/10.1084/jem.20130212>
- Liang, X.-F., Wang, H.-Q., Wang, J.-Z., Fang, H.-H., Wu, J., Zhu, F.-C., Li, R.-C., Xia, S.-L., Zhao, Y.-L., Li, F.-J., Yan, S.-H., Yin, W.-D., An, K., Feng, D.-J., Cui, X.-L., Qi, F.-C., Ju, C.-J., Zhang, Y.-H., Guo, Z.-J., ... Wang, Y. (2010). Safety and immunogenicity of 2009 pandemic influenza a h1n1 vaccines in china: A multicentre, double-blind, randomised, placebo-controlled trial. *The Lancet*, 375(9708), 56–66. [https://doi.org/10.1016/s0140-6736\(09\)62003-1](https://doi.org/10.1016/s0140-6736(09)62003-1)
- Liu, F., Tzeng, W. P., Horner, L., Kamal, R. P., Tatum, H. R., Blanchard, E. G., Xu, X., York, I., Tumpey, T. M., Katz, J. M., Lu, X., & Levine, M. Z. (2018). Influence of immune priming and egg adaptation in the vaccine on antibody responses to circulating a(h1n1)pdm09 viruses after influenza vaccination in adults. *J Infect Dis*, 218(10), 1571–1581. <https://doi.org/10.1093/infdis/jiy376>
- Liu, F., Veguilla, V., Gross, F. L., Gillis, E., Rowe, T., Xu, X., Tumpey, T. M., Katz, J. M., Levine, M. Z., & Lu, X. (2017). Effect of priming with seasonal influenza a(h3n2) virus on the prevalence of cross-reactive hemagglutination-inhibition antibodies to swine-origin a(h3n2) variants. *J Infect Dis*, 216(suppl_4), S539–S547. <https://doi.org/10.1093/infdis/jix093>
- Liu, M., Zhao, X., Hua, S., Du, X., Peng, Y., Li, X., Lan, Y., Wang, D., Wu, A., Shu, Y., & Jiang, T. (2015). Antigenic patterns and evolution of the human influenza a (h1n1) virus. *Sci Rep*, 5, 14171. <https://doi.org/10.1038/srep14171>
- Liu, S., Ji, K., Chen, J., Tai, D., Jiang, W., Hou, G., Chen, J., Li, J., & Huang, B. (2009). Panorama phylogenetic diversity and distribution of type a influenza virus. *PLoS One*, 4(3), e5022. <https://doi.org/10.1371/journal.pone.0005022>
- Liu, S. T. H., Behzadi, M. A., Sun, W., Freyn, A. W., Liu, W. C., Broecker, F., Albrecht, R. A., Bouvier, N. M., Simon, V., Nachbagauer, R., Krammer, F., & Palese, P. (2018). Antigenic sites in influenza h1 hemagglutinin display species-specific immunodominance. *J Clin Invest*, 128(11), 4992–4996. <https://doi.org/10.1172/JCI122895>

- Lorusso, A., Vincent, A. L., Harland, M. L., Alt, D., Bayles, D. O., Swenson, S. L., Gramer, M. R., Russell, C. A., Smith, D. J., Lager, K. M., & Lewis, N. S. (2010). Genetic and antigenic characterization of h1 influenza viruses from united states swine from 2008. *Journal of General Virology*, 92(4), 919–930. <https://doi.org/10.1099/vir.0.027557-o>
- Luksza, M., & Lassig, M. (2014). A predictive fitness model for influenza. *Nature*, 507(7490), 57–61. <https://doi.org/10.1038/nature13087>
- Lycett, S. J., Baillie, G., Coulter, E., Bhatt, S., Kellam, P., McCauley, J. W., Wood, J. L., Brown, I. H., Pybus, O. G., Leigh Brown, A. J., & Combating Swine Influenza Initiative, C. C. (2012). Estimating reassortment rates in co-circulating eurasian swine influenza viruses. *J Gen Virol*, 93(Pt II), 2326–36. <https://doi.org/10.1099/vir.0.044503-o>
- Ma, W., Vincent, A. L., Lager, K. M., Janke, B. H., Henry, S. C., Rowland, R. R., Hesse, R. A., & Richt, J. A. (2010). Identification and characterization of a highly virulent triple reassortant h1n1 swine influenza virus in the united states. *Virus Genes*, 40(1), 28–36. <https://doi.org/10.1007/s11262-009-0413-7>
- Machalaba, C. C., Elwood, S. E., Forcella, S., Smith, K. M., Hamilton, K., Jebara, K. B., Swayne, D. E., Webby, R. J., Mumford, E., Mazet, J. A., Gaidet, N., Daszak, P., & Karesh, W. B. (2015). Global avian influenza surveillance in wild birds: A strategy to capture viral diversity. *Emerg Infect Dis*, 21(4), e1–7. <https://doi.org/10.3201/eid2104.141415>
- Maher, J. A., & DeStefano, J. (2004). The ferret: An animal model to study influenza virus. *Lab Anim (NY)*, 33(9), 50–3. <https://doi.org/10.1038/labani004-50>
- Maier, H. E., Nachbagauer, R., Kuan, G., Ng, S., Lopez, R., Sanchez, N., Stadlbauer, D., Gresh, L., Schiller, A., Rajabhathor, A., Ojeda, S., Guglia, A. F., Amanat, F., Balmaseda, A., Krammer, F., & Gordon, A. (2020). Pre-existing antineuraminidase antibodies are associated with shortened duration of influenza a(h1n1)pdm virus shedding and illness in naturally infected adults. *Clin Infect Dis*, 70(11), 2290–2297. <https://doi.org/10.1093/cid/ciz639>
- Mainer, G., Sanchez, L., Ena, J. M., & Calvo, M. (1997). Kinetic and thermodynamic parameters for heat denaturation of bovine milk igg, iga and igm. *Journal of Food Science*, 62(5), 1034–1038. <https://doi.org/10.1111/j.1365-2621.1997.tb15032.x>
- Mancera Gracia, J. C., Pearce, D. S., Masic, A., & Balasch, M. (2020). Influenza a virus in swine: Epidemiology, challenges and vaccination strategies. *Front Vet Sci*, 7, 647. <https://doi.org/10.3389/fvets.2020.00647>
- Mandon, E. C., Trueman, S. F., & Gilmore, R. (2013). Protein translocation across the rough endoplasmic reticulum. *Cold Spring Harb Perspect Biol*, 5(2). <https://doi.org/10.1101/cshperspect.a013342>
- Marriott, A. C., Dove, B. K., Whittaker, C. J., Bruce, C., Ryan, K. A., Bean, T. J., Rayner, E., Pearson, G., Taylor, I., Dowall, S., Plank, J., Newman, E., Barclay, W. S., Dimmock, N. J., Easton, A. J., Hallis, B., Silman, N. J., & Carroll, M. W. (2014). Low dose influenza virus challenge in the ferret leads to increased virus shedding and greater sensitivity to oseltamivir. *PLoS One*, 9(4), e94090. <https://doi.org/10.1371/journal.pone.0094090>
- Matsuoka, Y., Lamirande, E. W., & Subbarao, K. (2009a). The ferret model for influenza. *Curr Protoc Microbiol, Chapter 15*, Unit 15G 2. <https://doi.org/10.1002/9780471729259.mc15go2si3>
- Matsuoka, Y., Lamirande, E. W., & Subbarao, K. (2009b). The mouse model for influenza. *Curr Protoc Microbiol, Chapter 15*, Unit 15G 3. <https://doi.org/10.1002/9780471729259.mc15go3si3>

- Matsuzawa, Y., Iwatsuki-Horimoto, K., Nishimoto, Y., Abe, Y., Fukuyama, S., Hamabata, T., Okuda, M., Go, Y., Watanabe, T., Imai, M., Arai, Y., Fouchier, R. A. M., Yamayoshi, S., & Kawaoka, Y. (2019). Antigenic change in human influenza a(h2n2) viruses detected by using human plasma from aged and younger adult individuals. *Viruses*, 11(11). <https://doi.org/10.3390/v11110978>
- McElhaney, J. E. (2011). Influenza vaccine responses in older adults. *Ageing Res Rev*, 10(3), 379–88. <https://doi.org/10.1016/j.arr.2010.10.008>
- McElhaney, J. E., Meneilly, G. S., Lechelt, K. E., Beattie, B. L., & Bleackley, R. C. (1993). Antibody response to whole-virus and split-virus influenza vaccines in successful ageing. *Vaccine*, 11(10), 1055–1060. [https://doi.org/10.1016/0264-410X\(93\)90133-i](https://doi.org/10.1016/0264-410X(93)90133-i)
- McElwain, T. F., & Thumby, S. M. (2017). Animal pathogens and their impact on animal health, the economy, food security, food safety and public health. *Rev Sci Tech*, 36(2), 423–433. <https://doi.org/10.20506/rst.36.2.2663>
- McLaren, C., & Potter, C. W. (1973). Immunity to influenza in ferrets. 8. serological response of ferrets to influenza virus vaccines after infection with heterotypic strains of influenza. *Med Microbiol Immunol*, 159(1), 53–62. <https://doi.org/10.1007/bf02122649>
- McLaren, C., & Potter, C. W. (1974). Immunity to influenza in ferrets. vii. effect of previous infection with heterotypic and heterologous influenza viruses on the response of ferrets to inactivated influenza virus vaccines. *J Hyg (Lond)*, 72(1), 91–100. <https://doi.org/10.1017/s0022172400023251>
- McLaren, C., Potter, C. W., & Jennings, R. (1974a). Immunity to influenza in ferrets. 13. protection against influenza infection by serum antibody to homologous haemagglutinin or neuraminidase antigens. *Med Microbiol Immunol*, 160(1), 33–45. <https://doi.org/10.1007/bf02124341>
- McLaren, C., Potter, C. W., & Jennings, R. (1974b). Immunity to influenza in ferrets. x. intranasal immunization of ferrets with inactivated influenza a virus vaccines. *Infect Immun*, 9(6), 985–90. <https://www.ncbi.nlm.nih.gov/pubmed/4830530>
- McLaren, C., Verbonitz, M. W., Daniel, S., Grubbs, G. E., & Ennis, F. A. (1977). Effect of priming infection on serologic response to whole and subunit influenza virus vaccines in animals. *J Infect Dis*, 136 Suppl, S706–11. https://doi.org/10.1093/infdis/136.supplement_3.s706
- McLean, H. Q., Thompson, M. G., Sundaram, M. E., Meece, J. K., McClure, D. L., Friedrich, T. C., & Belongia, E. A. (2014). Impact of repeated vaccination on vaccine effectiveness against influenza a(h3n2) and b during 8 seasons. *Clin Infect Dis*, 59(10), 1375–85. <https://doi.org/10.1093/cid/ciu680>
- McMahon, M., Strohmeier, S., Rajendran, M., Capuano, C., Ellebedy, A. H., Wilson, P. C., & Krammer, F. (2020). Correctly folded - but not necessarily functional - influenza virus neuraminidase is required to induce protective antibody responses in mice. *Vaccine*, 38(45), 7129–7137. <https://doi.org/10.1016/j.vaccine.2020.08.067>
- Memoli, M. J., Shaw, P. A., Han, A., Czajkowski, L., Reed, S., Athota, R., Bristol, T., Fargis, S., Risos, K., Powers, J. H., Davey, J., R. T., & Taubenberger, J. K. (2016). Evaluation of antihemagglutinin and antineuraminidase antibodies as correlates of protection in an influenza a/h1n1 virus healthy human challenge model. *MBio*, 7(2), e00417-16. <https://doi.org/10.1128/mBio.00417-16>
- Middleton, D., Rockman, S., Pearse, M., Barr, I., Lowther, S., Klippel, J., Ryan, D., & Brown, L. (2009). Evaluation of vaccines for h5n1 influenza virus in ferrets reveals the potential for protective single-shot immunization. *J Virol*, 83(15), 7770–8. <https://doi.org/10.1128/JVI.00241-09>

- Miller, M. S., Gardner, T. J., Krammer, F., Aguado, L. C., Tortorella, D., Basler, C. F., & Palese, P. (2013). Neutralizing antibodies against previously encountered influenza virus strains increase over time: A longitudinal analysis. *Sci Transl Med*, 5(198), 198ra107. <https://doi.org/10.1126/scitranslmed.3006637>
- Min, J. Y., Chen, G. L., Santos, C., Lamirande, E. W., Matsuoka, Y., & Subbarao, K. (2010). Classical swine h1n1 influenza viruses confer cross protection from swine-origin 2009 pandemic h1n1 influenza virus infection in mice and ferrets. *Virology*, 408(1), 128–133. <https://doi.org/10.1016/j.virol.2010.09.009>
- Mitchell, R., Taylor, G., McGeer, A., Frenette, C., Suh, K. N., Wong, A., Katz, K., Wilkinson, K., Amihod, B., Gravel, D., & Canadian Nosocomial Infection Surveillance, P. (2013). Understanding the burden of influenza infection among adults in canadian hospitals: A comparison of the 2009-2010 pandemic season with the prepandemic and postpandemic seasons. *Am J Infect Control*, 41(11), 1032–7. <https://doi.org/10.1016/j.ajic.2013.06.008>
- Monsalvo, A. C., Batalle, J. P., Lopez, M. F., Krause, J. C., Klemenc, J., Hernandez, J. Z., Maskin, B., Bugna, J., Rubinstein, C., Aguilar, L., Dalurzo, L., Libster, R., Savy, V., Baumeister, E., Aguilar, L., Cabral, G., Font, J., Solari, L., Weller, K. P., ... Polack, F. P. (2011). Severe pandemic 2009 h1n1 influenza disease due to pathogenic immune complexes. *Nat Med*, 17(2), 195–9. <https://doi.org/10.1038/nm.2262>
- Monto, A. S. (2010). Seasonal influenza and vaccination coverage. *Vaccine*, 28 Suppl 4, D33–44. <https://doi.org/10.1016/j.vaccine.2010.08.027>
- Monto, A. S., Petrie, J. G., Cross, R. T., Johnson, E., Liu, M., Zhong, W., Levine, M., Katz, J. M., & Ohmit, S. E. (2015). Antibody to influenza virus neuraminidase: An independent correlate of protection. *J Infect Dis*, 212(8), 1191–9. <https://doi.org/10.1093/infdis/jiv195>
- Moriyama, M., Hugentobler, W. J., & Iwasaki, A. (2020). Seasonality of respiratory viral infections. *Annu Rev Virol*, 7(1), 83–101. <https://doi.org/10.1146/annurev-virology-012420-022445>
- Morris, D. H., Gostic, K. M., Pompei, S., Bedford, T., Luksza, M., Neher, R. A., Grenfell, B. T., Lassig, M., & McCauley, J. W. (2018). Predictive modeling of influenza shows the promise of applied evolutionary biology. *Trends Microbiol*, 26(2), 102–118. <https://doi.org/10.1016/j.tim.2017.09.004>
- Munier, S., Larcher, T., Cormier-Aline, F., Soubieux, D., Su, B., Guigand, L., Labrosse, B., Cherel, Y., Quere, P., Marc, D., & Naffakh, N. (2010). A genetically engineered waterfowl influenza virus with a deletion in the stalk of the neuraminidase has increased virulence for chickens. *J Virol*, 84(2), 940–52. <https://doi.org/10.1128/JVI.01581-09>
- Munoz, E. T., & Deem, M. W. (2005). Epitope analysis for influenza vaccine design. *Vaccine*, 23(9), 1144–8. <https://doi.org/10.1016/j.vaccine.2004.08.028>
- Muramoto, Y., Noda, T., Kawakami, E., Akkina, R., & Kawaoka, Y. (2013). Identification of novel influenza a virus proteins translated from pa mrna. *J Virol*, 87(5), 2455–62. <https://doi.org/10.1128/JVI.02656-12>
- Murphy, B. R., Kasel, J. A., & Chanock, R. M. (1972). Association of serum anti-neuraminidase antibody with resistance to influenza in man. *New England Journal of Medicine*, 286(25), 1329–1332.
- Murti, K. G., & Webster, R. G. (1986). Distribution of hemagglutinin and neuraminidase on influenza virions as revealed by immunoelectron microscopy. *Virology*, 149(1), 36–43. [https://doi.org/10.1016/0042-6822\(86\)90084-x](https://doi.org/10.1016/0042-6822(86)90084-x)

- Music, N., Reber, A. J., Lipatov, A. S., Kamal, R. P., Blanchfield, K., Wilson, J. R., Donis, R. O., Katz, J. M., & York, I. A. (2014). Influenza vaccination accelerates recovery of ferrets from lymphopenia. *PLoS One*, 9(6), e100926. <https://doi.org/10.1371/journal.pone.0100926>
- Music, N., Tzeng, W. P., Liaini Gross, F., Levine, M. Z., Xu, X., Shieh, W. J., Tumpey, T. M., Katz, J. M., & York, I. A. (2019). Repeated vaccination against matched h3n2 influenza virus gives less protection than single vaccination in ferrets. *NPJ Vaccines*, 4, 28. <https://doi.org/10.1038/s41541-019-0123-7>
- Myers, K. P., Olsen, C. W., Setterquist, S. F., Capuano, A. W., Donham, K. J., Thacker, E. L., Merchant, J. A., & Gray, G. C. (2006). Are swine workers in the united states at increased risk of infection with zoonotic influenza virus? *Clin Infect Dis*, 42(1), 14–20. <https://doi.org/10.1086/498977>
- Na, W., Yeom, M., Yuk, H., Moon, H., Kang, B., & Song, D. (2016). Influenza virus vaccine for neglected hosts: Horses and dogs. *Clin Exp Vaccine Res*, 5(2), 117–24. <https://doi.org/10.7774/cevr.2016.5.2.117>
- Nachbagauer, R., Choi, A., Hirsh, A., Margine, I., Iida, S., Barrera, A., Ferres, M., Albrecht, R. A., Garcia-Sastre, A., Bouvier, N. M., Ito, K., Medina, R. A., Palese, P., & Krammer, F. (2017). Defining the antibody cross-reactome directed against the influenza virus surface glycoproteins. *Nat Immunol*, 18(4), 464–473. <https://doi.org/10.1038/ni.3684>
- Ndifon, W., Wingreen, N. S., & Levin, S. A. (2009). Differential neutralization efficiency of hemagglutinin epitopes, antibody interference, and the design of influenza vaccines. *Proc Natl Acad Sci U S A*, 106(21), 8701–6. <https://doi.org/10.1073/pnas.0903427106>
- Neher, R. A., Bedford, T., Daniels, R. S., Russell, C. A., & Shraiman, B. I. (2016). Prediction, dynamics, and visualization of antigenic phenotypes of seasonal influenza viruses. *Proc Natl Acad Sci USA*, 113(12), E1701–9. <https://doi.org/10.1073/pnas.1525578113>
- Neher, R. A., Russell, C. A., & Shraiman, B. I. (2014). Predicting evolution from the shape of genealogical trees. *eLife*, 3. <https://doi.org/10.7554/eLife.03568>
- Nelson, M. I., Gramer, M. R., Vincent, A. L., & Holmes, E. C. (2012). Global transmission of influenza viruses from humans to swine. *J Gen Virol*, 93(Pt 10), 2195–203. <https://doi.org/10.1099/vir.vir.0.044974-o>
- Nelson, M. I., Lemey, P., Tan, Y., Vincent, A., Lam, T. T., Detmer, S., Viboud, C., Suchard, M. A., Rambaut, A., Holmes, E. C., & Gramer, M. (2011). Spatial dynamics of human-origin h1 influenza a virus in north american swine. *PLoS Pathog*, 7(6), e1002077. <https://doi.org/10.1371/journal.ppat.1002077>
- Ng, P. S., Bohm, R., Hartley-Tassell, L. E., Steen, J. A., Wang, H., Lukowski, S. W., Hawthorne, P. L., Trezise, A. E., Coloe, P. J., Grimmond, S. M., Haselhorst, T., von Itzstein, M., Paton, A. W., Paton, J. C., & Jennings, M. P. (2014). Ferrets exclusively synthesize neu5ac and express naturally humanized influenza a virus receptors. *Nat Commun*, 5, 5750. <https://doi.org/10.1038/ncomms6750>
- Ng, S., Cowling, B. J., Fang, V. J., Chan, K. H., Ip, D. K., Cheng, C. K., Uyeki, T. M., Houck, P. M., Malik Peiris, J. S., & Leung, G. M. (2010). Effects of oseltamivir treatment on duration of clinical illness and viral shedding and household transmission of influenza virus. *Clin Infect Dis*, 50(5), 707–14. <https://doi.org/10.1086/650458>
- Nobusawa, E., Aoyama, T., Kato, H., Suzuki, Y., Tateno, Y., & Nakajima, K. (1991). Comparison of complete amino-acid-sequences and receptor-binding properties among 13 serotypes of hemagglutinins of influenza a-viruses. *Virology*, 182(2), 475–485. [https://doi.org/10.1016/0042-6822\(91\)90588-3](https://doi.org/10.1016/0042-6822(91)90588-3)

- Nordholm, J., Petitou, J., Ostbye, H., da Silva, D. V., Dou, D., Wang, H., & Daniels, R. (2017). Translational regulation of viral secretory proteins by the 5' coding regions and a viral rna-binding protein. *J Cell Biol*, 216(8), 2283–2293. <https://doi.org/10.1083/jcb.201702102>
- Novel Swine-Origin Influenza, A. V. I. T., Dawood, F. S., Jain, S., Finelli, L., Shaw, M. W., Lindstrom, S., Garten, R. J., Gubareva, L. V., Xu, X., Bridges, C. B., & Uyeki, T. M. (2009). Emergence of a novel swine-origin influenza a (h1n1) virus in humans. *N Engl J Med*, 360(25), 2605–15. <https://doi.org/10.1056/NEJMoa0903810>
- Nunez, I. A., Carlock, M. A., Allen, J. D., Owino, S. O., Moehling, K. K., Nowalk, P., Susick, M., Diagle, K., Sweeney, K., Mundie, S., Vogel, T. U., Delagrave, S., Ramgopal, M., Zimmerman, R. K., Kleanthous, H., & Ross, T. M. (2017). Impact of age and pre-existing influenza immune responses in humans receiving split inactivated influenza vaccine on the induction of the breadth of antibodies to influenza a strains. *PLoS One*, 12(11), e0185666. <https://doi.org/10.1371/journal.pone.0185666>
- Ochi, A., Danesh, A., Seneviratne, C., Banner, D., Devries, M. E., Rowe, T., Xu, L., Ran, L., Czub, M., Bosinger, S. E., Cameron, M. J., Cameron, C. M., & Kelvin, D. J. (2008). Cloning, expression and immunoassay detection of ferret ifn-gamma. *Dev Comp Immunol*, 32(8), 890–7. <https://doi.org/10.1016/j.dci.2007.12.008>
- O'Donnell, C. D., Wright, A., Vogel, L. N., Wei, C. J., Nabel, G. J., & Subbarao, K. (2012). Effect of priming with h1n1 influenza viruses of variable antigenic distances on challenge with 2009 pandemic h1n1 virus. *J Virol*, 86(16), 8625–33. <https://doi.org/10.1128/JVI.00147-12>
- Oh, J. Z., Ravindran, R., Chassaing, B., Carvalho, F. A., Maddur, M. S., Bower, M., Hakimpor, P., Gill, K. P., Nakaya, H. I., Yarovinsky, F., Sartor, R. B., Gewirtz, A. T., & Pulendran, B. (2014). Tlr5-mediated sensing of gut microbiota is necessary for antibody responses to seasonal influenza vaccination. *Immunity*, 41(3), 478–492. <https://doi.org/10.1016/j.immuni.2014.08.009>
- O'Hagan, D. T., Rappuoli, R., De Gregorio, E., Tsai, T., & Del Giudice, G. (2011). Mf59 adjuvant: The best insurance against influenza strain diversity. *Expert Rev Vaccines*, 10(4), 447–62. <https://doi.org/10.1586/erv.11.23>
- Ohmit, S. E., Thompson, M. G., Petrie, J. G., Thaker, S. N., Jackson, M. L., Belongia, E. A., Zimmerman, R. K., Gaglani, M., Lamerato, L., Spencer, S. M., Jackson, L., Meece, J. K., Nowalk, M. P., Song, J., Zervos, M., Cheng, P. Y., Rinaldo, C. R., Clipper, L., Shay, D. K., ... Monto, A. S. (2014). Influenza vaccine effectiveness in the 2011-2012 season: Protection against each circulating virus and the effect of prior vaccination on estimates. *Clin Infect Dis*, 58(3), 319–27. <https://doi.org/10.1093/cid/cit736>
- Olsen, C. W. (2002). The emergence of novel swine influenza viruses in north america. *Virus Res*, 85(2), 199–210. <https://www.ncbi.nlm.nih.gov/pmc/articles/PMC12034486/>
- O'Neill, E., Krauss, S. L., Riberdy, J. M., Webster, R. G., & Woodland, D. L. (2000). Heterologous protection against lethal a/hongkong/156/97 (h5nr) influenza virus infection in c57bl/6 mice. *J Gen Virol*, 81(Pt 11), 2689–96. <https://doi.org/10.1099/0022-1317-81-11-2689>
- Organization, W. H. (2019). *Recommended composition of influenza virus vaccines for use in the 2019- 2020 northern hemisphere influenza season* (Report).
- Organization, W. H., & Network, W. G. I. S. (2011). *Manual for the laboratory diagnosis and virological surveillance of influenza*. World Health Organization. <https://books.google.com/books?id=kYajuAAACAAJ>

- Ostbye, H., Gao, J., Martinez, M. R., Wang, H., de Gier, J. W., & Daniels, R. (2020). N-linked glycan sites on the influenza a virus neuraminidase head domain are required for efficient viral incorporation and replication. *J Virol*, 94(19). <https://doi.org/10.1128/JVI.00874-20>
- Paccha, B., Jones, R. M., Gibbs, S., Kane, M. J., Torremorell, M., Neira-Ramirez, V., & Rabinowitz, P. M. (2016). Modeling risk of occupational zoonotic influenza infection in swine workers. *J Occup Environ Hyg*, 13(8), 577–87. <https://doi.org/10.1080/15459624.2016.1159688>
- Paget, J., Spreeuwenberg, P., Charu, V., Taylor, R. J., Iuliano, A. D., Bresee, J., Simonsen, L., Viboud, C., Global Seasonal Influenza-associated Mortality Collaborator, N., & Teams*, G. L. C. (2019). Global mortality associated with seasonal influenza epidemics: New burden estimates and predictors from the glamor project. *J Glob Health*, 9(2), 020421. <https://doi.org/10.7189/jogh.09.020421>
- Paillet, R., Hannant, D., Kydd, J. H., & Daly, J. M. (2006). Vaccination against equine influenza: Quid novi? *Vaccine*, 24(19), 4047–61. <https://doi.org/10.1016/j.vaccine.2006.02.030>
- Pan, K., Subieta, K. C., & Deem, M. W. (2011). A novel sequence-based antigenic distance measure for hini, with application to vaccine effectiveness and the selection of vaccine strains. *Protein Eng Des Sel*, 24(3), 291–9. <https://doi.org/10.1093/protein/gzq105>
- Paquette, S. G., Huang, S. S. H., Banner, D., Xu, L., Leomicronn, A., Kelvin, A. A., & Kelvin, D. J. (2014). Impaired heterologous immunity in aged ferrets during sequential influenza a hini infection. *Virology*, 464–465, 177–183. <https://doi.org/10.1016/j.virol.2014.07.013>
- Paramsothy, A., Lartey Jalloh, S., Davies, R. A., Guttermson, A. B., Cox, R. J., & Mohn, K. G. (2021). Humoral and cellular immune responses in critically ill influenza a/hini infected patients. *Scand J Immunol*, e13045. <https://doi.org/10.1111/sji.13045>
- Park, A. W., Daly, J. M., Lewis, N. S., Smith, D. J., Wood, J. L., & Grenfell, B. T. (2009). Quantifying the impact of immune escape on transmission dynamics of influenza. *Science*, 326(5953), 726–8. <https://doi.org/10.1126/science.1175980>
- Park, J. K., Han, A., Czajkowski, L., Reed, S., Athota, R., Bristol, T., Rosas, L. A., Cervantes-Medina, A., Taubenberger, J. K., & Memoli, M. J. (2018). Evaluation of preexisting anti-hemagglutinin stalk antibody as a correlate of protection in a healthy volunteer challenge with influenza a/hinipdm virus. *mBio*, 9(1). <https://doi.org/10.1128/mBio.02284-17>
- Park, S., Il Kim, J., Lee, I., Bae, J. Y., Yoo, K., Nam, M., Kim, J., Sook Park, M., Song, K. J., Song, J. W., Kee, S. H., & Park, M. S. (2017). Adaptive mutations of neuraminidase stalk truncation and deglycosylation confer enhanced pathogenicity of influenza a viruses. *Sci Rep*, 7(1), 10928. <https://doi.org/10.1038/s41598-017-11348-o>
- Parra, G. I., Bok, K., Taylor, R., Haynes, J. R., Sosnovtsev, S. V., Richardson, C., & Green, K. Y. (2012). Immunogenicity and specificity of norovirus consensus gii.4 virus-like particles in monovalent and bivalent vaccine formulations. *Vaccine*, 30(24), 3580–6. <https://doi.org/10.1016/j.vaccine.2012.03.050>
- Paules, C. I., & Fauci, A. S. (2019). Influenza vaccines: Good, but we can do better. *J Infect Dis*, 220(Supplement_1), S1–S4. <https://doi.org/10.1093/infdis/jiy633>
- Paules, C. I., Marston, H. D., Eisinger, R. W., Baltimore, D., & Fauci, A. S. (2017). The pathway to a universal influenza vaccine. *Immunity*, 47(4), 599–603. <https://doi.org/10.1016/j.jimmuni.2017.09.007>

- Pauly, M. D., Procario, M. C., & Lauring, A. S. (2017). A novel twelve class fluctuation test reveals higher than expected mutation rates for influenza a viruses. *eLife*, 6. <https://doi.org/ARTNe2643710.7554/eLife.26437>
- Pearce, M. B., Belser, J. A., Houser, K. V., Katz, J. M., & Tumpey, T. M. (2011). Efficacy of seasonal live attenuated influenza vaccine against virus replication and transmission of a pandemic 2009 h1n1 virus in ferrets. *Vaccine*, 29(16), 2887–94. <https://doi.org/10.1016/j.vaccine.2011.02.014>
- Pearce, M. B., Jayaraman, A., Pappas, C., Belser, J. A., Zeng, H., Gustin, K. M., Maines, T. R., Sun, X., Raman, R., Cox, N. J., Sasisekharan, R., Katz, J. M., & Tumpey, T. M. (2012). Pathogenesis and transmission of swine origin a(h3n2)v influenza viruses in ferrets. *Proc Natl Acad Sci USA*, 109(10), 3944–9. <https://doi.org/10.1073/pnas.1119945109>
- Pei, Z., Jiang, X., Yang, Z., Ren, X., Gong, H., Reeves, M., Sheng, J., Wang, Y., Pan, Z., Liu, F., Wu, J., & Lu, S. (2015). Oral delivery of a novel attenuated salmonella vaccine expressing influenza a virus proteins protects mice against h5n1 and h1n1 viral infection. *PLoS One*, 10(6), e0129276. <https://doi.org/10.1371/journal.pone.0129276>
- Peng, Y., Wang, D., Wang, J., Li, K., Tan, Z., Shu, Y., & Jiang, T. (2017). A universal computational model for predicting antigenic variants of influenza a virus based on conserved antigenic structures. *Sci Rep*, 7, 42051. <https://doi.org/10.1038/srep42051>
- Pentiah, K., Lees, W. D., Moss, D. S., & Shepherd, A. J. (2015). N-linked glycans on influenza a h3n2 hemagglutinin constrain binding of host antibodies, but shielding is limited. *Glycobiology*, 25(1), 124–32. <https://doi.org/10.1093/glycob/cwu097>
- Petrie, J. G., Ohmit, S. E., Johnson, E., Truscon, R., & Monto, A. S. (2015). Persistence of antibodies to influenza hemagglutinin and neuraminidase following one or two years of influenza vaccination. *J Infect Dis*, 212(12), 1914–22. <https://doi.org/10.1093/infdis/jiv313>
- Philippon, D. A. M., Wu, P., Cowling, B. J., & Lau, E. H. Y. (2020). Avian influenza human infections at the human-animal interface. *J Infect Dis*, 222(4), 528–537. <https://doi.org/10.1093/infdis/jiaa105>
- Pohl, M. O., Lanz, C., & Stertz, S. (2016). Late stages of the influenza a virus replication cycle-a tight interplay between virus and host. *J Gen Virol*, 97(9), 2058–2072. <https://doi.org/10.1099/jgv.o.000562>
- Potier, M., Mameli, L., Belisle, M., Dallaire, L., & Melancon, S. B. (1979). Fluorometric assay of neuraminidase with a sodium (4-methylumbelliferyl-alpha-d-n-acetylneuraminate) substrate. *Anal Biochem*, 94(2), 287–96. [https://doi.org/10.1016/0003-2697\(79\)90362-2](https://doi.org/10.1016/0003-2697(79)90362-2)
- Potter, C. W. (2001). A history of influenza. *J Appl Microbiol*, 91(4), 572–9. <https://doi.org/10.1046/j.1365-2672.2001.01492.x>
- Potter, C. W., Jennings, R., Marine, W. M., & McLaren, C. (1973). Potentiation of the antibody response to inactivated a2-hong kong vaccines by previous heterotypic influenza virus infection. *Microbios*, 8(30), 101–10. <https://www.ncbi.nlm.nih.gov/pubmed/4801251>
- Potter, C. W., McLaren, C., & Shore, S. L. (1973). Immunity to influenza in ferrets. v. immunization with inactivated virus in adjuvant 65. *J Hyg (Lond)*, 71(1), 97–106. <https://doi.org/10.1017/s0022172400046258>
- Potter, C. W., Oxford, J. S., Shore, S. L., McLaren, C., & Stuart-Harris, C. (1972). Immunity to influenza in ferrets. i. response to live and killed virus. *Br J Exp Pathol*, 53(2), 153–67. <https://www.ncbi.nlm.nih.gov/pubmed/5032092>

- Potter, C. W., Shore, S. L., McLaren, C., & Stuart-Harris, C. (1972). Immunity to influenza in ferrets. ii. influence of adjuvants on immunization. *Br J Exp Pathol*, 53(2), 168–79. <https://www.ncbi.nlm.nih.gov/pubmed/4338059>
- Pritchett, T. J., & Paulson, J. C. (1989). Basis for the potent inhibition of influenza virus infection by equine and guinea pig alpha 2-macroglobulin. *J Biol Chem*, 264(17), 9850–8. <https://www.ncbi.nlm.nih.gov/pubmed/2470765>
- Pulit-Penaloza, J. A., Jones, J., Sun, X., Jang, Y., Thor, S., Belser, J. A., Zanders, N., Creager, H. M., Ridenour, C., Wang, L., Stark, T. J., Garten, R., Chen, L. M., Barnes, J., Tumpey, T. M., Wentworth, D. E., Maines, T. R., & Davis, C. T. (2018). Antigenically diverse swine origin h1n1 variant influenza viruses exhibit differential ferret pathogenesis and transmission phenotypes. *J Virol*, 92(11). <https://doi.org/10.1128/JVI.00095-18>
- Putri, W., Muscatello, D. J., Stockwell, M. S., & Newall, A. T. (2018). Economic burden of seasonal influenza in the united states. *Vaccine*, 36(27), 3960–3966. <https://doi.org/10.1016/j.vaccine.2018.05.057>
- Quinn, S. C., Kumar, S., Freimuth, V. S., Musa, D., Casteneda-Angarita, N., & Kidwell, K. (2011). Racial disparities in exposure, susceptibility, and access to health care in the us h1n1 influenza pandemic. *Am J Public Health*, 101(2), 285–93. <https://doi.org/10.2105/AJPH.2009.188029>
- Raghwani, J., Thompson, R. N., & Koelle, K. (2017). Selection on non-antigenic gene segments of seasonal influenza a virus and its impact on adaptive evolution. *Virus Evol*, 3(2), vexo034. <https://doi.org/10.1093/ve/vexo034>
- Rajao, D. S., Anderson, T. K., Kitikoon, P., Stratton, J., Lewis, N. S., & Vincent, A. L. (2018). Antigenic and genetic evolution of contemporary swine h1 influenza viruses in the united states. *Virology*, 518, 45–54. <https://doi.org/10.1016/j.virol.2018.02.006>
- Rajaram, S., Boikos, C., Gelone, D. K., & Gandhi, A. (2020). Influenza vaccines: The potential benefits of cell-culture isolation and manufacturing. *Ther Adv Vaccines Immunother*, 8, 2515135520908121. <https://doi.org/10.1177/2515135520908121>
- Rasmussen, T. S., de Vries, L., Kot, W., Hansen, L. H., Castro-Mejia, J. L., Vogensen, F. K., Hansen, A. K., & Nielsen, D. S. (2019). Mouse vendor influence on the bacterial and viral gut composition exceeds the effect of diet. *Viruses*, 11(5). <https://doi.org/10.3390/v11050435>
- Raymond, D. D., Stewart, S. M., Lee, J., Ferdman, J., Bajic, G., Do, K. T., Ernandes, M. J., Suphaphiphat, P., Settembre, E. C., Dormitzer, P. R., Del Giudice, G., Finco, O., Kang, T. H., Ippolito, G. C., Georgiou, G., Kepler, T. B., Haynes, B. F., Moody, M. A., Liao, H. X., ... Harrison, S. C. (2016). Influenza immunization elicits antibodies specific for an egg-adapted vaccine strain. *Nat Med*, 22(12), 1465–1469. <https://doi.org/10.1038/nm.4223>
- Remmert, M., Biegert, A., Hauser, A., & Soding, J. (2011). HHblits: Lightning-fast iterative protein sequence searching by hmm-hmm alignment. *Nat Methods*, 9(2), 173–5. <https://doi.org/10.1038/nmeth.1818>
- Reneer, Z. B., Jamieson, P. J., Skarlupka, A. L., Huang, Y., & Ross, T. M. (2020). Computationally optimized broadly reactive h2 ha influenza vaccines elicited broadly cross-reactive antibodies and protected mice from viral challenges. *J Virol*, 95(2). <https://doi.org/10.1128/JVI.01526-20>
- Reneer, Z. B., & Ross, T. M. (2019). H2 influenza viruses: Designing vaccines against future h2 pandemics. *Biochem Soc Trans*, 47(1), 251–264. <https://doi.org/10.1042/BST20180602>

- Richmond, J., & McKinney, R. (1993). *Biosafety in microbiological and biomedical laboratories* (4th ed.). U.S. Government Printing Office.
- Rockman, S., Brown, L. E., Barr, I. G., Gilbertson, B., Lowther, S., Kachurin, A., Kachurina, O., Klippel, J., Bodle, J., Pearse, M., & Middleton, D. (2013). Neuraminidase-inhibiting antibody is a correlate of cross-protection against lethal h5n1 influenza virus in ferrets immunized with seasonal influenza vaccine. *J Virol*, 87(6), 3053–61. <https://doi.org/10.1128/JVI.02434-12>
- Rohatgi, A. (2020). Webplotdigitizer. Version 4.3. <https://automeris.io/WebPlotDigitizer>
- Rolfes, M. A., Flannery, B., Chung, J. R., O'Halloran, A., Garg, S., Belongia, E. A., Gaglani, M., Zimmerman, R. K., Jackson, M. L., Monto, A. S., Alden, N. B., Anderson, E., Bennett, N. M., Billing, L., Eckel, S., Kirley, P. D., Lynfield, R., Monroe, M. L., Spencer, M., ... Prevention. (2019). Effects of influenza vaccination in the united states during the 2017-2018 influenza season. *Clin Infect Dis*, 69(11), i845–i853. <https://doi.org/10.1093/cid/ciz075>
- Ross, T. M., DiNapoli, J., Giel-Moloney, M., Bloom, C. E., Bertran, K., Balzli, C., Strugnell, T., Sa, E. S. M., Mebatson, T., Bublot, M., Swayne, D. E., & Kleanthous, H. (2019). A computationally designed h5 antigen shows immunological breadth of coverage and protects against drifting avian strains. *Vaccine*, 37(17), 2369–2376. <https://doi.org/10.1016/j.vaccine.2019.03.018>
- Ross, T. M., Xu, Y., Bright, R. A., & Robinson, H. L. (2000). C3d enhancement of antibodies to hemagglutinin accelerates protection against influenza virus challenge. *Nat Immunol*, 1(2), 127–31. <https://doi.org/10.1038/77802>
- Rossmann, J. S., & Lamb, R. A. (2011). Influenza virus assembly and budding. *Virology*, 411(2), 229–36. <https://doi.org/10.1016/j.virol.2010.12.003>
- Roubidoux, E. K., & Schultz-Cherry, S. (2021). Animal models utilized for the development of influenza virus vaccines. *Vaccines (Basel)*, 9(7). <https://doi.org/10.3390/vaccines9070787>
- Rowe, T., Leon, A. J., Crevar, C. J., Carter, D. M., Xu, L., Ran, L., Fang, Y., Cameron, C. M., Cameron, M. J., Banner, D., Ng, D. C., Ran, R., Weirback, H. K., Wiley, C. A., Kelvin, D. J., & Ross, T. M. (2010). Modeling host responses in ferrets during a/california/07/2009 influenza infection. *Virology*, 401(2), 257–65. <https://doi.org/10.1016/j.virol.2010.02.020>
- R-Project. (2017). R a language and environment for statistical computing. <https://www.R-project.org>
- Rust, M. J., Lakadamyali, M., Zhang, F., & Zhuang, X. (2004). Assembly of endocytic machinery around individual influenza viruses during viral entry. *Nat Struct Mol Biol*, 11(6), 567–73. <https://doi.org/10.1038/nsmb769>
- Ryan, K. A., Slack, G. S., Marriott, A. C., Kane, J. A., Whittaker, C. J., Silman, N. J., Carroll, M. W., & Gooch, K. E. (2018). Cellular immune response to human influenza viruses differs between h1n1 and h3n2 subtypes in the ferret lung. *PLoS One*, 13(9), e0202675. <https://doi.org/10.1371/journal.pone.0202675>
- Ryan-Poirier, K. A., & Kawaoka, Y. (1993). Alpha 2-macroglobulin is the major neutralizing inhibitor of influenza a virus in pig serum. *Virology*, 193(2), 974–6. <https://doi.org/10.1006/viro.1993.1208>
- Sandbulte, M. R., & Eichelberger, M. C. (2014). Analyzing swine sera for functional antibody titers against influenza a neuraminidase proteins using an enzyme-linked lectin assay (ella). *Animal Influenza Virus, Second Edition*, 1161, 337–345. https://doi.org/10.1007/978-1-4939-0758-8_28
- Sandbulte, M. R., Gauger, P. C., Kitikoon, P., Chen, H., Perez, D. R., Roth, J. A., & Vincent, A. L. (2016). Neuraminidase inhibiting antibody responses in pigs differ between influenza a virus n2 lineages and by vaccine type. *Vaccine*, 34(33), 3773–9. <https://doi.org/10.1016/j.vaccine.2016.06.001>

- Sandbulte, M. R., Westgeest, K. B., Gao, J., Xu, X., Klimov, A. I., Russell, C. A., Burke, D. F., Smith, D. J., Fouchier, R. A., & Eichelberger, M. C. (2011). Discordant antigenic drift of neuraminidase and hemagglutinin in h1n1 and h3n2 influenza viruses. *Proc Natl Acad Sci U S A*, 108(51), 20748–53. <https://doi.org/10.1073/pnas.1113801108>
- Sautto, G. A., Kirchenbaum, G. A., Abreu, R. B., Ecker, J. W., Pierce, S. R., Kleanthous, H., & Ross, T. M. (2020). A computationally optimized broadly reactive antigen subtype-specific influenza vaccine strategy elicits unique potent broadly neutralizing antibodies against hemagglutinin. *J Immunol*, 204(2), 375–385. <https://doi.org/10.4049/jimmunol.1900379>
- Sautto, G. A., Kirchenbaum, G. A., Diotti, R. A., Criscuolo, E., & Ferrara, F. (2019). Next generation vaccines for infectious diseases. *J Immunol Res*, 2019, 5890962. <https://doi.org/10.1155/2019/5890962>
- Sautto, G. A., Kirchenbaum, G. A., Ecker, J. W., Bebin-Blackwell, A. G., Pierce, S. R., & Ross, T. M. (2018). Elicitation of broadly protective antibodies following infection with influenza viruses expressing h1n1 computationally optimized broadly reactive hemagglutinin antigens. *Immunohorizons*, 2(7), 226–237. <https://doi.org/10.4049/immunohorizons.1800044>
- Sautto, G. A., Kirchenbaum, G. A., & Ross, T. M. (2018). Towards a universal influenza vaccine: Different approaches for one goal. *Virology*, 51(1), 17. <https://doi.org/10.1186/s12985-017-0918-y>
- Sautto, G. A., & Ross, T. M. (2019). Hemagglutinin consensus-based prophylactic approaches to overcome influenza virus diversity. *Vet Ital*, 55(3), 195–201. <https://doi.org/10.12834/VetIt.1944.10352.1>
- Scheiblhofer, S., Laimer, J., Machado, Y., Weiss, R., & Thalhamer, J. (2017). Influence of protein fold stability on immunogenicity and its implications for vaccine design. *Expert Rev Vaccines*, 16(5), 479–489. <https://doi.org/10.1080/14760584.2017.1306441>
- Schon, J., Breithaupt, A., Hoper, D., King, J., Pohlmann, A., Parvin, R., Behr, K. P., Schwarz, B. A., Beer, M., Stech, J., Harder, T., & Grund, C. (2021). Neuraminidase-associated plasminogen recruitment enables systemic spread of natural avian influenza viruses h3n1. *PLoS Pathog*, 17(4), e1009490. <https://doi.org/10.1371/journal.ppat.1009490>
- Schotsaert, M., Ibanez, L. I., Fiers, W., & Saelens, X. (2010). Controlling influenza by cytotoxic t-cells: Calling for help from destroyers. *J Biomed Biotechnol*, 2010, 863985. <https://doi.org/10.1155/2010/863985>
- Schulman, J. L., & Kilbourne, E. D. (1965). Induction of partial specific heterotypic immunity in mice by a single infection with influenza a virus. *J Bacteriol*, 89, 170–4. <https://www.ncbi.nlm.nih.gov/pubmed/14255658>
- Sederdahl, B. K., & Williams, J. V. (2020). Epidemiology and clinical characteristics of influenza c virus. *Viruses*, 12(1). <https://doi.org/10.3390/v12010089>
- Seitz, C., Casalino, L., Konecny, R., Huber, G., Amaro, R. E., & McCammon, J. A. (2020). Multiscale simulations examining glycan shield effects on drug binding to influenza neuraminidase. *Biophys J*, 119(11), 2275–2289. <https://doi.org/10.1016/j.bpj.2020.10.024>
- Sekiya, T., Ohno, M., Nomura, N., Handabile, C., Shingai, M., Jackson, D. C., Brown, L. E., & Kida, H. (2021). Selecting and using the appropriate influenza vaccine for each individual. *Viruses*, 13(6). <https://doi.org/10.3390/v13060971>
- Selimova, L. M., Zaides, V. M., & Zhdanov, V. M. (1982). Disulfide bonding in influenza virus proteins as revealed by polyacrylamide gel electrophoresis. *J Virol*, 44(2), 450–7. <https://doi.org/10.1128/JVI.44.2.450-457.1982>

- Sellers, S. A., Hagan, R. S., Hayden, F. G., & Fischer, Z., W. A. (2017). The hidden burden of influenza: A review of the extra-pulmonary complications of influenza infection. *Influenza Other Respir Viruses*, 11(5), 372–393. <https://doi.org/10.1111/irv.12470>
- Selman, M., Dankar, S. K., Forbes, N. E., Jia, J. J., & Brown, E. G. (2012). Adaptive mutation in influenza a virus non-structural gene is linked to host switching and induces a novel protein by alternative splicing. *Emerging Microbes & Infections*, 1. <https://doi.org/ARTNe4210.1038/emi.2012.38>
- Shi, W., Lei, F., Zhu, C., Sievers, F., & Higgins, D. G. (2010). A complete analysis of ha and na genes of influenza a viruses. *PLoS One*, 5(12), e14454. <https://doi.org/10.1371/journal.pone.0014454>
- Shie, J. J., & Fang, J. M. (2019). Development of effective anti-influenza drugs: Congeners and conjugates - a review. *J Biomed Sci*, 26(1), 84. <https://doi.org/10.1186/s12929-019-0567-0>
- Shoji, Y., Chichester, J. A., Palmer, G. A., Farrance, C. E., Stevens, R., Stewart, M., Goldschmidt, L., Deyde, V., Gubareva, L., Klimov, A., Mett, V., & Yusibov, V. (2011). An influenza n1 neuraminidase-specific monoclonal antibody with broad neuraminidase inhibition activity against h5n1 hpai viruses. *Hum Vaccin, 7 Suppl*, 199–204. <https://doi.org/10.4161/hv.7.0.14595>
- Shtyrya, Y. A., Mochalova, L. V., & Bovin, N. V. (2009). Influenza virus neuraminidase: Structure and function. *Acta Naturae*, 1(2), 26–32. <https://www.ncbi.nlm.nih.gov/pubmed/22649600>
- Shultz, P. K., Crofts, K. F., Holbrook, B. C., & Alexander-Miller, M. A. (2020). Neuraminidase-specific antibody responses are generated in naive and vaccinated newborn nonhuman primates following virus infection. *JCI Insight*, 5(24). <https://doi.org/10.1172/jci.insight.141655>
- Simon-Grife, M., Martin-Valls, G. E., Vilar, M. J., Busquets, N., Mora-Salvaterra, M., Bestebroer, T. M., Fouchier, R. A., Martin, M., Mateu, E., & Casal, J. (2012). Swine influenza virus infection dynamics in two pig farms; results of a longitudinal assessment. *Vet Res*, 43, 24. <https://doi.org/10.1186/1297-9716-43-24>
- Simonsen, L., Reichert, T. A., & Miller, M. A. (2004). The virtues of antigenic sin: Consequences of pandemic recycling on influenza-associated mortality. *International Congress Series*, 1263, 791–794. <https://doi.org/10.1016/j.ics.2004.01.029>
- Skarlupka, A. L., Bebin-Blackwell, A. G., Sumner, S. F., & Ross, T. M. (2021). Universal influenza virus neuraminidase vaccine elicits protective immune responses against human seasonal and pre-pandemic strains. *J Virol*, JVI0075921. <https://doi.org/10.1128/JVI.00759-21>
- Skarlupka, A. L., Handel, A., & Ross, T. M. (2020). Dataset of antigenic distance measures, hemagglutination inhibition, viral lung titers, and weight loss in mice and ferrets when exposed to ha-based vaccination or sub-lethal a(h1) influenza infection. *Data Brief*, 32, 106118. <https://doi.org/10.1016/j.dib.2020.106118>
- Skarlupka, A. L., Owino, S. O., Suzuki-Williams, L. P., Crevar, C. J., Carter, D. M., & Ross, T. M. (2019). Computationally optimized broadly reactive vaccine based upon swine h1n1 influenza hemagglutinin sequences protects against both swine and human isolated viruses. *Hum Vaccin Immunother*, 15(9), 2013–2029. <https://doi.org/10.1080/21645515.2019.1653743>
- Skarlupka, A. L., Reneer, Z. B., Abreu, R. B., Ross, T. M., & Sautto, G. A. (2020). An influenza virus hemagglutinin computationally optimized broadly reactive antigen elicits antibodies endowed with group 1 heterosubtypic breadth against swine influenza viruses. *J Virol*, 94(8). <https://doi.org/10.1128/JVI.02061-19>
- Skarlupka, A. L., & Ross, T. M. (2020). Immune imprinting in the influenza ferret model. *Vaccines (Basel)*, 8(2). <https://doi.org/10.3390/vaccines8020173>

- Skarupka, A. L., & Ross, T. M. (2021). Inherent serum inhibition of influenza virus neuraminidases. *Frontiers in Veterinary Science*, 8. <https://doi.org/10.3389/fvets.2021.677693>
- Skountzou, I., Koutsonanos, D. G., Kim, J. H., Powers, R., Satyabhama, L., Masseoud, F., Weldon, W. C., Martin Mdel, P., Mittler, R. S., Compans, R., & Jacob, J. (2010). Immunity to pre-1950 h1n1 influenza viruses confers cross-protection against the pandemic swine-origin 2009 a (h1n1) influenza virus. *J Immunol*, 185(3), 1642–9. <https://doi.org/10.4049/jimmunol.1000091>
- Skowronski, D. M., Chambers, C., Sabaiduc, S., De Serres, G., Winter, A. L., Dickinson, J. A., Gubbay, J. B., Drews, S. J., Martineau, C., Charest, H., Krajden, M., Bastien, N., & Li, Y. (2017). Beyond antigenic match: Possible agent-host and immuno-epidemiological influences on influenza vaccine effectiveness during the 2015-2016 season in canada. *J Infect Dis*, 216(12), 1487–1500. <https://doi.org/10.1093/infdis/jix526>
- Smith, D. J., Forrest, S., Ackley, D. H., & Perelson, A. S. (1999). Variable efficacy of repeated annual influenza vaccination. *Proc Natl Acad Sci USA*, 96(24), 14001–6. <https://doi.org/10.1073/pnas.96.24.14001>
- Smith, D. J., Lapedes, A. S., de Jong, J. C., Bestebroer, T. M., Rimmelzwaan, G. F., Osterhaus, A. D., & Fouchier, R. A. (2004). Mapping the antigenic and genetic evolution of influenza virus. *Science*, 305(5682), 371–6. <https://doi.org/10.1126/science.1097211>
- Smith, G. E., Sun, X., Bai, Y., Liu, Y. V., Massare, M. J., Pearce, M. B., Belser, J. A., Maines, T. R., Creager, H. M., Glenn, G. M., Flyer, D., Pushko, P., Levine, M. Z., & Tumpey, T. M. (2017). Neuraminidase-based recombinant virus-like particles protect against lethal avian influenza a(h5n1) virus infection in ferrets. *Virology*, 509, 90–97. <https://doi.org/10.1016/j.virol.2017.06.006>
- Smith, G. J., Vijaykrishna, D., Bahl, J., Lycett, S. J., Worobey, M., Pybus, O. G., Ma, S. K., Cheung, C. L., Raghwani, J., Bhatt, S., Peiris, J. S., Guan, Y., & Rambaut, A. (2009). Origins and evolutionary genomics of the 2009 swine-origin h1n1 influenza a epidemic. *Nature*, 459(7250), 1122–5. <https://doi.org/10.1038/nature08182>
- Solano, M. I., Woolfitt, A. R., Williams, T. L., Pierce, C. L., Gubareva, L. V., Mishin, V., & Barr, J. R. (2017). Quantification of influenza neuraminidase activity by ultra-high performance liquid chromatography and isotope dilution mass spectrometry. *Anal Chem*, 89(5), 3130–3137. <https://doi.org/10.1021/acs.analchem.6bo4902>
- Spackman, E., Pantin-Jackwood, M. J., Sitaras, I., Stephens, C. B., & Suarez, D. L. (2020). Identification of efficacious vaccines against contemporary north american h7 avian influenza viruses. *Avian Dis*. <https://doi.org/10.1637/aviandiseases-D-20-00109>
- Stadlbauer, D., Zhu, X., McMahon, M., Turner, J. S., Wohlbold, T. J., Schmitz, A. J., Strohmeier, S., Yu, W., Nachbagauer, R., Mudd, P. A., Wilson, I. A., Ellebedy, A. H., & Krammer, F. (2019). Broadly protective human antibodies that target the active site of influenza virus neuraminidase. *Science*, 366(6464), 499–504. <https://doi.org/10.1126/science.aayo678>
- Stech, O., Veits, J., Abdelwhab, E. M., Wessels, U., Mettenleiter, T. C., & Stech, J. (2015). The neuraminidase stalk deletion serves as major virulence determinant of h5n1 highly pathogenic avian influenza viruses in chicken. *Sci Rep*, 5, 13493. <https://doi.org/10.1038/srep13493>
- Steel, J., Staeheli, P., Mubareka, S., Garcia-Sastre, A., Palese, P., & Lowen, A. C. (2010). Transmission of pandemic h1n1 influenza virus and impact of prior exposure to seasonal strains or interferon treatment. *J Virol*, 84(1), 21–6. <https://doi.org/10.1128/JVI.01732-09>

- Steinbruck, L., Klingen, T. R., & McHardy, A. C. (2014). Computational prediction of vaccine strains for human influenza a (h3n2) viruses. *J Virol*, 88(20), 12123–32. <https://doi.org/10.1128/JVI.01861-14>
- Steinbruck, L., & McHardy, A. C. (2012). Inference of genotype-phenotype relationships in the antigenic evolution of human influenza a (h3n2) viruses. *PLoS Comput Biol*, 8(4), e1002492. <https://doi.org/10.1371/journal.pcbi.1002492>
- Suguitan, J., A. L., Matsuoka, Y., Lau, Y. F., Santos, C. P., Vogel, L., Cheng, L. I., Orandle, M., & Subbarao, K. (2012). The multibasic cleavage site of the hemagglutinin of highly pathogenic a/vietnam/1203/2004 (h5n1) avian influenza virus acts as a virulence factor in a host-specific manner in mammals. *J Virol*, 86(5), 2706–14. <https://doi.org/10.1128/JVI.05546-11>
- Sultana, I., Yang, K., Getie-Kebtie, M., Couzens, L., Markoff, L., Alterman, M., & Eichelberger, M. C. (2014). Stability of neuraminidase in inactivated influenza vaccines. *Vaccine*, 32(19), 2225–30. <https://doi.org/10.1016/j.vaccine.2014.01.078>
- Sun, H., Yang, J., Zhang, T., Long, L. P., Jia, K., Yang, G., Webby, R. J., & Wan, X. F. (2013). Using sequence data to infer the antigenicity of influenza virus. *mBio*, 4(4). <https://doi.org/10.1128/mBio.00230-13>
- Sun, W., Luo, T., Liu, W., & Li, J. (2020). Progress in the development of universal influenza vaccines. *Viruses*, 12(9). <https://doi.org/10.3390/vr12091033>
- Sun, X., Li, Q., Wu, Y., Wang, M., Liu, Y., Qi, J., Vavricka, C. J., & Gao, G. F. (2014). Structure of influenza virus n7: The last piece of the neuraminidase "jigsaw" puzzle. *J Virol*, 88(16), 9197–207. <https://doi.org/10.1128/JVI.00805-14>
- Sutton, T. C., Chakraborty, S., Mallajosyula, V. V. A., Lamirande, E. W., Ganti, K., Bock, K. W., Moore, I. N., Varadarajan, R., & Subbarao, K. (2017). Protective efficacy of influenza group 2 hemagglutinin stem-fragment immunogen vaccines. *NPJ Vaccines*, 2, 35. <https://doi.org/10.1038/s41541-017-0036-2>
- Suzuki, Y., Ito, T., Suzuki, T., Holland, J., R. E., Chambers, T. M., Kiso, M., Ishida, H., & Kawaoka, Y. (2000). Sialic acid species as a determinant of the host range of influenza a viruses. *J Virol*, 74(24), 11825–31. <https://doi.org/10.1128/jvi.74.24.11825-11831.2000>
- Sylte, M. J., & Suarez, D. L. (2009). Influenza neuraminidase as a vaccine antigen. *Curr Top Microbiol Immunol*, 333, 227–41. https://doi.org/10.1007/978-3-540-92165-3__12
- Takahashi, T., & Suzuki, T. (2015). Low-ph stability of influenza a virus sialidase contributing to virus replication and pandemic. *Biol Pharm Bull*, 38(6), 817–26. <https://doi.org/10.1248/bpb.b15-00120>
- Tan, M., & Jiang, X. (2014). Vaccine against norovirus. *Hum Vaccin Immunother*, 10(6), 1449–56. <https://doi.org/10.4161/hv.28626>
- Tate, M. D., Job, E. R., Deng, Y. M., Gunalan, V., Maurer-Stroh, S., & Reading, P. C. (2014). Playing hide and seek: How glycosylation of the influenza virus hemagglutinin can modulate the immune response to infection. *Viruses*, 6(3), 1294–316. <https://doi.org/10.3390/v6031294>
- Tesini, B. L., Kanagaiah, P., Wang, J., Hahn, M., Halliley, J. L., Chaves, F. A., Nguyen, P. Q. T., Nogales, A., DeDiego, M. L., Anderson, C. S., Ellebedy, A. H., Strohmeier, S., Krammer, F., Yang, H., Bandyopadhyay, S., Ahmed, R., Treanor, J. J., Martinez-Sobrido, L., Golding, H., ... Sangster, M. Y. (2019). Broad hemagglutinin-specific memory b cell expansion by seasonal influenza virus infection reflects early-life imprinting and adaptation to the infecting virus. *J Virol*, 93(8). <https://doi.org/10.1128/JVI.00169-19>

- Thacker, E., & Janke, B. (2008). Swine influenza virus: Zoonotic potential and vaccination strategies for the control of avian and swine influenzas. *J Infect Dis*, *197 Suppl 1*, S19–24. <https://doi.org/10.1086/524988>
- Tomley, F. M., & Shirley, M. W. (2009). Livestock infectious diseases and zoonoses. *Philos Trans R Soc Lond B Biol Sci*, *364*(1530), 2637–42. <https://doi.org/10.1098/rstb.2009.0133>
- Tong, S., Li, Y., Rivailler, P., Conrardy, C., Castillo, D. A., Chen, L. M., Recuenco, S., Ellison, J. A., Davis, C. T., York, I. A., Turmelle, A. S., Moran, D., Rogers, S., Shi, M., Tao, Y., Weil, M. R., Tang, K., Rowe, L. A., Sammons, S., ... Donis, R. O. (2012). A distinct lineage of influenza a virus from bats. *Proc Natl Acad Sci U S A*, *109*(11), 4269–74. <https://doi.org/10.1073/pnas.1116200109>
- Transportation, sale, and handling of certain animals. (2015). <https://uscode.house.gov/view.xhtml?path=/prelim%5C@title7/chapter54%5C&edition=prelim>
- Treanor, J. J., Campbell, J. D., Zangwill, K. M., Rowe, T., & Wolff, M. (2006). Safety and immunogenicity of an inactivated subvirion influenza a (h5ni) vaccine. *N Engl J Med*, *354*(13), 1343–51. <https://doi.org/10.1056/NEJMoa055778>
- Treanor, J. J., Hayden, F. G., Vrooman, P. S., Barbarash, R., Bettis, R., Riff, D., Singh, S., Kinnersley, N., Ward, P., & Mills, R. G. (2000). Efficacy and safety of the oral neuraminidase inhibitor oseltamivir in treating acute influenza: A randomized controlled trial. us oral neuraminidase study group. *JAMA*, *283*(8), 1016–24. <https://doi.org/10.1001/jama.283.8.1016>
- Treanor, J. J., Wilkinson, B. E., Massoud, F., Hu-Primmer, J., Battaglia, R., O'Brien, D., Wolff, M., Rabinovich, G., Blackwelder, W., & Katz, J. M. (2001). Safety and immunogenicity of a recombinant hemagglutinin vaccine for h5 influenza in humans. *Vaccine*, *19*(13–14), 1732–7. [https://doi.org/10.1016/s0264-410x\(00\)00395-9](https://doi.org/10.1016/s0264-410x(00)00395-9)
- Treanor, J. J., Kotloff, K., Betts, R. F., Belshe, R., Newman, F., Iacuzio, D., Wittes, J., & Bryant, M. (1999). Evaluation of trivalent, live, cold-adapted (caiv-t) and inactivated (tiv) influenza vaccines in prevention of virus infection and illness following challenge of adults with wild-type influenza a (hini), a (h3n2), and b viruses. *Vaccine*, *18*(9–10), 899–906. [https://doi.org/10.1016/s0264-410x\(99\)00334-5](https://doi.org/10.1016/s0264-410x(99)00334-5)
- Tricco, A. C., Chit, A., Soobiah, C., Hallett, D., Meier, G., Chen, M. H., Tashkandi, M., Bauch, C. T., & Loeb, M. (2013). Comparing influenza vaccine efficacy against mismatched and matched strains: A systematic review and meta-analysis. *BMC Med*, *11*, 153. <https://doi.org/10.1186/1741-7015-11-153>
- Tsuchiya, E., Sugawara, K., Hongo, S., Matsuzaki, Y., Muraki, Y., Li, Z. N., & Nakamura, K. (2001). Antigenic structure of the haemagglutinin of human influenza a/h2n2 virus. *J Gen Virol*, *82*(Pt 10), 2475–84. <https://doi.org/10.1099/0022-1317-82-10-2475>
- UniProt, C. (2021). Uniprot: The universal protein knowledgebase in 2021. *Nucleic Acids Res*, *49*(D1), D480–D489. <https://doi.org/10.1093/nar/gkaa1100>
- Uno, N., & Ross, T. M. (2020). A universal dengue vaccine elicits neutralizing antibodies against strains from all four dengue serotypes. *J Virol*. <https://doi.org/10.1128/JVI.00658-20>
- Upadhyay, A. A., Kauffman, R. C., Wolabaugh, A. N., Cho, A., Patel, N. B., Reiss, S. M., Havenar-Daughton, C., Dawoud, R. A., Tharp, G. K., Sanz, I., Pulendran, B., Crotty, S., Lee, F. E., Wrammert, J., & Bosinger, S. E. (2018). Baldr: A computational pipeline for paired heavy and light chain immunoglobulin reconstruction in single-cell rna-seq data. *Genome Med*, *10*(1), 20. <https://doi.org/10.1186/s13073-018-0528-3>

- Uyeki, T. M. (2020). High-risk groups for influenza complications. *JAMA*, 324(22), 2334. <https://doi.org/10.1001/jama.2020.21869>
- Vahey, M. D., & Fletcher, D. A. (2019). Influenza a virus surface proteins are organized to help penetrate host mucus. *eLife*, 8. <https://doi.org/10.7554/eLife.43764>
- Valcarcel, J., Portela, A., & Ortín, J. (1991). Regulated mi mrna splicing in influenza virus-infected cells. *J Gen Virol*, 72 (Pt 6), 1301–8. <https://doi.org/10.1099/0022-1317-72-6-1301>
- Valkenburg, S. A., Fang, V. J., Leung, N. H., Chu, D. K., Ip, D. K., Perera, R. A., Wang, Y., Li, A. P., Peiris, J. M., Cowling, B. J., & Poon, L. L. (2019). Cross-reactive antibody-dependent cellular cytotoxicity antibodies are increased by recent infection in a household study of influenza transmission. *Clin Transl Immunology*, 8(ii), e1092. <https://doi.org/10.1002/ctiz.e1092>
- van den Brand, J. M., Haagmans, B. L., van Riel, D., Osterhaus, A. D., & Kuiken, T. (2014). The pathology and pathogenesis of experimental severe acute respiratory syndrome and influenza in animal models. *J Comp Pathol*, 151(1), 83–112. <https://doi.org/10.1016/j.jcpa.2014.01.004>
- Varghese, J. N., Colman, P. M., van Donkelaar, A., Blick, T. J., Sahasrabudhe, A., & McKimm-Breschkin, J. L. (1997). Structural evidence for a second sialic acid binding site in avian influenza virus neuraminidases. *Proc Natl Acad Sci U S A*, 94(22), 11808–12. <https://doi.org/10.1073/pnas.94.22.11808>
- Vatti, A., Monsalve, D. M., Pacheco, Y., Chang, C., Anaya, J. M., & Gershwin, M. E. (2017). Original antigenic sin: A comprehensive review. *J Autoimmun*, 83, 12–21. <https://doi.org/10.1016/j.jaut.2017.04.008>
- Vaughan, K., Kim, Y., & Sette, A. (2012). A comparison of epitope repertoires associated with myasthenia gravis in humans and nonhuman hosts. *Autoimmune Dis*, 2012, 403915. <https://doi.org/10.1155/2012/403915>
- Vemula, S. V., Sayedahmed, E. E., Sambhara, S., & Mittal, S. K. (2017). Vaccine approaches conferring cross-protection against influenza viruses. *Expert Review of Vaccines*, 16(ii), 1141–1154. <https://doi.org/10.1080/14760584.2017.1379396>
- Vester, D., Lagoda, A., Hoffmann, D., Seitz, C., Heldt, S., Bettenbrock, K., Genzel, Y., & Reichl, U. (2010). Real-time rt-qpcr assay for the analysis of human influenza a virus transcription and replication dynamics. *J Virol Methods*, 168(1-2), 63–71. <https://doi.org/10.1016/j.jviromet.2010.04.017>
- Viboud, C., Simonsen, L., Fuentes, R., Flores, J., Miller, M. A., & Chowell, G. (2016). Global mortality impact of the 1957–1959 influenza pandemic. *J Infect Dis*, 213(5), 738–45. <https://doi.org/10.1093/infdis/jiv534>
- Vincent, A. L., Ma, W., Lager, K. M., Gramer, M. R., Richt, J. A., & Janke, B. H. (2009). Characterization of a newly emerged genetic cluster of h1n1 and h1n2 swine influenza virus in the united states. *Virus Genes*, 39(2), 176–85. <https://doi.org/10.1007/s11262-009-0386-6>
- Vincent, A. L., Ma, W., Lager, K. M., Janke, B. H., & Richt, J. A. (2008). Swine influenza viruses a north american perspective. *Adv Virus Res*, 72, 127–54. [https://doi.org/10.1016/S0065-3527\(08\)00403-X](https://doi.org/10.1016/S0065-3527(08)00403-X)
- Wagner, R., Matrosovich, M., & Klenk, H. D. (2002). Functional balance between haemagglutinin and neuraminidase in influenza virus infections. *Rev Med Virol*, 12(3), 159–66. <https://doi.org/10.1002/rmv.352>
- Walters, K. A., Zhu, R., Welge, M., Scherler, K., Park, J. K., Rahil, Z., Wang, H., Auvil, L., Bushell, C., Lee, M. Y., Baxter, D., Bristol, T., Rosas, L. A., Cervantes-Medina, A., Czajkowski, L., Han, A.,

- Memoli, M. J., Taubenberger, J. K., & Kash, J. C. (2019). Differential effects of influenza virus na, ha head, and ha stalk antibodies on peripheral blood leukocyte gene expression during human infection. *mBio*, *10*(3). <https://doi.org/10.1128/mBio.00760-19>
- Walz, L., Kays, S. K., Zimmer, G., & von Messling, V. (2018). Sialidase-inhibiting antibody titers correlate with protection from heterologous influenza virus strains of the same neuraminidase subtype. *J Virol*. <https://doi.org/10.1128/JVI.01006-18>
- Wan, H., Gao, J., Xu, K., Chen, H., Couzens, L. K., Rivers, K. H., Easterbrook, J. D., Yang, K., Zhong, L., Rajabi, M., Ye, J., Sultana, I., Wan, X. F., Liu, X., Perez, D. R., Taubenberger, J. K., & Eichelberger, M. C. (2013). Molecular basis for broad neuraminidase immunity: Conserved epitopes in seasonal and pandemic h1n1 as well as h5n1 influenza viruses. *J Virol*, *87*(16), 9290–300. <https://doi.org/10.1128/JVI.01203-13>
- Wang, F., Wang, Y., Wan, Z., Shao, H., Qian, K., Ye, J., & Qin, A. (2020). Generation of a recombinant chickenized monoclonal antibody against the neuraminidase of h9n2 avian influenza virus. *AMB Express*, *10*(1), 151. <https://doi.org/10.1186/s13568-020-01086-4>
- Wang, H., Dou, D., Ostbye, H., Revol, R., & Daniels, R. (2019). Structural restrictions for influenza neuraminidase activity promote adaptation and diversification. *Nat Microbiol*, *4*(12), 2565–2577. <https://doi.org/10.1038/s41564-019-0537-z>
- Wang, J., Hilchey, S. P., DeDiego, M., Perry, S., Hyrien, O., Nogales, A., Garigen, J., Amanat, F., Huertas, N., Krammer, F., Martinez-Sobrido, L., Topham, D. J., Treanor, J. J., Sangster, M. Y., & Zand, M. S. (2018). Broad cross-reactive igg responses elicited by adjuvanted vaccination with recombinant influenza hemagglutinin (rha) in ferrets and mice. *PLoS One*, *13*(4), e0193680. <https://doi.org/10.1371/journal.pone.0193680>
- Wang, N., Glidden, E. J., Murphy, S. R., Pearse, B. R., & Hebert, D. N. (2008). The cotranslational maturation program for the type ii membrane glycoprotein influenza neuraminidase. *J Biol Chem*, *283*(49), 33826–37. <https://doi.org/10.1074/jbc.M806897200>
- Wang, P., Zhu, W., Liao, B., Cai, L., Peng, L., & Yang, J. (2018). Predicting influenza antigenicity by matrix completion with antigen and antiserum similarity. *Front Microbiol*, *9*, 2500. <https://doi.org/10.3389/fmicb.2018.02500>
- Wang, T., Wei, F., & Liu, J. (2020). Emerging role of mucosal vaccine in preventing infection with avian influenza a viruses. *Viruses*, *12*(8). <https://doi.org/10.3390/v12080862>
- Ward, C. W., Colman, P. M., & Laver, W. G. (1983). The disulphide bonds of an asian influenza virus neuraminidase. *FEBS Letters*, *153*(1), 29–33. [https://doi.org/10.1016/0014-5793\(83\)80113-6](https://doi.org/10.1016/0014-5793(83)80113-6)
- Waterhouse, A., Bertoni, M., Bienert, S., Studer, G., Tauriello, G., Gumienny, R., Heer, F. T., de Beer, T. A. P., Rempfer, C., Bordoli, L., Lepore, R., & Schwede, T. (2018). Swiss-model: Homology modelling of protein structures and complexes. *Nucleic Acids Res*, *46*(W1), W296–W303. <https://doi.org/10.1093/nar/gky427>
- Webby, R. J., Rossow, K., Erickson, G., Sims, Y., & Webster, R. (2004). Multiple lineages of antigenically and genetically diverse influenza a virus co-circulate in the united states swine population. *Virus Res*, *103*(1-2), 67–73. <https://doi.org/10.1016/j.virusres.2004.02.015>
- Webster, R. G. (1966). Original antigenic sin in ferrets: The response to sequential infections with influenza viruses. *J Immunol*, *97*(2), 177–83. <https://www.ncbi.nlm.nih.gov/pubmed/5921310%20https://www.jimmunol.org/content/97/2/177.long>

- Webster, R. G., & Laver, W. G. (1980). Determination of the number of nonoverlapping antigenic areas on hong kong (h3n2) influenza virus hemagglutinin with monoclonal antibodies and the selection of variants with potential epidemiological significance. *Virology*, *104*(1), 139–148. [https://doi.org/10.1016/0042-6822\(80\)90372-4](https://doi.org/10.1016/0042-6822(80)90372-4)
- Wei, C. J., Boyington, J. C., Dai, K., Houser, K. V., Pearce, M. B., Kong, W. P., Yang, Z. Y., Tumpey, T. M., & Nabel, G. J. (2010). Cross-neutralization of 1918 and 2009 influenza viruses: Role of glycans in viral evolution and vaccine design. *Sci Transl Med*, *2*(24), 24ra21. <https://doi.org/10.1126/scitranslmed.3000799>
- Weiss, C. D., Wang, W., Lu, Y., Billings, M., Eick-Cost, A., Couzens, L., Sanchez, J. L., Hawksworth, A. W., Seguin, P., Myers, C. A., Forshee, R., Eichelberger, M. C., & Cooper, M. J. (2020). Neutralizing and neuraminidase antibodies correlate with protection against influenza during a late season a/h3n2 outbreak among unvaccinated military recruits. *Clin Infect Dis*, *71*(12), 3096–3102. <https://doi.org/10.1093/cid/ciz198>
- Westgeest, K. B., Bestebroer, T. M., Spronken, M. I., Gao, J., Couzens, L., Osterhaus, A. D., Eichelberger, M., Fouchier, R. A., & de Graaf, M. (2015). Optimization of an enzyme-linked lectin assay suitable for rapid antigenic characterization of the neuraminidase of human influenza a(h3n2) viruses. *J Virol Methods*, *217*, 55–63. <https://doi.org/10.1016/j.jviromet.2015.02.014>
- Wetherall, N. T., Trivedi, T., Zeller, J., Hodges-Savola, C., McKimm-Breschkin, J. L., Zambon, M., & Hayden, F. G. (2003). Evaluation of neuraminidase enzyme assays using different substrates to measure susceptibility of influenza virus clinical isolates to neuraminidase inhibitors: Report of the neuraminidase inhibitor susceptibility network. *Journal of Clinical Microbiology*, *41*(2), 742–750. <https://doi.org/10.1128/Jcm.41.2.742-750.2003>
- White, L. A., Torremorell, M., & Craft, M. E. (2017). Influenza a virus in swine breeding herds: Combination of vaccination and biosecurity practices can reduce likelihood of endemic piglet reservoir. *Prev Vet Med*, *138*, 55–69. <https://doi.org/10.1016/j.prevetmed.2016.12.013>
- Whittle, J. R., Zhang, R., Khurana, S., King, L. R., Manischewitz, J., Golding, H., Dormitzer, P. R., Haynes, B. F., Walter, E. B., Moody, M. A., Kepler, T. B., Liao, H. X., & Harrison, S. C. (2011). Broadly neutralizing human antibody that recognizes the receptor-binding pocket of influenza virus hemagglutinin. *Proc Natl Acad Sci USA*, *108*(34), 14216–21. <https://doi.org/10.1073/pnas.1111497108>
- Wikramaratna, P. S., & Rambaut, A. (2015). Relationship between haemagglutination inhibition titre and immunity to influenza in ferrets. *Vaccine*, *33*(41), 5380–5385. <https://doi.org/10.1016/j.vaccine.2015.08.065>
- Wiley, D. C., Wilson, I. A., & Skehel, J. J. (1981). Structural identification of the antibody-binding sites of hong kong influenza haemagglutinin and their involvement in antigenic variation. *Nature*, *289*(5796), 373–8. <https://doi.org/10.1038/289373a0>
- Wilkinson, K., Wei, Y., Szwajcer, A., Rabbani, R., Zarychanski, R., Abou-Setta, A. M., & Mahmud, S. M. (2017). Efficacy and safety of high-dose influenza vaccine in elderly adults: A systematic review and meta-analysis. *Vaccine*, *35*(21), 2775–2780. <https://doi.org/10.1016/j.vaccine.2017.03.092>
- Williams, J. A., Gui, L., Hom, N., Mileant, A., & Lee, K. K. (2018). Dissection of epitope-specific mechanisms of neutralization of influenza virus by intact igg and fab fragments. *J Virol*, *92*(6). <https://doi.org/10.1128/JVI.02006-17>

- Winter, G., Fields, S., & Brownlee, G. G. (1981). Nucleotide sequence of the haemagglutinin gene of a human influenza virus h1 subtype. *Nature*, 292(5818), 72–5. <https://www.ncbi.nlm.nih.gov/pubmed/7278968>
- Wise, H. M., Foeglein, A., Sun, J., Dalton, R. M., Patel, S., Howard, W., Anderson, E. C., Barclay, W. S., & Digard, P. (2009). A complicated message: Identification of a novel pb1-related protein translated from influenza a virus segment 2 mrna. *J Virol*, 83(16), 8021–31. <https://doi.org/10.1128/JVI.00826-09>
- Wise, H. M., Hutchinson, E. C., Jagger, B. W., Stuart, A. D., Kang, Z. H., Robb, N., Schwartzman, L. M., Kash, J. C., Fodor, E., Firth, A. E., Gog, J. R., Taubenberger, J. K., & Digard, P. (2012). Identification of a novel splice variant form of the influenza a virus m2 ion channel with an antigenically distinct ectodomain. *PLoS Pathog*, 8(11), e1002998. <https://doi.org/10.1371/journal.ppat.1002998>
- Wohlbold, T. J., & Krammer, F. (2014). In the shadow of hemagglutinin: A growing interest in influenza viral neuraminidase and its role as a vaccine antigen. *Viruses*, 6(6), 2465–94. <https://doi.org/10.3390/v6062465>
- Wohlbold, T. J., Nachbagauer, R., Xu, H., Tan, G. S., Hirsh, A., Brokstad, K. A., Cox, R. J., Palese, P., & Krammer, F. (2015). Vaccination with adjuvanted recombinant neuraminidase induces broad heterologous, but not heterosubtypic, cross-protection against influenza virus infection in mice. *MBio*, 6(2), e02556. <https://doi.org/10.1128/mBio.02556-14>
- Wohlbold, T. J., Podolsky, K. A., Chromikova, V., Kirkpatrick, E., Falconieri, V., Meade, P., Amanat, F., Tan, J., tenOever, B. R., Tan, G. S., Subramaniam, S., Palese, P., & Krammer, F. (2017). Broadly protective murine monoclonal antibodies against influenza b virus target highly conserved neuraminidase epitopes. *Nat Microbiol*, 2(10), 1415–1424. <https://doi.org/10.1038/s41564-017-0011-8>
- Wong, S. S., Duan, S., DeBeauchamp, J., Zanin, M., Kercher, L., Sonnberg, S., Fabrizio, T., Jeevan, T., Crumpton, J. C., Oshansky, C., Sun, Y., Tang, L., Thomas, P., & Webby, R. (2017). The immune correlates of protection for an avian influenza h5n1 vaccine in the ferret model using oil-in-water adjuvants. *Sci Rep*, 7, 44727. <https://doi.org/10.1038/srep44727>
- Wong, S. S., Waite, B., Ralston, J., Wood, T., Reynolds, G. E., Seeds, R., Newbern, E. C., Thompson, M. G., Huang, Q. S., Webby, R. J., & Team, S. I. (2020). Hemagglutinin and neuraminidase antibodies are induced in an age- and subtype-dependent manner after influenza virus infection. *J Virol*, 94(7). <https://doi.org/10.1128/JVI.01385-19>
- Wong, T. M., Allen, J. D., Bebin-Blackwell, A. G., Carter, D. M., Alefantis, T., DiNapoli, J., Kleanthous, H., & Ross, T. M. (2017). Computationally optimized broadly reactive hemagglutinin elicits hemagglutination inhibition antibodies against a panel of h3n2 influenza virus cocirculating variants. *J Virol*, 91(24). <https://doi.org/10.1128/JVI.01581-17>
- Worobey, M., Han, G. Z., & Rambaut, A. (2014a). Genesis and pathogenesis of the 1918 pandemic h1n1 influenza a virus. *Proc Natl Acad Sci U S A*, 111(22), 8107–12. <https://doi.org/10.1073/pnas.1324197111>
- Worobey, M., Han, G. Z., & Rambaut, A. (2014b). A synchronized global sweep of the internal genes of modern avian influenza virus. *Nature*, 508(7495), 254–7. <https://doi.org/10.1038/nature13016>
- Wozniak-Kosek, A., Kempinska-Miroslawska, B., & Hoser, G. (2014). Detection of the influenza virus yesterday and now. *Acta Biochim Pol*, 61(3), 465–70. <https://www.ncbi.nlm.nih.gov/pubmed/25180218>

- Xiong, F. F., Liu, X. Y., Gao, F. X., Luo, J., Duan, P., Tan, W. S., & Chen, Z. (2020). Protective efficacy of anti-neuraminidase monoclonal antibodies against h7n9 influenza virus infection. *Emerg Microbes Infect*, 9(1), 78–87. <https://doi.org/10.1080/22221751.2019.1708214>
- Xiong, X., McCauley, J. W., & Steinhauer, D. A. (2014). Receptor binding properties of the influenza virus hemagglutinin as a determinant of host range. *Curr Top Microbiol Immunol*, 385, 63–91. https://doi.org/10.1007/82_2014_423
- Xu, J., Davis, C. T., Christman, M. C., Rivailler, P., Zhong, H., Donis, R. O., & Lu, G. (2012). Evolutionary history and phylodynamics of influenza a and b neuraminidase (na) genes inferred from large-scale sequence analyses. *PLoS One*, 7(7), e38665. <https://doi.org/10.1371/journal.pone.0038665>
- Xu, R., Ekiert, D. C., Krause, J. C., Hai, R., Crowe, J., J. E., & Wilson, I. A. (2010). Structural basis of preexisting immunity to the 2009 h1n1 pandemic influenza virus. *Science*, 328(5976), 357–60. <https://doi.org/10.1126/science.1186430>
- Xu, R., Zhu, X., McBride, R., Nycholat, C. M., Yu, W., Paulson, J. C., & Wilson, I. A. (2012). Functional balance of the hemagglutinin and neuraminidase activities accompanies the emergence of the 2009 h1n1 influenza pandemic. *J Virol*, 86(17), 9221–32. <https://doi.org/10.1128/JVI.00697-12>
- Yakubogullari, N., Genc, R., Coven, F., Nalbantsoy, A., & Bedir, E. (2019). Development of adjuvant nanocarrier systems for seasonal influenza a (h3n2) vaccine based on astragaloside viii and gum tragacanth (aps). *Vaccine*, 37(28), 3638–3645. <https://doi.org/10.1016/j.vaccine.2019.05.038>
- Yamayoshi, S., Uraki, R., Ito, M., Kiso, M., Nakatsu, S., Yasuhara, A., Oishi, K., Sasaki, T., Ikuta, K., & Kawaoka, Y. (2017). A broadly reactive human anti-hemagglutinin stem monoclonal antibody that inhibits influenza a virus particle release. *EBioMedicine*, 17, 182–191. <https://doi.org/10.1016/j.ebiom.2017.03.007>
- Yang, X., Steukers, L., Forier, K., Xiong, R., Braeckmans, K., Van Reeth, K., & Nauwynck, H. (2014). A beneficiary role for neuraminidase in influenza virus penetration through the respiratory mucus. *PLoS One*, 9(10), e110026. <https://doi.org/10.1371/journal.pone.0110026>
- Yetter, R. A., Barber, W. H., & Small, J., P. A. (1980). Heterotypic immunity to influenza in ferrets. *Infect Immun*, 29(2), 650–3. <https://www.ncbi.nlm.nih.gov/pmc/articles/PMC3716432/> <https://www.ncbi.nlm.nih.gov/pmc/articles/PMC3716432/pdf/infectimmun02650.pdf>
- Yetter, R. A., Lehrer, S., Ramphal, R., & Small, J., P. A. (1980). Outcome of influenza infection: Effect of site of initial infection and heterotypic immunity. *Infect Immun*, 29(2), 654–62. <https://www.ncbi.nlm.nih.gov/pmc/articles/PMC3716433/> <https://www.ncbi.nlm.nih.gov/pmc/articles/PMC3716433/pdf/infectimmun02654.pdf>
- Yoo, B. W., Kim, C. O., Izu, A., Arora, A. K., & Heijnen, E. (2018). Phase 4, post-marketing safety surveillance of the mf59-adjuvanted influenza vaccines fluad(r) and vantaflu(r) in south korean subjects aged >/=65 years. *Infect Chemother*, 50(4), 301–310. <https://doi.org/10.3947/ic.2018.50.4.301>
- Yoshida, R., Igarashi, M., Ozaki, H., Kishida, N., Tomabechi, D., Kida, H., Ito, K., & Takada, A. (2009). Cross-protective potential of a novel monoclonal antibody directed against antigenic site b of the hemagglutinin of influenza a viruses. *PLoS Pathog*, 5(3), e1000350. <https://doi.org/10.1371/journal.ppat.1000350>
- Yoshida, T., Mei, H., Dorner, T., Hiepe, F., Radbruch, A., Fillatreau, S., & Hoyer, B. F. (2010). Memory b and memory plasma cells. *Immunol Rev*, 237(1), 117–39. <https://doi.org/10.1111/j.1600-065X.2010.00938.x>

- Zambon, M. C. (2001). The pathogenesis of influenza in humans. *Rev Med Virol*, 11(4), 227–41. <https://doi.org/10.1002/rmv.319>
- Zhang, Y., Zhu, J., Li, Y., Bradley, K. C., Cao, J., Chen, H., Jin, M., & Zhou, H. (2013). Glycosylation on hemagglutinin affects the virulence and pathogenicity of pandemic h1n1/2009 influenza a virus in mice. *PLoS One*, 8(4), e61397. <https://doi.org/10.1371/journal.pone.0061397>
- Zheng, A., Sun, W., Xiong, X., Freyn, A. W., Peukes, J., Strohmeier, S., Nachbagauer, R., Briggs, J. A. G., Krammer, F., & Palese, P. (2020). Enhancing neuraminidase immunogenicity of influenza a viruses by rewiring rna packaging signals. *J Virol*, 94(16). <https://doi.org/10.1128/JVI.00742-20>
- Zhou, J., & Teo, Y. Y. (2016). Estimating time to the most recent common ancestor (tmrca): Comparison and application of eight methods. *Eur J Hum Genet*, 24(8), 1195–201. <https://doi.org/10.1038/ejhg.2015.258>
- Zhu, X., Turner, H. L., Lang, S., McBride, R., Bangaru, S., Gilchuk, I. M., Yu, W., Paulson, J. C., Crowe, J., J. E., Ward, A. B., & Wilson, I. A. (2019). Structural basis of protection against h7n9 influenza virus by human anti-n9 neuraminidase antibodies. *Cell Host Microbe*, 26(6), 729–738 e4. <https://doi.org/10.1016/j.chom.2019.10.002>
- Zhuang, Q., Wang, S., Liu, S., Hou, G., Li, J., Jiang, W., Wang, K., Peng, C., Liu, D., Guo, A., & Chen, J. (2019). Diversity and distribution of type a influenza viruses: An updated panorama analysis based on protein sequences. *Virol J*, 16(1), 85. <https://doi.org/10.1186/s12985-019-1188-7>
- Zimmerman, R. K., Nowalk, M. P., Chung, J., Jackson, M. L., Jackson, L. A., Petrie, J. G., Monto, A. S., McLean, H. Q., Belongia, E. A., Gaglani, M., Murthy, K., Fry, A. M., Flannery, B., Investigators, U. S. F. V., & Investigators, U. S. F. V. (2016). 2014-2015 influenza vaccine effectiveness in the united states by vaccine type. *Clin Infect Dis*, 63(12), 1564–1573. <https://doi.org/10.1093/cid/ciw635>
- Zost, S. J., Parkhouse, K., Gumina, M. E., Kim, K., Diaz Perez, S., Wilson, P. C., Treanor, J. J., Sant, A. J., Cobey, S., & Hensley, S. E. (2017). Contemporary h3n2 influenza viruses have a glycosylation site that alters binding of antibodies elicited by egg-adapted vaccine strains. *Proc Natl Acad Sci USA*, 114(47), 12578–12583. <https://doi.org/10.1073/pnas.1712377114>

APPENDIX A

DESIGN CONSIDERATIONS FOR PRE-IMMUNE INFLUENZA FERRET STUDIES^I

A.1 Vaccination as a Surrogate for Viral Infection Pre-Immunity

A pre-immune animal model should be established through an initial viral infection instead of through a vaccination regimen. Vaccination cannot be a surrogate for viral imprinting and pre-immunity due to the inequivalence in the immune responses to an active influenza infection versus an intramuscular unadjuvanted vaccination (Ellebedy et al., 2011). Administering a vaccine matched to the challenge virus does not produce a vaccine with 100% efficacy. Healthy volunteers vaccinated with inactivated or cold-adapted live influenza vaccines were not all protected from challenges with homologous viruses; the estimated protective efficacies were 71% and 85%, respectively (Treanor et al., 1999). Vaccination does not induce a robust T-cell response compared to infection, which, in ferrets, has been found to contribute to sterilizing immunity (Dutta et al., 2016). Furthermore, in ferrets, vaccination and viral pre-immunity differ in their

^ISkarupka, A. L., & Ross, T. M. (2020). Immune Imprinting in the Influenza Ferret Model. *Vaccines (Basel)*, 8(2). doi:10.3390/vaccines8020173. Reprinted here with permission of the publisher.

protective outcomes as well (Dutta et al., 2016). Significant immunological differences, such as ratios of IgG and IgA influenza-specific antibodies and targeted antigenic sites (Houser et al., 2013), cannot be discerned and identified with the commonly used hemagglutinin inhibition assay (HAI).

A pre-immune-vaccination ferret model was used to investigate the phenomenon of low efficacy from repeat vaccination with commercial quadrivalent inactivated influenza vaccine that occurs in humans (Music et al., 2019). When matched to ferrets vaccinated once, repeatedly vaccinated ferrets had less protection, higher viral shedding, and lower T-lymphocyte counts, whereas the serological responses, cell-mediated immunity, and histopathological changes did not differ. It was hypothesized that although the magnitude of the serological response was similar, the composition differed, resulting in the difference of protection. A larger ratio of non-neutralizing to neutralizing antibodies may have been recalled in the repeat vaccination group. Hence, the repeat vaccination group had lower vaccine efficacy compared to one vaccination. Encouragingly, the repeat vaccination group was still better protected than the no-vaccine group. The relevance of using these results to explain the decreased vaccine efficacy in humans is limited due to the lack of pre-immunity establishment in ferrets. Even with well-planned studies, not establishing pre-immunity creates a confounding factor when extrapolating the findings to the human population.

A.2 Low Vaccine Seroconversion Proportions in Naïve Ferrets

In early ferret vaccination studies, the administration of unadjuvanted vaccines elicited no measurable antibody outcome. Not all naïve ferrets seroconvert to influenza vaccination (Bodewes et al., 2011; McLaren & Potter, 1974; Middleton et al., 2009; Potter, McLaren, et al., 1973). Even with the addition of an adjuvant, the immune response can be weak, especially when compared to the immune response elicited by a live homologous infection (Potter, McLaren, et al., 1973; Potter, Oxford, et al., 1972). The lack of an antibody response is associated with a lack of protection (S. S. Wong et al., 2017). For instance, naïve ferrets immunized with A/Hong Kong/X31/1968 H₃N₂ vaccine were all susceptible to homologous challenge, and none produced vaccine-specific serum HAI antibodies (McLaren & Potter, 1974). This low reactivity to the vaccine may be attributed to the outbred nature of the animal model (Music et al., 2019).

Low seroconversion ratios may also be due to the low immunogenicity of the influenza vaccine. In humans, vaccines vary in immunogenicity (Bart et al., 2014; Clark et al., 2009; Fries et al., 2013), particularly in immunocompromised adults and children (Liang et al., 2010). Due to this issue, pandemic influenza vaccines can be adjuvanted to ensure an efficient immune response (Belshe et al., 2011; Hilgers et al., 2017; Treanor et al., 2006; Treanor et al., 2001). With the inclusion of different adjuvants, different magnitudes of seroconversion and protection can be achieved (S. S. Wong et al., 2017). Some studies used virus-like particle (VLP) vaccines produced from insect cells using a baculoviral system which results in 100% seroconversion in ferrets (Bright et al., 2007; G. E. Smith et al., 2017). The manufacturing process of these VLPs retains insect protein that acts as an adjuvant contributing to seroconversion. Research groups have attempted to solve this phenomenon through multiple vaccinations, i.e., a prime-boost or prime-boost-boost regimen or with the addition of an adjuvant to elicit an antibody response (Jeong et al., 2019).

The establishment of pre-immunity overcomes this phenomenon; pre-immune ferrets respond to vaccination at a higher proportion than immunologically naïve ferrets. With either type, A homosubtypic (Carter et al., 2017) or heterosubtypic (McLaren & Potter, 1974) pre-immunity, the vaccine-specific serum hemagglutinin inhibition titers are increased. Imprinting primed the immune system towards future influenza vaccinations. This priming phenomenon is not only present in the ferret animal model but also occurs in mice and hamsters (Jennings & Potter, 1973; McLaren et al., 1977; Potter, Jennings, et al., 1973).

A.3 Historic Pre-Immune Ferret Models

One of the earliest works with pre-immunity in ferrets was conducted by Webster in 1966, investigating the presence of original antigenic sin in ferrets by conducting sequential infections (Webster, 1966). Following this, in the 1970s, a vast amount of pre-immunity work was conducted with ferrets. These studies focused on characterizing the ferret immune system response to live and killed virus, vaccination, adjuvant and heterotypic and heterologous infections (McLaren & Potter, 1973, 1974; McLaren et al., 1974a, 1974b; Potter, McLaren, et al., 1973; Potter, Oxford, et al., 1972; Potter, Shore, et al., 1972). Further, heterosubtypic immunity was shown not to wane over a period of up to eighteen months (Yetter, Barber, et al.,

1980). This historical collection of ferret research laid the foundation for showing that low vaccination seroconversion proportions for naïve ferrets can be overcome by the development and optimization of a pre-immune animal model. The pre-immune model never advanced after this time, potentially due to the lack of immunological reagents and tools needed to properly characterize the model and general ignorance of the magnitude imprinting and pre-immunity contributes towards vaccination and infection.

A.4 Current Pre-Immune Ferret Models in Practice

A.4.1 H1N1 2009 Pandemic

After a lull in the pre-immune ferret research, the H1N1 2009 swine influenza pandemic initiated the dramatic increase of the investigative effort into imprinting, pre-immunity, and heterologous protection. The early epidemiological and serological studies that inspired this interest suggested that pre-existing immunity may have altered the pandemic virus' morbidity and mortality in the human population (Hancock et al., 2009; Y. Itoh et al., 2009). The resultant pre-immunity models were based upon the historical model: (1) establish anti-influenza virus immune memory with a sub-lethal viral challenge; (2) assess for seroconversion; (3) vaccinate, if necessary; (4) challenge with A/California/2009 H1N1. A prolonged period of rest between imprinting and vaccination or challenge allows the ferret to return to an assumed immunological baseline after the generation of an adaptive memory response and recovery from damage and local cellular activation in the lung tissue. Compared to the 1970s, the drastic increase in the understanding of the immune system, the effects induced from influenza challenge and vaccination, and the ability to measure and quantify these important details allowed for a well-defined model. The worldwide 2009 pandemic inspired much research looking at the protective effects of seasonal H1N1 imprinting on the H1N1 2009 pandemic strain. Therefore, much of the published research has focused on the H1N1 subtype (please refer to the original publication for Tables S1 and S2; Skarlupka and Ross, 2020).

Sterilizing immunity in ferrets, an immune state that blocks viral infection (Dutta et al., 2016), can be achieved through establishing pre-immunity (Laurie et al., 2010). Whereas, with an intramuscular

vaccination, subsequent infection was not inhibited, although virus shedding was reduced. The gathered data from this study were restricted to viral characteristics, such as virus shedding, transmission frequency and morbidity, and mortality due to the lack of ferret immunological reagents. From these data, an ideal state of protection against the re-infection of the influenza virus was defined along with a goal to generate a vaccine that will elicit similar protection. Although not sterilizing, it was found that seasonal H1N1 pre-immune animals exhibited immunity and mitigated infection against the pandemic H1N1 virus (Laurie et al., 2010).

Through multiple infections and vaccination schemes, vaccination with the trivalent influenza vaccine (TIV; containing only one Type B strain instead of two) was unable to lessen the resulting morbidity or contact transmission in ferrets following challenge with the pandemic H1N1 (Ellebedy et al., 2011). Conversely, imprinting with a seasonal H1N1 virus altered the morbidity, but not the transmission characteristics of the pandemic H1N1 (Ellebedy et al., 2011). Although these viral traits were muted, there was only minimal detection of cross-reactive serum antibodies.

The 2009 pandemic was characterized by distinct protective responses seen between different age groups of people. Older adults were more protected than young adults and children against the H1N1 pandemic virus, A/California/07/2009 . This older population was captured in the pre-immune ferret model by imprinting with historical antigenically distinct viruses (O'Donnell et al., 2012). The protective responses to a pandemic challenge were then measured. The historical viruses from the 1950s and earlier elicited more protective responses than the naïve ferrets (O'Donnell et al., 2012). This corroborated the human data that the older population was more protected than, the younger to pandemic challenges. Next, the effects of imprinting on the response to a pandemic vaccine were determined. Ferrets imprinted with seasonal H1N1 received a pandemic H1N1 vaccine. This seasonal H1N1 priming did not diminish the antibody response to either infection or vaccination with the pandemic virus (O'Donnell et al., 2012). Furthermore, original antigenic sin was not observed in the context of seasonal H1N1 to pandemic H1N1. Additionally, the priming of the seasonal H1N1 virus provided cross-protection against the pandemic virus. However, it did not impact the transmission efficiency (Pearce et al., 2011).

A human's pre-immune history can be recapitulated in ferrets by conducting repeated infections. Carter et al. (2013) utilized this technique by sequentially infecting two different ferret groups with seasonal H1N1: one with historical H1N1 from 1934 to 1957 and another with contemporary H1N1 viruses from 1999 to 2007. The abilities of the differing pre-immunities to protect against an A/California/07/2009 H1N1 challenge were compared. Both sequential groups were protected from the challenge; they exhibited no weight loss, minimal recoverable virus, and no transmission compared to ferrets pre-immunized with only one of the viruses. Unique to sequentially infected ferrets, the elicited antibody profile was broader and interacted with pandemic H1N1 HA compared to the single pre-immunity groups as measured with HA-specific ELISA binding. The recall and adaptation of the antibody profile over time in response to sequential exposures are complex and still not completely understood. However, these interactions help to explain the puzzling epidemiological and serological observations surrounding the pandemic H1N1 outbreak. Carter et al. (2013) hypothesized that the older adults were exposed to more antigenically variant strains and had extensive protection compared to young adults with less exposure.

In addition, the changes in the elicited antibody profile point to the possibility of achieving broad vaccine-induced protection against influenza viruses by sequential immunization with a series of antigenic variants. Further analysis with these ferret samples and the infection/immunization scheme confirmed the change in antibody profile observed previously. Anti-HA stalk antibodies increased, even in the absence of receptor-binding site antibodies, leading to the observed cross-reactivity and reduction in clinical signs and transmission (Kirchenbaum et al., 2016). In contrast to previous reports that pre-immunity-induced protection does not wane (Yetter, Barber, et al., 1980), the boosts in anti-HA stalk antibodies and the cross-reactivity induced from sequential infection with antigenically distinct seasonal H1N1 declined over time (Kirchenbaum et al., 2016).

The pandemic outbreak occurred from a transmission event of an avian-human-swine reassortant virus from a swine host into the human population (G. J. Smith et al., 2009). Whereas many groups investigated the effects of human seasonal H1N1 imprinting, the effects of imprinting with a classical swine virus were also determined. Min et al. (2010) exhibited that infection with classical swine viruses

elicited cross-reactive neutralizing antibody activity and provided protection against the pandemic H1N1 virus.

Over time, a natural breakpoint occurred between the investigation into the pandemic mystery and the examination of the immune system response within the context of imprinting and pre-immunity. Within a seasonal and pandemic H1N1 sequential infection study, the changes in polyclonal serum antibodies responses were measured. Ferrets pre-immunized with the seasonal A/Texas/36/1991 H1N1 were followed up with an A/California/07/2009 H1N1 infection. The elicited serum antibody specificity shifted to target a different region of the HA compared to the H1N1/Texas/36/1991 only serum (Y. Li et al., 2013). The overall antibody response moved to epitopes near the HA receptor-binding domain, sites where homology between these two strains is shared (Y. Li et al., 2013). These findings resulted in research in the basic science of how imprinting and pre-immunity affect vaccination and infection and subsequent immune responses.

A.4.2 Contemporary H1N1/H3N2 Models

The current pre-immunity models are moving away from investigating the differences in disease symptoms and vaccine effectiveness observed in the human population in response to the pandemic virus. Resources are now focused on how pre-immunity affects vaccination responses and general vaccine efficacies to any virus, not just in terms of the pandemic H1N1 (please refer to the original publication for Tables S2 and S3; Skarlupka and Ross, 2020). Furthermore, the pre-immune model is now being used, in replacement of a naïve model, to test novel vaccine candidates and methods currently in research and development (Allen et al., 2019). Sequential infections of antigenically distinct viruses lead to a broader antibody response than that of just one strain (Carter et al., 2017; Nachbagauer et al., 2017). This illustrated the importance of using a pre-immune model for antigenic characterization and vaccine testing. In fact, when H3N2 antigenic maps were produced using sera from naïve or pre-immune ferrets, the maps were poorly correlated; the classification of whether two viruses were antigenically distinct or similar varied with the model (naïve or pre-immune) (Kosikova et al., 2018). The broader antibody response characterized with H1N1 or H3N2

sequential infections was extremely informative at the hetero-subtype level (Nachbagauer et al., 2017). However, the impacts of other subtypes, such as H₅N₁ and H₇N₉, were not investigated, and neither were the nuances of how protective different antigenically drifted strains within a subtype investigated.

The antibody profiles of sequentially infected ferrets with H₃N₂ viruses revealed that H₃N₂ pre-immunity affected both the quantity and quality of antibodies elicited (Kosikova et al., 2018). With high HAI titers against the imprinting virus, lower titers were observed toward the most recent isolate, H₃N₂/Hong Kong/4801/2014. After repeated H₃N₂ infections, the antibody avidities gradually increased for H₃N₂ compared to those from a single homologous infection. This repeated H₃N₂ exposure expanded the cross-reactivity breadth against the same HAI panel. With computationally optimized HA vaccines, the same increased breadth phenomenon, back-boosting, occurred. Pre-immunity to a historical H₃N₂ virus helped boost the magnitude and breadth of the broadly neutralizing antibodies elicited by computationally optimized broadly reactive antigen (COBRA) immunogens compared to a naïve ferret group (Allen et al., 2019). Emphasis was placed on the concept that testing vaccine candidates in naïve ferrets do not reflect the performance of the vaccines in the human population. In an H₁N₁ primed model, greater protection after vaccination was observed (Francis, McNeil, et al., 2019).

Vaccine effectiveness varies in the human population from season to season. Epidemiological data from people suggests that pre-existing immunity can result in decreased vaccine effectiveness (McLean et al., 2014; Ohmit et al., 2014; Skowronski et al., 2017). The pre-immune model has been used to study how vaccines can overcome pre-existing immunity to mount a new response with M₂-deficient single replicon vaccine candidates for H₁N₁ and H₃N₂ subtypes (Hatta et al., 2018). Type B and H₁N₁ heterosubtypic pre-immunity followed by H₃N₂ vaccination provided protection against an antigenically distinct H₃N₂ challenge. H₁N₁ pandemic homosubtypic imprinting negatively affected the ability of a FluMist-like vaccine to elicit protection towards seasonal H₁N₁ (Hatta et al., 2018). These key findings highlight the difficulty with inducing immunity to a novel HA in the presence of pre-existing heterotypic, heterosubtypic, and homosubtypic immunity.

Although the questions surrounding the 2009 outbreak have been sufficiently answered, there still remains the possibility for a second swine-origin pandemic. Even of the same subtype and species origin, pandemic H1N1 pre-existing immunity was unable to induce sterilizing immunity to current circulating swine-origin H1N1 viruses (Pulit-Penaloza et al., 2018). Furthermore, other subtypes – H3N2 and H1N2 - circulate in the swine and transmit into the human population (T. K. Anderson et al., 2015). The swine-origin H3N2 subtype raises concerns due to human's documented susceptibility to H3N2 viruses and transmission in ferrets being as efficient as human-origin seasonal H3N2 viruses (Pearce et al., 2012). Differing pre-immunity may be protective against these swine-origin viruses; pre-immunity with the human H3N2/Perth/16/2009 cross-protected against a swine-origin variant H3N2, whereas other human strains did not (Houser et al., 2013). Hence, prior seasonal virus infections may be protective by limiting viral replication and reducing transmission. This may suggest that within the human population, different age groups are more susceptible to certain transmission events depending on the subtypes of influenza virus that they have previously been exposed to (F. Liu et al., 2017).

The ferret immune response to re-infection is strikingly different compared to the response after primary infection (Leon et al., 2013). When comparing the H1N1/Mexico/4108/2009 challenge in naïve and H1N1/Mexico/4108/2009 pre-immune ferrets, the pre-immunity status limited viral titers. The virus was still detectable at low levels at day seven post-infection. Assessment of the ferret transcriptome during this challenge provided invaluable data for unraveling the immune response to infection. In a primary challenge, the innate immune system and inflammatory genes were upregulated in both the lung and lymph node tissues. Comparatively, in the pre-immune ferret, the adaptive immune response genes (CXCL10, CCL5) were upregulated in the lungs, with no upregulation in the lymph nodes. The lack of lymph node gene activity suggested influenza-specific CD8+ T-cells and B-cells may have originally resided within the lungs before infection, or the adaptive immune response originated from another unidentified peripheral compartment (Leon et al., 2013).

Influenza virus infection also imprints on the influenza-specific T-cell memory compartment. In an H1N1/H1N1 homologous and an H1N1/H3N2 heterologous challenge, H1N1 imprinting partially pro-

tected against the H₃N₂ challenge, reducing virus shedding duration, but not the peak virus titer. The inflammatory immune response was increased, but less than that of the immunologically naïve infected ferrets (Gooch et al., 2019). Differences between interferon-gamma (IFN- γ) producing peripheral blood mononuclear cells (PBMCs) in naïve vs. H₁N₁ pre-immunized ferrets with a homologous H₁N₁ challenge were not discernable. However, the pre-immune ferrets had IFN- γ producing PBMCs that were stimulated by heterosubtypic viruses. The imprinting event did not lessen the quantity of IFN- γ producing PBMCs compared to mock/H₃N₂ infected ferrets. However, heterosubtypic pre-immunity affected the reactivity of the IFN- γ producing lung mononuclear cells (MNCs) and induced whole-blood IFN- γ producing cells quicker. H₁N₁/H₃N₂ pre-immune ferrets had high reactivity of IFN- γ producing lung MNCs to H₁N₁ virus compared to H₁N₁/H₁N₁ ferrets that had no increase. Although the classification of these T-cells as CD8+ or CD4+ was not conducted as of yet, pre-immune ferrets can be used to model T-cell population contributions to influenza-specific memory and recognition.

Future studies will investigate the different cellular and humoral responses to influenza virus infection and clarify the differences between T-cell subsets. The study conducted by Hay et al. (Hay et al., 2019) analyzed data derived from a previous study (Laurie et al., 2010) to mathematically model the short-term antibody kinetics from either influenza infection or vaccination with and without adjuvant. Their results, although limited in sample size, highlight the potential future applications and data analysis of the serological, cellular, and virological data that can be collected during a pre-immune study.

A.4.3 H₅N₁ Models

The effects of H₁N₁ and H₃N₂ pre-immunity on the H₅N₁ subtype or the effect of H₅N₁ on H₁N₁ or H₃N₂ vaccination or subsequent viral challenge are not well known. Although studies have been performed in pre-immune mice (Kreijtz et al., 2009; O'Neill et al., 2000), few studies have addressed pre-immunity using the viruses of the H₅N₁ subtype (Cheng et al., 2009) (please refer to the original publication for Table S4; Skarupka and Ross, 2020). Pandemic vaccines for H₅N₁ influenza viruses elicited low seroconversion proportions in immunologically naïve ferrets. When primed with seasonal

live attenuated influenza vaccine (LAIV), H₅N₁ HA-specific IgG antibody-secreting cells (ASC) were stimulated compared to unprimed ferrets. Expansion of the H₁N₁ or H₃N₂ specific memory B-cells may cross-react with the H₅N₁ HA antigen. When imprinted with the individual vaccine strains, the IgG ASC levels were similar to the LAIV imprinted cells, with the H₁N₁ imprinting influenza virus eliciting higher responses than H₃N₂ imprinting viruses. This effect may be a response to the HA molecule rather than the H₁N₁ NA protein because an H₁N₂ reassortant virus elicited a similar response. But a synergistic or additive effect was not determined with an H₅N₁ reassortant virus to confirm the lack of protective contribution from the NA. However, upon closer inspection, the protection afforded by the H₁N₁ HA was temporary and waned to levels similar to naïve ferrets three weeks after the second dose was administered.

A.4.4 Priming and pre-immune strain selection

The main hypothesis and question being addressed will determine strains selected for use in a pre-immune model. The priming method, whether by vaccination or infection should be evaluated based on the target population of the vaccine/study. An infant or child target demographic may warrant that priming actually occur through vaccination followed by viral challenge. This instance recapitulates if the vaccine was administered before exposure to influenza. In contrast, to target populations whose first exposure is through infection, live influenza virus would be the appropriate priming method.

The initial imprinting strain should be antigenically representative for the population being modeled. Therefore, the timing and order of the infections are variable. After imprinting, ferrets may be re-infected to add to the pre-immune history or be vaccinated or challenged according to study design. However, the magnitude of the contributions of a full pre-immunity history compared to just the initial imprinting virus on the immune response has not been adequately quantified. For instance, if attempting to recapitulate a person born in 1970, it is unclear if it is only necessary to pre-immunize with an H₃N₂ 1970s virus, followed by H₁N₁ influenza virus, or if all of the antigenically distinct H₃N₂ viruses are needed to establish a true pre-immune state. Studies investigating the effects of heterosubtypic and heterotypic imprinting and pre-

immunity can be expanded to include: 1.) Type B imprinting followed by an H₁N₁ or H₃N₂ vaccination or challenge, 2.) H₂N₂ imprinting, 3.) H₁N₁ imprinting and H₃N₂ pre-immunity and vice versa on which combination results in more protection against H₁N₁, H₃N₂, H₂N₂, or H₅N₁ challenge. Limited research is available on the serological, cellular, and immunological effects of infections with varying infection doses, but there have been observed differences (Marriott et al., 2014).

A.5 Immune system cool-down

The immunological system should return to the baseline immunological state before attempting another repeat infection or vaccination. This period should encompass the cool-down time for both the innate and adaptive immune systems, including the induction and contraction of B- and T-cells into their memory states. Studies similar to Leon et al. (Leon et al., 2013) are of great importance for understanding the inner workings of the ferret immune system during imprinting and re-infection. Without these studies, this cool-down component will need to continuously be stated as a study limitation. For example, Pilit-Penaloza et al. (Pilit-Penaloza et al., 2018) indicated that a thirty-one day interval between primary and secondary challenges for their studies may have been too short, allowing for elevated non-specific innate responses from the primary infection to affect the secondary. Without letting the immune system return to baseline, misrepresentation of cross-protection may be observed. Cheng et al. (Cheng et al., 2009) found that the heterologous protective titers waned to levels not significantly different than the negative naïve control ferret group providing only temporary protection.

A.6 Age/Sex/Vendor specific responses

The age and sex of the animals being used may be a confounding factor especially when comparing humoral responses (Fischinger et al., 2019; van den Brand et al., 2014). The ages for male and female ferrets ranged from two to twelve months. Ferrets were considered aged when they were greater than four years of age (Paquette et al., 2014). Reporting results by sex may reveal new avenues for influenza virus research. The

breeding vendor and housing conditions of the animals should also be reported. Within the mouse model, the microbiome differs by vendor in the gut (Hufeldt et al., 2010; Rasmussen et al., 2019) and in the lungs (Dickson et al., 2018), contributing to different responses to vaccination and influenza infection (C. J. Chen et al., 2017; Hagan et al., 2019; Oh et al., 2014). Therefore, it is recommended that when mice or ferrets are housed in separate holding rooms, bedding or enrichment equipment is shared between the cages to merge the microbiomes together (Oh et al., 2014). Inclusion of the ferret health history is also beneficial. Metadata such as whether they were castrated, spayed, de-scented, or received any previous vaccinations or treatments may shed light on immunological results.

The ferret model captures special at-risk populations. Ferret age was varied to encompass different age groups: young, adult and old. Adult and aged ferrets, similar to humans, exhibit significant immune response differences when comparing homologous and heterologous H1N1 priming and challenges suggesting immune senescence in the aged ferret population (Paquette et al., 2014). Therefore, the use of this model would contribute to vaccine testing and efficacy studies. Currently, a vaccine specifically formulated for aged individuals already exists due to their high-risk status and substantial contributions to influenza-associated hospitalizations and deaths (McElhaney, 2011; Mitchell et al., 2013; Wilkinson et al., 2017); this high dose vaccine contains 60 ug of each vaccine strain HA, compared to the standard 15 ug. The National Institute of Allergy and Infectious Diseases' (NIAID) goal for the development of a universal influenza vaccine requires a protection equal to or greater than 75% against symptomatic disease lasting at least one year in all populations, including, at-risk populations (Paules et al., 2017). The addition of pre-existing immune responses to these various at-risk population models more accurately reflects the variation of the human population and allows for appropriate testing of novel vaccine candidates.

A.7 Validation and Further Work of the Pre-Immune Model

The pre-immune ferret model is within its early stages of development; to become a mainstay within the scientific community and used reliably in the context of influenza virus research, the baseline effects of infection, re-infection, and vaccination within the ferret need to be addressed first. This involves

determining the cool-down time of the ferret immune system following infection and the differences compared to a vaccination. Furthermore, studies of the different immunological ferret responses such as cytokine quantity and diversity, B- and T-cell repertoire, and B- and T-cell recall responses are important to characterize. In addition, advancements in high-throughput, single cell sequencing technology allow depiction of the B-cell evolution from a single ancestral B-cell (Upadhyay et al., 2018).

The ferret model is used to study influenza virus infection because of the ferret's natural susceptibility, shared clinical signs of illness, and possession of similarities in respiratory physiology, cell composition, and distribution of sialic acid receptors. Although present, these components may not interact in the same manner as human immune system following influenza virus infection (Nachbagauer et al., 2017). Comparisons of different pre-immune influenza animal models (mice, guinea pigs, and ferrets) to human serology data emphasized that the use of different animal models should be heavily considered for pre-clinical vaccine studies due to the biases between them. Basic research of the ferret physiology can be compared and validated against data from human studies. Cross-validation will either bolster the ferret findings or they will provide researchers the ability to determine which immunological findings are relevant for further investigation and which are solely ferret-specific phenomena. This process focuses on the ferret model being a surrogate for the human. The decision-making process of vaccine selection and therapeutics relies on the ferret, and it is important that human-ferret shared traits are appropriately distinguished. Therefore, further study, comparison, and validation are needed to fully grasp the predispositions and limitations of the model.

A.8 Conclusions

Although initially developed in the 1970s, recently, the pre-immune ferret model has rapidly progressed into a vital tool for the development of a broadly neutralizing influenza vaccine. In conclusion, care needs to be taken to begin planning studies to incorporate the effects of imprinting and pre-immunity within the animal model to apply the results to the human system. Animal models used for influenza research are available and widely used. However, as more findings and reagents become available, the models need

to be updated appropriately. In addition, more research on the immunological effects of imprinting in ferrets, which is then compared to the research on the effects of imprinting on humans, will contribute to the validation of using the ferret as an appropriate animal model to study influenza virus in humans. Altogether, the major goal of developing a broadly neutralizing influenza vaccine by priming the immune system adequately to produce the same sterilizing immunity as infection, but without the deleterious effects, could be tested in these models.

APPENDIX B

INHERENT SERUM INHIBITION OF INFLUENZA VIRUS NEURAMINIDASE¹

¹Skarupka, A. L. & Ross, T. M. Inherent Serum Inhibition of Influenza Virus Neuraminidases. *Front. Vet. Sci.* 2021. 8:677693. doi: 10.3389/fvets.2021.677693. Reprinted here with permission of the publisher.

B.1 Abstract

Influenza virus vaccines have been designed for human and veterinary medicine. The development for broadly protective influenza virus vaccines has propelled the vaccine field to investigate and include neuraminidase (NA) components into new vaccine formulations. The antibody-mediated protection induced by NA vaccines is quantified by inhibition of sialic acid cleavage. Non-immune inhibitors against influenza viruses naturally occur in varying proportions in sera from different species. In this brief report, the inherent ability of raw animal sera to inhibit a panel of influenza virus NA was determined. Raw sera from the same species inhibited more than 50% of influenza viruses tested from 4 different subtypes, but the breadth of inhibiting NA activity depended on the source of sera. Furthermore, different influenza viruses were inhibited by different sources of sera. Overall, additional studies are needed to ensure that scientific methods are consistent across studies in order to compare NA inhibition results. Through future investigation into the differences between sera from different animal species and how they influence NA inhibition assays, there can be effective development of a broadly-protective influenza virus vaccines for veterinary and human use.

B.2 Introduction

Influenza viruses are global zoonotic and human pathogens and vaccination remains the main preventative measure against infection. The influenza virus is a member of the Orthomyxoviridae family. The genome is composed of eight negative single sense RNA segments that determines the viral genus, alpha-, beta-, delta-, and gammainfluenzavirus that correspond to the species influenza A, B, D, and C viruses, respectively. Of the four influenza types, Types A and D are commonly isolated from animals. Whereas, influenza Types B and C is most commonly associated with human infection especially in children (Sederdahl & Williams, 2020). The Type A influenza viruses are further classified into subtypes determine by the two major surface proteins, hemagglutinin (HA) and neuraminidase (NA). Currently there are eighteen HA subtypes and eleven NA subtypes that can be paired to create different influenza subtypes.

Influenza viruses are of international importance due to the widespread infection in different livestock leading to vaccination being utilized across the veterinary field (Tomley & Shirley, 2009). Equine influenza viruses are important horse pathogens with policies in place that require horses be vaccinated for equine influenza viruses before participation in events or importation (Allkofer et al., 2021; Paillet et al., 2006). Furthermore, due to the transmission of influenza viruses from horses to dogs, as well as the endemic infection of influenza viruses in the canine population, canine vaccination is also recommended by the American Veterinary Medical Association for dogs with high risk of exposure (“Canine influenza”, 2021; H. H. Kim et al., 2018; Na et al., 2016). The swine industry uses primarily whole inactivated vaccines (WIVs – reviewed in reference (Mancera Gracia et al., 2020)) that are developed using split-inactivated technologies (Everett et al., 2021; Mancera Gracia et al., 2020). The poultry industry utilizes the greatest variety of vaccine platforms, including: split-inactivated virus, HA protein antigens, HA DNA vaccines, and recombinant technologies with other backbone viruses (Spackman et al., 2020; T. Wang et al., 2020).

However, during infection both HA and NA proteins are targets for neutralizing antibodies (Y. Q. Chen et al., 2018). The NA glycoprotein mediates viral egress and virion de-aggregation by cleaving sialic acids as well as contributing to motility through cleaving mucins in the upper respiratory tract (Cohen

et al., 2013; Murti & Webster, 1986). Polyclonal NA-specific sera and NA inhibition (NAI) titers reduce, modulate, and protect against disease (Gilbert et al., 2019; Kilbourne, 1976). Further research has identified monoclonal NA-specific antibodies that neutralize viral growth (F. F. Xiong et al., 2020). Although NA antibodies hinder viral replication, the induction of NAI antibody titers following vaccination is not as great as the induction of HAI titers, potentially due to either the split-inactivated vaccines lacking a standardized concentration of NA protein or the NA protein being destroyed during the split-inactivation process (Gilbert et al., 2019). Recently, research and vaccine development have focused on live-attenuated viruses that elicit NA antibodies, or protein vaccines that include the NA (Krammer et al., 2018).

Currently, the enzyme linked lectin assay (ELLA), MUNANA substrate, thiobarbituric acid (TBA) fluorescent-based assay, and NA-Star chemiluminescent assay are methods for measuring antibodies against the NA molecule (Buxton et al., 2000; Couzens et al., 2014; Potier et al., 1979; Sandbulte & Eichelberger, 2014; Westgeest et al., 2015; Wetherall et al., 2003). As the NA glycoprotein undergoes antigenic drift, the protein's ability to cleave sialic acid can be measured and the quantified using these assays. All techniques assess the elicited antibody-specific inhibition of the NA after vaccination or infection. The ELLA measures the ability of the viral NA to cleave sialic acids from a large substrate (fetuin) similar to infection when sialic acids are expressed on the surface of the host cell, whereas the MUNANA and NA-Star techniques measure cleavage of small soluble chemical substrates (Shie & Fang, 2019). However, only the ELLA was proposed as the assay for measuring serum NA inhibiting antibodies as a correlate for protection for humans (Krammer et al., 2020).

Components in raw sera have non-specific inhibitory activity against NA activity (Westgeest et al., 2015). These initial findings were conducted with ferret sera that varied using different viruses from different influenza subtypes. However, treating sera with receptor-destroying enzyme (RDE) overnight and then heat-inactivating the sera for 8 h at 55°C mitigated the non-specific inhibition without loss of NA or HA specific inhibitory activity (Westgeest et al., 2015). The animal models used for influenza virus research are growing and now include more species. Not only is there a need to compare serological results between animal models that are used for human influenza viruses, but also endemic influenza virus infection in

agricultural animal species requires a consistent method to quantify the NA inhibiting antibodies as well. Therefore, it may be necessary to handle sera from different species differently when quantifying the NA inhibition responses, which may be key to determining overall vaccine effectiveness.

Therefore, animal sera from different species were characterized for their inherent inhibition of the enzyme linked lectin assay with a panel of influenza viruses. Sera were compared for their ability to non-specifically inhibit the NA proteins of many influenza viruses representing different viral subtypes. Sera was collected and tested from varying animal sera sources against H₁ and H₃ human- and swine-isolated influenza strains as well as avian-isolated viruses with N₂ and N₃ proteins. Overall, there are many different variables that contribute to the interpretation of the ELLA assay, and understanding the innate characteristics of host-origin of the sera is critical to conducting the assay and interpreting the results. Therefore, it is important to standardized methodologies that will allow for consistent and reproducible results to assess anti-NA antibodies.

B.3 Materials and Methods

B.3.1 Viruses

All swine viruses were passaged once in Madin-Darby canine kidney (MDCK) cell culture at 37°C, which was the same growth conditions as they were received in (Organization & Network, 2011). Harvested virus was centrifuged at 2500 rpm for 10 min to remove cell debris. Human and avian influenza viruses were propagated in 11-day old embryonated chicken eggs. Virus lots were aliquoted for single-use applications and stored at -80°C. Viral titer of the frozen aliquots was determined with a plaque assay using MDCK cell culture in plaque forming units per ml (PFU) (Table B.1). The panel of viruses covered a range of N₁ to N₃ influenza NA subtypes, including: A/Brisbane/59/2007 (H₁N₁) (Bris/07), A/California/07/2009xPR8 (6:2 viral reassortant with 6 internal genes from A/Puerto Rico/8/1934, and NA and HA external protein genes from virus indicated) (H₁N₁) (CA/09), A/swine/Nebraska/A10444614/2013 (H₁N₁) (Sw/NE/13), A/Vietnam/1203/2004xPR8 (H₅N₁) (Viet/04; HA gene contains mutation in multibasic cleavage site

for BSL-2 level research), A/swine/Missouri/A10444664/2013 (H1N2) (Sw/MO/13), A/swine/North Carolina/152702/2015 (H1N2) (Sw/NC/15), A/white fronted goose/Netherlands/22/1999 (H2N2) (Wfg/Neth/99), A/quail/Rhode Island/16-018622-1/2016 (H2N2) (Qu/RI/16), A/Port Chalmers/1/1973 (H3N2) (PC/73), A/Hong Kong/4801/2014 (H3N2) (HK/14), A/swine/Missouri/2124514/2006 (H2N3) (Sw/MO/06), and A/mallard/Minnesota/A108-3437/2008 (H2N3) (Mal/MN/08).

B.3.2 Animal Serum

Animal serum was either commercially sourced or generated in house. Sera were confirmed to be negative for preexisting antibodies to currently circulating human influenza viruses by HAI. Ferret sera originated from 6-8 month female finch ferrets (*Mustela putorius furo*, spayed, female, 6-8 months, descented) purchased from Triple F Farms (Sayre, PA); porcine sera originated from piglets at Auburn University; and rhesus macaque (*Macaca mulatta*) sera originated from previous dengue virus studies performed in the lab (Uno & Ross, 2020). The rat (catalogue number: 10710C), goat (catalogue number: 01-6201), horse (catalogue number: 31874), and mouse (catalogue number: 01-6501; NIH Swiss mouse) normal serum were harvested from non-immune animals (Invitrogen, Carlsbad, CA, USA), and rehydrated according to manufacturer's specification; only one lot was tested for each commercial serum. Raw serum was not diluted any further before experimentation.

B.3.3 NA Activity and Inhibition Assay

High affinity Immunoblot 4HBX 96-well flat-bottom plates (ThermoFisher Scientific, Waltham, MA, USA) were coated overnight with 100 µl of 25 µg/ml fetuin (Sigma-Aldrich, St. Louis, MO, USA) in coating buffer (KPL coating solution concentrate; Seracare Life Sciences Inc, Milford, MA, USA) and stored away from light for a maximum of 2 months at 4°C until use. Viruses were diluted to an initial dilution of 1:10 with Dulbecco's phosphate-buffered saline (DPBS) with Tween-20 and 1% BSA (DPBS-T-B), a PBS which contains 0.133 g/L CaCl₂ and 0.1g/L MgCl₂ further supplemented with 1% BSA, and 0.5% Tween-20. Before virus addition, fetuin plates were washed three times in PBS-T (PBS + 0.05%

Tween-20). Virus was diluted in two-fold serial dilutions within a range that allowed for linear regression analysis. After which, 50 μ l of the viral dilutions were added to the fetauin-coated plate containing 50 μ l of DPBS-T-B in duplicate. A negative control column was included containing 100 μ l DPBS-T-B only. Plates were sealed and incubated for 16-18 h at 37°C and 5% CO₂. After incubation, plates were washed six times in PBS-T. After washing, a diluted lectin was added to the plates to bind exposed galactose. Specifically, 100 μ l of peanut agglutinin-HRPO (Sigma-Aldrich, St. Louis, MO, USA) diluted 1000-fold in DPBS-B (DPBS, 1% BSA). Plates were incubated at RT for 2 h. Plates were washed three times in PBS-T, and 100 μ l (500 μ g/ml) of o-phenylenediamine dihydrochloride (OPD; Sigma-Aldrich, St. Louis, MO, USA) in 0.05 M phosphate-citrate buffer with 0.03% sodium perborate pH 5.0 (Sigma-Aldrich, St. Louis, MO, USA) was added to the plates. Plates were immediately incubated in the dark for 10 mins at room temperature (20-22°C). The reaction was stopped with 100 μ l of 1 N sulfuric acid. The absorbance was read at 490nm. NA activity was determined after subtracting the mean background absorbance of the negative control wells. Linear regression analysis was used to determine the dilution of NA antigen necessary to achieve 90-95% NA activity and was used for subsequent NA inhibition ELLAs.

From each virus titration at least five serial dilutions within the linear range were used to calculate the linear regression after transforming the dilutions by \log_2 . The R-squared value above 0.9 was considered acceptable. The best-fit values for the slope (m) and y-intercept (b) were used to determine the 90-95% range (Equation B.1). The lowest titer dilution used for regression was defined as the 100% NA activity dilution (Equation B.2). Using the fitted linear regression equation, the optical density (OD_{100%}) value for 100% NA activity was calculated. Then the OD_{95%} and OD_{90%} were calculated by multiplying OD_{100%} by 0.95 and 0.9 respectively (Equation B.4). The range of viral dilution for 90-95% NA activity was then determined by using the OD_{95%} and OD_{90%} values in the linear regression equation to obtain lower and upper bounds for the virus dilution (Equation B.4). Virus dilutions were then chosen between that range as indicated (Table B.1).

Table B.1: Linear regression fit of the NA activity of the viruses tested in the panel.

Strain	PFU/ml	Fitted Equation (OD=)	R ²	100%	95%	90%	ELLA
Briso7	4.2 × 10 ⁸	-0.5796log ₂ T + 7.72	0.9867	160	197	243	200
CA/o9	1.0 × 10 ⁸	-0.5903log ₂ T + 8.804	0.9835	320	402	505	450
Sw/NE/13	1.15 × 10 ⁸	-0.5694log ₂ T + 7.556	0.9867	100	196	241	200
Viet/o4	1.75 × 10 ⁸	-0.4799log ₂ T + 5.66	0.9738	100	119	143	130
Sw/MO/13	1.31 × 10 ⁷	-0.5177log ₂ T + 5.932	0.9786	40	49	61	50
Sw/NC/15	8.45 × 10 ⁵	-0.4144log ₂ T + 3.913	0.9430	10	12	15	15
Wfg/Neth/99	1.0 × 10 ⁸	-0.6189log ₂ T + 10.86	0.9900	6,400	7,576	8,981	8,000
Qu/RI/16	8.0 × 10 ⁹	-0.6213log ₂ T + 10.82	0.9896	6,400	7,551	8,911	8,000
PC/73	9.0 × 10 ⁸	-0.6022log ₂ T + 8.33	0.9789	640	749	875	800
HK/14	3.0 × 10 ⁷	-0.4438log ₂ T + 3.773	0.9903	10	12	14	13
Sw/MO/o6	2.0 × 10 ⁸	-0.676log ₂ T + 9.549	0.9899	320	390	477	400
Mal/MN/o8	4.0 × 10 ⁶	-0.6394log ₂ T + 11.19	0.9862	3,200	3,911	4,792	4,000

The plaque-forming units (PFU/ml) and the fitted linear regression equation using a minimum of five two-fold serial dilution data points with the final R-squared value are provided. From the 100% NA activity titer (T), the 95% and 90% activity titers were calculated from the fitted equation. The viral dilution used for the ELLA assay were chosen between that range.

$$OD = m * \log_2(\text{Titer}) + b \quad (\text{B.1})$$

$$OD_{100\%} = m * \log_2(\text{Lowest Titer}) + b \quad (\text{B.2})$$

$$OD_{90\%} = 0.9 * OD_{100\%} \quad OD_{95\%} = 0.95 * OD_{100\%} \quad (\text{B.3})$$

$$Titer_{90\%} = 2^{\frac{OD_{90\%}-b}{m}} \quad Titer_{95\%} = 2^{\frac{OD_{95\%}-b}{m}} \quad (\text{B.4})$$

The NI ELLA titers were determined from two-fold serially diluting sera in DPBS-T-B from 1:10 to 1:1280. Duplicate dilutions were added to fetauin plates in 50μl. The NA antigen was diluted to 90-95% NA activity in DPBS-T-B and 50μl were added to the plate. Controls were each a minimum of 8 wells, and included a positive NA antigen control (50μl NA antigen + 50μl DPBS-T-B) and a negative control

(100 μ l of DPBS-T-B) on each plate. Plates were incubated for 16-18 h at 37°C and 5% CO₂ after which they were washed, processed, and absorbance was read as described above. Initially, the mean background absorbance from the negative control wells was subtracted from all wells. Then, NA percent activity was determined by dividing the serum absorbance by the mean virus positive control wells multiplied by 100 (Equation B.5)

$$\text{NA Activity \%} = \frac{\text{Individual well absorbance}}{\text{Mean absorbance of virus only control wells}} \cdot 100 \quad (\text{B.5})$$

Non-linear regression fits were performed using GraphPad Prism version 9.1.1 (223) for MacOS (GraphPad Software, San Diego, CA, USA; www.graphpad.com”), and the 50% NAI titer was estimated. Briefly, the “[Agonist] vs. normalized response – Variable slope” model was chosen which fits the model presented in Equation B.6, which estimates the Hill slope and the half effective concentration (EC_{50}). Outliers were not detected for or removed, and least squares regression with no weighting was used for the fitting. The model was constrained in that the EC_{50} was greater than 0. Asymmetrical profile-likelihood 95% confidence intervals of the EC_{50} were determined as well.

$$y = 100x^{\frac{\text{Hill slope}}{EC_{50}^{\text{Hill slope}} + x^{\text{Hill slope}}}} \quad (\text{B.6})$$

The lower limit of detection was 1:10, and the upper limit of detection was 1:1280 due to the range of sera dilution tested.

B.4 Results

B.4.1 NA titers of influenza viruses

The lowest dilution of virus needed to induce 100% NA activity varied between 1:10 and 1:6400 for different influenza viruses (Table B.1). Three HXN₂ viruses had 100% NA titers below 100, 1:40 for Sw/MO/1₃ (H₁N₂), and 1:10 for both Sw/NC/1₅ (H₁N₂) and HK/1₄ (H₃N₂). Of these, the virus titer for only

Sw/NC/15 was comparatively low at 8.45×10^5 PFU/ml. While the virus titers for Sw/MO/13 and HK/14 were 2.0×10^8 PFU/ml and 3.0×10^7 PFU/ml respectively. The avian lineage H₂N₂ and H₂N₃ viruses had the highest 100% NA titers of 1:3200 for Mal/MN/08 (H₂N₃), and 1:6400 for both Wfg/Neth/99 (H₂N₂) and Qu/RI/16 (H₂N₂). The virus titer was not greater for these viruses than the others, therefore indicating that the increase in activity is not due to solely an increase in replicating virus.

B.4.2 Animal-specific raw sera inhibition of the influenza NA

Sera collected from seven different sources were tested for the ability to inhibit the influenza virus NA activity as tested in the ELLA assay with fetuin substrate (Fig. B.1). Each serum sample was tested against twelve influenza viruses containing either NA type N₁, N₂ or N₃. There were four swine origin viruses and three avian origin viruses. The 50% NAI titers were estimable for only some virus and sera pairs (Table B.2). Ferret sera inhibited ELLA activity by 11 of the 12 viruses with a dilution titer greater than 1:10 and 9 viruses with a titer greater than 1:100 (Table B.3). The rat sera inhibited the least number of viral NAs, inhibiting ELLA activity by three of the H₂ viruses. Interestingly, not all animal sera inhibited all the same viruses (Table B.3). For example, the Bris/07 (H₁N₁) virus was inhibited by ferret and mouse sera at a dilution greater than 1:100, by pig, goat and horse sera at a dilution greater than 1:10, and was not inhibited by either rat or monkey sera. This variation was observed for other subtypes and host origin isolates. The Wfg/Neth/99 (H₂N₂) had a similar inhibition profile. The HK/14 (H₃N₂) virus was inhibited by the greatest number of sera. There was no distinguishable viral characteristic, such as host origin or HA or NA subtype, that was correlated with pattern of sera inhibition.

B.5 Discussion

Influenza vaccine formulations, including live-attenuated virus, whole-inactivated virus, and protein sub-unit vaccines, use NA as a vaccine component to elicit NA-specific antibodies (Sandbulte et al., 2016). However, components in raw sera have anti-NA properties that results in inhibition of NA activity. The

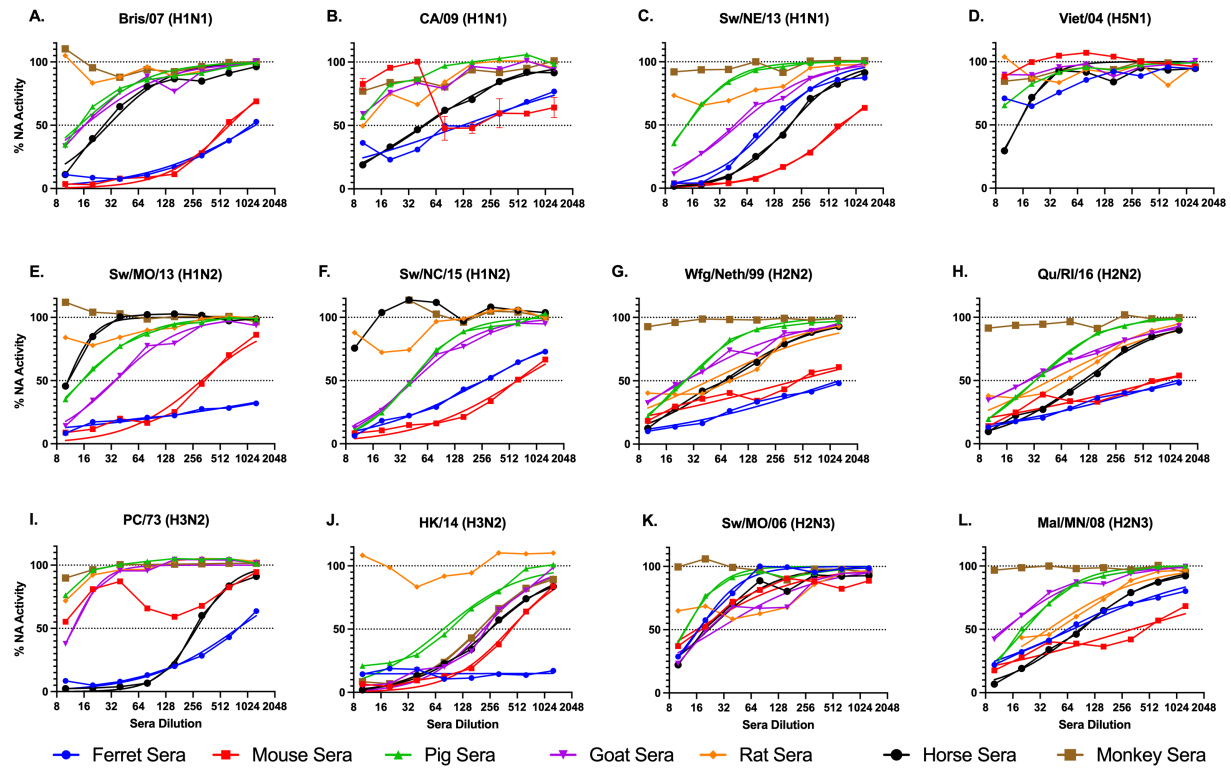


Figure B.1: A panel of influenza viruses were tested including N₁ (A-D), N₂ (E-J), and N₃ (K,L) NA subtypes. The sera were two-fold serially diluted from the reciprocal dilutions of 10-1,280. Non-linear regression was conducted, and the regression that resulted in estimable parameters (as indicated in Table B.2) are shown. The NA activity was normalized to 100% of a “virus only with no sera” control.

enzyme-linked lectin assay (ELLA) is used to measure antibody-mediated NA inhibition for cleaving a large substrate, and has been used to assess the effectiveness of NA-containing vaccines and anti-NA antibodies (Y. Desheva et al., 2020; Kaplan & Vincent, 2020; Paramsothy et al., 2021; F. Wang et al., 2020). In this study, seven raw animal sera were tested for inhibition of virus in the ELLA assay (Table B.2). All sera, regardless of species, inhibited at least one influenza virus (50% inhibition) with a dilution of greater than 1:10. Five of the seven samples inhibited 50% NAI activity at a titer of greater than 1:100. Sera contains innate host influenza inhibitors, such as complement protein of the α -, β -, and γ -class serum inhibitors. In horse and pig sera, the α -2-macroglobulin (γ -class) is one of the major innate influenza virus neutralizing factors (Pritchett & Paulson, 1989; Ryan-Poirier & Kawaoka, 1993). The γ -class inhibitors express sialic acids that bind specifically to the HA protein on influenza viruses and may inhibit the NA through steric interactions. These γ -class inhibitors are inactivated through receptor-destroying enzyme (RDE) treatment using *Vibrio cholerae* NA and are resistant to viral sialidase activity (Cwach et al., 2012; Pritchett & Paulson, 1989). There appear to be minor innate factors that results in the ability of horse and pig sera to inhibit different viruses in the panel.

Not all sera inhibited NA activity of all viruses. There were distinct inhibition profiles against specific influenza viruses in the panel. Innate inhibitors interact with influenza viruses through competitive binding of sialic acids to the HA protein receptor binding site (RBS) (α - and γ -class) and with mannose-binding lectins (β -class) (Anders et al., 1990; Krizanova & Rathova, 1969). Depending on the host origin of the virus, the HA RBS may have stronger affinity for α -2,3 or α -2,6 sialic acids. The glycosylation of HA proteins has been associated with mannose-binding lectins (Anders et al., 1990). Further research into the contributions of HA sialic acid binding specificity and the glycosylation of HA and NA surface proteins is needed to determine if it is significantly impacting the variation of NA inhibition observed here across the different viruses. The innate NA inhibition of different species sera is useful for determining the appropriate treatment before conducting for ELLA assays. To account for the innate inhibitors observed here sera may either be heat treated or RDE treated overnight at 37°C to cleave competing sialic acids from α - and γ -class inhibitors and heat inactivated at 56°C for a minimum of 30 minutes to inactivate

the heat-labile β -class inhibitors and up to 8 hours to fully inactivate the *V. cholerae* NA, when used with ferret sera (Westgeest et al., 2015). Immunoglobulins vary in their heat stability with IgG being more stable than IgA which is more stable than IgM (Mainer et al., 1997). With researchers using different inactivation methods, it may be inappropriate to compare titers between sera heat inactivated for 30 min to RDE treated sera that is heat inactivated for 8 h.

However, one of the major limitations of the study design was the inability to quantify within-species variability due to the limited sources of the sera. This variability can be further investigated to determine if age, sex or husbandry practices, such as farm or laboratory origin animals, have any effect on the results. Furthermore, the sera inactivation procedure for conducting the ELLA may be different between species. To determine the appropriate method, positive control antiserum is necessary to confirm that no loss in NA-specific antibodies is observed during treatment. Given the wide panel of viruses and different animal models tested here, those samples were not available. Lastly, the wide variability in the NA activity titers observed between viruses (Table B.1) may either be from increased enzymatic capacity, i.e., a virus' NA protein cleaves more sialic acid at a higher rate than another viral NA, or from having a higher NA content per PFU. Therefore, why different viruses had such variability in NA activity was undetermined.

In conclusion, with the increase in NA research, the RDE treatment, the inactivation time and temperature used to inactivate sialidases should be clearly described with the negative control data provided for each viral strain with serum species used for the assay in order to accurately interpret the results. This information will allow for comparison across species or if comparison of anti-NA serological results need to be assessed within the same species.

B.6 Acknowledgements

The authors would like to thank Harrison Bergeron, Naoko Uno, and Z. Beau Reneer for assistance in obtaining sera. Furthermore, we would like to thank the following individuals for providing influenza viruses: Dr. Mark Tompkins at UGA for A/swine/North Carolina/152702/2015 (H1N2), Dr. Ralph Tripp at UGA for A/swine/Nebraska/Ao1444614/2013 (H1N1) and A/swine/Missouri/Ao1444664/2013

(H₁N₂), Dr. David Stallkrecht at UGA for A/mallard/MN/2008 (H₂N₃), and Dr. Ron Fouchier at Erasmus MC for providing A/white fronted goose/Netherlands/22/1999 (H₂N₂). Lastly, remaining influenza A viruses were obtained through Virapur, BEI Resources, the International Reagent Resources (IRR) or from the Centers for Disease Control and Prevention, Atlanta, GA, USA.

B.7 Competing Interests

No competing interests.

B.8 Funding Information

This work has been funded by the National Institute of Allergy and Infectious Diseases, a component of the NIH, Department of Health and Human Services, under the Collaborative Influenza Vaccine Innovation Centers (CIVICs) contract 75N93019C00052 and in part, by the University of Georgia (UGA) (MRA-001). In addition, TMR is supported by the Georgia Research Alliance as an Eminent Scholar.

Table B.2: Non-linear regression fits of raw serum inhibition of Type A influenza viruses.

	Result	Ferret	Mouse	Pig	Goat	Rat	Horse	Monkey
Bris/o7	EC_{50}	1,251	647.7	14.32	16.33		29.90	
	95% EC_{50}	997.3, 1,685	588.3, 717.2	11.79, 16.77	10.84, 21.99		24.86, 36.02	
	Adj. R^2	0.9493	0.9837	0.9541	0.8703		0.9497	
CA/o9	EC_{50}	125.4					48.24	
	95% EC_{50}	78.76, 200.4					41.95, 55.31	
	Adj. R^2	0.8110					0.9799	
Sw/NE/13	EC_{50}	117.4	725.9	13.89	51.26		189.7	
	95% EC_{50}	102.9, 134.3	674.2, 785.2	13.25, 14.53	43.64, 60.15		172.5, 208.8	
	Adj. R^2	0.9821	0.9917	0.9946	0.9737		0.9903	
Viet/o4	EC_{50}						14.04	
	95% EC_{50}						11.71, 16.51	
	Adj. R^2						0.8780	
Sw/MO/13	EC_{50}	23,011	318.1	15.51	35.70		10.66	
	95% EC_{50}	10,183, 75,817	258.1, 392.4	14.72, 16.30	30.74, 41.39		10.04, 11.27	
	Adj. R^2	0.9040	0.9466	0.9954	0.9721		0.9782	
Sw/NC/15	EC_{50}	270.4	636.1	41.73	45.57			
	95% EC_{50}	244.0, 300.5	538.2, 770.2	37.61, 46.28	38.96, 53.28			
	Adj. R^2	0.9891	0.9653	0.9866	0.9723			
Wfg/Neth/99	EC_{50}	1,279	425.0	26.01	25.89	47.34	69.02	
	95% EC_{50}	997.4, 1,727	265.3, 816.6	24.16, 27.96	18.98, 33.75	30.45, 68.96	62.62, 76.01	
	Adj. R^2	0.9651	0.8161	0.9920	0.9261	0.8721	0.9907	
Qu/RI/16	EC_{50}	1,214	817.3	32.91	27.97	48.04	III.I	
	95% EC_{50}	957.5, 1,611	491.6, 1749	29.91, 36.16	23.18, 33.17	34.61, 64.45	96.41, 127.9	
	Adj. R^2	0.9695	0.8347	0.9889	0.9710	0.9182	0.9804	
PC/73	EC_{50}	798.4			12.10		280.0	
	95% EC_{50}	666.1, 992.5			10.83, 13.39		262.2, 299.1	
	Adj. R^2	0.9555			0.9519		0.9936	
HK/14	EC_{50}		424.5	78.03	216.6		258.7	194.9
	95% EC_{50}		379.5, 475.3	57.20, 104.9	178.9, 261.1		240.4, 278.4	179.7, 211.4
	Adj. R^2		0.9810	0.9193	0.9618		0.9941	0.9927
Sw/MO/o6	EC_{50}	16.96	16.00	11.98	27.26		21.67	
	95% EC_{50}	15.25, 18.78	10.44, 21.55	10.65, 13.23	16.58, 40.81		15.70, 28.64	
	Adj. R^2	0.9745	0.8812	0.9534	0.8365		0.8724	
Mal/MN/o8	EC_{50}	72.27	329.5	21.98	12.77	39.23	87.82	
	95% EC_{50}	61.88, 84.12	222.4, 537.1	20.23, 23.84	10.09, 15.37	30.55, 48.54	81.79, 94.29	
	Adj. R^2	0.9753	0.8585	0.9883	0.9505	0.9505	0.9950	

The 50% NA inhibitory concentration estimate (EC_{50} , half maximal effective concentration), the 95% profile-likelihood confidence intervals, and the adjusted R-squared (Adj. R^2) were determined for each fit. Sera and virus pairs that resulted in an unstable estimate or did not have an estimate > 10 are not shown.

Table B.3: NA inhibition of raw sera stratified by host origin.

NA	HA	Host	Strain	Ferret	Mouse	Pig	Goat	Rat	Horse	Monkey	> 10	> 100
N ₁	H ₁	Human	Bris/07	1,251	648	14	16	< 10	30	< 10	5	2
	H ₁	Human	CA/09	125	< 10	< 10	< 10	< 10	48	< 10	2	1
	H ₁	Swine	Sw/NE/13	117	726	14	51	< 10	190	< 10	5	3
	H ₅	Human	Viet/04	< 10	< 10	< 10	< 10	< 10	14	< 10	1	0
N ₂	H ₁	Swine	Sw/MO/13	> 1,280	318	16	36	< 10	11	< 10	5	2
	H ₁	Swine	Sw/NC/15	270	636	42	46	< 10	< 10	< 10	4	2
	H ₂	Avian	Wfg/Neth/99	> 1,280	425	26	26	47	69	< 10	6	2
	H ₂	Avian	Qu/RI/16	1,214	817	33	28	48	III	< 10	6	2
	H ₃	Human	PC/73	798	< 10	< 10	12	< 10	280	< 10	3	2
	H ₃	Human	HK/14	> 1,280	425	78	217	< 10	259	195	6	5
N ₃	H ₂	Swine	Sw/MO/o6	17	16	12	27	< 10	22	< 10	5	0
	H ₂	Avian	Mal/MN/o8	72	330	22	13	39	88	< 10	6	1
Number of viruses with NAI > 10				11	9	9	10	3	11	1	54	-
Number of viruses with NAI > 100				9	9	0	1	0	4	1	-	23

Viruses tested are separated by NA subtype, HA subtype, and host origin. The reciprocal NAI 50% titer for each virus and serum pair is shown from the non-linear regression estimates. The number of viruses or sera with NAI 50% titers > 1 : 10 and > 1 : 100 is tabulated by serum origin and by virus, respectively.

APPENDIX C

COBRA VACCINE BASED UPON SWINE H1N1 INFLUENZA HA SEQUENCES PROTECTS AGAINST BOTH SWINE AND HUMAN ISOLATED VIRUSES¹

C.1 Abstract

Swine and human influenza viruses have coevolved for more than a century. Swine H1N1 influenza viruses were stable within pigs for nearly 70 years until in 1998 when a classical swine virus reassorted with avian and human influenza viruses to generate the novel triple reassortant H1N1 strain that eventually led to the 2009 influenza pandemic. Previously, our group demonstrated broad protection against a panel of human H1N1 viruses using HA antigens derived by the COBRA (computationally optimized broadly reactive antigen) methodology. These vaccines were derived using either only human hemagglutinin (HA)

¹Skarupka, A. L., Reneer, Z. B., Abreu, R. B., Ross, T. M., & Sautto, G. A. An influenza virus hemagglutinin computationally optimized broadly reactive antigen elicits antibodies endowed with group 1 heterosubtypic breadth against swine influenza viruses. *J Virol.* 2020. 94:e02061-19. <https://doi.org/10.1128/JVI.02061-19>. Accepted by *Journal of Virology*. Reprinted here with permission of publisher.

sequences (X₃ and X₆) or a combination of human and swine HA sequences (P₁). In this report, the effectiveness of swine COBRA HA antigens (SW₁, SW₂, SW₃ and SW₄) which were designed using only HA sequences from swine H₁N₁ and H₁N₂ isolates were tested in BALB/c mice. Vaccines, such as SW₂ and SW₄, that elicited antibodies that detected the pandemic-like virus, A/California/07/2009 (CA/09), had antibodies with HAI activity against almost all the panel of classical swine influenza viruses isolated from 1973-2015 and all of the Eurasian viruses. However, sera collected from mice vaccinated with SW₂ or SW₄ had HAI activity against 25% of the human seasonal-like influenza viruses isolated from 2009-2015. Several wild-type swine HA-based vaccines elicited antibodies that detected a similar number of classical swine viruses in the panel. In contrast to the COBRA HA vaccines designed with only swine H₁ HA sequences, the P₁ COBRA HA vaccine, derived from both swine and human sequences, elicited antibodies that had HAI activity against both swine and human H₁ influenza viruses and protected against CA/09 challenge, but not a human seasonal-like swine H₁N₂ virus challenge, A/Swine/North Carolina/152702/2015 (SW/NC/15). However, the SW₁ vaccine protected against this challenge as well as the homologous vaccine. The H₁ HAs from the Eurasian swine H₁ viruses elicited antibodies with HAI activity against most of the North American swine viruses, suggesting a possible conserved antigenic link and also supporting the idea that a pan-swine influenza virus vaccine is possible.

C.2 Introduction

The domestic pig (*Sus scrofa domesticus*), also referred to as swine or hog, can be infected by both avian and human influenza viruses through the expression of $\alpha_{2,3}$ - and $\alpha_{2,6}$ - sialic acid receptors in the respiratory tract. Approximately 25% of the swine population in the United States is infected with a swine influenza virus (Y. K. Choi et al., 2002). Infected pigs show influenza-like symptoms including weight loss, fever, respiratory distress, coughing, and nasal discharge, but little mortality. Currently swine influenza viruses of the subtypes H₁N₁, H₃N₂, and H₁N₂ are circulating in North America (Olsen, 2002). In Asia, North America, and much of Europe, H₁N₁ swine influenza viruses are significantly prevalent in the populations and remain an important infection with zoonotic potential (Thacker & Janke, 2008; Vincent et al., 2008).

The H₁N₁ influenza subtype was originally isolated from pigs in 1932, and these swine H₁N₁ influenza viruses remained genetically and antigenically stable in North American pigs until a series of reassortment events in 1998. The triple reassortant H₃N₂ virus originated from a classical swine lineage virus (Np, M, NS) reassorting with a human seasonal H₃N₂ virus (PB₁, HA, NA) with an avian virus (PB₂, PA). This H₃N₂ virus then went on to reassort with co-circulating classical lineage H₁N₁ swine viruses (HA and NA or HA). This was marked by the introduction of human and avian influenza virus gene segments with swine influenza virus genes and resulted in generation of novel strains with pandemic potential (Vincent et al., 2008). Based on phylogenetic analysis and ancestry studies, the swine H₁ viruses belong to four distinctive clades: alpha, beta, gamma and delta (Karasim et al., 2002; Vincent et al., 2009; Webby et al., 2004). Alpha viruses are considered classical isolates and are related to viruses that circulated from 1930s to 1998 (cH₁N₁) (T. K. Anderson et al., 2016; Ma et al., 2010; Vincent et al., 2009). Viruses classified in the Beta clade developed due to reassortment events between cH₁N₁ isolates and H₃N₂ viruses in pigs that led to H₁N₁ viruses expressing cH₁N₁ HA and NA surface proteins with H₃N₂ internal genes. Gamma clade swine influenza viruses are referred to as H₁N₂-like isolates and are the result of a triple reassortant event between H₃N₂ and cH₁N₁ viruses. Swine influenza viruses of the Gamma clade include both H₁N₁ and H₁N₂ viruses (Vincent et al., 2009). Delta clade swine influenza viruses are highly divergent, containing both H₁N₁ and H₁N₂ swine influenza viruses, and contain H₁ human seasonal influenza virus genes (Lewis et al., 2016). In 2009, the first pandemic of the 21st century occurred with the introduction of a swine-origin influenza virus of the cH₁N₁ subtype into the human population that transmitted easily between people (Gibbs et al., 2009).

Ultimately, the expansive divergence of the swine hemagglutinin makes all the clades antigenically distinct; a wild-type H₁ hemagglutinin vaccination would leave the host open to infection from a mismatched virus, of which, there are plenty. Therefore, to address the need for more broadly reactive influenza vaccines, our group has previously reported on the methodology of antigen design, termed computationally optimized broadly reactive antigen (COBRA), using multiple rounds of layered consensus building to generate influenza vaccine HA immunogens. COBRA HA vaccines elicit antibodies that target both the

globular head and stem regions of HA. Recently, we reported the characterization of a COBRA-based vaccine for highly pathogenic H₅N₁ (Crevar & Ross, 2008; Giles, Bissel, et al., 2012; Giles, Crevar, et al., 2012; Giles & Ross, 2011b; Monto, 2010) and both human seasonal and pandemic H₁N₁ influenza virus isolates. (Carter et al., 2016b). For H₁N₁, these COBRA HA candidates were designed to recognize H₁N₁ viruses isolated within the last 30 years. In addition, several COBRA HA candidate designs were based on sequences of H₁N₁ viruses spanning the past 100 years, including modern pandemic H₁N₁ isolates. Three of the nine H₁N₁ COBRA HA proteins (X₃, X₆, and P₁) had intense broad hemagglutination inhibition (HAI) activity against a panel of fifteen H₁N₁ viruses. These vaccines were derived using HA sequences from human isolates, except for P₁, which was based on a combination of both human and H₁N₁ swine isolates. Mice vaccinated with a virus-like particle (VLP) expressing the P₁ COBRA HA antigen had little or no detectable viral replication following challenge with the A/California/07/2009 (CA/09) pandemic-like H₁N₁ virus, which was comparable to a homologous matched CA/09 vaccine.

In this study, a set of H₁ COBRA HA vaccines designed using only swine H₁N₁ and H₁N₂ viruses (SW₁, SW₂, SW₃, SW₄) were assessed for their ability to elicit protective antibodies with HAI activity against both human and swine H₁ influenza viruses. Those results were then compared to the P₁ swine-human COBRA HA, as well as, the human COBRA HA vaccines (Carter et al., 2016c). While swine COBRA HA vaccines elicited antibodies with HAI activity against a diverse panel of swine H₁ viruses, these same elicited antibodies did not recognize human seasonal H₁N₁ viruses. The SW₂ and SW₄ vaccines elicited antibodies with HAI activity against classical swine H₁ viruses, and the SW₁ vaccine elicited protective immune responses against human seasonal-like H₁ swine influenza viruses. Only the P₁ COBRA vaccine was able to elicit antibodies that effectively recognized historical and contemporary human seasonal H₁N₁ viruses, in addition to, different lineages of H₁N₁ and H₁N₂ swine viruses.

C.3 Materials and Methods

C.3.1 COBRA HA antigen construction and synthesis

Nucleotide sequences ($N=721$) for swine H₁N₁ and H₁N₂ influenza A hemagglutinin (HA) proteins, isolated from 1930-2013, were downloaded from the NCBI Influenza Virus Resource database (Giles, Bissel, et al., 2012). The nucleotide sequences were translated into protein sequences using the standard genetic code. Full-length swine H₁N₁ and H₁N₂ sequences from viral infections covering the period from 1930 to 2013 were analyzed. Specifically, the SW₁ COBRA was designed to include both H₁N₁ and H₁N₂ sequences from 1998 to 2013. SW₂ incorporated only H₁N₁ sequences, and SW₃ included sequences that included only H₁N₂ sequences from 1998 to 2013. SW₄ included historical sequences from 1930 to 1997, in addition to, the 1998 to 2013 period (Fig. C.1). The HAo amino acid sequences were aligned, and the most common amino acid at each position was determined resulting in primary consensus sequences representing each genotypic group. The resulting primary sequences from each group were then realigned to generate a secondary consensus. This process was continued until a single final consensus was obtained. Finally, the ultimate amino acid sequence was reverse translated and optimized for expression in mammalian cells, including codon usage and RNA optimization (Genewiz, Washington, DC, USA). The resulting sequence was termed a computationally optimized broadly reactive antigen (COBRA). H₁ HA genes were synthesized and inserted into the pTR600 expression vector, as previously described (Ross et al., 2000).

C.3.2 Viruses and HA antigens

H₁ viruses were obtained through the Influenza Reagents Resource (IRR), BEI Resources, the Centers for Disease Control (CDC), or provided by Sanofi-Pasteur. Viruses were passaged once in the same growth conditions as they were received or as per the instructions provided by the WHO, in either embryonated chicken eggs or Madin-Darby canine kidney (MDCK) cell culture (Organization & Network, 2011). Virus

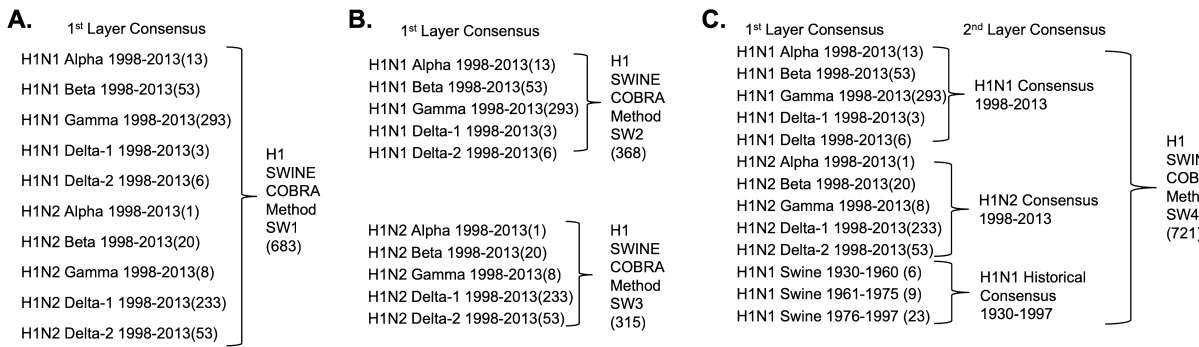


Figure C.1: Designs of Swine COBRA HA sequences. Swine and human COBRA swine genotypic characteristics. (A–C) Description of the number of original sequences from each of phylogenetic clade input into SW₁ (A), SW₂, SW₃ (B), and SW₄ (C).

lots were aliquoted for single-use applications and stored at -80°C. Titer of the frozen aliquots was determined with turkey RBCs.

The classification of the swine HA was determined using the Swine H1 Clade Classification Tool (<http://www.fludb.org>) (T. K. Anderson et al., 2016) which takes the HA nucleotide sequence and infers both the global (T. K. Anderson et al., 2016) and US (T. K. Anderson et al., 2015; T. K. Anderson et al., 2013) swine H1 clade classification. When available, virus was used for HAI assays where indicated (*), otherwise HA VLPs were used. The protein accession numbers for the HA amino acid sequences used for VLP production, phylogenetic analysis, *p_{epitope}* calculation, and glycosylation prediction are provided. If no accession number was available, the amino acid sequences are provided (Table C.1). The following HA VLP vaccines were included for both viral challenges: SW-1 COBRA (SW₁), SW-2 COBRA (SW₂), SW-3 COBRA (SW₃), SW-4 COBRA (SW₄), P-1 COBRA (P₁), X-3 COBRA (X₃), X-6 COBRA (X₆), and A/California/07/2009 (CA/o9*; YP_009118626.i). The A/Swine/North Carolina/152702/2015 (SW/NC/152702/15*) included a matched HA VLP vaccine. The CA/o9 challenge included swine wild-type HA VLP vaccines representing different lineages and clades (Fig. C.2) including: A/Swine/Wisconsin/125/1997 (SW/WI/97; AAF87274.i), A/Swine/Indiana/P12439/2000 (SW/IN/oo;

AAL87870.1), A/Swine/Spain/50047/2003 (SW/Spain/03; ABD78104.1), A/Swine/Korea/Asano4/2006 (SW/Korea/06; ACE77933.1), A/Swine/Zhejiang/1/2007 (SW/Zhejiang/07; ACJ06667.1), A/Swine/North Carolina/02744/2009 (SW/NC/02744/09), A/Swine/North Carolina/34543/2009 (SW/NC/34543/09; AEX25796.1), and A/Swine/Minnesota/A01489606/2015 (SW/MN/15; AKD00877.1).

Mice were only vaccinated with and not challenged with VLPs expressing the HA of human strains including A/Chile/1/1983 (Chile/83*; AFM72054.1), A/Singapore/6/1986 (Sing/86*; ABO38395.1), A/New Caledonia/20/1999 (New Cal/99*; AGQ47728.1), and A/Brisbane/59/2007 (Bris/07*; ACA28846.1). The following swine strains were used only for the HAI VLP panel: A/Swine/Iowa/1973 (SW/IA/73; ABV25637.1), A/Swine/North Carolina/93523/2001 (SW/NC/01; AAL87867.1), A/Swine/Ohio/511445/2007 (SW/OH/07; ACH69547.1), A/Swine/Colorado/SG1322/2009 (SW/CO/09; AHB21556.1), A/Swine/North Carolina/5043-1/2009 (SW/NC/5043-1/09; ADV69084.1), A/Swine/Missouri/A01203163/2012 (SW/MO/12; AFM47013.1), A/Swine/Nebraska/A10444614/2013 (SW/NE/13*; AGF68975.1) and A/Swine/North Carolina/A01377454/2014 (SW/NC/14; AJM70701.1). The following human H1N1 strains were used for only the HAI virus panel: A/Texas/36/1991 (TX/91*; ABF21276.1), A/Beijing/262/1995 (Beijing/95*; ACF41867.1), and A/Solomon Islands/3/2006 (SI/06*; ABU99109.1). The 25-member wild-type HA panel represented human viruses from 1980 to the introduction of CA/09 and swine viruses from different phylogenetic lineages and clades. Wild-type HA vaccine antigens were codon optimized for expression in mammalian cells. The additional eight swine and three human strains were included in the HAI panel to expand the breadth of the human and swine phylogenetic coverage from 1930 to 2015.

C.3.3 Phylogenetic comparison of swine, human, and COBRA HA sequences

Viruses used for the vaccination panel and HAI panel were visualized on a phylogenetic tree to confirm full coverage of swine and human influenza clades (Fig. C.2). Briefly, the HAo was aligned utilizing Geneious alignment with global alignment with free end gaps and a cost matrix Blosum62 with open

Table C.1: Accession numbers or amino acid sequences of the HA of H1 strains.

Virus	Protein Accession Number/HA sequence
A/Sw/NC/02744/2009	DTICVGYHAN NSTDTVDTVL EKNVTVTHSV NLLEDSHNGK LCLLKGIAPL QLGSCSVAGW ILGNPECELL ISKESWSYIV ETPNPENGTC YPGYFTDYEE LREQLSSVSS FKRFEIFPKE SS- WPNHNVNG VSSSCSHNGK SSFYRNLLWL TVKNGLYPNL SKSYTNKKEK EVLVLWGVHH PSNIGDQRAL YHTENAYVSV VSSHYSRRFT PEIAKRPKVR NQEGRINYYW TLLEPGDTII FEANGNLIAP RYAFELSKGF GSGIITSADP MGECNAKCQT PQGAINSSLP FQNVHPVTIG ECPKYVRSAK LRMTGLRNT PSIQSRLGLFG AIAGFIEGGW TGMVDGWYGY HHQNEQGSGY AADQQSTQNA INGITNKVNS VIEKMNTQFT AVGKEFNKLE RRMENLNKKI DDGFLDIWTY NAELLVLLEN ERTLDFHDSN VKNLYEKVKS QLKNNAKEIG NGCFEFYHHC NDECMESVKN GTYDYPKYSE ESKLNREKID GVKLESMGVY NILAIYSTVA SSLVLLVSLG AISFWMCSNG SLQCRICI
A/Sw/NC/152702/2015	DTICVGYHAN NSTDTVDTVL EKNVTVTHSV NLLEDSHNGK LCLLKGIAPL QLGSCSVAGW ILGNPECELL ISKESWSYIV ETPNPENGTC YPGYFEDYEE LREQLSSVSS FKRFEIFPKK SS- WPNHVTVG VSSSCSHNGN SSFYRNLLWL TVKNNLYPNL SKSYTNKKEK EILVLWGVHH PSNMEDQRAL YHTENAYVSV VSSHYSRRFT PEIAKRPKVR NQEGRINYYW TLLEPGDTII FEASGNLIAP RYAFELSKGF GSGIITSNAP MGECNAKCQT PQGAINSSLP FQNVHPVTIG ECPKYVRSAK LRMTGLRNT PSIQSRLGLFG AIAGFIEGGW TGMVDGWYGY HHQNEQGSGY AADQQSTQNA INGITNKVNS VIEKMNTQFT AVGKEFNKLE RRMENLNKKV DDGFLDIWTY NAELLVLLEN ERTLDFHDSN VKNLYEKVKS QLKNNAKEIG NGCFEFYHHC DDECMDSVKN GTYDYPKYSE ESKLNREKID GVKLESMGVY NILAIYSTVA SSLVLLVSLG AICFWMCSNG SLQCRICI
A/New Jersey/11/1976	ACU80014.I
A/South Carolina/1/1918	AAD17229.I
A/United Kingdom/1/1933	ACV49534.I
A/Puerto Rico/8/1934	BAV596II.I
A/Weiss/1/1943	ABD79101.I
A/Denver/1/1957	ADB15258.I
A/USSR/90/1977	AFM73477.I
A/Brazil/11/1978	ABO38065.I
A/California/10/1978	ABP49338.I

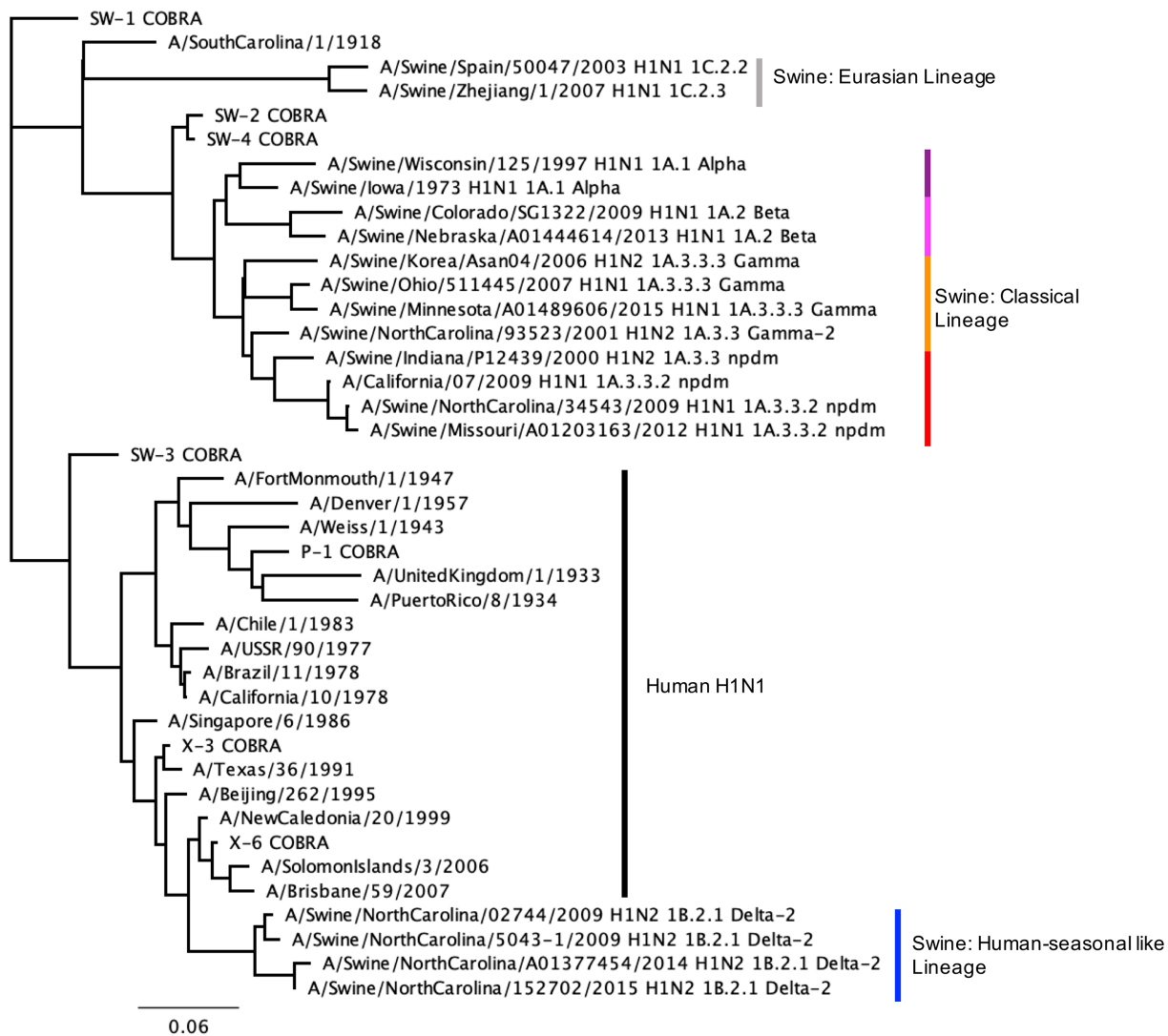


Figure C.2: The unrooted human and swine H1 HA phylogenetic tree was inferred from database HA amino acid sequences with the inclusion of COBRA HA sequences. Neighbor-joining tree built on the alignment of the amino acid sequences of the HA₁ (1–327) region. The swine isolates include the influenza subtype, H1 swine global classification, and swine North American classification. Scale bar length represents the number of amino acid substitutions per amino acid site.

gap penalty 12, and gap extension penalty 3, with refinement iterations of 2 (Geneious v7.1.5). The HA_I portions (1-327AA) were extracted from the alignment. Using only sequences with a full HA_I amino acid sequence, Geneious Tree Builder, which observed the same alignment characteristics, was used to obtain a neighbor-joining Jukes-Cantor phylogenetic tree with no indicated outgroup. The scale bar represents 0.06 amino acid substitutions per site, of a total of 347 amino acid sites (Kearse et al., 2012).

C.3.4 Predicted HA structures by Pymol

The known crystal structure were used for A/California/07/2009 (PDB accession: 3lzf (R. Xu et al., 2010)) and A/Swine/Indiana/P12439/2000 (PDB accession: 4f3z (R. Xu et al., 2012)). For all other HA vaccines the predicted protein structural models were constructed using SWISS-MODEL workspace (<https://swiss-model.expasy.org>) (Bienert et al., 2017; Waterhouse et al., 2018). The template for the target sequence was identified through parallel searches of the SWISS-MODEL template library (SMTL) using BLAST (Camacho et al., 2009) and HHBlits (Remmert et al., 2011). For all the target HA sequences two templates were chosen for model building (Guex et al., 2009). The crystal structures of A/Jiangsu/ALSI/2011 (H1N1) HA (PDB accession: 6d8w) was selected for the Eurasian strains, and A/Netherlands/002P1/1951 (H1N1) HA (PDB accession: 6n41) was selected for all remaining HAs. The template's quality was predicted from features of the target-template alignment. The templates with the highest quality were then selected for model building. Models were built based on the target-template alignment using ProMod3. Conserved coordinates between the target and the template were copied from the template to the model. Insertions and deletions were remodeled using a fragment library. Side chains were then rebuilt. Finally, by using a force field the geometry of the resulting model was regularized. Incase loop modelling with ProMod3 failed, an alternative model was built with PROMOD-II (Guex & Peitsch, 1997). The global model quality estimation (GMQE) determines the expected accuracy of the model based upon the alignment of the target to the template as well as the coverage of the target. The global and per-residue model quality was assessed using the QMEAN scoring function based upon geometrical properties (Benkert et al., 2011). QMEAN Z-scores close to zero indicate high quality, whereas less than -4.0 indicate low

quality models (Altschul et al., 1997; Guex & Peitsch, 1997). The quaternary structure prediction score (QSQE) indicates the quality of fit for the quaternary structure of the protein given that HA is naturally isolated as a homotrimer. Putative glycosylation sites were predicted using the online tool NetNGlyc 1.0 (<http://www.cbs.dtu.dk/services/NetNGlyc/>) (R. Gupta et al., 2004). The antigenic regions were defined as: Sa (124-125, 153-157, 159-164); Sb (184-195); Ca1 (166-170, 203-205, 235-237); Ca2 (137-142, 221-222); and Cb (70-75).

C.3.5 Calculation of p_{epitope} values

Due to the inclusion of the pandemic HAs, the A/California/04/2009 numbering scheme was used (Deem & Pan, 2009). The amino acid numbering begins following the seventeen amino acids in the signal peptide (Burke & Smith, 2014; Nobusawa et al., 1991; Winter et al., 1981). The epitope sites include the amino acids predicted to be important to vaccine efficacy: neutralizing-antibody binding residues, structure/sequence homologues of known H₃ epitopes, and protein surface residues with high information entropy (Table C.3; Deem and Pan, 2009. The p_{epitope} provides a quantitative value for the antigenic distance between two hemagglutinin amino acid sequences based upon the comparison of the five epitopes. For any two given sequences, the p-value was calculated for each epitope region to be the proportion of differing amino acids. The largest p-value of the five was then considered the dominant p_{epitope} , and the corresponding epitope was named the dominant epitope region (Table C.2). A p_{epitope} of less than 0.442 has been correlated with a vaccine effectiveness greater than zero in humans (Pan et al., 2011). Therefore, this cutoff was observed for the study.

C.3.6 Vaccine preparation

Human embryonic kidney 293T (HEK-293T) cells (1×10^6) were transiently transfected with 1 μg DNA of each of the three pTR600 mammalian expression vectors (Green et al., 2003) expressing the influenza neuraminidase (A/Mallard/Alberta/24/2001; H₇N₃), the HIV p55 Gag sequence, and one of the various H₁ wild-type or COBRA HAs. Following 72 h of incubation at 37°C, supernatants from transiently

Table C.2: Computationally optimized broadly reactive antigens used in the study.

HA Vaccine	Origin ^a	Subtype	Years ^b	Sequences ^c
SW-1 COBRA (SW ₁)	Swine	H ₁ N ₁ /H ₁ N ₂ Based	1998-2013	683
SW-2 COBRA (SW ₂)	Swine	H ₁ N ₁ Based	1998-2013	368
SW-3 COBRA (SW ₃)	Swine	H ₁ N ₂ Based	1998-2013	315
SW-4 COBRA (SW ₄)	Swine	H ₁ N ₁ /H ₁ N ₂ Based	H ₁ N ₁ only: 1930-1997 H ₁ N ₁ /H ₁ N ₂ : 1998-2013	721
P-1 COBRA (P ₁)	Human and Swine	H ₁ N ₁ Based	1918-2012	205
X-3 COBRA (X ₃)	Human	H ₁ N ₁ Based	1977-2008	116
X-6 COBRA (X ₆)	Human	H ₁ N ₁ Based	1999-2012	1096

^aSpecies of the H_iN_X isolates^bRange of years that the HA sequences from the H_iN_X viral strains were isolated^cNumber of HA sequences utilized for the input sequence alignments

Table C.3: Amino acid residues used to calculate the ADM of vaccine and challenge virus combinations.

Antigenic Site	Amino Acid Residue
A (SA)	118, 120, 121, 122, 126, 129 1, 132-135, 137, 139-143, 146, 147, 149, 165, 252, 253
B (Sb)	124, 125, 152-157, 160, 162, 183-187 189-191, 193-196
C	34-38, 40, 41, 43-45, 269-274, 276-278, 283, 288, 292, 295, 297, 298, 302, 303, 305-310
D (Ca)	89, 94-96, 113, 117, 163, 164, 166174, 176-178, 200, 202, 204-216, 222-227, 235, 237, 241, 243-245
E (Cb)	47, 48, 50, 51, 53, 54, 56-58, 66, 68-75 78-80, 82-86, 102, 257-261, 263, 267

transfected cells were collected, centrifuged to remove cellular debris, and filtered through a 0.22 µm pore membrane. Mammalian virus-like particles (VLPs) were purified and sedimented by ultracentrifugation on a 20% glycerol cushion at 135,000 x g for 4 h at 4°C. VLPs were resuspended in phosphate buffered saline (PBS), and total protein concentration was determined with the Micro BCA Protein Assay Reagent kit (Pierce Biotechnology, Rockford, IL, USA). Hemagglutination activity of each preparation of VLP was determined by serially diluting volumes of VLPs and adding equal volume 0.8% turkey red blood cells (RBCs) (Lampire Biologicals, Pipersville, PA, USA) suspended in PBS to a V-bottom 96-well plate with a 30 min incubation at room temperature (RT). Prepared RBCs were stored at 4°C and used within 72 h. The highest dilution of VLP with full agglutination of RBCs was considered the endpoint HA titer.

C.3.7 Determination of HA content

Purified VLPs were mixed with 6X reducing Laemmli's SDS-sample buffer and incubated at 100°C for 5 min (Boston BioProducts, Ashland, MA, USA). Reduced VLPs were then electrophoresed on a 10% sodium dodecyl sulfate-polyacrylamide gel (SDS-PAGE) and transferred to a polyvinylidene difluoride (PVDF) membrane. The blot was probed 1:1000 with commercially sourced mouse anti-human HA clade 1 (15B7; Immune Technology Corporation, Lexington Ave, NY, USA). HA-antibody complexes were then detected using 1:4000 goat anti-mouse IgG labeled with horseradish peroxidase (HRP) (Southern Biotech, Birmingham, AL, USA). HRP activity was detected using Clarity™ Western ECL substrate (Bio-Rad Laboratories, Hercules, CA, USA) and digitally imaged using a cooled charged-coupled device camera (myECL Imager, ThermoFisher Scientific, Waltham, MA, USA). Linear regression standard curve analysis was performed using the known concentrations of the standard recombinant antigen (H1N1 A/California/07/2009) to estimate HA content in VLP lots. Quantifications were performed in duplicate.

C.3.8 Mouse vaccination and challenge studies

BALB/c mice (*Mus musculus*, females, 6 to 8 weeks old) were purchased from Jackson Laboratory (Bar Harbor, ME, USA) and housed in microisolator units and allowed free access to food and water. Mice (9 and 11 mice per group for CA/09 and SW/NC/152702/15, respectively) were vaccinated with a 1:1 mixture of purified VLP (1.0 µg HA/mouse) and an emulsified MF59-like, squalene-based oil-in-water adjuvant (Sanofi Pasteur, Lyon, France). Mice were vaccinated via intramuscular injection at week 0 and boosted with the same vaccine formulation at the same dose at weeks 4 and 8. PBS mixed 1:1 with adjuvant served as a mock vaccination. Blood samples were collected from mice via cheek bleeds twenty-eight days after each vaccination in 1.5 ml microcentrifuge tubes. The samples were incubated at RT for 30 min and then centrifuged at 5000 rpm for 5 min. Serum samples were removed and stored at -20°C.

Four weeks after final vaccination, mice were challenged intranasally with 5×10^4 plaque forming units (PFU) of A/California/07/2009 (H1N1) or 1×10^7 PFU of A/Swine/North Carolina/152702/2015 (H1N2).

in a volume of 50 µl. Challenge PFUs were calculated to be ten times the LD₅₀ for each challenge virus. For fourteen days after challenge, mice were monitored, at minimum, daily for weight loss, disease signs, and death for 14 days after infection. Three days post-infection, lungs (n=3) were harvested, transferred to dry ice, and stored at -80°C until enumeration of viral lung titers. Individual body weights were recorded daily post-infection for each group. Any animal exceeding 20% weight loss was humanely euthanized. Surviving mice were confirmed for successful infection indicative by seroconversion. All procedures were performed in accordance with the Guide for the Care and Use of Laboratory Animals, Animal Welfare Act, and Biosafety in Microbiological and Biomedical Laboratories.

C.3.9 Hemagglutination inhibition (HAI) assay

The hemagglutination inhibition (HAI) assay assessed functional antibodies to the HA able to inhibit agglutination of turkey erythrocytes. The protocols were adapted from the WHO laboratory influenza surveillance manual (Organization & Network, 2011). To inactivate nonspecific inhibitors, sera were treated with receptor-destroying enzyme (RDE) (Denka Seiken, Co., Japan) prior to being tested. Briefly, three parts RDE was added to one part sera and incubated overnight at 37°C. RDE was inactivated by incubation at 56°C for 30 min. After heat treatment, six parts PBS were added to the RDE-treated sera. RDE-treated sera were two-fold serially diluted in V-bottom microtiter plates. An equal volume of each virus (or VLP where applicable), adjusted to approximately 8 hemagglutination units (HAU)/50 µl, was added to each well. The plates were covered and incubated at RT for 20 min, and then 50 µl RBCs were added to each well. The plates were mixed by agitation and covered, and the RBCs were allowed to settle for 30 min at RT. The HAI titer was determined by the reciprocal dilution of the last well that contained non-agglutinated RBCs. Positive and negative serum controls were included for each plate. All mice were negative (HAI < 1:10) for preexisting antibodies to currently circulating human and swine influenza viruses prior to vaccination and seroprotection was defined as HAI titer greater than or equal to 1:40 and seroconversion as a 4-fold increase in titer compared to baseline, as per the WHO and European Committee for Medicinal Products to evaluate influenza vaccines (“Guideline on influenza vaccines”,

2014); however, we often examined a more stringent threshold of greater than or equal to 1:80. Mice were naïve and seronegative at the time of vaccination, thus seroconversion and seroprotection proportions were interchangeable in this study.

C.3.10 Determination of viral lung titers.

Whole lung samples were thawed on ice. CA/09 lung samples were weighed and per 0.1 g a volume of 1 ml of Dulbecco modified Eagle medium (DMEM) supplemented with penicillin-streptomycin (P/S) was added. For SW/NC/152702/15 lung samples, whole lungs were suspended in 1 ml of DMEM + P/S. The tissue was macerated through a 0.70 µm nylon filter (Corning Cell Strainer, Sigma Aldrich, St. Louis, MO, USA) until thoroughly homogenized. Lung filtrate was then enumerated for viral lung titers. Ten-fold serial dilutions of lung homogenate were overlaid onto MDCK cells seeded at 5×10^5 cells per well of a six-well plate. Samples were incubated for 1 h at RT with intermittent shaking every 15 min. Medium was removed, and the cells were washed twice with DMEM + P/S. Wash medium was replaced with 2 ml of L15 medium with 2 µg/ml TPCK-trypsin plus 0.8% agarose (Cambrex, East Rutherford, NJ, USA) and incubated at 37°C with 5% CO₂ for 72 h and 48 h for CA/09 and SW/NC/152702/15, respectively. Agarose was removed and discarded. MDCK cells were fixed with 10% buffered formalin for 10 min and stained with 1% crystal violet for 15 min. The plates were thoroughly washed in distilled water to remove excess crystal violet, and the plaques were counted and recorded to determine the PFU per ml lung homogenate.

C.3.11 ELISA for elicited antibody binding

A high-affinity, 96-well flat-bottom enzyme-linked immunosorbent assay (ELISA) plate was coated with 50 µl of 2 µg/ml of recombinant hemagglutinin of either CA/09 or SW/NC/152702/15 in ELISA carbonate buffer (50mM carbonate buffer [pH 9.5] with 5 µg/ml BS), and the plate was incubated overnight at 4°C. The next morning, the plates were washed in PBS, and nonspecific epitopes were blocked with 1% bovine serum albumin (BSA) in PBS with 0.05% Tween 20 (PBST+BSA) solution for 1 h at RT or overnight at 4°C. Buffer was removed and three-fold serial dilutions of RDE treated sera were added to the plate with a

highest initial dilution of 1:50. The initial dilution of SW/NC/02744/09 was 1:110 due to sera limitations. Plates were incubated at 37°C for 90 min. The plates were washed in PBS, and goat anti-mouse IgG-HRP was added 1:4000 in PBST+BSA. Plates were incubated at 37°C for 1 hr. After washing, 2,2'-azino-bis(3-ethylbenzothiazoline-6-sulphonic acid) (ABTS) substrate in McIlvain's Buffer (pH 5) was added to each well, and incubated at 37°C for 15 min. The colorimetric reaction was stopped with the addition of 1% SDS in ddH₂O, and the absorbance was measured at 414 nm.

C.3.12 Statistical analysis

Statistical significance was defined as a p-value less than 0.05. The means of the viral lung titers and day 6 weights were analyzed by an ordinary one-way ANOVA followed by Tukey's multiple comparisons test, with a single pooled variance (Table C.4). The viral lung titers were transformed by \log_{10} and the mean calculated. The lowest limit of detection for viral lung titers was 10 PFU/ml lung homogenate, and was used for the statistical analysis of samples below that. The day 6 weights were determined by dividing the measured weight on day 6 by the pre-challenge weight on day 0, multiplied by 100. The standard deviations for viral lung titers and day 6 weights were determined. If an animal was sacrificed before day 6 due to a greater than 20% drop in original weight, a percent weight of 80 was used as the limit of detection for the statistical analysis. The HAI titers were transformed by \log_2 and the mean calculated. The ELISAs were performed in quadruplicate. After subtraction of the background absorbance replicates were averaged and the standard deviations plotted. Analyses were done using GraphPad Prism software.

C.3.13 Nucleotide sequences

The nucleotide sequences for all three human and four swine COBRA HA sequences have been reported in U.S. patent filings.

Table C.4: Resultant p-values from ordinary one-way ANOVA followed by Tukey's multiple comparisons test.

Lung Titers CA/09 Challenge	PBS	SW1	SW2	SW3	SW4	Pr	X3	X6	CA/09	SW/Spain/03	SW/Zhejiang/07	SW/Korea/06	SW/WI/97	SW/NC/34543/09	SW/MN/15	SW/IN/00	SW/NC/02744/09
PBS	0.5138																
SW1	0.0001	0.1197															
SW2	>0.9999	0.5876	0.0002														
SW3	0.0001	0.1197	>0.9999	0.0002	>0.9999												
SW4	0.0001	0.1197	>0.9999	0.0002	>0.9999												
Pr	0.0001	0.1197	>0.9999	0.0002	>0.9999												
X3	>0.9999	0.9135	0.0011	>0.9999	0.0011	0.0011											
X6	>0.9999	0.4869	0.0001	>0.9999	0.0001	0.0001	>0.9999										
CA/09	0.0001	0.1197	>0.9999	0.0002	>0.9999	>0.9999	0.0011	0.0001	>0.9999								
SW/Spain/03	0.0004	0.2515	>0.9999	0.0006	>0.9999	>0.9999	0.0032	0.0004	>0.9999								
SW/Zhejiang/07	0.0001	0.1197	>0.9999	0.0002	>0.9999	>0.9999	0.0011	0.0001	>0.9999	>0.9999							
SW/Korea/06	0.5754	>0.9999	0.0078	0.6491	0.0578	0.9414	0.548	0.0978	0.2118	0.0578							
SW/WI/97	0.0314	>0.9999	0.5586	0.3131	0.5586	0.3186	0.3902	0.0944	0.5186	0.7912	0.5586	0.9998					
SW/NC/34543/09	0.0001	0.1197	>0.9999	0.0002	>0.9999	>0.9999	0.0011	0.0001	>0.9999	>0.9999	>0.9999	0.0978	0.5586				
SW/MN/15	>0.9999	0.2013	<0.0001	>0.9999	<0.0001	<0.0001	0.9956	>0.9999	<0.0001	<0.0001	<0.0001	0.3397	0.0161	<0.0001			
SW/IN/00	0.1029	>0.9999	0.3124	0.5761	0.124	0.3124	0.3077	0.4761	0.124	0.2952	0.3124	>0.9999	0.124	0.195			
SW/NC/02744/09	>0.9999	0.562	0.0002	>0.9999	0.0002	>0.9999	>0.9999	0.0002	0.0002	0.0002	0.6218	0.121	0.0002	>0.9999	0.5509		

Day 6 Weights CA/09 Challenge	PBS	SW1	SW2	SW3	SW4	Pr	X3	X6	CA/09	SW/Spain/03	SW/Zhejiang/07	SW/Korea/06	SW/WI/97	SW/NC/34543/09	SW/MN/15	SW/IN/00	SW/NC/02744/09
PBS	0.0325																
SW1	<0.0001	0.0351															
SW2	>0.9999	0.014	<0.0001														
SW3	>0.9999	0.014	<0.0001														
SW4	<0.0001	0.6982	0.9884	<0.0001													
Pr	<0.0001	0.1656	>0.9999	<0.0001	>0.9999												
X3	>0.9999	0.0152	<0.0001	>0.9999	<0.0001	<0.0001											
X6	>0.9999	0.0158	<0.0001	>0.9999	<0.0001	>0.9999	<0.0001	<0.0001	>0.9999	<0.0001	<0.0001	<0.0001	<0.0001	<0.0001	<0.0001		
CA/09	<0.0001	0.341	>0.9999	<0.0001	>0.9999	<0.0001	<0.0001	<0.0001	>0.9999	<0.0001	<0.0001	<0.0001	<0.0001	<0.0001	<0.0001		
SW/Spain/03	<0.0001	0.0653	0.9938	<0.0001	>0.9999	<0.0001	<0.0001	<0.0001	>0.9999	<0.0001	<0.0001	<0.0001	<0.0001	<0.0001	<0.0001		
SW/Zhejiang/07	<0.0001	0.0192	0.0009	<0.0001	0.9894	<0.0001	<0.0001	<0.0001	>0.9999	<0.0001	<0.0001	<0.0001	<0.0001	<0.0001	<0.0001		
SW/Korea/06	>0.9999	0.2184	<0.0001	>0.9999	0.0003	<0.0001	>0.9999	<0.0001	>0.9999	<0.0001	<0.0001	<0.0001	<0.0001	<0.0001	<0.0001	0.0846	
SW/WI/97	0.0387	>0.9999	0.1059	0.0034	0.9882	0.3772	0.0039	0.0226	0.6066	0.7803	0.1396						
SW/NC/34543/09	<0.0001	0.0126	>0.9999	<0.0001	0.9884	>0.9999	<0.0001	<0.0001	0.9898	0.9949	>0.9999	<0.0001	0.0452				
SW/MN/15	>0.9999	0.0047	<0.0001	>0.9999	<0.0001	<0.0001	>0.9999	>0.9999	<0.0001	<0.0001	<0.0001	<0.0001	0.2992	0.0011	<0.0001		
SW/IN/00	0.2928	>0.9999	0.0019	0.6562	0.1592	0.0117	0.2967	0.1365	0.0175	0.0945	0.0033	0.7641	0.3964	0.0005	0.0731		
SW/NC/02744/09	0.1	>0.9999	0.0048	0.481	0.413	0.0378	0.018	0.058	0.155	0.2631	0.0153	0.446	>0.9999	0.0032	0.0181	>0.9999	

Lung Titers SW/NC/15 Challenge	PBS	SW1	SW2	SW3	SW4	Pr	X3	X6	CA/09	SW/NC/15
PBS										
SW1	>0.9999	0.6477								
SW2	0.7603	0.3776	>0.9999							
SW3	0.4857	0.3776	>0.9999							
SW4	0.7799	0.3274	0.976	<0.0001						
Pr	0.4399	0.3904	>0.9999	>0.9999	0.9993					
X3	>0.9999	0.8694	0.8694	0.6217	0.2611	0.6364				
X6	0.9364	0.9841	0.9914	0.9113	0.6052	0.9778	0.0996			
CA/09	0.1498	0.2051	0.9887	0.9884	>0.9999	0.9979	0.2206	0.5418		
SW/NC/15	0.0085	0.0129	0.0002	<0.0001	<0.0001	<0.0001	0.0052	0.0013	<0.0001	

Day 6 Weights SW/NC/15 Challenge	PBS	SW1	SW2	SW3	SW4	Pr	X3	X6	CA/09	SW/NC/15
PBS										
SW1	0.0380									
SW2	0.028	0.0013								
SW3	>0.9999	0.0317	0.9751							
SW4	0.8111	0.0007	>0.9999	0.9729						
Pr	0.9181	0.0014	>0.9999	0.9798	>0.9999					
X3	0.9972	0.3124	0.4183	0.0891	0.3181	0.4815				
X6	0.8383	0.7986	0.1177	0.7168	0.0745	0.1274	0.9988			
CA/09	0.0988	0.2847	0.5174	0.092	0.3906	0.5112	>0.9999	0.9972		
SW/NC/15	0.0412	>0.9999	0.0009	0.0246	0.0005	0.001	0.2709	0.7299	0.2293	

A p-value less than 0.05 was reported as significant

Values greater than 0.05 were shaded in grey

C.4 Results

C.4.1 Design of H1N1 COBRA HA genes

Previous studies from our laboratory used the COBRA methodology to design H1N1 HA sequences to account for the evolution of H1N1 influenza viruses isolated in humans over the past 100 years (Carter et al., 2016c). The COBRA design utilized these chronologically different eras of primarily human H1 HA sequences to account for the unique antigenic types of HA domains. Three lead candidates (P1, X3, and X6) elicited broadly protected antibody responses in immunologically naïve mice and ferrets (Carter et al., 2016c), as well as ferrets with pre-existing antibodies to H1N1 influenza viruses (Carter et al., 2017). In this study, new H1 COBRA HA sequences were designed based exclusively on swine isolates. Examples of the COBRA sequence clustering are shown in Fig. C.1. Primary consensus HA sequences were aligned, and the most common amino acid was chosen resulting in secondary consensus sequences. The secondary and tertiary consensus sequences were aligned sequentially, and the most common amino acid at each position was selected ultimately resulting in the final consensus sequence referred to by one of four swine H1 COBRA HA designations (SW₁, SW₂, SW₃, SW₄) (Table C.2). Three of the four swine COBRA HA vaccines utilize HA amino acid sequences from H1N1 and H1N2 isolates in different configurations with the same representative years (Fig. C.1A and B). However, SW₄ was designed using swine HA sequences from isolates collected between 1930 and 2013 (Fig. C.1C).

An unrooted phylogenetic analysis of the aligned wild-type human, swine, and COBRA HA amino acid sequences determined that the COBRA sequences clustered into different lineages (Fig. C.2). One family has similarity to human seasonal influenza strains, and the other cluster is similar to the 2009 pandemic H1N1 swine strains. The alpha, beta, and gamma swine clades of the classical lineage cluster with the CA/09 pandemic-like virus, and the human seasonal viruses cluster with the delta lineage swine viruses. X₃ and X₆ both clustered with the human isolates most closely related to the human seasonal swine HA. P-1 COBRA was most closely related to the human isolates from the 1930-1950's which were unrelated to swine isolate HAs. SW-2 and SW-4 COBRAs were most closely related to each other, and

then to viruses in the classical swine lineage (Fig. C.2). Therefore, they were similar to the CA/09 HA sequence. Using p_{epitope} predictions, P₁, SW₂, and SW₄ should all elicit antibodies that neutralize CA/09 infection (Table C.5). In contrast, the SW₁ and SW₃ HA sequences, as well as X₃ and X₆ HA sequences, aligned closer to the human isolates and human seasonal-like swine lineage viruses (Fig. C.2). The p_{epitope} values indicate that these four HA antigens are similar to each other and human seasonal H1 viruses, such as A/Brisbane/59/2007 (Bris/07) or A/Swine/North Carolina/152702/2015 (SW/NC/15) (Table C.5). A BLAST search using each of the swine COBRA HA sequences revealed that each sequence was a unique sequence that has not been isolated from the environment (data not shown). The p_{epitope} values of the wild-type swine H1 influenza viruses indicated that classical lineage viruses may neutralize CA/09, such as A/Swine/Wisconsin/125/1997 (SW/WI/97), and that the human seasonal-like lineage viruses may protect against SW/NC/15, such as A/Swine/North Carolina/02744/2009 (SW/NC/02744/09). There were a few wild-type strains that had p_{epitope} values that predicted they would not bind or neutralize either classical or human seasonal-like lineage viruses, such as A/Swine/Spain/50047/2003 (SW/Spain/03).

Table C.5: The dominant p_{epitope} based predictions for vaccine effectiveness against the challenge strains.

Vaccine HA	A/California/07/2009		A/SW/North Carolina/152702/2015	
	Dominant p_{epitope}^a	Predicted Protection ^b	Dominant p_{epitope}^a	Predicted Protection ^b
PBS	-	-	-	-
SW ₁	0.455	-	0.375	+
SW ₂	0.235	+	0.636	-
SW ₃	0.727	-	0.25	+
SW ₄	0.235	+	0.682	-
P ₁	0.417	+	0.545	-
X ₃	0.727	-	0.227	+
X ₆	0.727	-	0.227	+
CA/09	0	+	0.636	-
SW/NC/15	0.636	-	0	+
A/SW/WI/125/97	0.292	+	0.682	-
A/SW/Korea/06	0.235	+	0.545	-
A/SW/MN/A01489606/15	0.25	+	0.727	-
A/SW/IN/P12439/00	0.121	+	0.636	-
A/SW/NC/34543/09	0.029	+	0.636	-
A/SW/NC/02744/09	0.682	-	0.167	+
A/SW/Spain/03	0.542	-	0.682	-
A/SW/Zhejiang/1/07	0.618	-	0.682	-
A/Chile/1/83	0.727	-	0.455	-
A/Singapore/06/86	0.636	-	0.273	+
A/New Caledonia/20/99	0.773	-	0.273	+

^aDominant p_{epitope} was the greatest p_{epitope} antigenic distance of the five antigenic sites

^b p_{epitope} value ≤ 0.442 was predicted to be more protective than a mock vaccination (+)

C.4.2 Predictive Structures and N-linked Glycosylation of the Swine COBRA HA antigens

Using a predictive structural modeling of swine COBRA H1 HA sequences, three-dimensional trimerized HA proteins were designed for the COBRA HA sequences (Fig. C.3A-G), nine wild-type swine HA sequences (Fig. C.3H-P), and five wild-type human HA sequences (Fig. C.3Q-U). Despite nearly identical predicted structures, the swine COBRA HA proteins did have subtle differences in the major antigenic antibody-binding and receptor-binding sites, more pronounced around the loop regions of the Sa and Sb sites (Fig. C.3). For example, all the H1 HA antigens have a Lys (K) at position 154 in the Sa region. However, classical lineage H1 HA proteins, including P1, SW2, and SW4 have a Gly (G) at position 155, whereas an Asp (N) is located at position 156 (Fig. C.3). In contrast, human or seasonal human-like swine influenza HA antigens have these amino acids transposed, with an Asp at position 155 and a Gly at 156. There are three exceptions. SW/Korea/o6 HA has a glutamic acid (E) at position 155 in the Sa region (Fig. C.3I). Interestingly, the COBRA SW1 HA has the N155 and N156 in the Sa region (Fig. C.3A), and the COBRA P1 HA has G155 and G156 in the Sa site (Fig. C.3E). Both these COBRA HA antigens represents a hybrid of classical and human seasonal-like HA amino acids in the Sa antigenic region.

There was little difference in the N-linked glycosylation patterns between any of the swine or human HA antigens, except in two locations (Figure C.4). Human and human seasonal-like swine HA, as well as SW1, SW3, X3, and X6 COBRA HA proteins, had putative glycosylation motif (N-X-S/T, where X is any amino acid except proline (J. I. Kim & Park, 2012; Wei et al., 2010)) at amino acids 125 and 160. No classical swine or pandemic-like HA antigens had these motifs. This includes P1, SW2, and SW4 COBRA HA antigens.

C.4.3 Vaccinated mice challenged with pandemic H1N1 influenza virus

BALB/c mice ($n>9$) were vaccinated three times at 4-week intervals via intramuscular injection with purified VLP vaccines expressing either COBRA HA, wild-type swine HA, or human HA plus an oil-in-

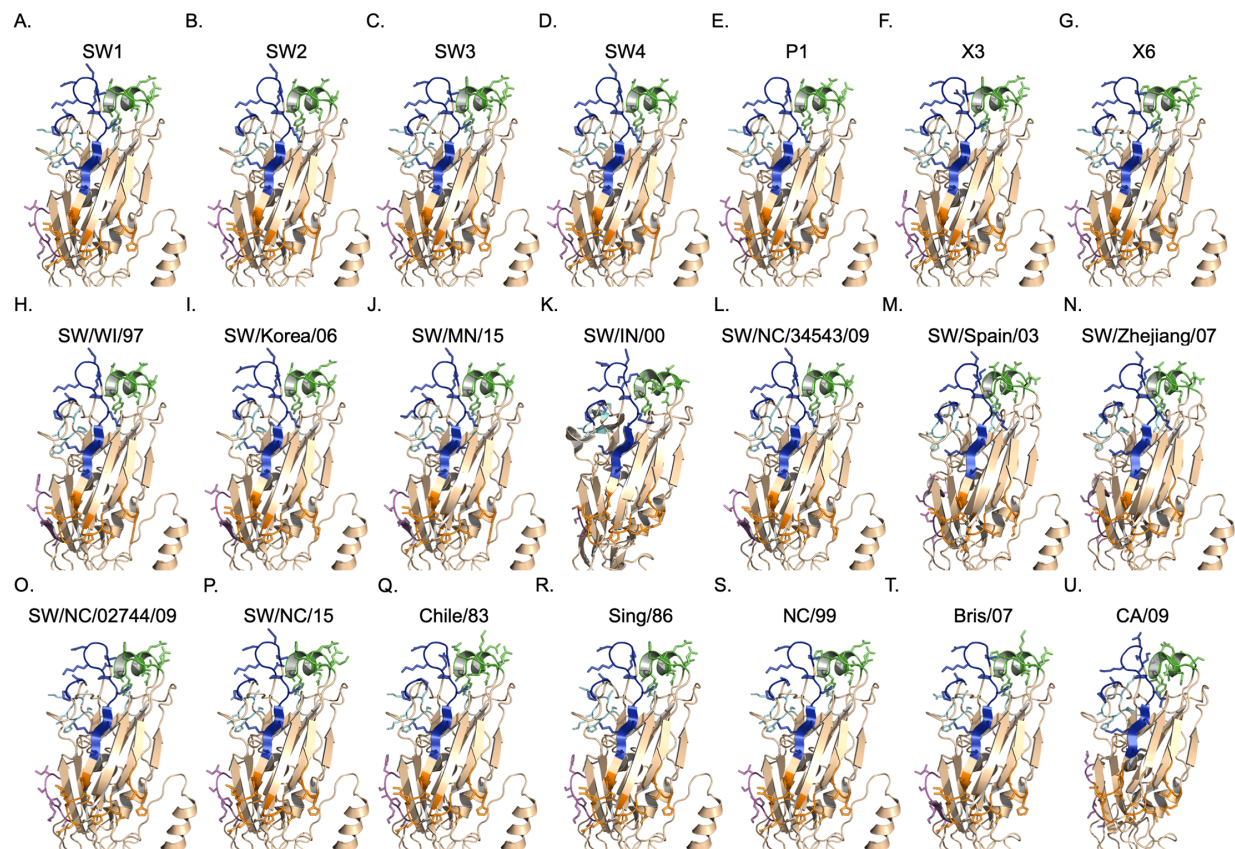


Figure C.3: Subtle differences in the Sa and Sb regions lead to structural differences among the COBRA and wild-type predicted structures surrounding the receptor-binding site. One monomer of each predicted trimer is shown for clarity. Protein structures predicted using SWISS-MODEL. CA/09's and SW/IN/oo's actual crystal structures were used. Antigenic sites Sa (blue), Sb (green), Cai (orange), Ca2 (teal), and Cb (purple) are indicated.

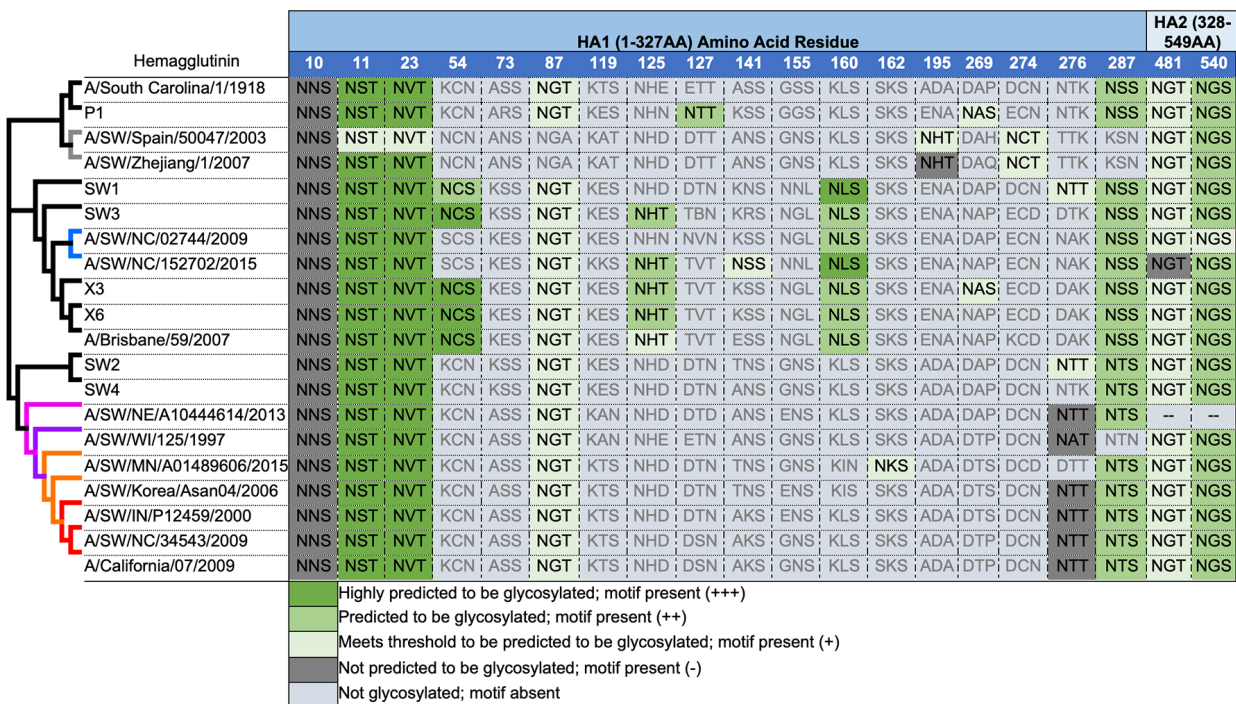


Figure C.4: Differential putative glycosylation sites between the human seasonal-like sequences and the classical swine sequences. A representative unrooted phylogenetic tree displays the genetic relationships, as well as, the clade classification.

water based adjuvant. To determine the protective efficacy of each swine COBRA HA vaccine, vaccinated mice were challenged with CA/09 influenza virus (5×10^4 PFU/ 50 µl) 4 weeks after the third vaccination (Fig. C.5). Mice vaccinated with SW₂, SW₄, P₁ or CA/09 HA VLP vaccines experienced little weight loss (Fig. C.5A and B) and all survived challenge (Fig. C.5E). Mock-vaccinated animals rapidly lost weight and many mice reached experimental endpoints (80% of original body weight) between 4-6 days post-infection (dpi). Mice vaccinated with SW₃, X₃, or X₆ had similar morbidity and mortality results as mock-vaccinated mice (Fig. C.5A and B). Mice vaccinated with SW₁ lost on average 10% of their original body weight by day 5 post-infection, but rapidly returned to original weight (Fig. C.5A). Some groups of mice vaccinated with wild-type swine VLP vaccines (SW/NC/34543/09, SW/WI/97) were protected against CA/09 challenge with little weight loss (Fig. C.5C and D). In contrast, mice vaccinated with VLPs expressing any of the other six wild-type swine HA antigens, lost between 10-15% of their body weight by day 6 post-infection with 50% of the mice in the SW/Korea/06 and SW/MN/15 groups succumbing to infection (Fig. C.5G). The range of weight loss observed at day 6 post-infection is shown in Figures 3H-J per individual mouse for each vaccine group. Mice vaccinated with SW₂, SW₄, and P₁ COBRA HA vaccines had little weight loss per group, which was consistent with the lack of detectable CA/09 virus in the lungs of mice collected at day 3 post-infection (Fig. C.5H-J). No virus was detected in mice vaccinated with SW₂, SW₄, P₁, SW/Zhejiang/07, SW/NC/34543/09 or CA/09 VLP vaccines (Fig. C.5K-M).

C.4.4 Vaccinated mice challenged with swine H1N2 influenza virus

To determine if these COBRA HA antigens would elicit protective immune responses against a human seasonal-like swine virus, vaccinated mice were challenged with SW/NC/152702/15 (H1N2) influenza virus (1×10^7 PFU/ 50 µl) 4 weeks after the third vaccination (Fig. C.6). All mice vaccinated with SW₁, X₃, and the homologous SW/NC/15 HA VLP vaccines quickly recovered from early weight loss and all survived challenge (Fig. C.6A-B). Mice vaccinated with SW₃, X₆ or CA/09 HA VLP vaccines had similar morbidity and mortality results as mock-vaccinated mice. By day 6 post-infection, mice vaccinated with SW₁ or SW/NC/15 lost on average 8% of their original body weight by day 6 (Fig. C.5C), but rapidly

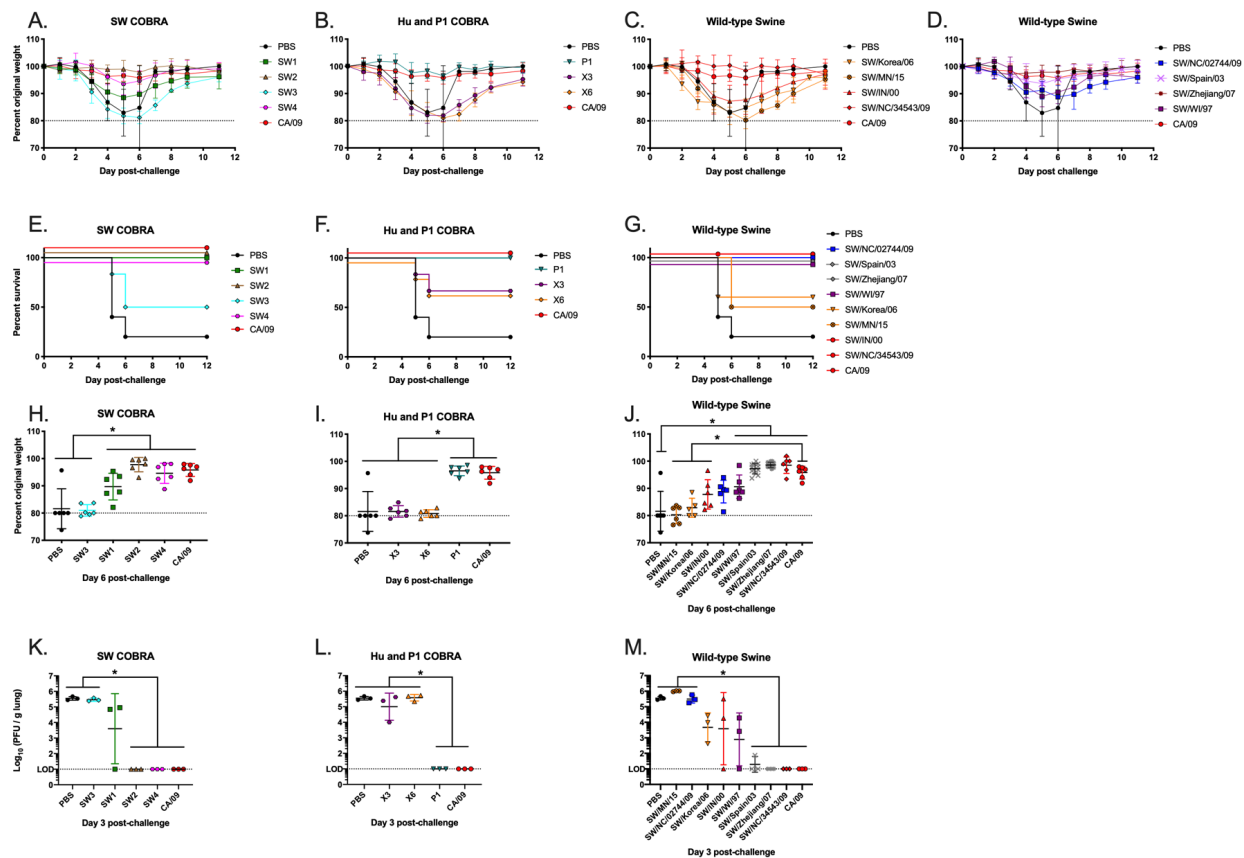


Figure C.5: A/California/07/2009 H1N1 viral challenge of vaccinated BALB/c mice. Mice vaccinated with either COBRA or wild-type HA VLP vaccines were challenged three weeks after final boost with 5×10^4 PFU of CA/09. Weight loss (A–D) and survival proportions (E–G) were monitored during the course of infection. The peak weight loss observed at six days post-infection was analyzed for statistical difference to the CA/09 group (H–J). The viral load of CA/09 was enumerated from challenged mice three days post-infection ($n = 3$) (K–M).

returned to their original weight. In contrast, mice vaccinated with VLPs expressing CA/o9 or any of the other six COBRA HA antigens, lost between 12-20% of their body weight by day 6 post-infection (Fig. C.5C-D). However, only mice vaccinated with SW/NC/15 HA VLPs had no detectable virus in their lungs at day 3 post-infection (Fig. C.5E-F). Mice vaccinated with SW1, X3, X6, or mock had lung viral titers between 10^4 to 10^5 PFU/lung. All the other groups had lung viral titers greater than 10^5 PFU/lung.

C.4.5 VLP vaccines with swine H1 HA antigens elicit antibodies with HAI activity against swine H1 strains, but not human H1 viruses

Serum was collected from vaccinated mice on day 56, following the third vaccination (Fig. C.7). Mice vaccinated with the SW1 VLP vaccine elicited antibodies with HAI activity exceeding 1:40 against 50% (2/4) of the human seasonal-like swine H1 lineage isolated from 2009 to 2015 and HAI activity against 45% (5/11) of the classical swine H1 lineage viruses in the panel (Fig. C.7A). Mice vaccinated with SW2 and SW4 had similar patterns of HAI activity against the viruses in the panel. Mice vaccinated with SW2 had antibodies with high HAI activity against one of four human seasonal-like swine H1 viruses and recognized all the classical swine H1 viruses (Fig. C.7B). SW4 had similar responses and recognized the same human seasonal-like swine virus (SW/NC/5043-1/09). However, these induced antibodies had lower HAI activity, and all the SW4 vaccinated mice did not detect SW/Korea/o6 and SW/MN/15 human classical H1 viruses to such a degree as SW2 (Fig. C.7D). The HAI activities induced by SW2 and SW4 antibodies were similar to antibodies induced by P1 COBRA HA (Fig. C.7E), which was designed using both human and swine H1 sequences. Mice vaccinated with SW3 recognized only one of seventeen swine viruses in the panel (Fig. C.7C), which was similar to HAI activities by antibodies induced by the X3 and X6 COBRA HA antigens (Fig. C.7F and G).

Mice vaccinated with seven of the nine VLP vaccines expressing wild-type swine H1 HA antigens had antibodies with HAI activity against at least thirteen of the seventeen viruses in the panel (Fig. C.8A-I). In addition, the CA/o9 HA VLP vaccine elicited antibodies with HAI activity against one human seasonal-like virus and all, except SW/NE/13, classical lineage viruses (Fig. C.8J). The SW/NC/15 elicited antibodies

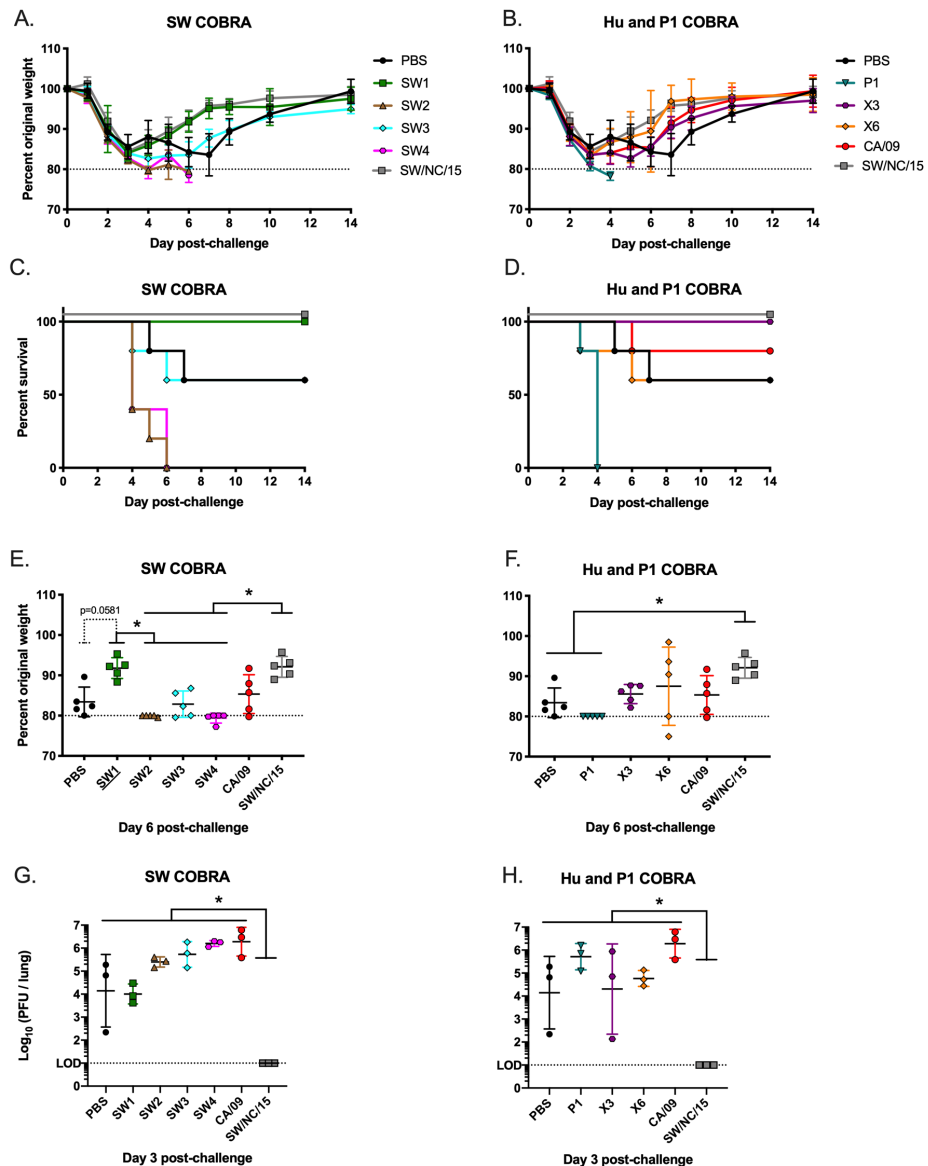


Figure C.6: A/Swine/North Carolina/152702/2015 H1N2 viral challenge of COBRA vaccinated BALB/c mice. Mice vaccinated with COBRA HA VLP vaccines ($n = 11$) were challenged three weeks after final boost with 1×10^7 PFU of A/Swine/North Carolina/152702/2015 H1N2. Survival proportions (A, B) and weight loss were monitored during the course of infection ($n = 5$). The peak weight loss observed at day six was analyzed for statistical difference to the SW/NC/15 group (C, D). The viral lung titer was determined from lungs ($n = 3$) harvested 3 days post-challenge (E, F).

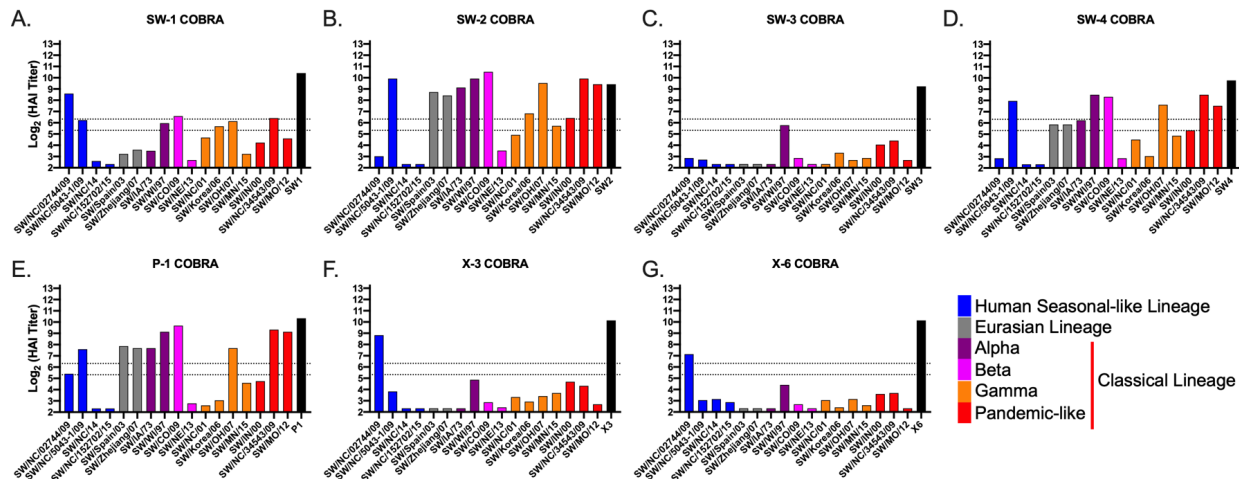


Figure C.7: HAI titers of COBRA VLP vaccinated mice sera against swine H1 VLPs. HAI titers were determined for each group of mice ($n \geq 5$) vaccinated at minimum twice (day 0 and 28) with wild-type HAs originating from swine or human H1 influenza viruses against a panel of seventeen swine H1 VLPs expressing their respective HA. HAIs were conducted with sera collected on day 56. Dotted lines indicate 1:40 and 1:80 HAI titer. Blue = Delta-2 human seasonal clade; Gray = Eurasian clade; Purple = alpha classical clade; Pink = beta classical clade; Orange = gamma classical clade; Red = pandemic classical clade.

with HAI activity against itself and SW/NC/14 (Fig. C.8B). Mice vaccinated with human seasonal HA VLP vaccines elicited antibodies with HAI activity against 73% of the viruses in the panel. Mice vaccinated with Sing/86 or Bris/07 had the same HAI pattern; detecting all viruses except two human seasonal-like viruses and two classic swine viruses (Fig. C.8L and N). None of the vaccines expressing human HA antigens detected SW/Zhejiang/07 or SW/MN/15. At least one of the four human seasonal HA VLP vaccines did not detect SW/NC/5043-1/09 (Chile/83 VLPs), SW/Spain/o3, SW/Korea/o6 (Sing/86, NC/99, Bris/o7 VLPs), SW/OH/o7 (Chile/83, NC/99 VLPs), and SW/IN/o0 (NC/99 VLPs). In contrast, when swine HA antigens were used in VLP vaccination, few elicited antibodies had HAI activity against human seasonal influenza viruses isolated from 1983 to 2007 (Fig. C.9). This same elicited antiserum from the Eurasian and classical swine lineage had HAI antibodies that recognized the CA/o9 virus (Fig. C.9C-I).

The antiserum from human seasonal-like lineage vaccinations, however, did not recognize any human virus (Fig. C.9A-B).

Although narrow breadth was seen in the elicited antiserum of the COBRA and wild-type HA vaccines to recognize the receptor binding site of the human seasonal-like SW/NC/15 hemagglutinin (Fig. C.7 and Fig. C.8) antibodies were elicited that bound to the HA by both COBRA (Fig. C.10A) and wild-type swine (Fig. C.10B). Against SW/NC/15 recombinant HA (rHA), SW₁, SW₃, X₃ and X₆ had intermediate antibody binding followed by the SW₂, SW₄, and P₁ COBRA vaccines. The classical swine strains SW/Korea/o6, SW/IN/oo and SW/NC/34543/o9 produced antibodies that bound to the human seasonal-like virus, but the titers decreased quicker. The human seasonal-like, Eurasian, and human seasonal vaccines all had minimal antibody binding (Fig. C.10C). When the vaccine antisera were tested against CA/o9 rHA (Fig. C.10D-F), all the COBRA groups had at least intermediate binding to the protein. The SW-2 COBRA and SW/NC/34543/o9 binding curves matched the CA/o9 elicited antisera profile. SW/MN/15 and SW/NC/o2744/o9 exhibited the lowest binding curves which correlated to the illness observed during challenge (Fig. C.5C, G, J, M).

C.5 Discussion

In the past 70 years, pig farming practices have changed from simple small-scale herds to immense herds in large, co-operate settings. These large herds are maintained by a constant introduction of young swine, leading to a constant supply of pathogen-susceptible animals and changes in farming practices (White et al., 2017) (Simon-Grife et al., 2012). Cross-species transmission and reassortment of avian and human influenza viruses in pigs has been documented (Castrucci et al., 1993; Lycett et al., 2012; Nelson et al., 2012; Vincent et al., 2008). These reassortment events result in emergence of genetically and antigenically diverse influenza viruses within the pig population with pandemic potential (C. S. Anderson et al., 2018; T. K. Anderson et al., 2013; Lorusso et al., 2010; Rajao et al., 2018). In 2009, a pandemic-like virus of swine origin, originated in Mexico and quickly spread to the United States and ultimately leading to a worldwide pandemic (Lemey et al., 2009). With the diversity of circulating swine-like H1 viruses, there is an urgent

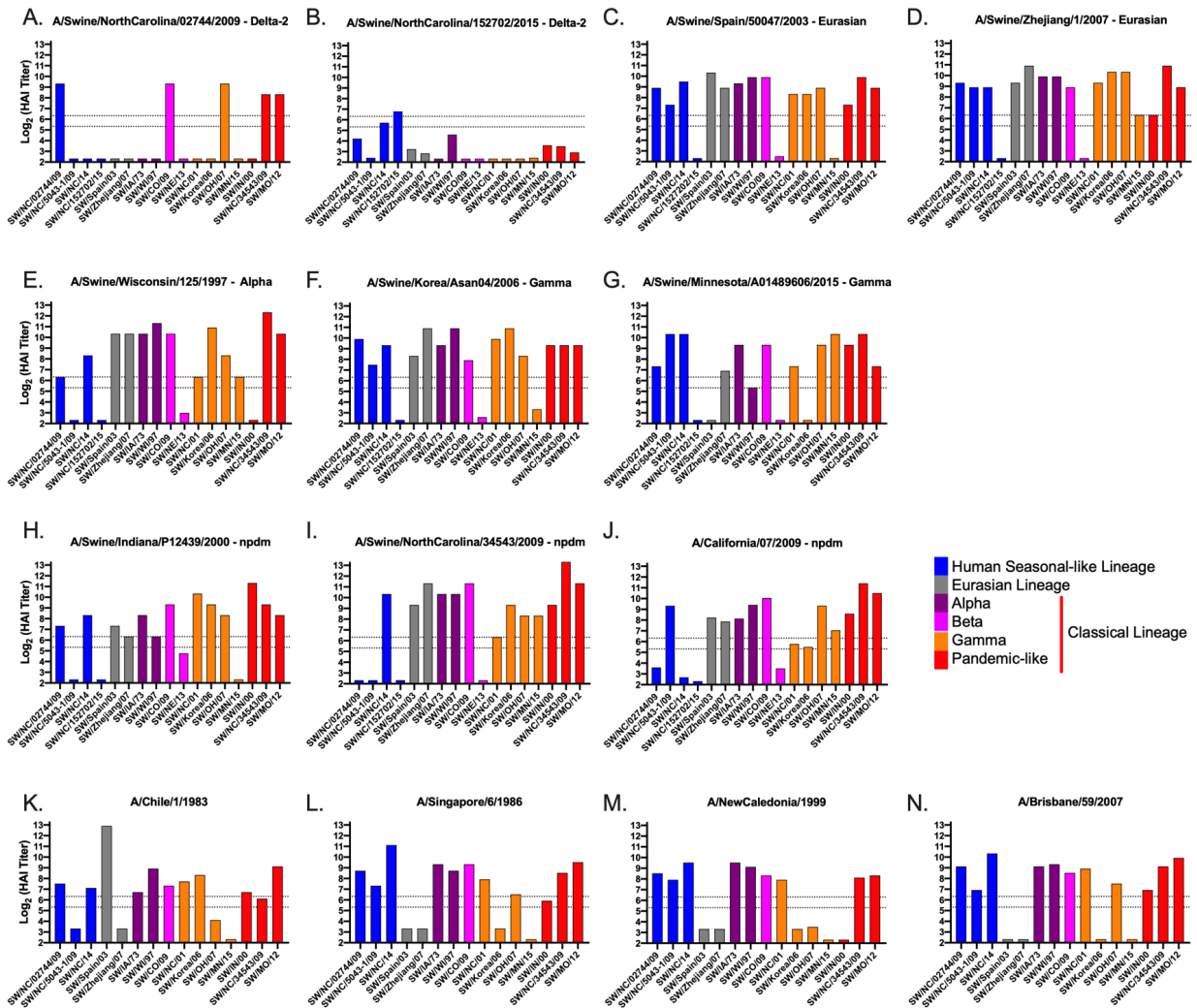


Figure C.8: HAI titers of swine and human wild-type HA VLP vaccinated mice sera against swine H1 VLPs. HAI titers were determined for each group of mice ($n \geq 5$) vaccinated at minimum twice (Day 0 and 28) with wild-type HAs originating from human and swine H1 influenza viruses against a panel of nineteen swine H1 VLPs expressing their respective HA. HAIs were conducted with equally pooled sera collected on day 56. Dotted lines indicate 1:40 and 1:80 HAI titer.

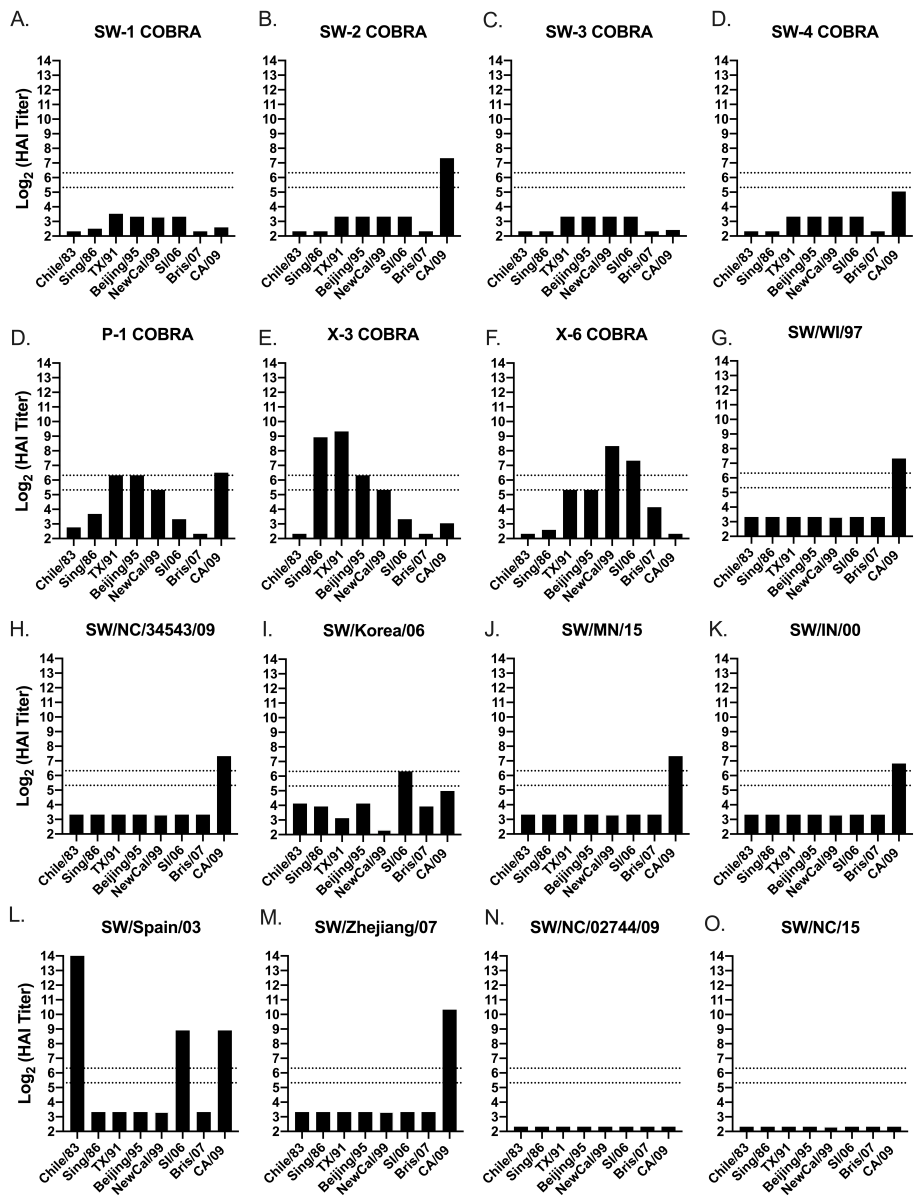


Figure C.9: HAI titers of swine wild-type HA VLP vaccinated mice sera against human H1N1 viruses. HAI titers were determined for each group of mice ($n \geq 5$) vaccinated at minimum twice (Day 0 and 28) with wild-type HAs originating from swine H1 influenza viruses against a panel of eight human H1N1 viruses. HAI titers were conducted with sera collected on Day 56. Dotted lines indicate 1:40 and 1:80 HAI titer.

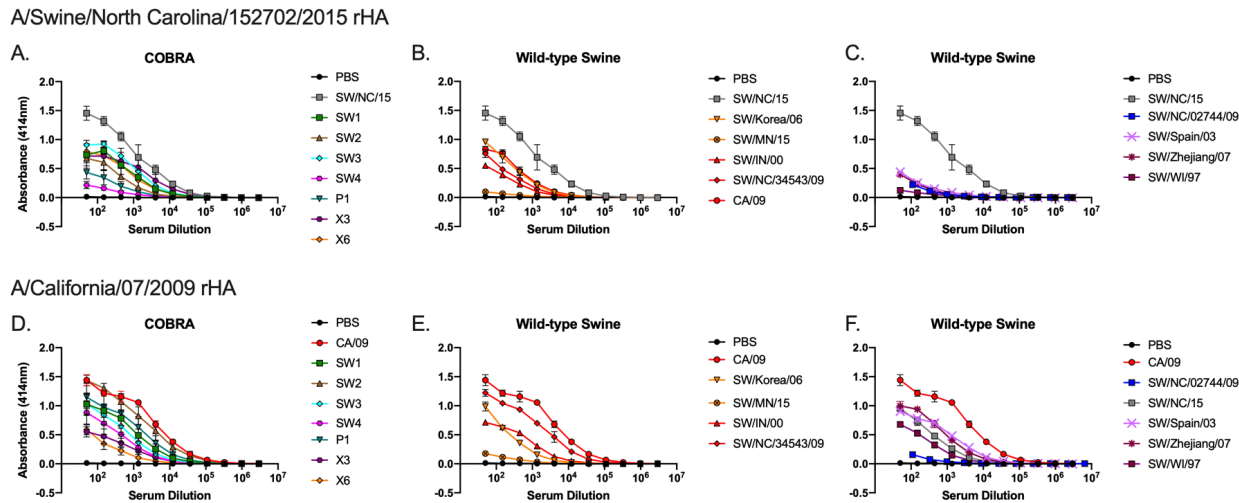


Figure C.10: ELISA of elicited antibodies against either SW/NC/15 or CA/09 recombinant HA protein. HA-specific IgG levels in the serum of mice vaccinated with various H1Nx VLP vaccines tested in an ELISA. (a-c) Antisera tested against rHA from SW/NC/15. (d-f) Antisera tested against rHA from CA/09. Antisera collected from mice vaccinated with (a and d) COBRA HA vaccines; (b, c, e and f) Wild-type HA vaccines.

unmet need to develop universal pandemic vaccine strategies to control spread of swine influenza viruses in pig populations, as well as, to control the potential spread of these viruses to humans. Despite the economic importance of swine influenza viruses, immune mechanisms of protection induced by natural infection or vaccination have been understudied in pigs compared to small animal models or humans. Neutralizing antibodies with HAI activity correlate with improved protection in humans and suggests that similar antibodies could protect against swine influenza viruses in pigs. However, immune mechanisms, such as cell-mediated immunity through direct killing, antibody dependent cellular cytotoxicity (ADCC), or induction of mucosal IgA may also contribute protection against swine influenza viruses in pigs. The administration of influenza vaccines that provide more “universal” protection against these viruses in both pigs and humans is needed.

The COBRA method uses multiple rounds of consensus building based upon not only the phylogenetic sequence of each isolate, but also the outbreak and specific time that each isolate was collected,

thereby eliminating the bias in the number of sequences uploaded to online databases. Previously, our group has demonstrated the effectiveness of the COBRA HA antigens for H₅N₁ (Giles, Crevar, et al., 2012; Giles & Ross, 2011b), H₃N₂ (Allen, Jang, et al., 2018; Allen, Ray, et al., 2018b; T. M. Wong et al., 2017), and H₁N₁ against human seasonal and pandemic influenza viruses (Carter et al., 2016b). These H₁N₁ COBRA HA proteins (X₃, X₆, and P₁) elicited antibodies with HAI activity against a range of human H₁N₁ viruses spanning the last 100 years. However, when antibodies elicited by these same three COBRA HA vaccines were tested against swine H₁ influenza viruses, the effectiveness of these vaccine antigens decreased. The X₃ and X₆ H₁N₁ HA COBRA proteins were designed from predominantly human seasonal H₁ influenza HA sequences (Carter et al., 2016b). The antibodies, while effective against human seasonal H₁N₁ influenza viruses, had little or no HAI activity against either classical or human seasonal-like swine influenza viruses (Fig. C.7). And the P₁ COBRA HA antigen, a hybrid derivative HA designed using both human and swine influenza HA input sequences (Carter et al., 2016b), while more effective at eliciting antibodies with HAI activity classical swine influenza viruses, was less effective against human seasonal-like swine influenza viruses.

In this study, we used the COBRA approach to design and develop HA vaccine candidates solely based upon swine H₁ HA input sequences. Four new COBRA HA antigens (SW₁₋₄) were developed following multiple rounds of sequence alignment to generate a single unique swine H₁ HA sequence only. The swine specific COBRA HA antigens, SW₁ and SW₃, elicited antibodies with HAI activity, but did not protect against classical swine influenza virus infections, which was similar to the previously published X₃ and X₆ COBRA HA antigens (Carter et al., 2016b). However, SW₁ was as effective at protecting mice against the H₁N₂ human seasonal-like swine influenza virus, SW/NC/15 (Fig. C.6). Furthermore, SW₂ and SW₄ COBRA HA antigens elicited antibodies with similar HAI activity as the P₁ COBRA HA. In addition, all three of these antigens protected against the CA/09 pandemic-like influenza virus, but none of them elicited protective immunity against the human seasonal-like swine virus. These results indicate that, while similar, the swine COBRA HA antigens have epitopes that allow for the elicitation of antibodies with HAI activity against subsets of swine influenza viruses, but are missing epitopes that

allow for elicitation of antibodies against human seasonal H1 influenza viruses. Concurrently, the human seasonal COBRA HA antigens, X₃ and X₆, elicit antibodies specific for human seasonal H1N1 influenza viruses only. However, since the COBRA P₁ HA incorporates both swine and human specific epitopes, this HA antigen elicits a broader breadth of HAI activity. However, the antibody profile indicates that P₁ elicited antibodies are still missing some critical epitopes found in both swine and human H1 influenza viruses, since P₁ elicited antibodies do not have HAI activity against some important H1 influenza viruses, such as A/Brisbane/59/2007 (Carter et al., 2016b). Future studies using monoclonal antibodies will need to determine the specific epitopes on each of these COBRA antigens (alone or in combination) that elicit specific protective antibodies against the panel of swine and human viruses.

Analysis of amino acids within the antigenic sites indicated a pattern that strongly suggests an existence of shared epitopes amongst swine and human influenza viruses (Fig. C.11). SW₁ and SW₃ have a more human seasonal-like set of amino acids in the antigenic sites and have similar predicted HA structures (Fig. C.3). Both these HA vaccines sequences were generated exclusively or predominately from H1N2 swine influenza viruses, which implies that the HA sequences in many H1N2 viruses are more closely related to the HA in human seasonal influenza viruses. This is consistent with the observation of cross-reactivity of human H1N1 antisera against swine H1 viruses (Myers et al., 2006). In contrast, the SW₂ and SW₄ HA sequences were developed using primarily HA sequences from H1N1 influenza viruses, which biases the HA to a classical or pandemic-like phenotype. Indeed, the major antigenic sites in SW₂ and SW₄ have many identical amino acids as the CA/09 and P₁ HA sequences. Structural analysis of the antigenic sites showed similarity especially around the Sa antigenic site that could potentially determine vaccine effectiveness.

There was little difference in the N-linked glycosylation patterns between any of the swine or human HA antigens (Table C.4), except in two locations at amino acids 125 and 160. No classical swine or pandemic-like HA antigens had these motifs, including P₁, SW₂, and SW₄ COBRA HA antigens. Glycosylation in HA is important for the folding and stability of the protein (Hebert et al., 1997), and, in some cases, significantly affects receptor binding and cleavage of the precursor HAo protein, influencing

Antigenic Site	Amino Acid Residues	CA/09	SW/NC/34543/09	SW/IN/00	SW/WI/97	SW/MN/15	SW/NE/13	SW/Korea/06	SW4	SW2	SW/Zhejiang/07	SW/Spain/03	P1	SW1	Sing/86	Chile/83	SW3	X3	Bris/07	X6	NewCal/99	SW/NC/02744/09	SW/NC/152702/15
Swine Lineage																							
Gap	130	K K R R K K R R R R R K R K K - K - - - - - -																					
Sa	153	K K K K K K K K K K K K K K K E V E G G G V V																					
	155	G G E G G E E G G G G G N N N N N N N N N N N N																					
	157	S S S S S S S S S S S S S S L S S L L L L L L L																					
	160	K K K K K K K K K K K K K K K N N N N N N N N N N																					
	184	T T T T T T N T T T T T T N N N N N N N N N N N																					
Sb	185	S S S S S S S S S S D D S I I I I I I I I I I I M																					
	186	A A A N A T A G G S R T G G E G G G G G G G G E																					
	189	Q Q Q Q Q Q R Q Q Q Q Q R R K R K R R R R R R R																					
	190	S S S S S T T S S T T S T T S T A T T A A A A A A A																					
	193	Q Q Q Q Q Q Q Q Q Q Q Q H R H H H H H H H H H H																					
	194	N N N N N N N N N N N N N N N T T K T T T T T T																					
	195	A A A A A A A A A A A A A N N E E E E E E E E E E																					
	166	I I I I T I I I I I T T V I V V I V A A V T T																					
Ca1	168	D D N N N N N N N N N N N N N N N D N N N N N K K																					
	170	G G G G E K G E E G G G E E E E E E E E E E E E																					
	205	R R R K K K R K K K K N H H H H H H H H H H H H																					
	137	P P P P P P P P P P S S S S S S S S S S S S S S S S																					
Ca2	139	A A A A A A A A A A A A S S A N K K N N N N N S N																					
	141	A A A A A T A T A T A A K K R K K K K E K R K N																					
	142	K K K N N N N N N N N N N S N S S R S S S S S S S																					
	222	D D D G D D G D D E E G D D N D D D D D D N																					
	71	S S F F S F I I I L L L I F F I F I I I I I I																					
Cb	72	T T T T T T A T T T T S S S S S S S S S S S S S S S																					
	73	A A A A A A A A A K K A A A K K K K K K K K K K K K																					
	74	S S S S S S S S S S N N R S K K S E E E E E E E E																					

Figure C.II: Comparison of antigenic site residues of CA/09 and SW/NC/152702/15. The order from left to right is based on decreasing similarity to CA/09 antigenic residues (red). For each SW/NC/15 residue (blue) a penalty was scored (-1). Completely different amino acid residues (white) scored no penalty. The narrowed antigenic site residues were used for the comparison. Sites where CA/09 and SW/NC/152702/15 were identical are not shown. The color legend for each antigenic site is associated with the matching PYMOL site.

the virulence and antigenicity of the virus (Zhang et al., 2013). Our group and others have shown that glycosylation on the HA globular head domain physically shields the antigenic sites, preventing antibody recognition and leading to viral evasion from antibody-mediated neutralization (Laursen & Wilson, 2013; Pentiah et al., 2015; Tate et al., 2014; Zhang et al., 2013; Zost et al., 2017). HA antigens acquire increased glycans as influenza viruses circulate in people (Altman et al., 2019), therefore it is not surprising that human-like wild-type or COBRA H1 HA antigens have additional glycans that classical swine viruses do not. More analysis aimed at elucidating the mechanism(s) of COBRA HA vaccines is needed to generate next-generation vaccine designs. An approach that maps out the antigenic epitopes on these vaccine candidates, as well as addressing effect of glycosylation, will provide a better understanding how these vaccines operate.

The P1, SW2, and SW4 COBRA HA antigens elicited antibodies with HAI activity against Eurasian H1 isolates. In Europe, an avian H1N1 influenza virus was first detected in pigs in Belgium in 1979, referred to as ‘avian-like’ swine H1N1 lineage (Nelson et al., 2011). This lineage slowly established itself in the pig population eventually replacing classical swine H1N1 influenza viruses and also reassorted in pigs with human H3N2 viruses (A/Port Chalmers/1/1973-like) (I. H. Brown, 2000). Importantly, to date, there are no notable cases of Eurasian avian-like swine H1N1 influenza viruses circulating in North America. However, the potential of introduction of viruses to North American herd is plausible, therefore, a vaccine that efficiently elicits protective immune responses against all H1 influenza viruses is highly desired. The SW2 and SW4 vaccines were effective in eliciting antibodies with HAI activity against the Eurasian derived swine viruses (Fig. C.6). However, it was surprising that wild-type HA antigens isolated from swine viruses induced antibodies with broad HAI activity. In particular, mice vaccinated with VLPs expressing wild-type Eurasian HA were the most efficient at eliciting broadly reactive antibodies against both Eurasian and North American isolates. This strongly supports the possibility of making a universal vaccine with worldwide application.

Despite the similarities between the human seasonal-like HA antigens and, for example, COBRA SW1 or SW3, these vaccines were not as effective as the SW/NC/15 HA homologous vaccine (Fig. C.6). There

is no clear explanation for why only mice vaccinated with SW/NC/15 HA VLP vaccine were protected when the antigenic sites of SW₁ and SW₃ HA antigens are highly similar to the SW/NC/15 HA, with similar predicted glycosylation patterns and similar predicted three-dimensional structures. Even though SW₁ HA VLP vaccinated mice had detectable virus in the lung (day 3 p.i.), mice vaccinated with the SW₁ vaccine all survived challenge and had the lowest viral lung titers, other than the homologous vaccine. The SW₁ vaccine antisera was, however, able to bind to SW/NC/15 rHA implying that the SW₁ COBRA was able to elicit antibodies against the HA, but these were not receptor site binding. Antibodies elicited by vaccination may have broader activity than just receptor binding site inhibiting, as seen by the lack of HAI titer, but the presence of antibody binding (Fig. C.10D). Future studies will need to tease out the specific epitopes on these HA antigens that elicit the most effective neutralizing antibodies.

It is estimated that more than 100,000 workers work in swine barns with live pigs, and in just Iowa alone – the leading swine-producing US state - more than 25 million hogs per year are reared (a ratio of more than 9 swine per human resident) (Myers et al., 2006). Therefore, it is likely that many people around the world have been exposed to multiple swine influenza viruses (Lantos et al., 2016) and have a B cell memory pool and antibody repertoire with HAI activity against multiple swine influenza viruses, but also historical human strains that represent various antigenic types (Paccha et al., 2016; T. Yoshida et al., 2010). Our group and others have demonstrated that ferrets pre-immune to H1N1 influenza viruses elicited antibodies with broader HAI activity against more antigenic variants following COBRA HA vaccination than using wild-type HA antigens (Carter et al., 2013; Kirchenbaum et al., 2016; Y. Li et al., 2013). Therefore, we would expect these COBRA vaccines to be even more effective in people pre-existing memory B cells to previous swine influenza exposures. Overall, this study demonstrated that computationally optimized HA antigens are a viable way of designing vaccines with broader application for both human and swine population, which is important given the zoonotic potential of influenza viruses. vaccines that are aimed at protecting both humans and swine population.

C.6 Acknowledgements

The authors would like to thank Dr. Ying Huang, Z. Beau Reneer, and James D. Allen for technical assistance, and Dr. Mark Tompkins' laboratory for graciously providing the A/Swine/North Carolina/152702/2015 virus. Furthermore, we thank both Drs. Mark Tompkins and Constantinos Kyriakis for helpful discussions. Certain H1N1 and H1N2 influenza A viruses were obtained through the Influenza Control of Influenza, Centers for Disease Control and Prevention, Atlanta, GA, USA. The authors would like to thank the University of Georgia Animal Resource staff, technicians, and veterinarians for animal care.

C.7 Competing Interests

No competing interests.

C.8 Funding Information

This work was funded, in part, by the University of Georgia (UGA) (MRA-001). In addition, TMR is supported by the Georgia Research Alliance as an Eminent Scholar.

APPENDIX D

AN INFLUENZA VIRUS HEMAGGLUTININ COMPUTATIONALLY OPTIMIZED BROADLY REACTIVE ANTIGEN ELICITS ANTIBODIES ENDOWED WITH GROUP I HETEROSUBTYPIC BREADTH AGAINST SWINE INFLUENZA VIRUSES¹

¹Skarupka, A. L., Reneer, Z. B., Abreu, R. B., Ross, T. M., & Sautto, G. A. An influenza virus hemagglutinin computationally optimized broadly reactive antigen elicits antibodies endowed with group 1 heterosubtypic breadth against swine influenza viruses. *J Virol.* 2020. 94:e02061-19. <https://doi.org/10.1128/JVI.02061-19>. Reprinted here with permission of the publisher.

D.1 Background

Computationally Optimized Broadly Reactive Antigens (COBRA) designed for different influenza virus subtypes (H₁N₁, H₃N₂ and H₅N₁) elicit a subtype-specific broad antibody (Ab) response in naïve as well as in pre-immune influenza virus animal models (Allen et al., 2019; Allen, Ray, et al., 2018a; Carter et al., 2017; Carter et al., 2016c; Giles, Crevar, et al., 2012; Sautto et al., 2019; Sautto, Kirchenbaum, Ecker, et al., 2018; Sautto, Kirchenbaum, & Ross, 2018; Sautto & Ross, 2019). In particular, an H₁ hemagglutinin (HA) COBRA candidate, named P₁, has been designed by a multiple-sequence alignment of HA sequences belonging to H₁ swine and human strains (Carter et al., 2016c) Importantly, immunization with P₁ elicits a broad neutralizing Ab response against H₁ human and swine viruses (Carter et al., 2016c; Sautto, Kirchenbaum, Ecker, et al., 2018; Skarlupka et al., 2019). Recently, we generated a panel of P₁-specific mouse monoclonal Abs (MAbs) with the aim to dissect the Ab response to P₁. As previously described, these MAbs feature different functional activities, spanning from narrowly to broadly reactive against H₁N₁ human viruses (Sautto et al., 2020). In this study, we investigated the breadth of hemagglutination inhibition (HAI) featured by representative P₁-elicited MAbs, along with those generated following immunization with wild-type historic H₁N₁ human vaccine strains in order to dissect the breadth of HAI activity of the P₁-elicited response against influenza swine viruses.

D.2 Results and Discussion

As shown in Fig. D.1A, P₁-specific MAbs featured a differentiating breadth of HAI activity, spanning from narrowly to broadly reactive against H₁N₁, H₁N₂, and H₂N₃ swine viruses. Interestingly, MAbs endowed with broad HAI activity against a panel of human H₁N₁ viruses featured a narrower HAI profile against swine viruses. Comparatively, those endowed with a narrower profile against human viruses featured a broader profile against swine viruses belonging to the Eurasian, classical, and human seasonal-like lineages (Sautto et al., 2020). Unsurprisingly, due to its swine origin, CA/09-specific MAbs, previously classified to have a narrow profile of neutralization activity against pandemic and pandemic-like viruses (Sautto

et al., 2020), collectively exhibited a broad HAI activity against H1N1 and H1N2 swine viruses and none against the A/Swine/Missouri/4296424/2006 H2N3 virus (Fig. D.1B).

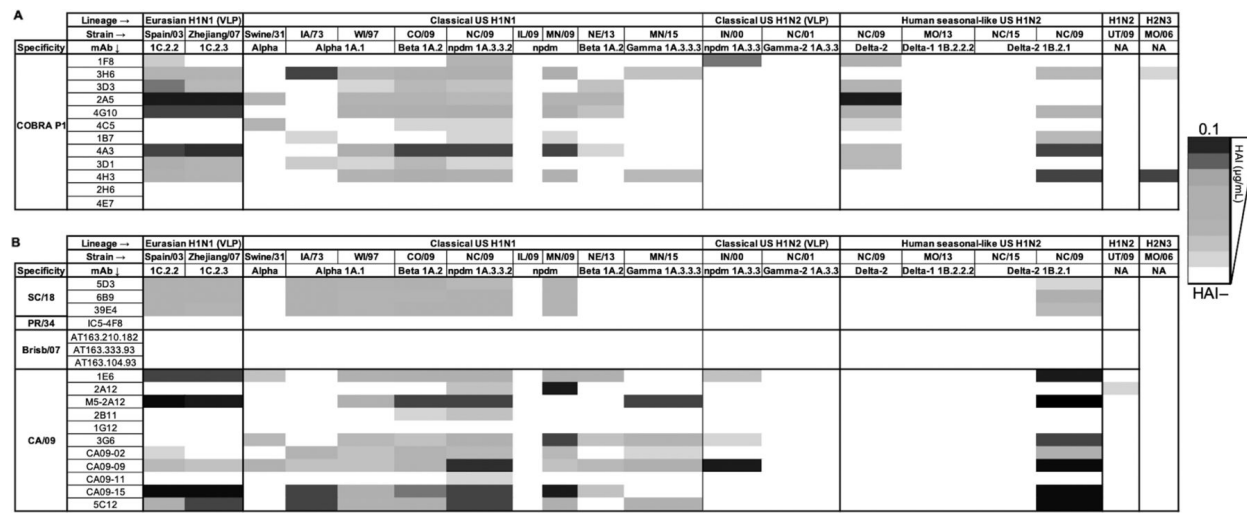


Figure D.1: HAI and neutralizing activity breadth of Pi- (A), seasonal-, and pandemic-specific (B) MAbs against influenza A H1N1, H1N2, and H2N3 swine viruses.

Interestingly, a Pi-specific MAb (4C5), previously demonstrated to have no HAI activity against any of the human H1N1 strains (Sautto et al., 2020), showed detectable HAI activity against H1N1 and H1N2 swine viruses, suggesting that its epitope is particular to swine viruses and not to human seasonal, pandemic, and pandemic-like HA proteins. The antigenic cartography segregates MAbs based on their HAI profile against human and swine viruses, with the Pi and pandemic-specific MAbs clustering together as opposed to the seasonal (Brishb/07)-specific MAbs (Fig. D.2) (Sautto et al., 2020; D.J. Smith et al., 2004). However, further investigation aimed at determining the amino acid contact residues of these MAbs will improve the resolution of the recognized epitopes, clarify distinctions between human- and swine-specific H1 epitopes, and elucidate the mechanism of breadth conferred by COBRA immunogens.

D.3 Acknowledgements

The MAbs 5D3, 6B9, 39E4, IC5-4F8, RA5-22, 1C5, 5C12, CA09-02, CA09-09, CA09-11, and CA09-15 were obtained from the Biodefense and Emerging Infections (BEI) Resources Repository while AT170.558.146,

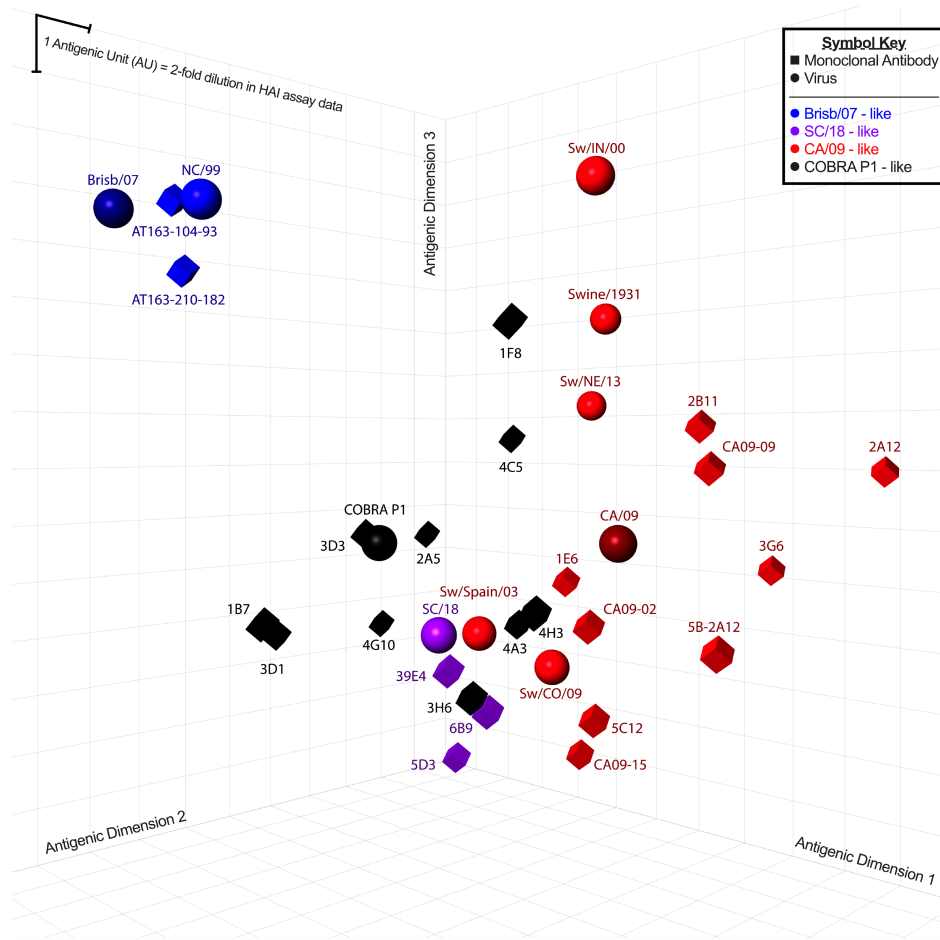


Figure D.2: Antigenic cartography map of PI-, seasonal-, and pandemic-specific MAbs. Map was drawn based on the minimum HAI concentration from this and previous studies (Sautto et al., 2020).

AT_{170.119.5}, AT_{163.272.54}, AT_{163.210.182}, AT_{163.333.93}, AT_{163.104.93}, AT_{163.329.189} MAbs were obtained from the Influenza Reagent Resource (IRR). The A/North Carolina/152702/2015, A/North Carolina/02744/2009, A/Illinois/02860/2009, A/Minnesota/02751/2009, A/Missouri/A01444664/2013, A/Swine/1931, A/Utah/02861/2009, and A/Nebraska/A01444614/2013 viruses were kindly provided by S. Mark Tompkins, Ralph Tripp (University of Georgia), and the Minnesota Veterinary Diagnostic Laboratory (University of Minnesota). Finally, we thank Silvia Carnaccini for helpful discussions.

D.4 Competing Interests

No competing interests.

APPENDIX E

INFLUENZA HEMAGGLUTININ
ANTIGENIC DISTANCE MEASURES
CAPTURE TRENDS IN HAI DIFFERENCES
AND INFECTION OUTCOMES, BUT ARE
NOT SUITABLE PREDICTIVE TOOLS¹

¹Skarupka, A. L., Handel, A. & Ross, T. M. (2020). Influenza hemagglutinin antigenic distance measures capture trends in HAI differences and infection outcomes, but are not suitable predictive tools. *Vaccine*, 38(36). 2020. doi:10.1016/j.vaccine.2020.06.042. Reprinted here with permission of the publisher.

E.I Abstract

Vaccination is the most effective method to combat influenza. Vaccine effectiveness is influenced by the antigenic distance between the vaccine strain and the actual circulating virus. Amino acid sequence based methods of quantifying the antigenic distance were designed to predict influenza vaccine effectiveness in humans. The use of these antigenic distance measures has been proposed as an additive method for seasonal vaccine selection. In this report, several antigenic distance measures were evaluated as predictors of hemagglutination inhibition titer differences and clinical outcomes following influenza vaccination or infection in mice or ferrets. The antigenic distance measures described the increasing trend in the change of HAI titer, lung viral titer and percent weight loss in mice and ferrets. However, the variability of outcome variables produced wide prediction intervals for any given antigenic distance value. The amino acid substitution based antigenic distance measures were no better predictors of viral load and weight loss than HAI titer differences, the current predictive measure of immunological correlate of protection for clinical signs after challenge.

E.2 Introduction

Type A influenza virus (IAV) causes annual, seasonal epidemics and occasionally devastating pandemics (Cox & Subbarao, 2000; Fedson, 2018; Rener & Ross, 2019). Influenza virus infections negatively affect the health of both the human population and the world economy (McElwain & Thumbi, 2017; Putri et al., 2018; Sellers et al., 2017). The most effective way to combat influenza is through vaccination. In general, the annual seasonal influenza vaccine is derived of two IAV strains and two influenza B strains (IBV), which represent dominant circulating strains in the human population. However, due to viral evolution and the time manufacturers need to produce the annual vaccine, there is often a mismatch in the antigenic version of the influenza strains selected in the vaccine compared to the influenza viral variants co-circulating during the next influenza season. The effectiveness of the annual vaccine is decreased if the vaccine strain significantly differs from infecting strains (Tricco et al., 2013).

Twice a year (once for each the Northern and Southern hemisphere), governmental agencies recommend to vaccine manufacturers strains to include in the annual vaccine (Grohskopf et al., 2019). Influenza experts in epidemiology, public health, and biomedical sciences decide if a change in the vaccine strain is recommended for the upcoming season based upon the most current surveillance, laboratory, and clinical study data at the time. Often, these recommendations are based upon the hemagglutination inhibition (HAI) assay, where the cross reactivity of ferret reference serum produced from infection with influenza vaccine strains is assessed to currently circulating viral variants (Organization, 2019). An 8-fold drop in HAI activity often results in a strain change recommendation for the next season.

Currently, there is a goal to develop universal influenza vaccines (Paules & Fauci, 2019). A variety of strategies are being used that rely on improved antigen development, delivery, adjuvants and immune assays (Vemula et al., 2017; Yakubogullari et al., 2019). These candidates are assessed for the elicitation of protective immune responses in pre-clinical, and then, clinical studies. To ease the burden of these expensive and time-consuming studies, computational tools have been developed to assist in vaccine

selection and to improve vaccine effectiveness (Bedford et al., 2014; Luksza & Lassig, 2014; Morris et al., 2018; Neher et al., 2014).

The antigenic differences between influenza viruses are defined by the ability of the antibodies to target the surface glycoprotein, the hemagglutinin (HA) and, in particular, the receptor binding site (RBS) domains on HA (Cattoli et al., 2011; M. Liu et al., 2015; Ndifon et al., 2009). The HA amino acid sequence is composed of highly conserved regions that are structurally and functionally necessary to bind to host cell sialic acid receptors and mediate viral fusion and entry to host cells (X. Xiong et al., 2014). In addition, there are highly variable head regions of the HA that are primary targets of the host antibody responses (Caton et al., 1982a; Tsuchiya et al., 2001; Webster & Laver, 1980). These regions, or antigenic sites, differ in size and number on each HA antigen subtype, with the greatest differences observed in HA between subtypes.

Computational methodologies can be used to assist with the vaccine selection process (Bedford et al., 2014; Klingen et al., 2018; Luksza & Lassig, 2014; Morris et al., 2018; Neher et al., 2016; Neher et al., 2014; Peng et al., 2017; Steinbrück et al., 2014; Steinbrück & McHardy, 2012). However, one difficulty is that the genetic similarity between two HA amino acid sequences does not correlate reliably with the antigenic distance between two strains (D. J. Smith et al., 2004). One or two amino acid differences in the HA can alter the profile of newly elicited antibodies or the ability of previously generated antibodies to neutralize (Koel et al., 2013; Koel et al., 2015; Koel et al., 2014). In vitro methods have been used to quantify and compare the antigenic distance of different influenza strains using HAI activity by ferret antisera with vaccine efficacy (Archetti & Horsfall, 1950; Bedford et al., 2014; Fonville et al., 2014; Harvey et al., 2016; Lee & Chen, 2004; D. J. Smith et al., 1999) or with sequence based antigenic distances to correlates of protection (C. S. Anderson et al., 2018). Measuring the HA epitope sequence based antigenic distances between strains in the annual vaccine and circulating strains (V. Gupta et al., 2006) has been found to correlate with vaccine effectiveness in humans (Bonomo & Deem, 2018; Deem & Pan, 2009; V. Gupta et al., 2006; X. Li & Deem, 2016; Munoz & Deem, 2005; Pan et al., 2011; H. Sun et al., 2013) or used to predict HAI titers (Neher et al., 2016). Analysis of just the immunodominant HA epitopes of the protein

sequence and not the entire molecule was proposed to improve the ability to predict HAI titers (Lee & Chen, 2004). The measure of antigenic distance derived from the assumed immunodominant epitope, known as the dominant p_{epitope} value, was validated using historical influenza vaccine effectiveness data from people reporting influenza illness-like symptoms following vaccination with commercial influenza vaccines (Bonomo & Deem, 2018; Deem & Pan, 2009; V. Gupta et al., 2006; X. Li & Deem, 2016; Pan et al., 2011). In this study, p_{epitope} and related measures that use protein sequence information to estimate antigenic distance (in the following referred to as antigenic distance measures (ADM)), were examined on whether they could be useful predictors of HAI differences and infection outcomes in animal studies.

E.3 Materials and Methods

E.3.1 Identities of vaccine, challenge, and HAI panel strains

The strains of influenza used as vaccine antigens, challenge strains, and as an antigen in a hemagglutination inhibition assay are detailed in Table E.1. The accession numbers, or appropriate reference, for the HA amino acid sequences used for the antigenic distance calculations are included in the dataset publication (Skarlupka, Handel, et al., 2020). Strains included H1 influenza from both human and swine origin as indicated.

Table E.1: HAs used as HAI antigens, vaccine components, and viral challenge strains.

HAI Antigen	Vaccine and HAI Antigen			Vaccine, HAI Antigen, and Challenge Strain
Swine Isolate	Human Isolate	Swine Isolate	Human Isolate	COBRA
A/Swine/Iowa/1973	A/South Carolina/1/1918	A/Swine/Wisconsin/125/1997	A/Chile/1/1983	SW1
A/Swine/North Carolina/93523/2001	A/Weiss/1/1943	A/Swine/Indiana/Pt2439/2000	A/Singapore/6/1986	SW2
A/Swine/North Carolina/A01377454/2014	A/Fort Monmouth/1/1947	A/Swine/Spain/50047/2003	A/New Caledonia/20/1999	SW3
A/Swine/Nebraska/A01444614/2013	A/Denver/1/1957	A/Swine/Korea/Asano4/2006	A/Brisbane/59/2007	SW4
A/Swine/Missouri/A01203163/2012	A/New Jersey/1/1976	A/Swine/Zhejiang/1/2007		X-3
A/Swine/Oklahoma/A0149501/2011	A/USSR/90/1977	A/Swine/North Carolina/02744/2009		X-6
A/Swine/North Carolina/5043-1/2009	A/Brazil/1/1978	A/Swine/North Carolina/34543/2009		P-1
A/Swine/Colorado/SG1322/2009	A/Texas/36/1991	A/Swine/Minnesota/A01489606/2015		
A/Swine/Ohio/511445/2007	A/Beijing/262/1995	A/Solomon Islands/3/2006		

E.3.2 Mouse vaccinations and infections

Mouse immunological and virological data were obtained from previous studies (Carter et al., 2013; Skarlupka et al., 2019). Briefly, BALB/c mice (*Mus musculus*, female, 6 to 8 weeks old) were purchased from

Envigo (Indianapolis, IN, USA) and housed in microisolator units. Animals were allowed free access to food and water and cared for under USDA guidelines for laboratory animals. All procedures were reviewed and approved by the University of Georgia Institutional Animal Care and Use Committee (IACUC) #2016-02-011-Y3-A7. Mice were randomly divided into 10 groups ($n=11$ /group) and were vaccinated with virus-like particles (VLPs) expressing H1 hemagglutinins (HA) of human, swine or COBRA origin. The corresponding HA and a wild-type mismatched influenza neuraminidase (A/mallard/Alberta/24/2001 H₇N₃) were pseudotyped onto an HIV GAG protein to generate a VLP. Mice were vaccinated with each VLP plus an MF59-like squalene oil-in-water adjuvant at day 0 and 28. A mock vaccinated group was included which received a phosphate-buffered saline (PBS) and adjuvant vaccination. Serum samples were collected at days 42 and 54 post-vaccination. Vaccinated mouse sera were tested for HAI activity against a panel of H1 viruses (Table E.1).

Vaccinated mice were challenged with 5×10^4 plaque forming unit (PFU) ($10 \times 50\%$ lethal doses [LD_{50}]) wild-type A/California/07/2009 (H1N1) or 1×10^7 PFU A/swine/North Carolina/152702/2015 H1N2 in a volume of 50 μ l. Mice were monitored daily for 14 days for weight loss, disease signs and death. Mice from each group ($n=3$) were euthanized on day 3 post-infection for lung harvest. Lung tissue was snap frozen on dry ice, and stored at -80°C for future viral titration. Mice were humanely euthanized when they reached the humane endpoint of 20% original body weight loss or a cumulative clinical disease score of 3 (lethargy=1, hunched posture=1, rough fur=1, weight loss 15%-20%=1, weight loss >20% of original body weight=3). All procedures were performed in accordance with the Guide for the Care and Use of Laboratory Animals (Council, 2011), Animal Welfare Act (“Transportation, sale, and handling of certain animals”, 2015), and Biosafety in Microbiological and Biomedical Laboratories (Richmond & McKinney, 1993).

E.3.3 Ferret infections

Immunological data of ferrets pre-immunized to A/California/07/2009 (H1N1), A/Brisbane/59/2007 (H1N1), or A/Singapore/6/1986 (H1N1) were obtained from previous publication (Carter et al., 2017).

Briefly, fitch ferrets (*Mustela putorius furo*, female, 6 to 12 months of age, de-scented) were purchased from Triple F Farms (Sayre, PA). Ferrets were pair housed in stainless steel cages (Shor-line, Kansas City, KS) containing Sani-Chips laboratory animal bedding (P.J. Murphy Forest Products, Montville, NJ). Ferrets were provided with Teklad Global Ferret Diet (Harlan Teklad, Madison, WI) and fresh water ad libitum. The University of Georgia Institutional Animal Care and Use Committee approved all experiments, which were conducted in accordance with the National Research Council's Guide for the Care and Use of Laboratory Animals, The Animal Welfare Act, and the CDC/NIH's Biosafety in Microbiological and Biomedical Laboratories guide. Ferrets ($n = 4$) were infected with one of the three H1N1 influenza viruses (10^6 PFU/ 1 ml) intranasally. Animals were monitored daily during the infection for adverse events, including weight loss, loss of activity, nasal discharge, sneezing, and diarrhea and allowed to recover. All blood was harvested from anesthetized ferrets via the anterior vena cava at day 14 post-infection. Blood was transferred to a centrifuge tube and centrifuged at 6000 rpm. Clarified serum was collected, frozen at $-20 \pm 5^\circ\text{C}$ and used for HAI assays.

E.3.4 Hemagglutination inhibition (HAI) assay

The hemagglutination inhibition (HAI) assay was used to assess functional antibodies specific to the receptor binding site of the HA that inhibit the agglutination of turkey erythrocytes. The protocols were adapted from the WHO laboratory influenza surveillance manual (Organization & Network, 2011) and were performed as previously described (Carter et al., 2016c). Briefly, to inactivate nonspecific inhibitors, sera were treated with receptor-destroying enzyme (RDE) (Denka Seiken, Co., Japan) prior to being tested. Three-parts RDE were added to one-part sera and incubated overnight at 37°C . Following RDE inactivation by incubation at 56°C for 30 min, six-parts phosphate-buffered saline pH 7.2 (PBS, Gibco) were added. RDE-treated sera were diluted in a series of two-fold dilutions in V-bottom microtiter plates. An equal volume of virus or virus-like particle, adjusted to approximately 8 hemagglutination units (HAU)/50 μl , was added to each well. The plates were agitated, covered, and incubated at room temperature (RT) for 20 min. Then, 0.8% of turkey red blood cells (RBCs; Lampire Biologicals, Pipersville, PA, USA) in PBS

were added. All RBCs were stored at 4°C and used within 72 h of preparation. The plates were agitated and covered. The RBCs were allowed to settle for 30 min at RT. The HAI titer was determined by the reciprocal dilution of the last well that contained agglutinated RBCs. Positive and negative serum controls were included for each plate. All mice and ferrets were negative (HAI < 1:10) for preexisting antibodies to currently circulating human influenza viruses prior to vaccination or challenge and seroprotection was defined as HAI titer \geq 1:40 and seroconversion as a 4-fold increase in titer compared to baseline, as per the WHO and European Committee for Medicinal Products to evaluate influenza vaccines (“Guideline on influenza vaccines”, 2014). The limit of detection for \log_2 HAI titer was 3.32. If below the limit of detection, 2.32 \log_2 HAI titer was used for mathematical calculations.

E.3.5 Viral lung titers

Plaque assay was performed according to previously described protocols (Gaush & Smith, 1968). In brief, lungs were homogenized in 1 ml Dulbecco’s Modified Eagle Medium (DMEM), and the supernatant was collected by spinning the homogenized samples at 2000 rpm for 5 min. Low passage (< 30) Madin-Darby Canine Kidney (MDCK) cells were plated at a confluence of 1×10^6 cell per well of a six-well plate (Greiner bio-one, NC, USA) one day before the assay. MDCK cells were infected with different dilutions of samples in 100 μ L of DMEM supplemented with penicillin-streptomycin. After 1 h incubation at RT, the medium was removed, and cells were washed twice with fresh DMEM. After the addition of 2 mL of Modified Eagle Medium (MEM) medium at 2 μ g/mL TPCK-trypsin and 0.8% agarose (Cambrex, East Rutherford, NJ, USA), cells were incubated for 72 h at 37°C with 5% CO₂. Agarose was removed, and the cells were fixed with 10% buffered formalin and stained with 1% crystal violet (Fisher Science Education) for 15 min. The crystal violet was removed by rinsing thoroughly in distilled water. The numbers of plaques were counted in duplicate. Duplicates were then averaged and transformed by log₁₀. The virus titer was analyzed as the average log₁₀ PFU/lung for each individual mouse.

E.3.6 Amino acid based antigenic distance measure (ADM) calculation

The five antigenic sites used in the calculation of the H₁ HA subtype antigenic distance were outlined previously (Deem & Pan, 2009). Due to the inclusion of the pandemic HAs, the A(H₁N₁)/California/04/2009 numbering scheme was used with a maximum length of 549 residues for the HAo (Deem & Pan, 2009). The amino acid numbering begins following the seventeen amino acids in the signal peptide (Burke & Smith, 2014; Nobusawa et al., 1991; Winter et al., 1981). The HA₁ region was defined as amino acids 1-327. The antigenic sites include the amino acids predicted to be important to vaccine efficacy: neutralizing-antibody binding residues, structure/sequence homologues of known H₃ epitopes, and protein surface residues with high information entropy (Table E.2) (Deem & Pan, 2009). The following equations were used to calculate the antigenic distances (Equations E.1, E.2, E.3, E.4, E.5):

$$p_{sequence} = \frac{\text{number of substitutions in entire HA sequence}}{\text{total number of amino acids in entire HA sequence}} \quad (\text{E.1})$$

$$p_{HA1} = \frac{\text{number of substitutions in HA}_1}{\text{total number of amino acids in HA}_1} \quad (\text{E.2})$$

$$p_{allepitope} = \frac{\text{number of substitutions in all epitopes}}{\text{total number of amino acids in all epitopes}} \quad (\text{E.3})$$

$$p_{epitopex} = \frac{\text{number of substitutions in epitope x}}{\text{total number of amino acids in epitope x}} \quad (\text{E.4})$$

$$p_{epitope} = \max p_{epitopex} \quad (\text{E.5})$$

Table E.2: Amino acid residues used to calculate the ADM of vaccine and challenge virus combinations.

Antigenic Site	Amino Acid Residue
A (SA)	118, 120, 121, 122, 126, 129, 132-135, 137, 139-143, 146, 147, 149, 165, 252, 253
B (Sb)	124, 125, 152-157, 160, 162, 183-187, 189-191, 193-196
C	34-38, 40, 41, 43-45, 269-274, 276-278, 283, 288, 292, 295, 297, 298, 302, 303, 305-310
D (Ca)	89, 94-96, 113, 117, 163, 164, 166-174, 176-178, 200, 202, 204-216, 222-227, 235, 237, 241, 243-245
E (Cb)	47, 48, 50, 51, 53, 54, 56-58, 66, 68-75, 78-80, 82-86, 102, 257-261, 263, 267

ADM were determined through protein alignment. Briefly, the HAo was aligned utilizing Geneious alignment with global alignment with free end gaps and a cost matrix Blosum62 with open gap penalty

12, and gap extension penalty 3, with refinement iterations of 2 (Geneious v7.1.5). The HAI portions (1-327AA) were extracted from the alignment. From which, all or individual antigenic sites were extracted and the differing number of amino acids between two viral strains were determined.

E.3.7 HAI titer difference calculation

The original raw HAI data were in two-fold serial dilution titers and transformed by \log_2 . From those transformed values, the mean \log_2 HAI titer was calculated for each vaccine:challenge virus combination. Outliers were not removed, but mock controls (PBS vaccinated) were removed from analysis. The difference between reference HAI titer and HAI titer for a specific strain was computed as $\Delta HAI = \log_2(HAI_{\text{reference}}) - \log_2(HAI_{\text{specific strain}})$.

E.3.8 Regression analysis between ADM and correlates of protection

Linear regression models, as done previously with antigenic measures (Wikramaratna & Rambaut, 2015), were fit to the data with the different antigenic measures as predictors, and HAI differences, lung titer and percent weight loss as outcomes. The adjusted R^2 was reported for all linear fits. The 95% confidence and prediction intervals were computed for each model with R version 3.6.2 using RStudio version 1.2.5033 (R-Project, 2017). The day 6 percent weight loss for mice was determined by dividing weight on day six post-challenge by the original day 0 weight and which was expressed as a percentage. Further analysis including the data below the limit of detection were analyzed separately.

E.4 Results

E.4.1 ADM describe the trend of Δ HAI titer of H1 influenza viruses in mice

The goal of this study was to determine if the ADM determined from influenza HA amino acid sequences may be a predictive measure for HA-induced HAI activity in collected antisera. These values – p_{sequence} ,

p_{HAI} , $p_{\text{all-epitope}}$, and p_{epitope} – are different attempts to measure the antigenic distance between two different viruses (V. Gupta et al., 2006).

Three hundred and sixteen ΔHAI titers from vaccinated mice (Skarlupka, Handel, et al., 2020) were examined for the linear relationship between the ΔHAI titers and ADM. The ADM had ranges starting at 0.0 with varying maximums ($p_{\text{sequence}} = 0.222$, $p_{\text{HAI}} = 0.303$, $p_{\text{all-epitope}} = 0.528$, $p_{\text{epitope}} = 0.864$). There was a linearly increasing trend of HAI titer difference as antigenic distance increased ($p < 0.0001$) (Fig. E.1; Fig. E.2). The adjusted R^2 increased as the antigenic measure became more specific ($p_{\text{sequence}} < p_{\text{HAI}} < p_{\text{all-epitope}} < p_{\text{epitope}}$). Thus, p_{epitope} was the best among the ADM in describing ΔHAI . Nevertheless, the R^2 values were all low, with a maximum value of 0.288 for the p_{epitope} antigenic distance (Table E.3; Table E.4). The variability of HAI differences for any value of antigenic distance was wide and ranged from a minimum of 0.868 ΔHAI at a p_{epitope} of 0.545 and a maximum of 12.5 ΔHAI at a value of 0.864 ADM, with a mean variability of 5.60 ΔHAI .

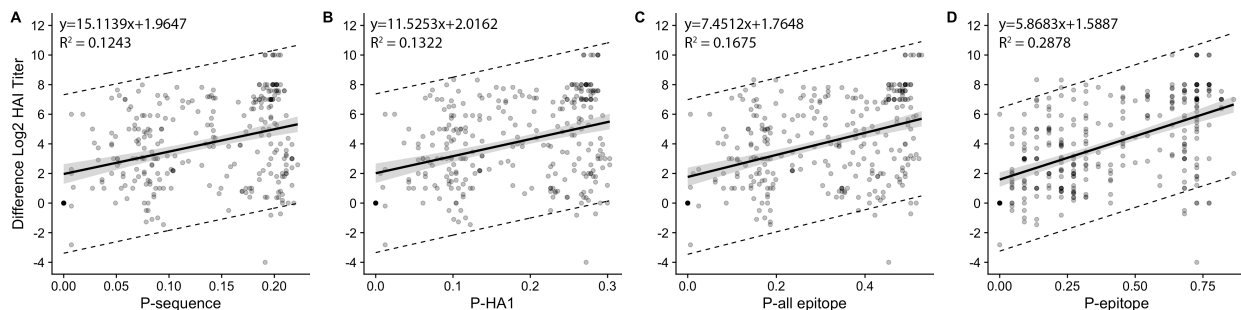


Figure E.1: Amino acid sequence based antigenic distances modeled against the change in HAI titer of H1 influenza in the mouse model. Linear regression of p_{sequence} (A), p_{HAI} (B), $p_{\text{all-epitope}}$ (C), and p_{epitope} antigenic distances (D) against the ΔHAI titers to homologous control elicited in BALB/C mice. The 95% confidence intervals are depicted with grey shading. The 95% prediction intervals are depicted by dashed lines.

E.4.2 ADM are poor predictors of Δ HAI titer of H1 influenza viruses in mice

To evaluate the ability of the ADM to predict ΔHAI , the 95% prediction intervals were computed. Those intervals are wide; the mean p_{epitope} , 0.420 units, has the narrowest prediction interval of the data. The

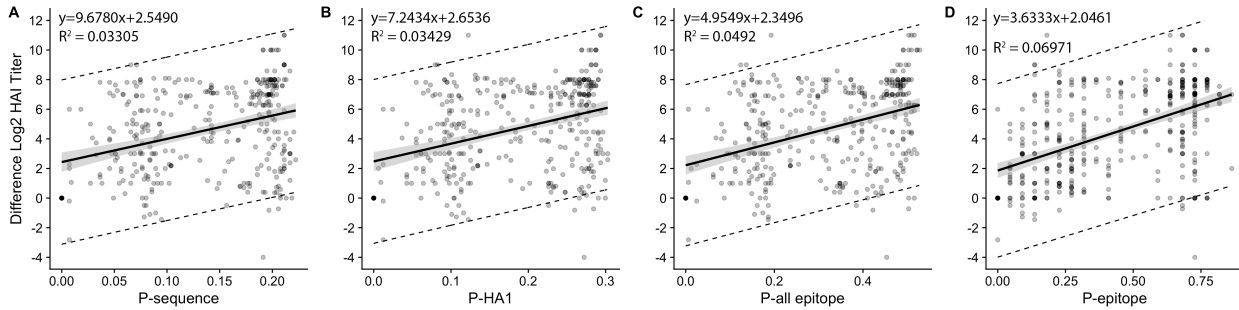


Figure E.2: Amino acid sequence based antigenic distances modeled against the change in HAI titer of H1 influenza in the mouse model including points below the limit of detection. Linear regression of p_{sequence} (A), p_{HA1} (B), $p_{\text{all epitope}}$ (C), and p_{epitope} antigenic distances (D) against the ΔHAI titers to homologous control elicited in BALB/C mice with the inclusion of point below the limit of detection. The 95% confidence intervals are depicted with grey shading. The 95% prediction intervals are depicted by dashed lines.

predictive interval for the mean, around the fitted estimate of 4.056 ΔHAI was $\pm 4.816 \Delta\text{HAI}$. The predictive intervals are wider than this range for any other given antigenic distance value. With widths greater than $\pm 2.0 \Delta\text{HAI}$, the measures were not suitable as predictive tools for outcomes of HAI assays.

E.4.3 p_{epitope} shows improved, but still limited, performance for COBRA vaccines

To evaluate if ADM might perform better for a specific type of vaccine, namely the COBRA vaccines (Carter et al., 2017; Skarupka et al., 2019), another analysis was performed on a subset of the data. Only mice vaccinated with a COBRA vaccine were analyzed. The p_{epitope} ADM was focused on since it performed best in the previous analyses. The prediction intervals for COBRA vaccinated mice tested against a wild-type human or swine H1 influenza strain were still wide, with a minimum spread of $\pm 4.479 \Delta\text{HAI}$ around the fitted value of 4.724 ΔHAI at the mean p_{epitope} ADM of 0.405 units (Fig. E.3A). However, the COBRA vaccinated mouse sera tested against COBRA VLPs in the HAI assay had smaller prediction intervals than most other combinations of $\pm 3.06 \Delta\text{HAI}$ around the fitted value of 4.154 ΔHAI at the

Table E.3: Summary of resultant equations from best-fit analysis.

Dependent Variable	Independent Variable	Equation	D.F.	t-value	p-value	Adjusted R ²
Mouse ΔHAI	P_{sequence}	$y = 15.1139x + 1.9647$	291	6.515	<0.0001	0.1243
	P_{HAI}	$y = 11.5253x + 2.0162$	301	6.856	<0.0001	0.1322
	$P_{\text{all-epitope}}$	$y = 7.4514x + 1.7648$	306	7.924	<0.0001	0.1675
	P_{epitope}	$y = 5.8683x + 1.5887$	314	11.328	<0.0001	0.2878
Ferret ΔHAI	P_{sequence}	$y = 32.7805x + 1.5102$	28	4.539	<0.0001	0.4034
	P_{HAI}	$y = 24.1281x + 1.4296$	28	4.648	<0.0001	0.5153
	$P_{\text{all-epitope}}$	$y = 12.8958x + 1.4243$	28	4.579	<0.0001	0.4078
	P_{epitope}	$y = 8.9706x + 0.9403$	28	5.616	<0.0001	0.5129
Mouse Day 3 Viral Lung Titer	P_{sequence}	$y = 9.1448x + 2.7541$	21	1.671	0.10960	0.0753
	P_{HAI}	$y = 7.3363x + 2.6468$	21	1.892	0.07232	0.105
	$P_{\text{all-epitope}}$	$y = 4.586x + 2.552$	21	2.189	0.040025	0.147
	P_{epitope}	$y = 5.0661x + 2.1251$	22	5.543	<0.0001	0.5638
	ΔHAI	$y = 0.41453x + 1.73092$	22	4.285	0.0003	0.4302
Mouse Day 6 Weight Loss	P_{sequence}	$y = 32.410x + 7.936$	21	1.556	0.13462	0.06069
	P_{HAI}	$y = 7.3363x + 2.6468$	21	1.763	0.09248	0.08742
	$P_{\text{all-epitope}}$	$y = 16.153x + 7.247$	21	2.013	0.05715	0.1218
	P_{epitope}	$y = 17.587x + 5.561$	22	4.816	<0.0001	0.491
	ΔHAI	$y = 1.4931x + 3.9187$	22	4.085	0.0005	0.4054

Table E.4: Summary of resultant equations from best-fit analysis including points below the limit of detection.

Dependent Variable	Independent Variable	Equation	D.F.	t-value	p-value	Adjusted R ²
Mouse ΔHAI	P_{sequence}	$y = 9.6780x + 2.5490$	417	3.910	0.0001	0.03305
	P_{HAI}	$y = 7.2434x + 2.6536$	433	4.051	<0.0001	0.03429
	$P_{\text{all-epitope}}$	$y = 4.9549x + 2.3496$	443	4.897	<0.0001	0.0492
	P_{epitope}	$y = 3.6333x + 2.0461$	475	6.055	<0.0001	0.06971
Ferret ΔHAI	P_{sequence}	$y = 21.6263x + 4.3229$	94	5.704	<0.0001	0.2492
	P_{HAI}	$y = 16.2446x + 4.1613$	94	6.032	<0.0001	0.2714
	$P_{\text{all-epitope}}$	$y = 8.993x + 4.058$	94	6.236	<0.0001	0.2851
	P_{epitope}	$y = 7.1259x + 3.1554$	94	8.031	<0.0001	0.4006

mean p_{epitope} of 0.364 (Fig. E.3B). The same subset was evaluated with the inclusion of the points below the limit of detection and a similar trend was observed (Fig. E.4; Table E.5).

E.4.4 p_{epitope} poorly describes ΔHAI for swine H1 influenza viruses in mice

One of the most novel aspects of this dataset was the inclusion of the swine origin influenza as HAI antigens and as vaccine antigens. When the swine antisera were matched with only human and swine wild-type HAI antigens (removal of COBRA HAI antigens), there was again an increasing trend between ADM and ΔHAI (Fig. E.5A). However, upon subsetting the HAI antigen by host origin, the swine

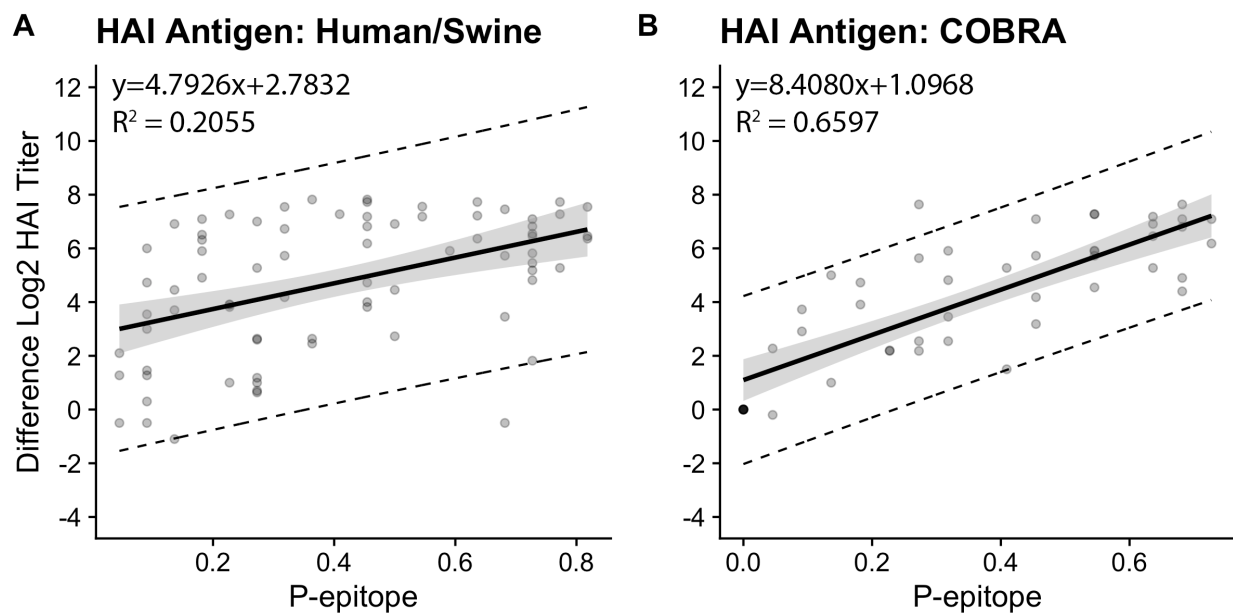


Figure E.3: The p_{epitope} antigenic distance better describes computationally designed interactions, than wild-type HAI antigen interactions. Linear regression of p_{epitope} antigenic distance against the ΔHAI titers to homologous control elicited in BALB/C mice. The vaccine antigen for all datapoints was a COBRA HA antigen. The HAI antigen was either of wild-type origin (A) or a COBRA VLP (B). The 95% confidence intervals are depicted with grey shading. The 95% prediction intervals are depicted by dashed lines.

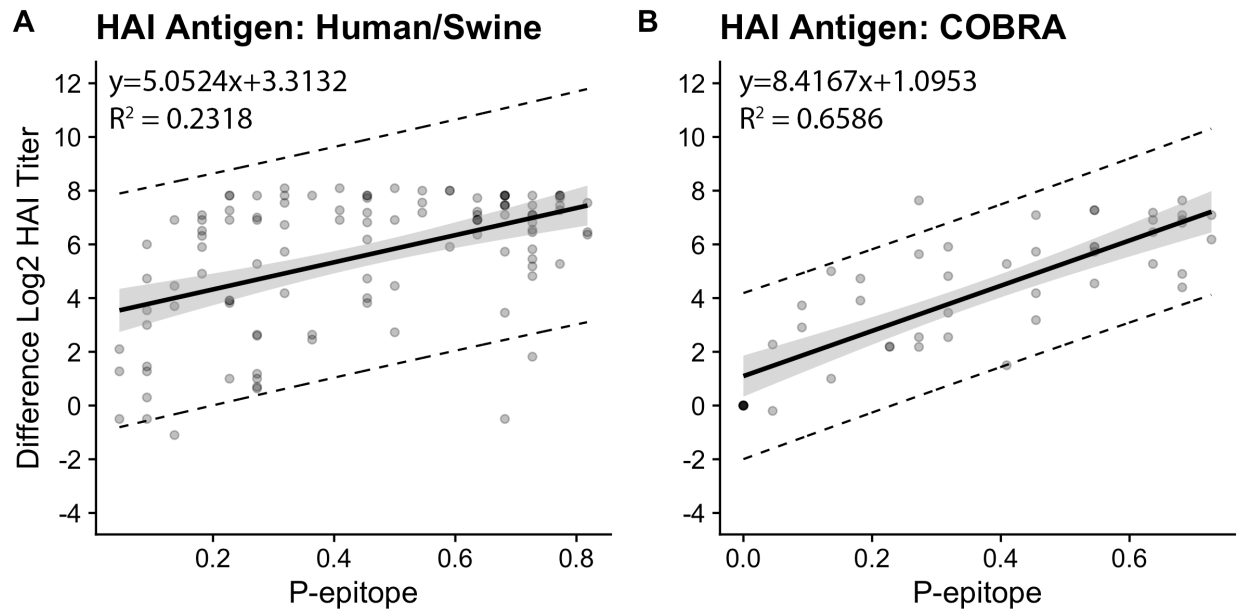


Figure E.4: The p_{epitope} antigenic distance better describes computationally designed interactions, than wild-type HAI antigen interactions including points below the limit of detection. Linear regression of p_{epitope} antigenic distance against the Δ HAI titers to homologous control elicited in BALB/C mice with the inclusion of point below the limit of detection. The vaccine antigen for all datapoints was a COBRA HA antigen. The HAI antigen was either of wild-type origin (A) or a COBRA VLP (B). The 95% confidence intervals are depicted with grey shading. The 95% prediction intervals are depicted by dashed lines.

Table E.5: Summary of resultant equations from best-fit analysis of sub-setted data with and without points below the limit of detection (LOD).

Vaccine Antigen	HAI Antigen	Inclusion of LOD	Equation	D.F.	t-value	p-value	Adjusted R ²
COBRA	Human/Swine	No	$y = 4.7926x + 2.7832$	75	4.545	0.0001	0.2055
	COBRA	No	$y = 8.4080x + 1.0968$	46	9.389	<0.0001	0.6597
	Human/Swine	Yes	$y = 5.0524x + 3.3132$	110	5.873	<0.0001	0.2318
	COBRA	Yes	$y = 8.4167x + 1.0953$	47	9.674	<0.0001	0.6586
Swine	Human/Swine	No	$y = 5.4889x + 1.5064$	164	7.473	<0.0001	0.2495
	Human	No	$y = 4.830x + 3.718$	52	2.848	0.00628	0.1183
	Swine	No	$y = 0.3155x + 2.2297$	110	0.7845	0.688	-0.00761
	Human/Swine	Yes	$y = 4.7544x + 1.7373$	211	5.472	<0.0001	0.1201
	Human	Yes	$y = 8.4599x + 0.8844$	64	6.182	<0.0001	0.3641
	Swine	Yes	$y = 0.9832x + 2.4704$	145	0.879	0.381	-0.00156

anti-sera were less HAI cross-reactive with the human antigens (Fig. E.5B), with most of the datapoints having a large p_{epitope} and a large ΔHAI titer. Interestingly, an analysis of swine antisera against different swine viruses did not show a correlation ($R^2 = -0.00761$) between p_{epitope} and ΔHAI (Fig. E.5C). The same subset was evaluated with the inclusion of the points below the limit of detection and a similar trend was also observed (Fig. E.6; Table E.5).

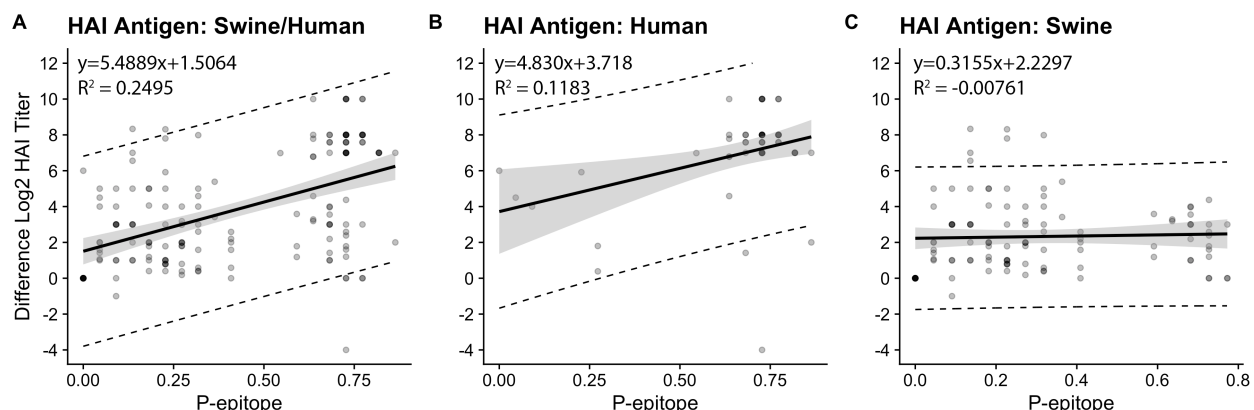


Figure E.5: The interactions of swine origin HA antigens with HAI antigens are not a function of the p_{epitope} antigenic distance. Linear regression of p_{epitope} antigenic distance against the ΔHAI titers to homologous control elicited in BALB/C mice. The vaccine antigen for all datapoints was a swine origin HA antigen. The HAI antigen was both human and swine (A), only human (B), or only swine (C) origin. The 95% confidence intervals are depicted with grey shading. The 95% prediction intervals are depicted by dashed lines.

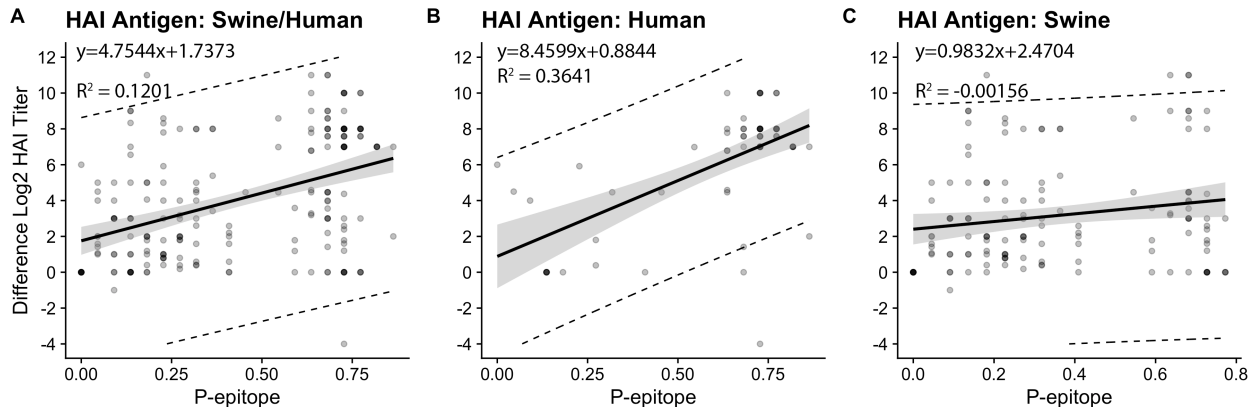


Figure E.6: The interactions of swine origin HA antigens with HAI antigens are not a function of the p_{epitope} antigenic distance even with inclusion of points below the limit of detection. Linear regression of p_{epitope} antigenic distance against the ΔHAI titers to homologous control elicited in BALB/C mice with the inclusion of point below the limit of detection. The vaccine antigen for all datapoints was a swine origin HA antigen. The HAI antigen was both human and swine (A), only human (B), or only swine (C) origin. The 95% confidence intervals are depicted with grey shading. The 95% prediction intervals are depicted by dashed lines.

E.4.5 ADM describe the trend of ΔHAI titer of H1 influenza viruses in ferrets

To determine if the trend observed in the mouse model was consistent across animal models or an artifact of the mouse model, the ΔHAI titer of antisera collected from ferrets infected with influenza virus was used for analysis (Skarlupka, Handel, et al., 2020). Thirty different antisera:HAI antigen combinations from challenged ferrets were examined for the linear relationship between the ΔHAI titers and ADM. The measures all had a range starting at 0.0 with varying maximums ($p_{\text{sequence}} = 0.199$, $p_{\text{HAI}} = 0.275$, $p_{\text{all-epitope}} = 0.522$, $p_{\text{epitope}} = 0.727$). There was a linearly increasing trend of HAI titer difference as antigenic distance increased ($p < 0.0001$) (Fig. E.7). The adjusted R^2 remained similar across the four ADM; there was no increasing trend, as seen with the mouse model. The ADM were higher than the mouse model, with a maximum value of 0.515 for the p_{HAI} antigenic distance (Table E.3), likely in part due to less data available for these analyses. There was, again, a wide spread in ΔHAI for any value of antigenic distance with a

mean variance of $4.78 \Delta\text{HAI}$ for the p_{epitope} ADM. The same dataset was evaluated with the inclusion of the points below the limit of detection and a similar trend was observed (Fig. E.8; Table E.5).

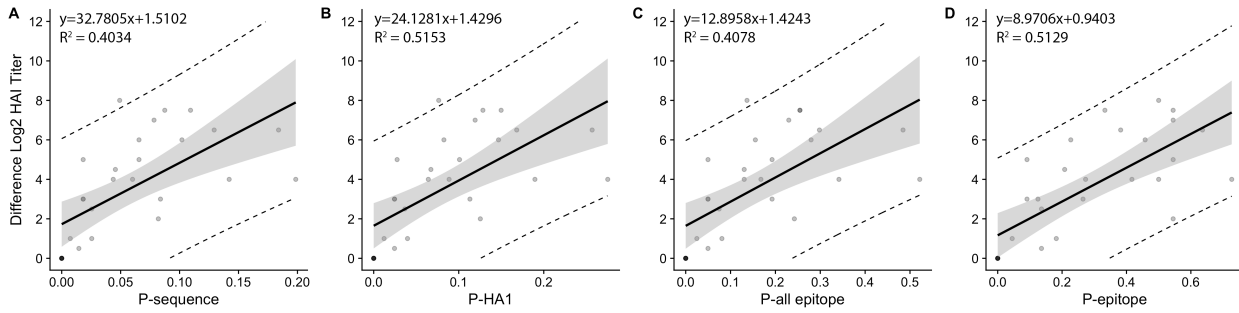


Figure E.7: Amino acid sequence based antigenic distances modeled against the change in HAI titer for human H1N1 subtype HAI data in the ferret model. Linear regression of p_{sequence} (A), p_{HA1} (B), $p_{\text{all-epitope}}$ (C), and p_{epitope} antigenic distances (D) against the ΔHAI titers to homologous control elicited in pre-immune ferrets. The 95% confidence intervals are depicted with grey shading. The 95% prediction intervals are depicted by dashed lines.

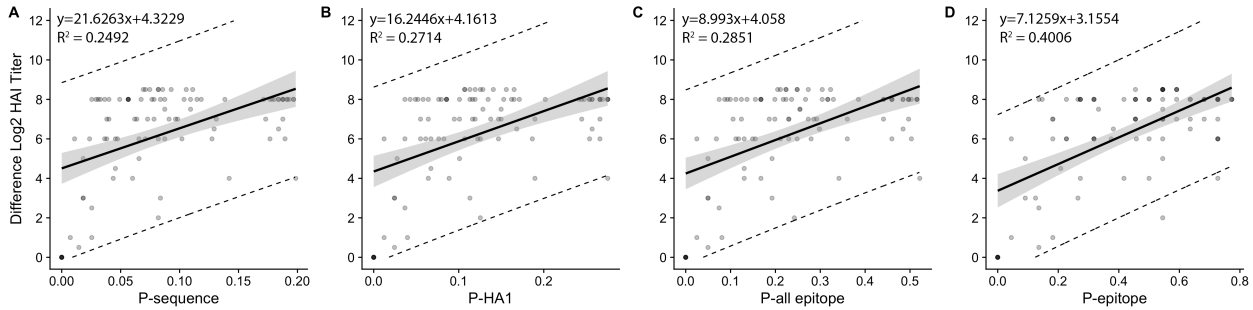


Figure E.8: Amino acid sequence based antigenic distances modeled against the change in HAI titer for human H1N1 subtype HAI data in the ferret model including points below the limit of detection. Linear regression of p_{sequence} (A), p_{HA1} (B), $p_{\text{all-epitope}}$ (C), and p_{epitope} antigenic distances (D) against the ΔHAI titers to homologous control elicited in pre-immune ferrets with the inclusion of point below the limit of detection. The 95% confidence intervals are depicted with grey shading. The 95% prediction intervals are depicted by dashed lines.

This suggests that similar to the mouse results, the ADM can capture the overall trend in ΔHAI but it is not possible to use them to predict outcomes of an HAI assay with much precision.

E.4.6 ADM and Δ HAI show similar correlations with viral load and weight loss following infection in mice.

In a last set of analyses, ADM or Δ HAI were assessed to determine if either correlated with two important infection outcomes, namely the peak viral lung titer and weight loss in mice. In total, there were twenty-four or twenty-three vaccine and challenge pairs analyzed depending on predictor variable (Table E.3; (Skarlupka, Handel, et al., 2020)). Among the ADM, $p_{\text{all-epitope}}$, and p_{epitope} , showed statistically significant correlations with lung virus titer, so did Δ HAI (Fig. E.9A-E; Table E.3). The $p_{\text{all-epitope}}$ had a smaller R^2 value of 0.147 compared to the other measures, such as 0.569 for p_{epitope} and 0.430 for Δ HAI titer. The p_{epitope} had the narrowest prediction intervals at the mean value of 0.337 ADM, for a fitted value of $3.833 \pm 2.3144 \log_{10}(\text{lung titer})$.

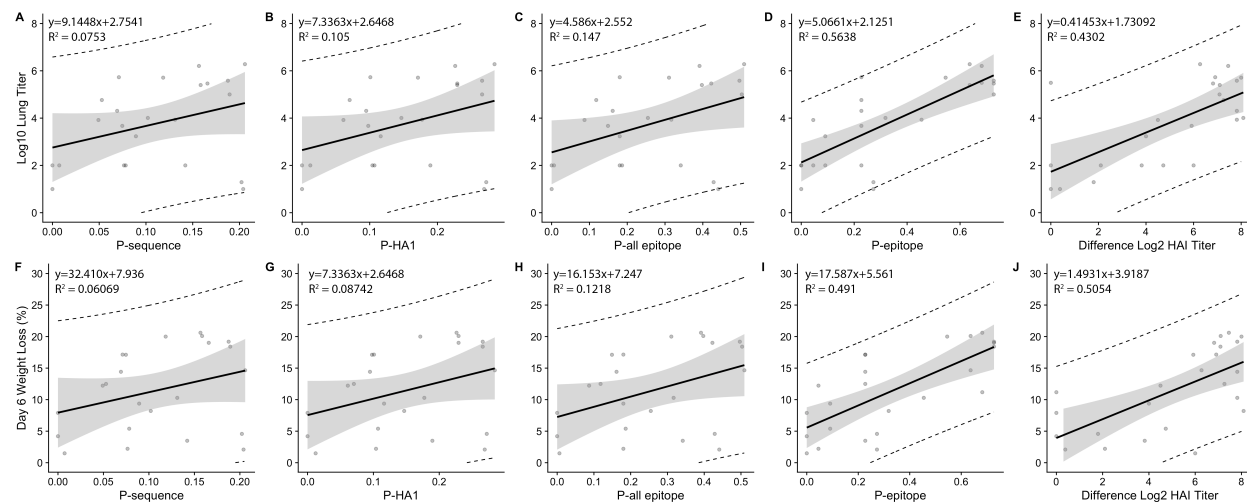


Figure E.9: The use of in vivo challenge data from the mouse model for linear regression with different antigenic distances. The sequence based and HAI based antigenic distances were linearly modeled with the mean \log_{10} lung viral titers (A-E) and day 6 percent weight loss (F-J) in mice after infection with either a human H1N1 (CA/09) or swH1N2 virus (SW/NC/15). The 95% confidence intervals are depicted with grey shading. The 95% prediction intervals are depicted by dashed lines.

The challenged mouse day 6 weight dataset revealed that of the ADM only the p_{epitope} and Δ HAI titer were significant (Fig. E.9F-J). The R^2 for these two measures were 0.491 and 0.405, respectively. Hence, the variation in weight loss in mice was better explained by the p_{epitope} than the other antigenic measures.

For all predictor and outcome variables in this analysis, prediction intervals were wide with the narrowest prediction intervals for the dataset at the p_{epitope} mean of 0.337 units with a fitted weight loss of $11.490 \pm 9.87\%$ (Fig. E.9), thus suggesting that while both p_{epitope} and ΔHAI can capture the overall trend, in lung titer and weight loss, neither quantity is useful for precise predictions.

E.5 Discussion

In this study, datasets from previous influenza virus vaccination and infection studies (Carter et al., 2017; Skarlupka et al., 2019) were used to determine the relationship between several ADM and HAI titer differences, viral lung titer, and weight loss. The ADM correlated with the difference in HAI titer but resulted in large prediction intervals (Fig. E.1, E.3, E.5). The relationships of ADM and ΔHAI were similar in the ferret and mouse models (Fig. E.1 and E.7; Table E.3). When comparing the ADM to viral lung titer and percent weight loss, only the p_{epitope} and ΔHAI adequately described the overall trends. The use of ADM as a predictive measure of ΔHAI titer, viral lung titer, and weight loss was determined not to be applicable due to wide predictive intervals for each outcome.

Previous studies compared HA-based computational ADM to ferret antisera HAI-based antigenic distances as predictors of inactivated influenza vaccine efficacy in humans and found that the computational ADMs correlated better with vaccine efficacy than HAI-based measures did (Bonomo & Deem, 2018; Deem & Pan, 2009; V. Gupta et al., 2006; X. Li & Deem, 2016; Pan et al., 2011). This study differed from the previous studies in that the outcome of interest was ΔHAI titer and murine clinical signs rather than influenza-like symptoms in vaccinated persons. Unlike in the human system used for the previous studies, the mice were not pre-immune to influenza. Although the mice were exposed to influenza HA through three vaccinations, the immune responses to infection and vaccination are not equivalent (Ghendon, 1990; Monto et al., 2015). The mechanism of exposure contributes to the epitope immunodominance of the antigen (Angeletti et al., 2017; Blackburne et al., 2008). Both vaccination and infection induce a systemic antibody response. Yet the live influenza infection leads to local immune and cytotoxic T-cell responses which could be captured in the original studies that used humans with pre-existing immunity and an out-

come of influenza-like illness through T-cell epitope similarity potentially having some multicollinearity with B-cell epitope similarity through the genetic distance of the two genomes being compared (Monto et al., 2015; Schotsaert et al., 2010). Furthermore, the ADMs may correlate better with vaccine efficacy in a pre-immune human model where immunodominance drives the antibody response to the measured dominant p_{epitope} . In a naïve vaccinated model, the antigen immunodominance could be directed to a different site thus not being captured by the ADM and contributing to the large variances of HAI titers observed at any given ADM, but further analysis would need to be conducted to confirm. In addition, the wide variability of HAI titers across ADM may have been influenced by including viruses isolated from different animal species (T. K. Anderson et al., 2015; Rajao et al., 2018). A host origin different from human may have species-specific epitope signatures that lead to uncommon antigenic regions not included in the definition of the antigenic regions since they are not shared across all species (Koedijk et al., 2017; Lee & Chen, 2004; S. T. H. Liu et al., 2018; Sutton et al., 2017; Vaughan et al., 2012). Considering all of these confounding factors, equating the immunodominant site to the most variable region, as used in this and previous analyses (Deem & Pan, 2009), may be inappropriate and may have contributed to the low correlation between the ADM and Δ HAI titers in an analysis with such variety of viral origins and animal models. The determination of these origin and species-specific antibody binding and immunodominance characteristics require future in depth studies on host antibody kinetics and viral escape mutant analysis. Inferences from antibody responses from animal data and the correlations between amino acid sequences, HAI titers, and viral protection should be cautiously made. Furthermore, strains may contain variations in their antigenic and neutralizing sites in undefined locations on the HA protein or on another component contributing to the observed poor correlation (Lees et al., 2010; A. W. Park et al., 2009). Other methods may be proposed over the purely amino acid sequence based methods such as including limited antisera data and genetic variation to achieve a finer resolution as previously shown with H₃N₂ (P. Wang et al., 2018). Other correlates of protection, such as total antibody binding or neutralization titers, which have been shown to be more reliable than HAI, could be investigated to determine if they correlate better with the ADM (Belshe et al., 2000; Lee et al., 2004). The protective contribution of T-cell epitopes should

be considered in pre-immune models especially due to human's pre-existing immunity (Jurchott et al., 2016).

The ability to accurately and precisely quantify antigenic distance at the amino acid sequence level would be a valuable tool for influenza virus research. Currently, the phylogenetic distance between a pair of viral gene segments is not an accurate predictor of antigenic distance (Lees et al., 2010). Therefore, in-silico methods for the antigenic characterization of influenza viruses are being developed and improved (Klingen et al., 2018). However, here we report that the ADM analyzed do not provide a method useful for predicting the Δ HAI response from a variety of influenza host origins and vaccine and challenge strain combinations, and the method did not correlate any better than Δ HAI titers in determining viral challenge outcomes. With the potentially additive confounding factors of the species of the virus and antibody origin, as well as, antigen delivery affecting the definition of antigenic regions. Hence, this antigenic distance measure needs to be further optimized before use in animal model based vaccine research and development.

E.6 Acknowledgments

The authors would like to thank Donald Carter for animal technical assistance and Dr. Mark Tompkins' laboratory for graciously providing the A/Swine/North Carolina/152702/2015 virus and HA amino acid sequence data. We would also like to thank Dr. Deborah A. Keys, Israel Rivera, Steven B. Hancock, and Z. Beau Reneer for helpful discussions and comments. Reagents were obtained through the NIH Biodefense and Emerging Infections Research Resources Repository, NIAID, NIH. TMR is supported, in part, by the Georgia Research Alliance as an Eminent Scholar.

E.7 Competing Interests

No competing interests.

APPENDIX F

DESIGN OF N₂ COBRA NA INFLUENZA

ANTIGENS¹

F.I Wild-type N₂ lineages

The N₂ influenza subtype has been present in the human population as either H₂N₂ (1956-1968) or H₃N₂ (1968-present). Similar to the N₁ subtype, N₂ is also isolated from animal reservoirs including swine, avian, and feline species (Fig. F.1). The wild-type N₂ proteins were confirmed for enzymatic activity (Fig. 3.1). Using the defined N₂ clades COBRA antigens were created to protect against either human and swine lineage viruses (Clade N_{2.2}) or to the most recent human-isolated viruses (Clade N_{2.2e}).

F.I.I Design of the N₂-A COBRA NA

The N₂-A COBRA NA was the resulting design of a COBRA antigen that would potentially elicit protective antibodies across the N_{2.2} clade. To begin, wild-type sequences from were downloaded from GISAID and saved with FASTA and accession ID information. Multiple sequence comparison by log expectation (MUSCLE) multiple sequence alignment was performed. All sequences with ambiguities or incomplete lengths were removed. The protein sequences were trimmed to include only the protein's

head region (N₂ residue numbering: 75-469). Unique sequences were then extracted, aligned, and used for phylogenetic tree generation. For the first consensus layer, the clades were condensed individually, with consensuses taken of strains had greater than 97% sequence identity (\leq 12 amino acid differences). The final sequence did not result in any ambiguities and is included below. Similar to the N₁ COBRA NAs the N₂ proteins were expressed either as full-length proteins for VLP production or as a soluble protein in the pcDNA3.1 expression vector.

F.I.2 Design of the N₂-B COBRA NA

The N₂-B COBRA NA was designed similarly to the N₂-A COBRA NA. However, instead of using all of the sequences available, only the wild-type sequences from the N₂.2e clade were used. The goal for this COBRA antigen was to protect against the most recently circulating H₃N₂ viruses in the human population. Ideally, this antigen would be paired with an H₃ antigen as a supplemental component. Therefore, the final sequence which contained ambiguities was aligned to the 2017-2019 vaccine strains and in the ambiguities were chosen to match the consensus residues of those strains.

Table F.1: Summary of N₂-A and N₂-B COBRA NA antigen design. The motivation, wild-type sequences, time frames and methods used to create the N₂ COBRA NA antigens.

Group #	Sub-Lineage	Years	Descriptor	# Trimmed Unique Sequences	Clustering
N ₂ -A COBRA	2.2	Human:1957-2019 Swine:1977-2019	Antigen to protect against human and swine originating N ₂ viruses	30 2.2a 64 2.2b 52 2.2c 310 2.2d 8960 2.2e 3174 N ₂ .swine	1°: 97% similarity (clades done separately) 2°+: Combine all primary consensus then combined
N ₂ -B COBRA	2.2e	Human:2000-2019	Antigen to protect against current circulating human H ₃ N ₂ viruses	8960 2.2e	1°: 97% similarity 2°+: Based on tree layout; consensus sequences; Ambiguities in the final sequence chosen based on: Alignment to 2017-2019 vaccine strains

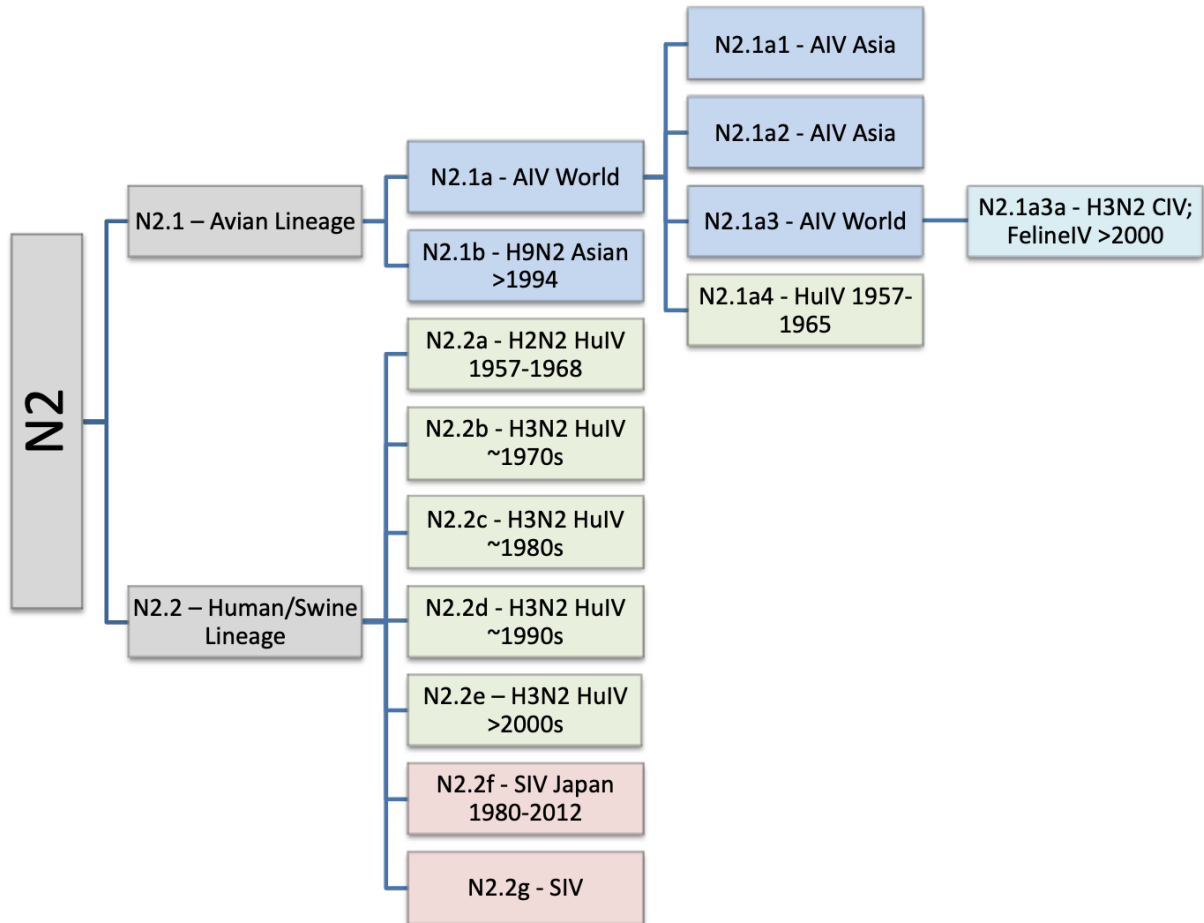


Figure F.1: The clades of the N₂ NA genetic lineages were determined through previous phylogenetic analysis (J. M. Chen et al., 2007; Fanning et al., 2000; S. Liu et al., 2009; Schon et al., 2021; Zhuang et al., 2019). Clades are color coded based upon host viruses are isolated from: grey: multiple host species; blue: avian host species; red: swine host species; green: human host species; light blue: feline and canine host species. AIV: Avian influenza virus; SIV: Swine influenza virus; HuIV: Human influenza virus; CIV: Canine influenza virus; FelineIV: Feline influenza virus.